INFORMATION TO USERS

This manuscript has been reproduced from the microfilm master. UMI films the text directly from the original or copy submitted. Thus, some thesis and dissertation copies are in typewriter face, while others may be from any type of computer printer.

The quality of this reproduction is dependent upon the quality of the copy submitted. Broken or indistinct print, colored or poor quality illustrations and photographs, print bleedthrough, substandard margins, and improper alignment can adversely affect reproduction.

In the unlikely event that the author did not send UMI a complete manuscript and there are missing pages, these will be noted. Also, if unauthorized copyright material had to be removed, a note will indicate the deletion.

Oversize materials (e.g., maps, drawings, charts) are reproduced by sectioning the original, beginning at the upper left-hand corner and continuing from left to right in equal sections with small overlaps.

ProQuest Information and Learning
300 North Zeeb Road, Ann Arbor, MI 48106-1346 USA
800-521-0600

Metamorphic petrology of siliceous marbles and associated gneissic rocks in the Grenville Province of southeastern Ontario.

by

Jo-Anne Goodwin-Bell, B.Sc. (Hons.), M.Sc.

A thesis submitted to the Faculty of Graduate Studies and Research

in partial fulfilment of the requirements for the degree of

Doctor of Philosophy

Department of Earth Sciences, Carleton University

Ottawa-Carleton Geoscience Centre

Ottawa, Ontario

June 29, 2005

Abstract

The marbles of the Carleton Place area are described within the CaO-MgO-SiO_2-$KAlSi_3O_8$-CO_2-H_2O system. An invariant point involving the phases calcite, dolomite, quartz, potassium feldspar, phlogopite, tremolite, diopside, and fluid in pressure-temperature space exists at ~ 625 °C and 6.0 kbars. This invariant point controls the phase relations of the polybaric T-X_{CO2} diagrams, resulting in significantly different diagrams for conditions above and below this invariant point.

The following isograds were mapped in the study area:

1 Talc-out: 2 talc + 3 calcite = tremolite +dolomite + H_2O + CO_2

2 Tremolite-in: 5 dolomite + 8 quartz +H_2O = tremolite +3 calcite + 7 CO_2

3 Tremolite + K-feldspar-in: 24 quartz + 6 calcite + 5 phlogopite = 3 tremolite + 5 K-feldspar + 2 H_2O + 6 CO_2

4 Diopside-in: tremolite + 3 calcite + 2 quartz = 5 diopside + 3 CO_2 + H_2O

5 Diopside-dolomite-in: tremolite + 3 calcite = dolomite + 4 diopside + H_2O + CO_2

6 Forsterite-in: tremolite + 11 dolomite = 8 forsterite + 13 calcite + 9 CO_2 + H_2O

Evidence from the petrology of the marbles indicates fluid composition was controlled by both internal and external buffering.

Thermobarometric data obtained from the various gneissic and plutonic rocks associated with the marbles suggest different metamorphic conditions prevailed on either side of the Clayton Lake shear zone. Relatively high temperature (554 °C) and low pressure (3.3 kbars) conditions existed in the west based on the Lavant Gabbro Complex. High temperature and high pressure regional metamorphism are suggested by the Wolf

Grove Structure which recorded a mean temperature and pressure of 713 °C at 7.8 kbars. Gneisses of the Pakenham Dome experienced P-T conditions of 598 °C and 8.5 kbars. These data were used to calculate approximate field gradients for the study area. A gradient of ~ 47 °C/km was obtained for the rocks west of the Clayton Lake shear zone and ~ 26-32 °C/km for rocks to the east.

Based on the differences in mineralogy, metamorphic grade, structural deformation, and associated rock types for the Carleton Place area marbles, it is apparent that two marble units are present in the field area juxtaposed against each other by the Clayton Lake shear zone. Rocks to the west of the shear zone are characterized by marble intercalated with metavolcanic rocks and intruded by the Lavant Gabbro Complex, with evidence of both contact metamorphism and low grade regional metamorphism in the presence of water-rich fluids. East of the shear zone, marble appears to be an integral part of a metasedimentary package containing various gneisses, and quartzite, intruded by granitic to granodioritic plutons. This package has experienced complex deformation and prolonged high grade metamorphism with dominantly CO_2-rich conditions.

This evidence supports the regional thrust model of Hildebrand and Easton (1995) in which the high grade rocks of the Frontenac terrane were thrust over the low grade rocks of the Sharbot Lake terrane. However, the presence of two marble units indicates that marbles are present in the footwall as suggested by Davidson and Carmichael (1997) and the terrane boundary coincides with the Clayton Lake shear zone rather than the Maberly shear zone.

Acknowledgements

First, I want to thank George Skippen, my thesis supervisor for proposing such a fascinating project and then letting me see what direction it took me.

My thesis examining board provided very sound and thoughtful criticisms which served to improve the final manuscript. I would particularly like to thank Anthony Williams-Jones (McGill) for his exhortation to "enjoy the day" and Mike Easton (Ontario Geological Survey) for taking time out of his field season to participate.

My field assistants and the property owners of the Carleton Place area made my field seasons much easier. Sharon Carr generously provided accommodation at her retreat at Wolfe Lake during work in the Westport area.

Mike Jackson and Peter Jones were immense help in the creation of numerous thin sections and their subsequent analysis by electron microprobe. My fellow grad students, friends, and family patiently listened to me rave (or rant, depending on the day) about the intricacies of marbles and metamorphic petrology for hours on end.

Finally I am tremendously grateful for the encouragement, support, cheerleading, and even the nagging of my husband Steven. An amateur geologist-in-the-making, he ably assisted during weekend forays into my field area, spent hours with Mike cutting and polishing rocks and listening to me rattle on about my project. I could not have done it without him.

Table of Contents

List of Figures

List of Tables

List of Photos

Chapter 1 - Introduction

1.1 Introduction

The Carleton Place area of southeastern Ontario (figures 1.1, 1.3, and 1.4) is underlain by one of the best preserved and most easily accessible marble belts in North America. The area lies along a major terrane boundary within the Central Metasedimentary Belt of the Grenville Province. Previous work (see Easton, 1992, Davidson, 1998, Carr et al., 2000 and the references therein) in the area examined various aspects of the geology and its structural and tectonic history. However, the metamorphic history of the marbles and their relationship to the various gneissic and plutonic rocks was ambiguous. This study evolved out of a desire to address such questions as: do the siliceous marbles in the Carleton Place area have the same metamorphic history as the adjacent gneissic and plutonic rocks within the Wolf Grove Structure of the Frontenac terrane and how might the siliceous marbles and the gneissic rocks be linked to the tectonic framework proposed for this area (Wynne-Edwards, 1967; Hildebrand and Easton, 1995; Easton and Davidson, 1997). A key aspect of this study was how best to employ petrologic tools to answer tectonic questions such as those posed above.

1.2 Purpose of Research

This study has the following objectives:

1) Describe the mineralogy and petrography of marbles from the Sharbot Lake and Frontenac terrane in the Carleton Place area of southeastern Ontario.

2) Determine the pressure and temperature conditions of prograde metamorphism of gneisses and metaplutonic rocks associated with marbles, using the world-wide web based thermobarometry program WEBINVEQ (Gordon, 1998).

3) Calculate appropriate field gradients for the marbles, using the thermobarometric data from 2.

4) Derive polybaric T-X_{CO2} diagrams related to Grenville metamorphic conditions based on the field gradients calculated in 3.

5) Map and describe the mineral isograd distribution in marbles developed during metamorphism of the Sharbot Lake and Frontenac terranes.

6) Map and describe the trace of invariant points from the polybaric T-X_{CO2} diagrams within the Sharbot Lake and Frontenac terrane marbles.

7) Relate the variation in fluid composition within the marbles to the polybaric T-X_{CO2} diagrams calculated in 4.

8) Provide an overview of the metamorphic history (prograde, overprinting or retrograde events) of the rocks within the Carleton Place area.

9) Revise the tectonic model for the Sharbot Lake and Frontenac terrane boundary based on petrological and field evidence from marbles of the Carleton Place area.

1.3 Location and Regional Geology

The study area is located in southeastern Ontario, within the Central Metasedimentary Belt (CMB) of the Grenville Province (Wynne-Edwards, 1972; figure 1.1). Rocks of the Grenville Province are exposed from the coast of Labrador through the

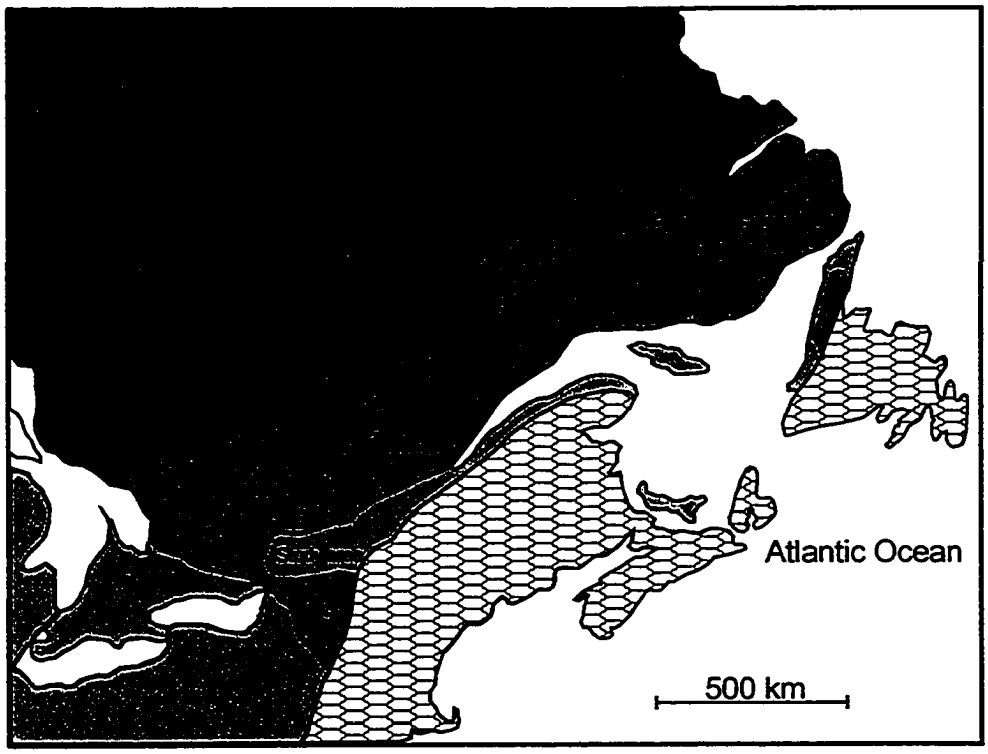

Paleozoic rocks

Appalachian Orogen

Grenville Province

Laurentian craton: includes the Southern, Superior, Churchill, Nain, and Makkovik provinces

Terrane boundary: subdivisions from Wynne-Edwards (1972)

CMB Central Metasedimentary Belt

CGT Central Granulite Terrain

Figure 1.1 Distribution of rocks of the Grenville Province within eastern Canada and their position relative to the Laurentian craton and the Appalachian Orogen. Terrane boundaries of the Grenville Province from Wynne-Edwards (1972). Study area is outlined in red. After Moore (1986).

southern portions of Quebec and southeastern Ontario to upper New York state. The Grenville province was first recognized as a structurally distinct entity from the predominantly supracrustal rocks of the Paleoproterozoic Southern and Archean Superior provinces by Wilson (1918, 1925) with the Grenville Province distinctly younger than the Archean foreland (Wynne-Edwards, 1972).

Wynne-Edwards (1972) established the Grenville Orogeny as a "major mountain-building episode" and proposed that the present exposed surface had originated from deep within the orogenic belt. He identified five distinct belts as shown in figure 1.1: the Central Granulite Terrain, Central Metasedimentary Belt, Central Gneiss Belt, Baie Comeau Segment, and the Eastern Grenville Province. The Grenville Tectonic Front forms the boundary between the Grenville Province and the Laurentian Craton.

Subsequent work by Rivers et al. (1989) resulted in the recognition of three first-order longitudinal belts within the Grenville Province (figure 1.2a). The Parautochthonous Belt has a distinctive pre-Grenvillian tectonometamorphic history and is characterized by a lithologic continuity with the Laurentian margin. The next two belts are composed of allochthonous material. The Allochthonous polycyclic belt shows evidence of having undergone major orogeny(-ies) prior to the Grenville orogenic events, in contrast to the Allochthonous monocyclic belt which appears to have been affected only by Grenvillian age metamorphic and deformational events.

Carr et al. (2000) further revised the tectonic subdivisions (figure 1.2b) of Rivers et al. (1989). The authors present three tectonic elements namely: pre-Grenvillian Laurentia and its margin which incorporates the Parautochthonous Belt and the

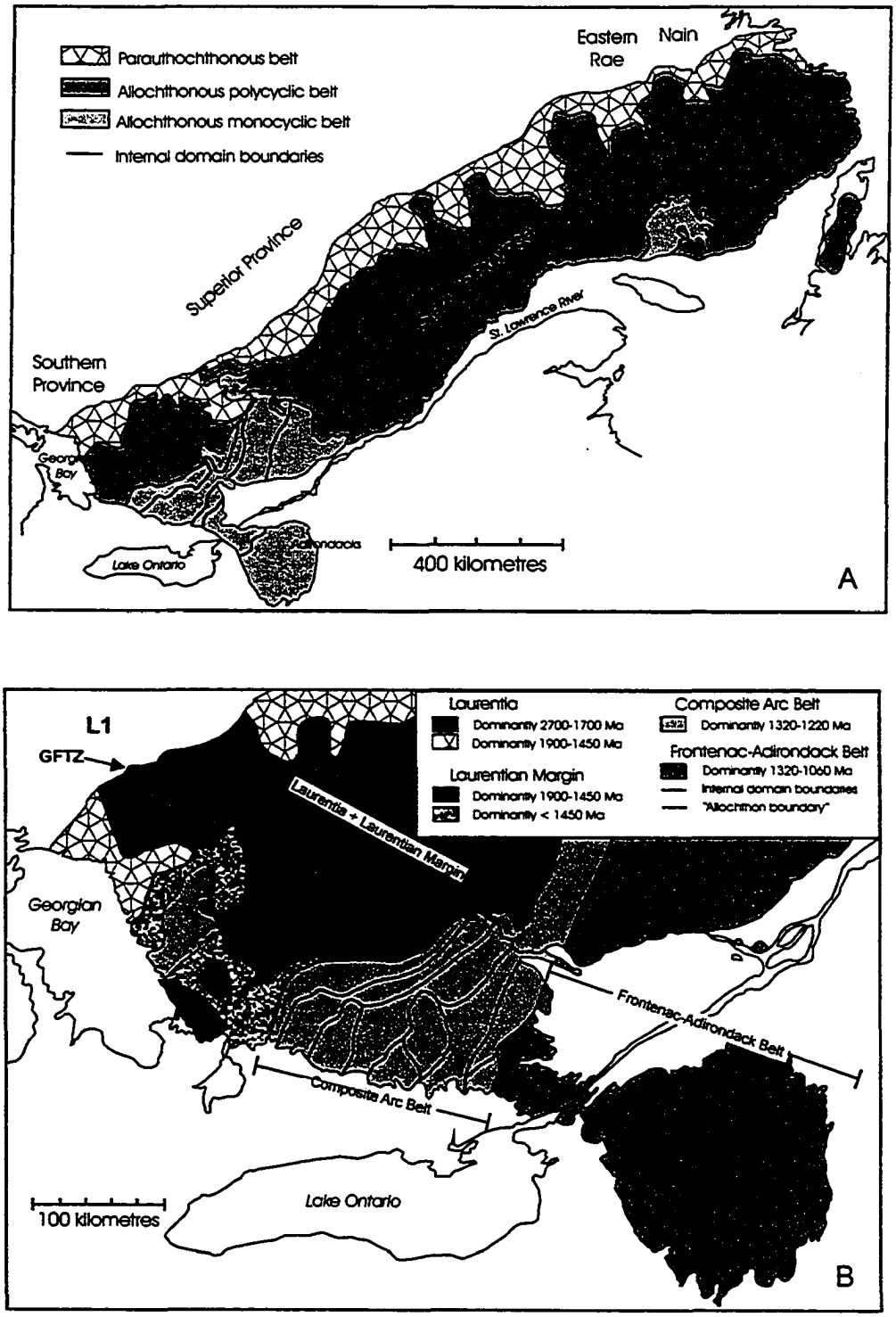

Figure 1.2 A) First-order tectonic subdivisions of the Grenville Province proposed by Rivers et al (1989). B) Positions of the internal terrane/domian boundaries within the CMB remain unchanged (Wynne-Edwards, 1972). After Carr et al., 2000.

Allochthonous polycyclic belt, the Composite Arc Belt which corresponds to the Allochthonous monocyclic belt, and the Frontenac-Adirondack Belt, formerly part of the Allochthonous monocyclic belt.

Currently, it is generally accepted that the Grenville Province formed as a result of a Himalayan-scale collision producing northwest-directed thrusting of a composite belt of continental and magmatic rocks onto the margin of the Laurentian craton (Easton, 1992; Carr et al., 2000; Percival et al., 2004). The Grenville orogeny encompasses a series of tectonic events grouped into two distinct age categories (Moore and Thompson, 1980), the Elzevirian Orogeny (~1.3-1.2 Ga) and the Ottawan Orogeny (~1.1-1.0 Ga.). The Elzevirian Orogeny is dominantly an accretionary stage involving folding, metamorphism and plutonism affecting the Grenville Supergroup (Davidson, 1998; Carr et al., 2000). The Ottawan Orogeny is defined by a period of sedimentation, folding and metamorphism (Moore and Thompson, 1980; Davidson, 1998; Carr et al., 2000). More recently events in the intermediate age range of 1.2-1.1 Ga have been identified (Davidson, 1998) including widespread magmatism, deformation and metamorphism (Easton, 1992, Davidson, 1998, Carr et al., 2000).

1.4 Central Metasedimentary Belt or Composite Arc Belt

Easton (1992) subdivided the CMB into five lithotectonic terranes (figure 1.3) based on lithological, geochronological, structural, and geophysical data. From the northwestern boundary of the CMB, these are the Bancroft, Elzevir, Mazinaw, Sharbot Lake and Frontenac terranes. Carr et al. (2000) employed the same terrane subdivisions

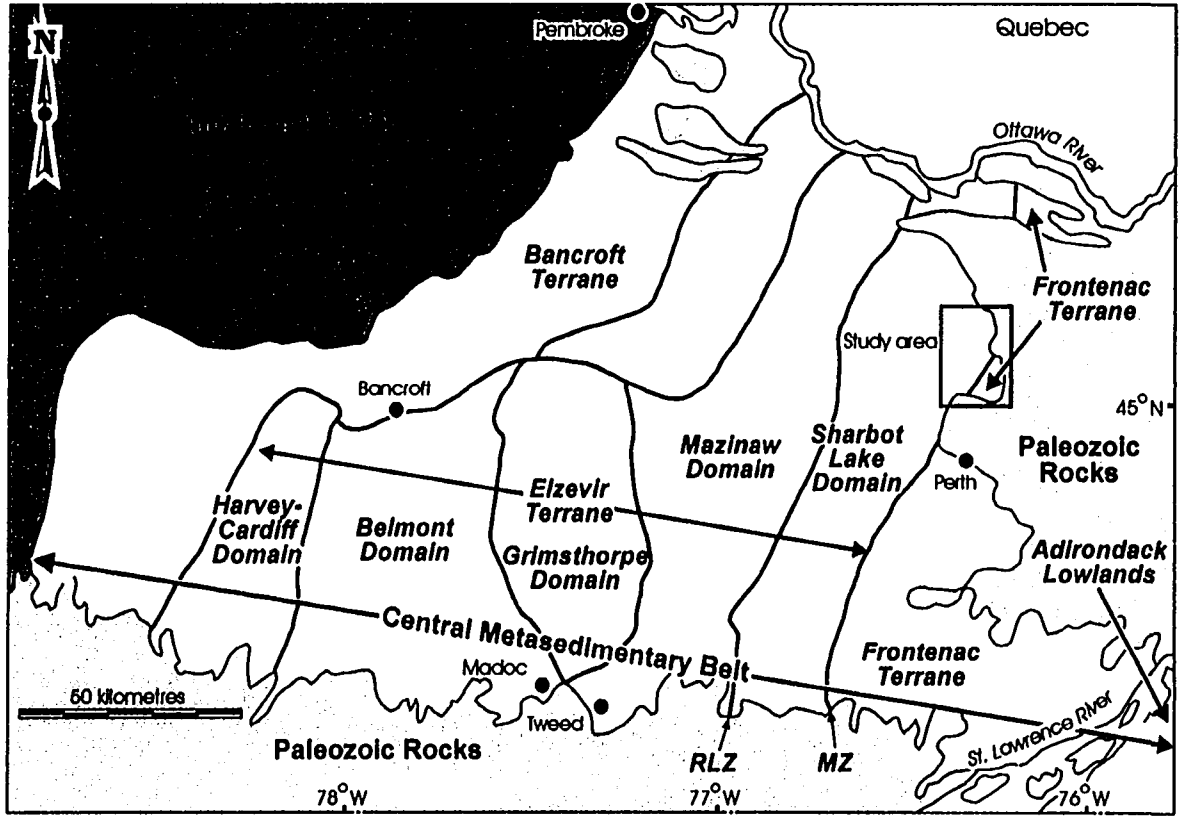

Figure 1.3 Terrane/domain subdivisions of the Central Metasedimentary Belt from Easton (1992). Study area is outlined in red.. RLZ = Robertson Lake shear zone. MZ = Maberly shear zone. (After Praamsma et al., 2000)

for the Composite Arc Belt grouping the Frontenac terrane with the Adirondack Lowlands into a separate belt. The present study area is located along the boundary between Sharbot Lake and Frontenac terranes to the south of Carleton Place (figure 1.4).

1.5 Tectonic settings of the Sharbot Lake and Frontenac terranes

The dominant rock types comprising the Sharbot Lake terrane are marbles interlayered with minor siliciclastic metasedimentary rocks. Deposition of the carbonate and clastic sediments occurred between ca. 1300-1250 Ma (Carr et al., 2000) and was coeval with the emplacement of mafic to felsic volcanic rocks. Plutonic rocks of the terrane include gabbro, granodiorite, monzonite, and granite of the Elzevir and Frontenac suites (Davidson and van Breemen, 2000). Age ranges for plutonism fall into two groups, namely ca. 1250-1220 Ma and ca. 1090-1060 Ma (Carr et al. 2000; Davidson and van Breemen, 2000). Overall metamorphic grade is greenschist- to lower amphibolite-facies (Easton, 1992). Metamorphism is largely syn-deformational but there is some evidence that metamorphism outlasted deformation.

The Sharbot Lake terrane is a lithologically and structurally distinct member of the Composite Arc Belt (Carr et al., 2000). The primary tectonic environments for this belt are interpreted to have been arcs, rifted arcs and possible continental fragments with associated carbonate and clastic sediments of the and related basins. These fragments formed and subsequently amalgamated offshore of Laurentia before tectonic juxtaposition against the Laurentian margin (Easton, 1992; Carr et al., 2000).

The Frontenac terrane is a distinct part of the Frontenac-Adirondack Belt (Carr et

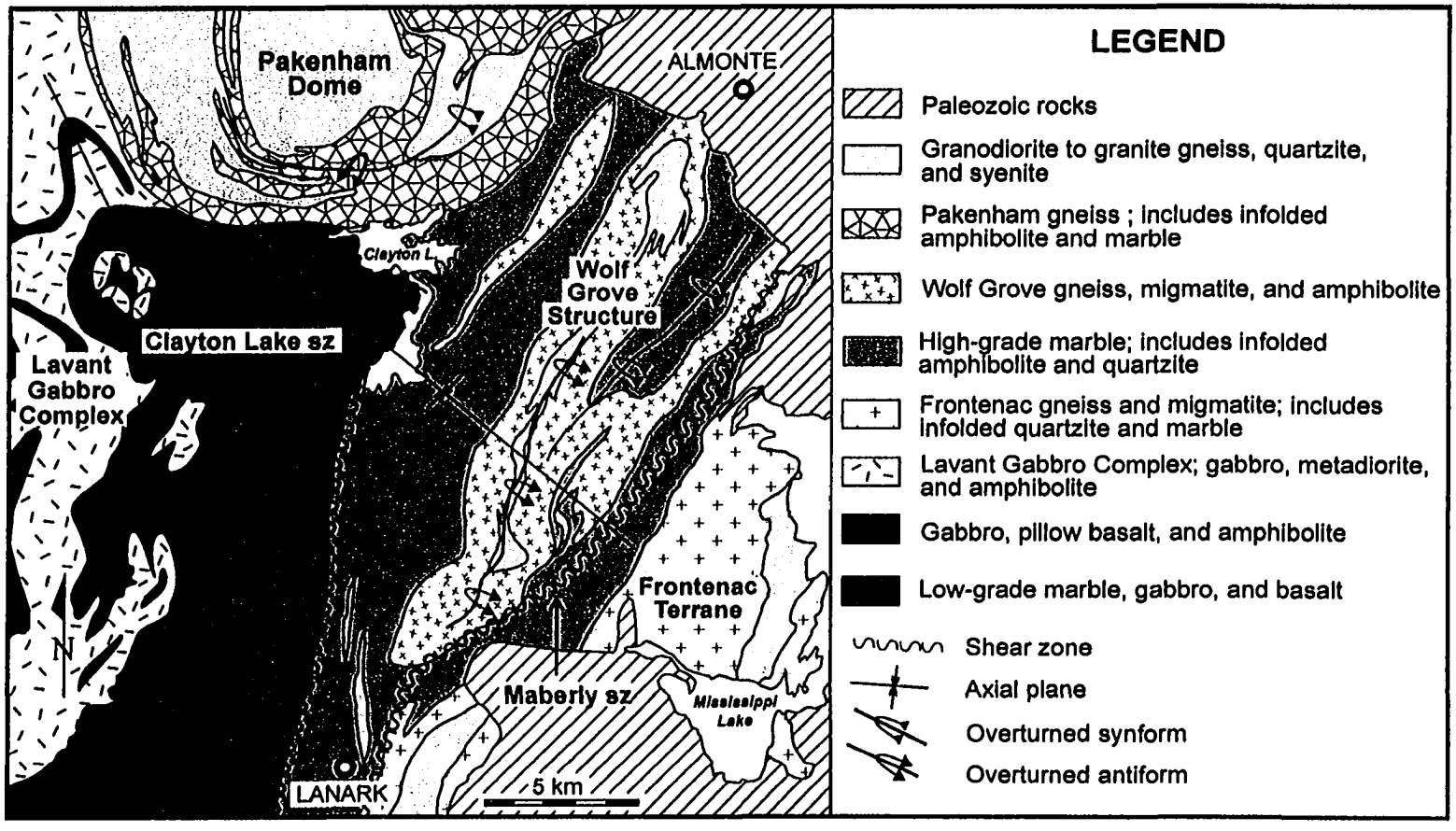

Figure 1.4 Simplified geological map of the Carleton Place area (modified from Reinhardt and Liberty, 1973). UTM coordinates of top left corner = 383000 5011000, bottom left corner = 383000 4985000; top right corner = 420000 5010000, bottom right corner = 420000 4984000.

al., 2000) which shares a common 1180-1140 Ma structural, metamorphic, and magmatic history. The Frontenac terrane consists of predominantly supracrustal rocks such as quartzofeldspathic gneiss, marble, and quartzite (Wynne-Edwards, 1967 a). Detrital zircons from quartzite indicate deposition of the platformal carbonate-clastic sedimentary sequence occurred after ca. 1300 Ma (Kinsman and Parrish, 1990). Basement of these rocks is unknown but based on Nd isotopic data it is unlikely to have been a thick crustal fragment (Marcantonio et al., 1990; McLelland et al., 1993). The Nd model ages suggest interaction between mantle-derived magmas and adjacent paragneiss, and derivation from a juvenile source terrane. Plutonism occurred between ca. 1180-1160 Ma and ca. 1090-1060 Ma (Carr et al., 2000; Davidson and van Breemen, 2000). Deformation appears to coincide with the earlier plutonic suite. At ca 1160 Ma the terrane was metamorphosed under low pressure granulite-facies conditions (Carr et al., 2000). The terrane had cooled below 500 °C by ca. 1110 Ma (Cosca et al., 1991). The juxatposition of the Sharbot Lake and Frontenac terranes along the Maberly shear zone had to have occurred by ca. 1160 Ma but may have taken place earlier (Davidson and van Breemen, 2000).

1.6 Sharbot Lake Terrane

Rocks of the Sharbot Lake terrane mainly consist of marble and mafic metavolcanics, with minor siliciclastic metasedimentary rocks, intruded by gabbros and granodiorite to granite plutons (Easton, 1992; Easton and Davidson, 1997; Davidson, 1998). Marbles of the terrane show considerable variation in texture, mineralogy and metamorphic grade. The marble consists of fine- to medium-grained calcitic to dolomitic

marble containing variable amounts of phlogopite, talc, tremolite, potassium feldspar, apatite, chondrodite, pyrite, and garnet. Small, positively weathering pods of white pegmatite outcrop locally within the marble.

Mafic metavolcanic rocks occur locally along the margins of, or as rafts within the Lavant gabbro complex (figure 1.4), the Dalhousie amphibolite complex and the Mountain Grove gabbro (Easton and Davidson, 1997). Thin selvaged pillows, beds of tuff breccia, lapilli tuff and variably bedded metatuffs are also present. Geochemical data (Wolff, 1982; Easton, 1988 a) suggest that the mafic metavolcanic rocks within the Sharbot Lake terrane formed in an oceanic environment as either ocean-floor basalts or island-arc tholeiites.

The Lavant Gabbro Complex is a composite intrusion (Easton, 1992; Easton and Davidson, 1997), approximately 50 km long and 15 km wide, which outcrops along the western edge of the Carleton Place map sheet and forms part of the Elzevir suite of plutons within the Sharbot Lake terrane (Davidson, 1998). The complex is dominated by medium-grained gabbro to diorite, locally retaining igneous layering and cross-cutting relationships between compositionally distinct phases. A slightly younger granodiorite to monzogranite suite forms small intrusive bodies and dykes cutting the gabbro.

The metamorphic grade of the complex is variable and ranges from upper greenschist to lower amphibolite facies. The complex does not have an extensive metamorphic aureole but it has caused local mineralization in the surrounding marbles. Inclusions and roof pendants of all the country rocks are present within the complex (Easton, 1988 b; Pauk, 1989 b).

The Pakenham structure (figure 1.4) forms a broad dome of ovoid shape (map view) in the northern portion of the Sharbot Lake terrane. It consists of a number of sill-like appendages of foliated granodiorite and gneiss with screens of marble and migmatitic gneiss (Reinhardt and Liberty, 1973). The Wolf Grove Structure (figure 1.4) is an elongate package which contains a variety of gneisses, amphibolite, and quartzite. Fabric of the gneissic rocks is cross-cut by the foliated Wolf Grove granodiorite and granite. Migmatitc rocks are common and leucosome roughly parallels the foliation and cross-cuts it (Reinhardt and Liberty, 1973; Easton and Hildebrand, 1994). Textural observations and the presence of relict high grade parageneses within gneisses of the Wolf Grove Structure suggest an earlier high-temperature metamorphic event (see chapters 2,3, and 6). Rocks from both the Wolf Grove and Pakenham structures display refolded folds and possibly record at least three folding episodes (Easton and Hildebrand, 1994).

Reinhardt and Liberty (1973) suggested the rocks of the Pakenham Dome and the Wolf Grove Structure were correlative of Frontenac terrane rocks in the Perth or Westport areas. Moore (1992) assigned the two gneissic bodies to the Sharbot Lake terrane. This terrane assignment was questioned by Easton (1992) and Hildebrand and Easton (1995). Hildebrand and Easton (1995) placed the two structures within the Frontenac terrane on the basis of a shared metamorphic and deformational history, although they are regarded as atypical of Frontenac terrane gneisses which are typically more pelitic (Easton, 1992, Corfu and Easton, 1997).

Basement to the Sharbot Lake terrane is unknown; however, Hildebrand and Easton (1995) have suggested that the Pakenham and Wolf Grove Structures may

represent basement to the terrane and are exposed through structural windows.

Two shear zones have been identified in the Carleton Place area. The first, previously unnamed shear zone (Easton and Hildebrand, 1994), is contained within marbles and is recognizable by a zone of intense deformation and marble breccia. It appears to be a steep, northwest-southeast-trending, ductile fault which may be related to the Maberly shear zone. The breccia is similar to that exposed along the Maberly shear zone (figure 1.4). Rocks on either side of the shear zone do not preserve the same metamorphic grade or degree of deformation. Evidence for this is explored in detail in chapters 5 and 6. This shear zone is hereafter referred to as the Clayton Lake shear zone, based on its exposure along the western shore of Clayton Lake.

The Maberly Shear Zone, mapped by Easton (1988 a), is defined as the Sharbot Lake-Frontenac terrane boundary (Wolff, 1985; Easton 1988 a; Davidson and Ketchum, 1993). The shear zone appears to be a moderately to steeply dipping reverse fault that juxtaposes granulite facies gneisses of the Frontenac terrane against amphibolite facies marble of the Sharbot Lake terrane (Easton and Davidson, 1997). In the Carleton Place area, the boundary between the two terranes is complex and possibly represents a basement-cover sequence that has been repeated by folding and stacking along the Maberly shear zone (Easton and Hildebrand, 1994). Hildebrand and Easton (1995) suggested the shear zone represents a regional-scale thrust fault interpreted as a "fundamental suture" which places hot, "pluton- riddled" metamorphic rocks over "cool, platformal marbles". Movement on the fault is constrained by the youngest of the transported plutons (1163 ± 3 Ma; van Breemen and Davidson, 1988) and is older than a

set of northwest trending diabase dykes (Kingston dykes) which cut the proposed thrust yet are unmetamorphosed (Easton and Davidson, 1994 a). The dykes were dated at ca.1160 Ma using U-Pb ratios from baddeleyite (Hildebrand and Easton, 1995). Locally, the shear zone is cut by syn- to post-tectonic granitic intrusions.

The predominant metamorphic grade within the Sharbot Lake terrane is lower amphibolite facies with grade appearing to increase towards the southeastern boundary of the terrane. The age of regional metamorphism is unknown but the terrane appears to have been unaffected by the high-grade metamorphism at ca. 1168 Ma which characterizes the Frontenac terrane (Corfu and Easton, 1997) and does not appear to record the deformation and ca. 1.03 Ga metamorphism of the Flinton Group of the Elzevir terrane (Davidson, 1998).

1.7 Frontenac Terrane:

The Frontenac terrane consists of a succession of multiply deformed, relatively low-pressure granulite facies quartzofeldspathic and pelitic gneiss, quartzite and marble intruded by various plutonic rocks (Wynne-Edwards, 1967 a; Carmichael et al., 1978; Easton, 1992; Hildebrand and Easton, 1995; Easton and Davidson, 1997). Wynne-Edwards (1967 a) proposed a hypothetical stratigraphy consisting of "two stacked sets of tripartite units composed of from bottom to top, gneiss, quartzite and marble" (Hildebrand and Easton, 1995).

The gneissic units contain a variety of paragneisses which are dominantly pelitic or quartzofeldspathic in composition associated with granulite, amphibolite and thin

layers of quartzite. The gneiss/granulite unit is overlain by quartzite and minor arkose with sparse feldspar granulestone (Wynne-Edwards, 1967 a). Hildebrand and Easton (1995) interpreted the relationship as unconformable cover on the gneisses. The main gneiss unit (Wynne-Edwards, 1967 a), above the major marble unit, is difficult to distinguish from the lower gneiss unit; division is made primarily based on structural interpretation of the field relations versus lithological differences between the units (Wynne-Edwards, 1967 a; Easton, 1992).

Marble is a regionally extensive unit within the Frontenac terrane. It has been interpreted as part of the metasedimentary sequence overlying the quartzite (Wynne-Edwards, 1967 a) or as structurally underlying the gneiss, quartzite and Frontenac suite plutonic rocks along a thrust fault (Hildebrand and Easton, 1995). The marble/gneiss contact is marked in places by a distinctive zone of marble breccia (Hildebrand and Easton, 1995; Easton and Davidson, 1997).

The major marble unit (Wynne-Edwards, 1967 a) consists of medium- to coarse-grained calcitic to dolomitic marble containing variable amounts of graphite, phlogopite, diopside, sepentine, scapolite, apatite, pyrite, and tourmaline that define a faint layering (Easton, 1992; Hildebrand and Easton, 1995). Disrupted layers and blocks of pyroxenite, rusty paragneiss and calc-silicate gneiss are also locally found within the marble. White granite and pegmatite is commonly present within the marble (Wynne-Edwards, 1967 a).

An upper marble and quartzite unit (Wynne-Edwards, 1967 a; 1967 b) is present in the eastern part of the Frontenac terrane. It consists of calcitic and minor dolomitic marble, quartzite and garnet-sillimanite gneiss, and a "quartzite-limestone" transition

rock which is comprised of centimetre-scale interlayered bands of quartzite and marble (Wynne-Edwards, 1967 a; Easton, 1992).

There is limited evidence that older basement underlies the supracrustal sequence of the Frontenac terrane. Nd model ages from Frontenac paragneisses (Marcantonio et al., 1990) are all in the 2045-1560 Ma range indicating derivation from a Paleoproterozoic crustal source (Easton, 1992). The reported juvenile ca. 1300-1400 Ma Nd model ages from Frontenac and Adirondack plutonic rocks (Marcantonio et al., 1990; Daly and McLelland, 1990; McLelland et al., 1993) are contradictory to the suggestion of a thick, older continental fragment serving as Frontenac basement. However, the geochemical data of Shieh, (1985) and Marcantonio et al. (1990) suggest juvenile mafic magma may have been underplating the terrane and been involved in plutonic petrogenesis. Detrital zircons from Frontenac quartzites indicate deposition after ca. 1300 Ma with source rocks of mainly ca. 1900-1700 Ma (Kinsman, 1990; Kinsman and Parrish, 1990).

The Frontenac terrane is intruded by a number of plutons. Wynne-Edwards (1965) identified Frontenac-type plutonic rocks in both the Sharbot Lake and Frontenac terranes. The Frontenac suite of plutons consists of slightly alkaline, synmetamorphic and syndeformational to late deformational intrusions including noritic gabbro, anorthosite, monzodiorite, pyroxene monzonite, quartz syenite and leucogranite (Easton, 1992; Easton and Davidson, 1997; Davidson, 1998). All the plutons are chemically distinct from the older calc-alkaline Elzevir suite (Davidson, 1998) of the Sharbot Lake terrane and plot as I-type granites with within-plate affinity (Marcantonio et al., 1990;

Lumbers et al., 1990). Metavolcanic rocks and Elzevir suite plutons (ca. 1270 and ca. 1225 Ma) are absent from the terrane (Easton and Davidson, 1997; Davidson, 1998). The Skootamatta suite of plutons (Easton, 1992; Easton and Davidson, 1997) is not found south of the Rideau-Canoe Lake Fault in the Frontenac terrane. The suite consists of alkaline gabbro, monzonite, syenite, and leucogranite stocks.

The Frontenac terrane has had a complex structural history as summarized by Wynne-Edwards (1963, 1967 a). At least two major periods of folding have occurred in the area resulting in a complex interference pattern. Carmichael et al. (1987) suggested that early thrusts might be present in the metasedimentary sequence. Easton and Ford (1991) noted that the structural history of the Mazinaw and Frontenac terranes and the Adirondack Lowlands are similar and all these areas have been affected by early thrust faults. Extensional mylonite zones occur throughout the terrane (Easton, 1992).

The Frontenac terrane appears to have experienced regional metamorphism under amphibolite to granulite conditions. The common occurrence of rocks bearing garnet-cordierite and orthopyroxene-cordierite assemblages indicates metamorphism at 700 °C and ~5 kbars (Hildebrand and Easton, 1995). The occurrence of the assemblage sillimanite-orthopyroxene-potassium feldspar-melt indicates pressures were locally above 7 kbars (Lonker, 1980; Carmichael et al., 1987). At several locations within the Frontenac terrane, there is evidence of an overprinting amphibolite-facies event (Carmichael, 1978; Lonker, 1980; Easton and Hildebrand, 1994).

Chapter 2 - Mineralogy and Petrography of Siliceous Marbles

2.1 Introduction

Mapping by Reinhardt and Liberty (1973) placed marble in the Carleton Place area in a single unit. These authors delineated an irregular zone of marble containing coarse tremolite in the center of the map area between Clayton Lake and Lanark (figure 2.1). They concluded that the marble was part of an interlayered metasedimentary sequence comprising the Grenville Supergroup. However, these same authors also noted that the rocks are divisible into two major lithological groupings along a line extending from Clayton Lake to the region just west of Lanark. Rocks to the west are composed of marbles, mafic igneous rocks and amphibolites, whereas the eastern grouping is composed of marble in association with quartzite and metasedimentary gneisses intruded by felsic to intermediate plutonic rocks. This grouping is comparable to rocks found in the Perth and Westport map area (Wynne-Edwards, 1967 a and 1967 b). The boundary between these groupings corresponds to the shear zone originally mapped by Easton and Hildebrand (1994) and referred to as the Clayton Lake shear zone in this study.

Ewert (1977) divided marble in the field area into four textural assemblages and used coexisting mineral assemblages to outline areas of varying metamorphic grade. He mapped five isograds, one of which represents the trace of an isobaric invariant point involving the minerals; calcite, dolomite, quartz, tremolite and diopside. The isograds are oblique to the Wolf Grove Structure. Ewert concluded that the overall metamorphic grade is low (i.e. greenschist to lower amphibolite facies) and appeared to be related to

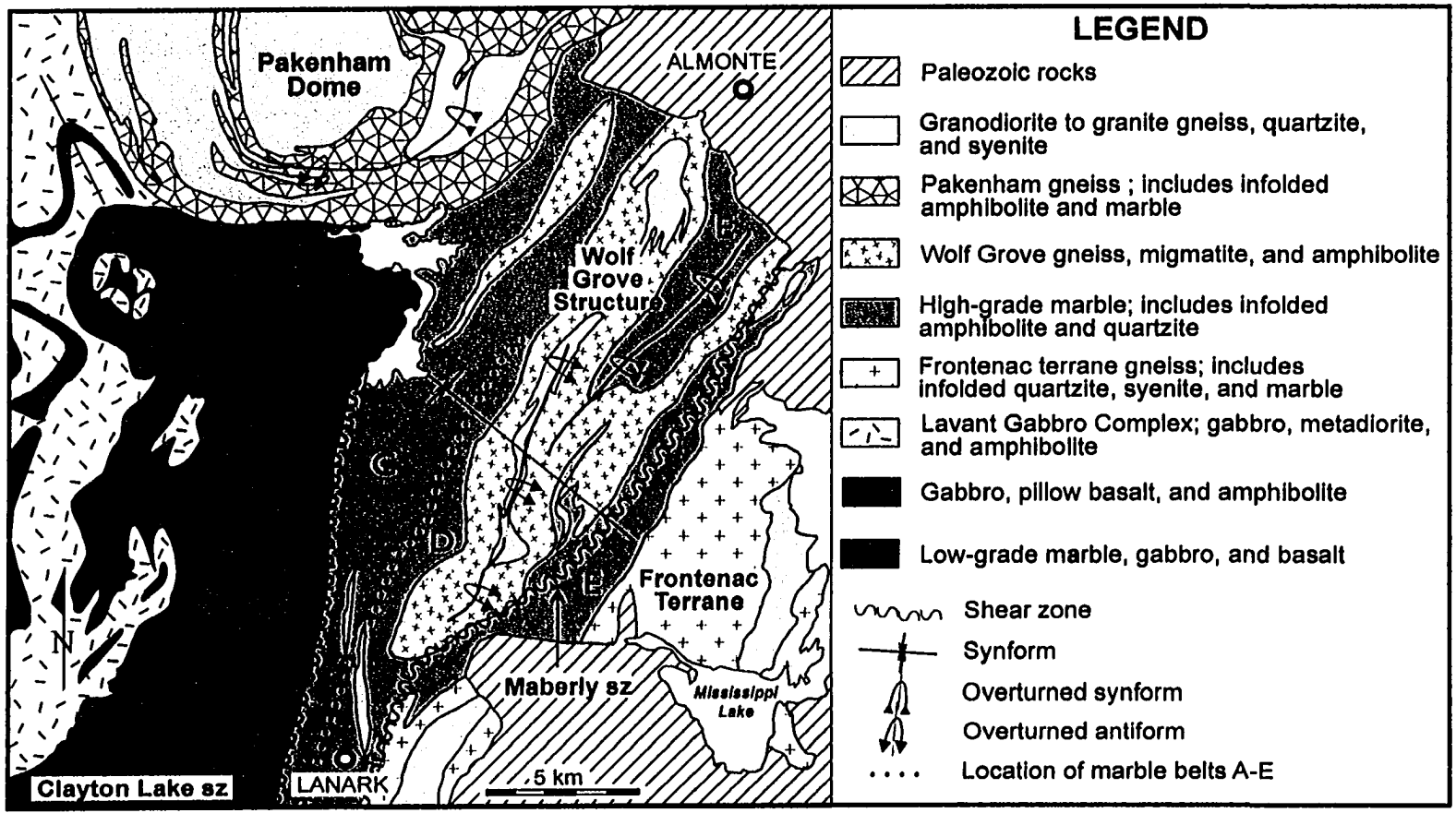

Figure 2.1 Simplified geological map of the Carleton Place area showing the location of the five major marble assemblages described by Easton and Hildebrand (1994) and Easton (1995). (After Easton, 1995; geology modified from Reinhardt and Liberty, 1973)

plutonic igneous activity along the western, northern, and eastern margins of the map area (figure 6.4). He also indicated that petrographic evidence suggested normal prograde metamorphic conditions within the carbonates.

Abercrombie (1983) collected samples of siliceous marble within the Carleton Place area in order to study the partitioning of fluorine between tremolite, talc and phlogopite. He concluded that with increasing F content the stabilities of assemblages containing tremolite, talc or phlogopite are enhanced. His calculations indicated that with increased F content, the upper stability limit of calcite-talc assemblages entered the sillimanite field over a restricted range of pressures, partially explaining the presence of prograde talc within the sillimanite zone of the CMB.

Kornik (1986) proposed a steep temperature gradient based on the proximity of the isograds mapped by Ewert (1977). Significant variation in the deformation and apparent metamorphic grade of the marbles within the area indicated a possible structural discontinuity. He suggested that these differences could be explained by polymetamorphism and/or the existence of two marble units. The hypothesis that two marble units are present in the Carleton Place area is compatible with the interpretation of Wynne-Edwards (1967 a); he concluded that there were at least two major marble units within the Westport area, which are in contact at Morton.

Marble of the Carleton Place area was subdivided into 5 major marble belts by Easton and Hildebrand (1994) and Easton (1995). Assemblages A, B, and C (figure 2.1) are characterized by fine- to medium-grained layered calcite and dolomite marbles which may contain tremolite. Assemblage A is intruded by the Lavant Gabbro Complex.

Assemblages B and C locally contain gabbroic sills, pillowed basalts and minor amphibolite. The Clayton Lake shear zone separates assemblages B and C. Assemblages A, B, and C were previously assigned to the Sharbot Lake terrane (Easton and Hildebrand, 1994). Assemblages D and E (figure 2.1) consist of massive to layered coarse-grained, graphitic, calcite and dolomite marble intruded by pink pegmatite and amphibolite. Lenses of rusty schist and quartzite are common in assemblage E. Assemblage E is transected by the Maberly shear zone and lies partly within the Frontenac terrane (Easton, 1988).

2.2 Field Description of Marble

Marble in the Carleton place area was mapped to determine the coexisting mineral assemblages, clarify the variation in metamorphic grade, the degree of deformation, and the relationship of marble to other rocks units within the field area. The Clayton Lake shear zone divides the area into two broad zones (Reinhardt and Liberty, 1973). The western half of the map area is referred to as the Lavant Gabbro block, as the Lavant Gabbro Complex forms the western margin of this section. The eastern portion of the area is referred to as the Wolf Grove block based on the presence of the Wolf Grove Structure within the marbles.

2.2.1 Marble of the Lavant Block

Marble, west of the Clayton Lake shear zone, is characterized by thick sequences of relatively pure calcite and calcite-dolomite marble (photo 2.1a) interlayered with

Photo 2.1 A) Relatively pure, massive calcite marble (UTM coordinates 869 924) exposed along Highway 511 in the Lavant Gabbro Block. Outcrop is approximately 2 m across.

B) Greyish black weathering surface of layered calcite marble from west of the Clayton Lake shear zone (UTM coordinates 932 014). Tremolite-rich layers are easily distinguished on the weathered surface and contain tremolite crystals up to 8 cm long. Similar textures are also present in marble of the Wolf Grove Block. Hammer is 40 cm long and hammer head is 13 cm across.

All 6 figure UTM locations are from the Carleton Place map sheet 31 F/1 (1994), zone 18T, NAD 83. The 6-figure coordinates are found by dropping the first digit and the last two digits for the easting and the first two digits and the last two digits from the northing. For example, the full UTM reference for 869 924 from photo 2.1 A would read as 386900 (easting) 4992400 (northing). The 6-figure grid references are considered accurate to the nearest 100m. When 7 figures are quoted, the grid references is accurate to the nearest 50m.

A

B

siliceous calcite marble with layers of tremolite or talc and tremolite (photo 2.1b). Grain size is dominantly fine- to medium-grained, although very coarse-grained patches may occur locally. The fresh surface is white to blue-gray and the weathered surface is typically buff to black. Dolomite-rich layers tend to have a higher weathering profile than the calcite-rich layers.

Marble of the western block of the Carleton Place map area is typically massive to moderately foliated. The foliation is expressed as an alternation of light and dark bands a few centimetres in width. Tremolite is frequently concentrated along the foliation surfaces. The occurrence of foliation increases within the marble as the Clayton Lake shear zone is approached. Outcrop-scale tight to isoclinal folds are common within a two kilometer-wide zone immediately west of the shear zone.

The most common mineral assemblage contains calcite, dolomite, quartz, tremolite ± phlogopite or potassium feldspar. Phlogopite is the primary mica. However, talc is found in a few regions: in the northwestern corner of the map sheet near the Tatlock Quarry area, along the western edge of Clayton Lake and in the southern portion of the map area west of Lanark, extending in narrow zone to Dalhousie Lake. Other minerals present include diopside, forsterite (replaced by sepentine), chondrodite, apatite, and pyrite.

Marbles from the western block have been intruded by gabbroic (photo 2.2a) and dioritic phases (photo 2.2b) of the Lavant Gabbro Complex along an irregular contact. The gabbro is fine-grained along the contact with marble and locally contains garnet (photo 2.2c). The marble is medium- to coarse-grained and may contain diopside or

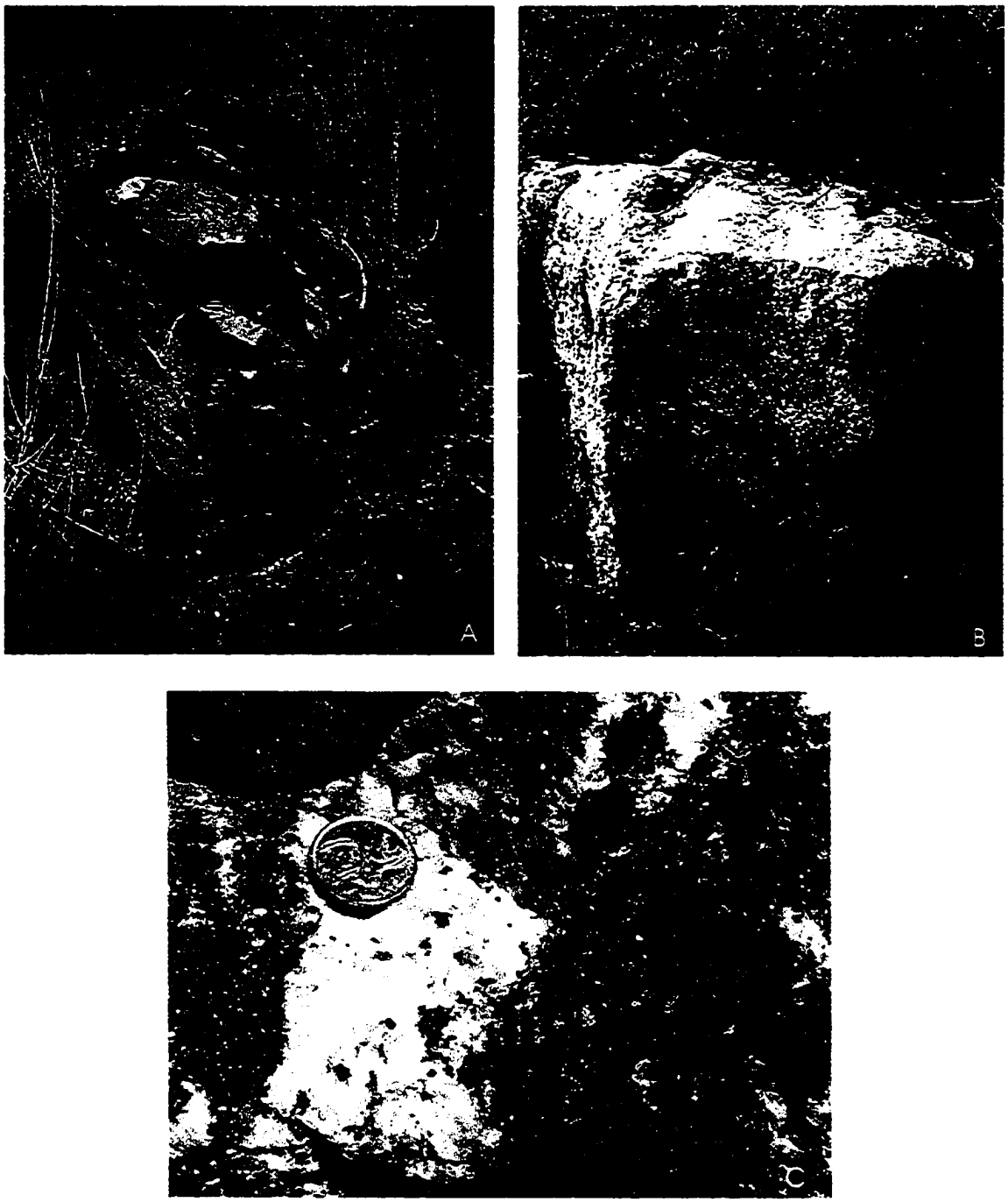

Photo 2.2 A) Fine-grained gabbro of the Lavant Gabbro Complex exposed along Highway 511 (UTM coordinates 894 894) in the western block of the study area.
B) Medium-grained metadiorite of the Lavant Gabbro Complex (UTM coordinates 836 025). This unit is locally pegmatitic.
C) Close-up of a gabbro-marble contact (UTM coordinates 832 966). Marble has been re-crystallized. Grain size in gabbro increases as contact is approached and locally contains garnet up to 20% as seen in this photo.

serpentinized forsterite near the contact.

Dolomitic marbles tend to be concentrated along the eastern margin of the zone west of the Clayton Lake shear zone. These marbles commonly contain fine-grained metavolcanics (photo 2.3a) and pillowed basalts (photo 2.3b). The marble is fine-grained and grey to buff on the fresh surface. Foliation within the dolomitic marbles is easily distinguishable on the weathered surface and has been folded. The metavolcanics have been boudinaged and appear flattened parallel to layering.

2.2.2 Marble Breccia

A zone of marble breccia separates the Lavant Gabbro and Wolf Grove blocks of marble and corresponds to the trend of the Clayton Lake shear zone (figure 2.2). The marble breccia consists of medium- to coarse-grained white or grey marble containing variably sized (1-2 cm up to 10+ cm across), sub-angular to rounded blocks of fine- to medium grained marble (photos 2.4a, b, and c). Some blocks within the breccia are more resistant to weathering than the surrounding matrix. A similar zone of marble breccia is associated with the Maberly shear zone (Easton and Davidson, 1997) and is exposed east of the Wolf Grove Structure. Breccia associated with the Maberly shear zone also contains blocks of migmatite and rusty gneiss.

2.2.3 Marble of the Wolf Grove Block

Marble of the Wolf Grove block is characterized by medium- to coarse-grained calcite and dolomite marble which is typically banded (photo 2.5a) but may be massive.

Photo 2.3 A) Boudinaged, aphanitic to fine-grained metavolcanics within dolomitic marble (UTM coordinates 896 895). Marble is medium-grained and contains ~10-20% tremolite.

Photo 2.3 B) Pillow basalt exposed along Herron Mills Road, west of the Clayton Lake shear zone (UTM coordinates 903 924).

Photo 2.4 A) Marble breccia exposed along Galbraith Road (UTM coordinates 914 034) southwest of Clayton Lake. Matrix is fine-to medium-grained grey marble conaining sub-angular blocks of coarse white calcite marble. Clasts are moderately aligned in the foliation. Hammer is 40 cm long and hammer head is 13 cm across.

B) Marble breccia containing sub-rounded clasts of marble (UTM coordinates 933 0135). Breccia clasts are more resistant to weathering than the matrix. Hammer is 40 cm long and hammer head is 13 cm across.

C) Close-up of marble breccia (UTM coordinates 931 012) containing clasts similar to A. Clasts are moderately aligned in the foliation. Brunton compass is aligned along strike.

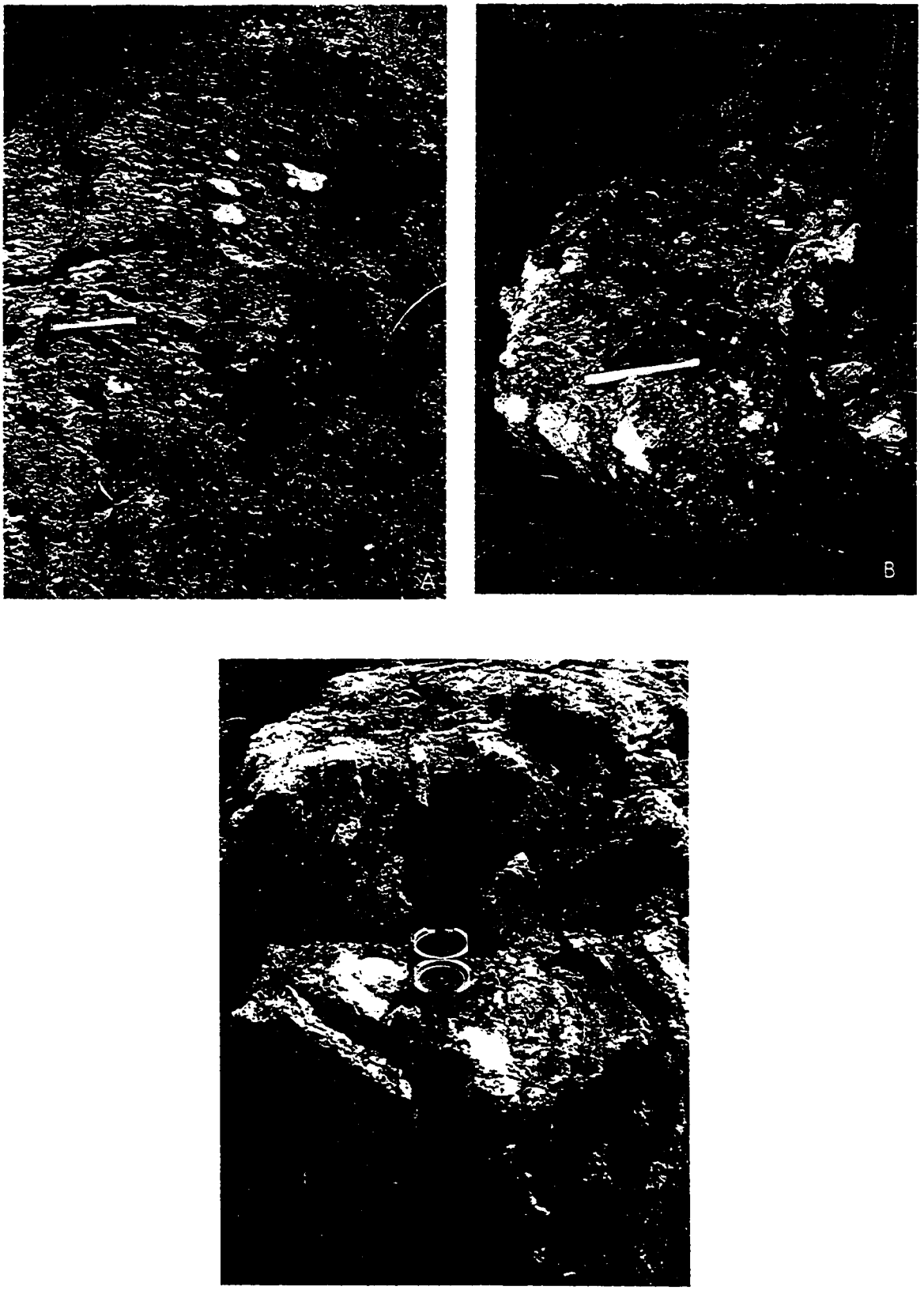

Photo 2.5 A) Typical grey and white banded marble of the Wolf Grove Block of the Carleton Place area (UTM coordinates 940 965) Darker layers contain finely disseminated graphite. Hammer is 40 cm long.

B) Outcrop-scale isoclinal folding of banded marble. Hammer is 25 cm long.

C) Greyish black weathered surface on pavement outcrop of coarse-grained calcite marble exposed along Forest Road (UTM coordinates 025 971). Hammer is 40 cm long.

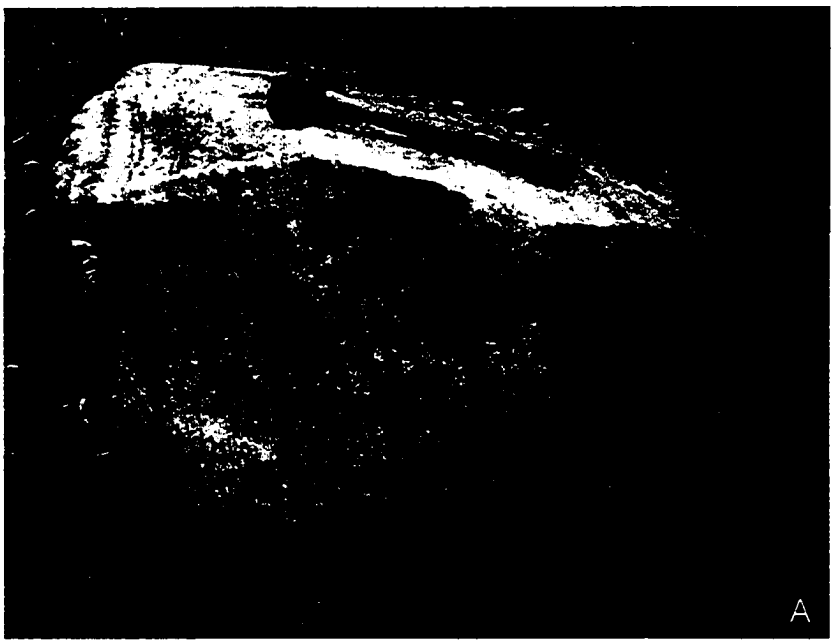

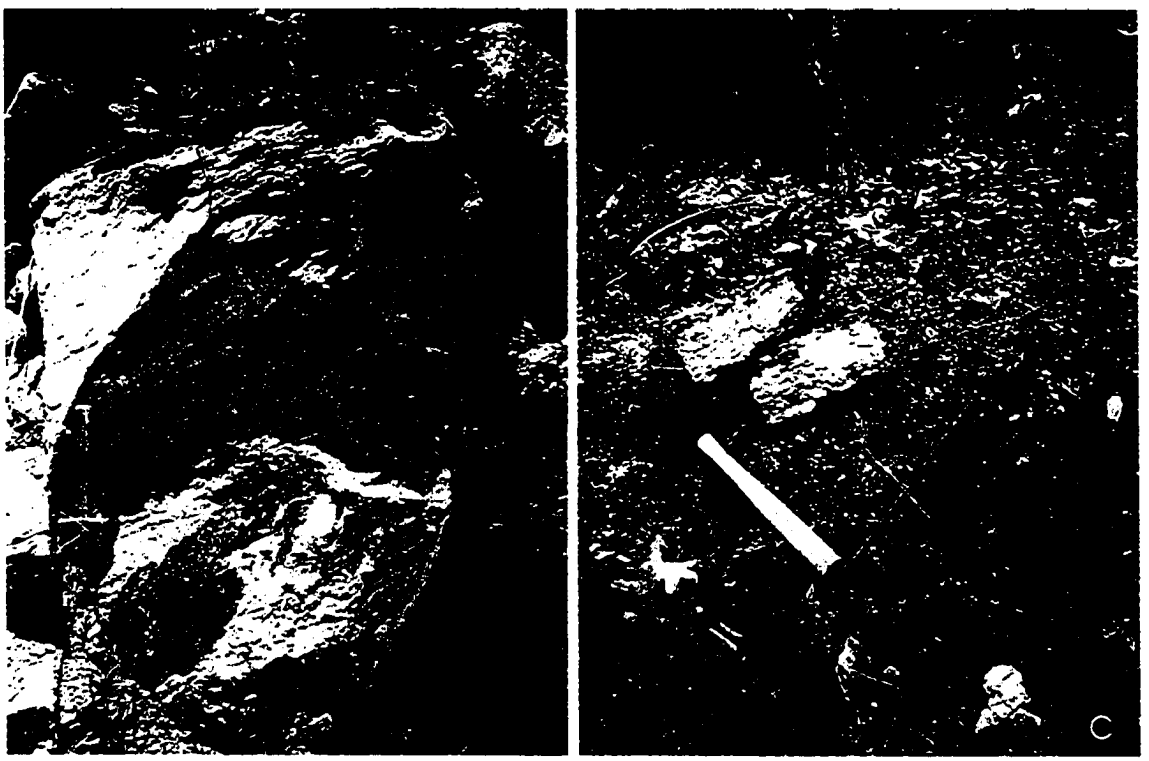

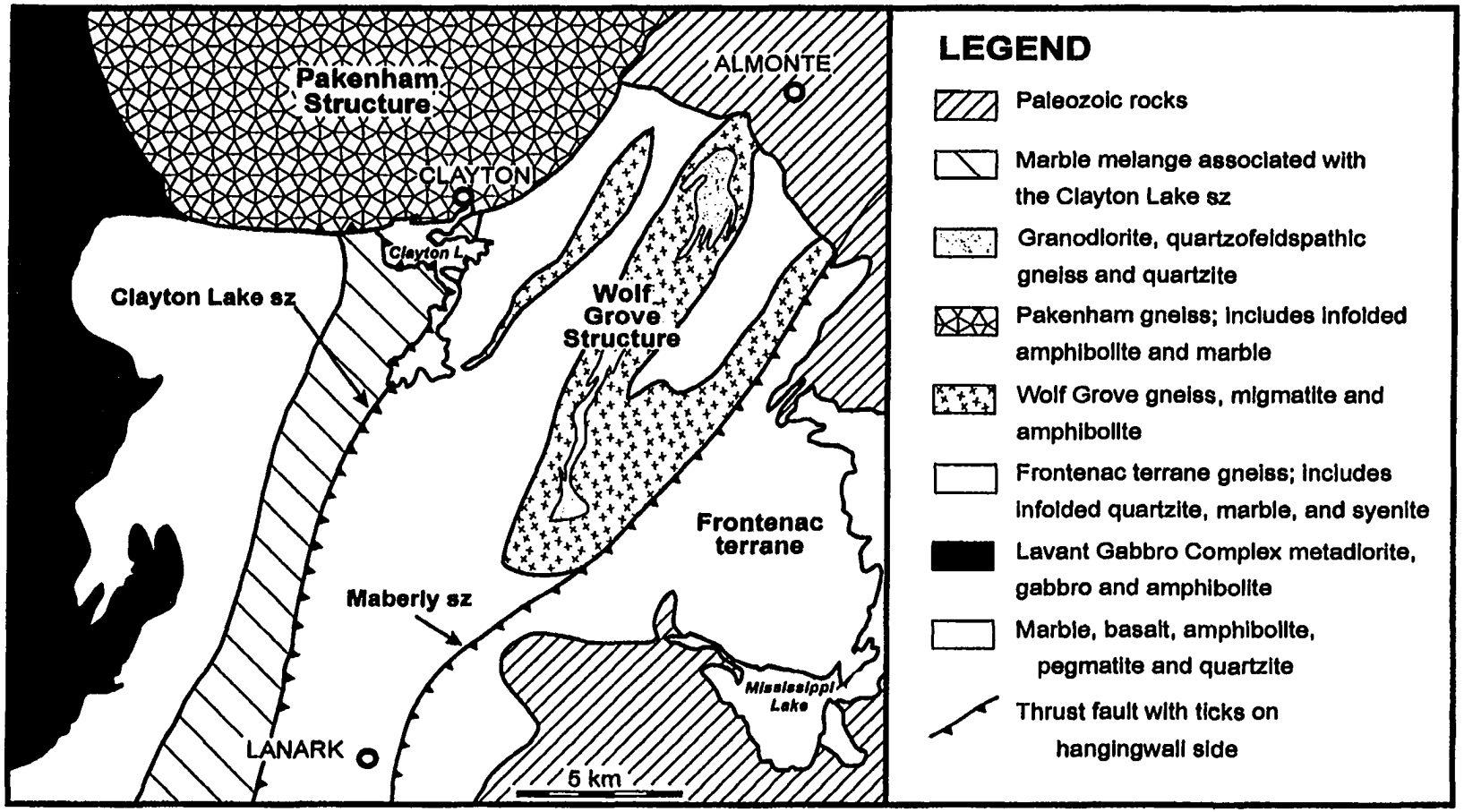

Figure 2.2 Simplified geological map showing the positions of the Clayton Lake and Maberly shear zones and the location of the marble breccia zone associated with the CLSZ. (Modified from Reinhardt and Liberty, 1973)

Banding is defined by alternating layers of white and blue-grey marble of varying widths (1-2 cm-5 cm spacing) and is commonly folded (photo 2.5b). Graphite is commonly concentrated in the darker bands. The weathered surface is typically dark gray to black (photo 2.5c).

The dominant mineral assemblage is calcite, dolomite, quartz, phlogopite, and tremolite. Diopside and forsterite may also be present. Accessory minerals include zircon, tourmaline, garnet, apatite, chalcopyrite or pyrite. Graphite and phlogopite are very coarse-grained locally.

Marble, east of the Clayton Lake shear zone is in contact with a variety of rock types. Rusty quartzofeldspathic-biotite and quartzite occur as pods and discontinuous layers within marble on the east side of the Wolf Grove Structure and the Maberly shear zone. Marble-amphibolite contacts are interlayered, sharp (photos 2.6a and b) or irregular with small blocks of amphibolite within the marble (photo 2.6c). On the west side of the Wolf Grove Structure, elongated ridges of Lanark granodiorite outcrop within the recessively weathered marble.

At least two generations of mafic dykes are present in the marble. Dimensions of both types of dykes vary considerably but most range between 15 cm and 2 m in width. Fine-grained, rusty weathered, metamorphosed mafic dykes (photo 2.7a) appear to follow the dominant foliation in the marbles and have been locally folded with the carbonate rocks. Unmetamorphosed, very fine-grained mafic dykes (photo 2.7b) cross-cut foliation in the marbles. Possible contact metamorphism has been partially obscured due to recrystallization of the marble. However, the orange colour of the marble and presence of

Photo 2.6 A) Sharp contact bewteen coarse-grained white marble and amphibolite from Tatlock Road (County Road 9; UTM coordinates 027 9715), near intersection with Forest Road. Outcrop is approximately 3 m high.

B) Interlayered contact between marble and amphibolite (UTM coordinates 929 936). Hammer is 30 cm long.

C) Irregular contact between marble and amphibolite (UTM coordinates 027 9715). Marble contains blocks of amphibolite and displays an increase in the percentage of calc-silicate minerals adjacent to the contact.

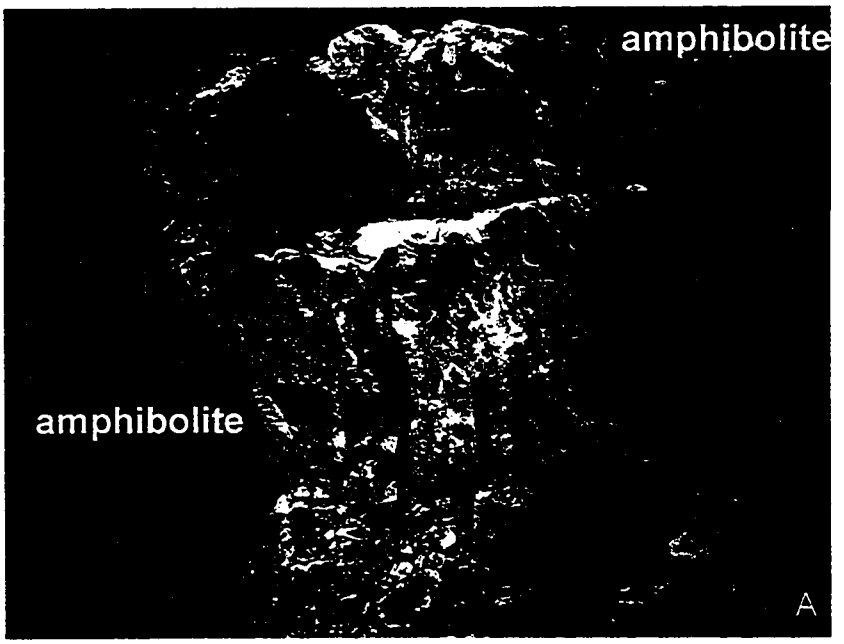

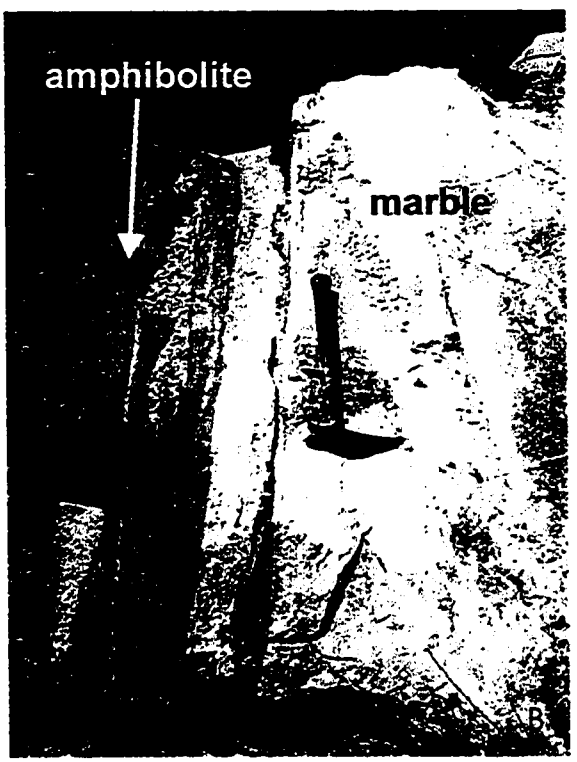

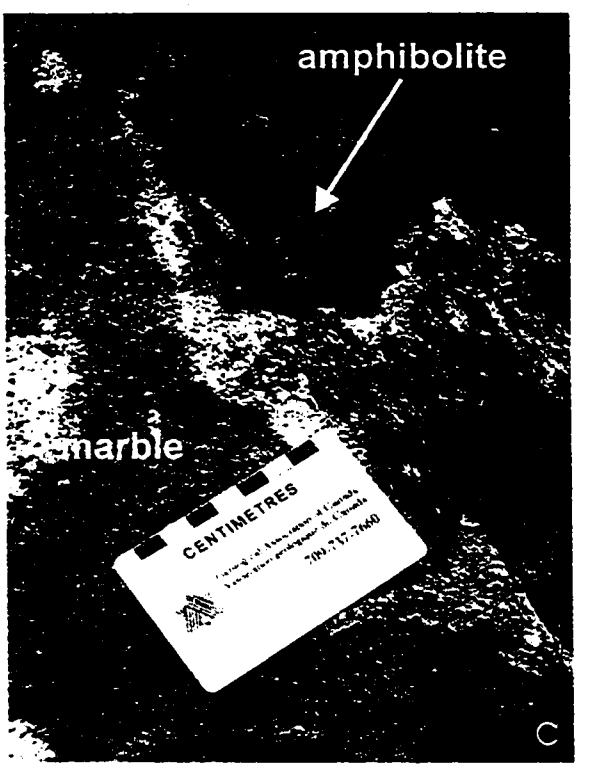

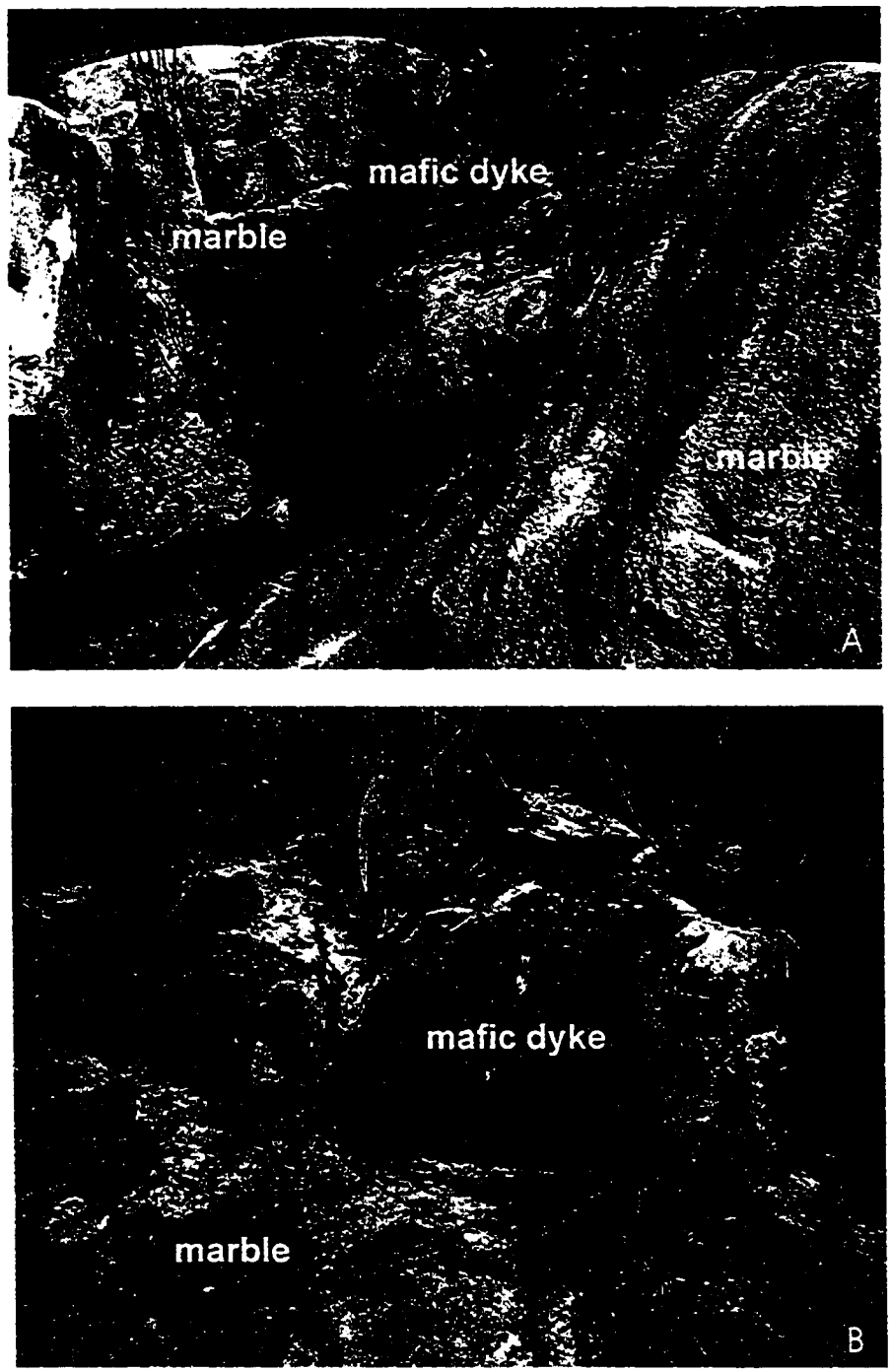

Photo 2.7 A) Hammer rests on metamorphosed aphanitic dyke within banded marble. Hammer is 36 cm long. Marble-dyke contact is outlined in red. Rusty weathered surface of dyke reflects the presence of pyrite.
B) Unmetamorphosed mafic dyke cross-cutting foliation in marble (UTM coordinates 943 975).

abundant diopside next to the contact indicates contact metamorphism may have occurred. Fine- to medium-grained intermediate dykes also intrude the marble.

Approximately 5 km northeast of the village of Middleville along Wolf Grove Road (County Road 16) at UTM coordinates 943 975, both metamorphosed and unmetamorphosed dyke rocks are in contact with marble. Medium-grained tremolite-bearing, banded marble outcrops on one side of the road. The banding is variably oriented as the rock has been folded. A metamorphosed mafic dyke approximately 30 cm wide roughly parallels the fabric in the marble and has been boudinaged. On the opposite side of the road, the outcrop consists of a tonalitic to quartz diorite dyke with breccia of dominantly mafic igneous fragments. This dyke cuts across the banding in the marble and is undeformed. One kilometer further north (UTM coordinates 953 983), outcrops on both sides of the road expose banded, medium-grained marble of varying colour and mineralogy. Green diopside is present in orange marble and finer grained green calc-silicate layers. Tremolite crystals and quartz-rich knots are prominent on the black weathered surfaces. Boudinaged and folded mafic dykes are found within the marble and typically are in contact with 5-10 cm green calc-silicate layers. At the southeast end of the outcrops the marble has been cut by fine-grained dykes, of roughly intermediate to felsic composition 0.5 to 1.5 m thick.

2.3 Mineralogy and Petrography

The coexisting mineral assemblages which form stable assemblages within the

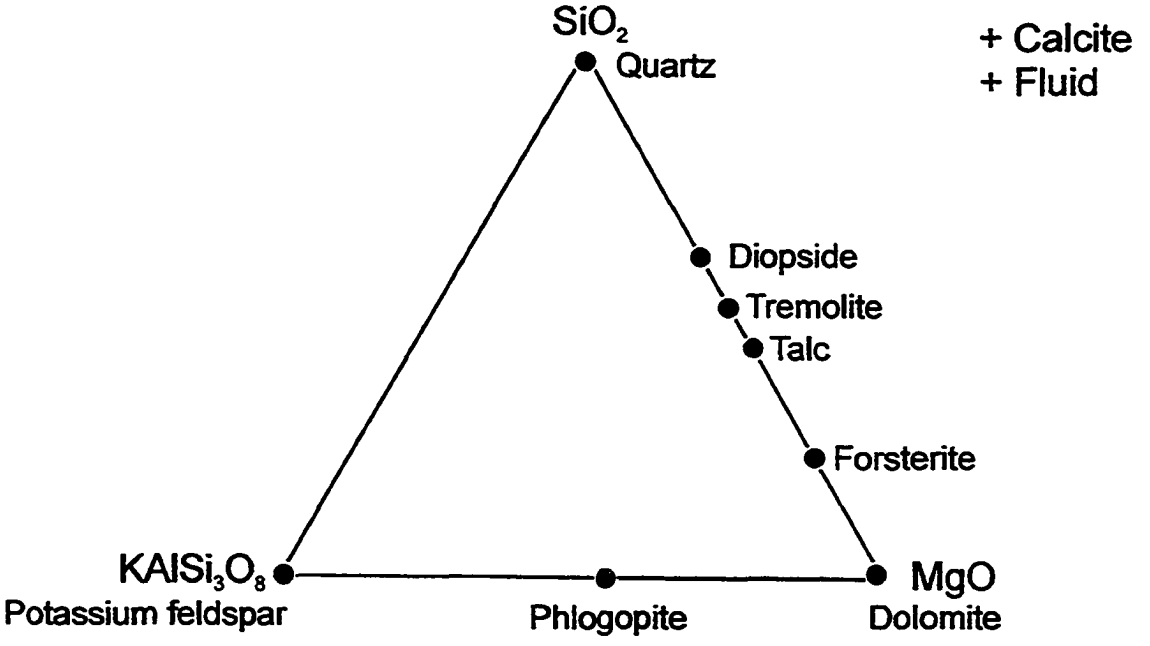

Figure 2.3 Ternary diagram for the CaO-MgO-SiO_2-$KAlSi_3O_8$-H_2O-CO_2 system.

siliceous marbles of the Carleton Place area can be represented within the system CaO-MgO-SiO_2-$KAlSi_3O_8$-H_2O-CO_2 (figure 2.3). Minerals formed within this system include calcite, dolomite, quartz, phlogopite, talc, tremolite, diopside, forsterite (sepentine), and potassium feldspar. The chemistry of the mineral assemblages can be projected from CO_2, H_2O and $CaCO_3$ on the premise that all of these components are present in excess. SiO_2-$KAlSi_3O_8$-MgO ternary diagrams have been utilized to subdivide the siliceous marbles within the thesis area into seven distinct lithologic assemblages:

1) phlogopite-bearing marble

2) talc-bearing marble

3) talc-tremolite-bearing marble

4) tremolite-bearing marble

5) tremolite-diopside-bearing marble

6) diopside-bearing marble

7) forsterite-bearing (sepentine) marble

In general, the mineralogy and petrography of the components of each assemblage are distinctive and can be characterized as follows:

2.3.1 Calcite-Dolomite

Calcite and dolomite form the basic framework of all the lithologic assemblages and occur in varying proportions together with siliceous minerals. Calcite and dolomite vary in texture from cloudy, untwinned crystals with vague crystal outlines to clear, well-twinned, granoblastic crystals. Dolomite is distinguishable from calcite in the field by its

buff to tan colour, greater hardness and its greater resistance to weathering. It is more difficult to differentiate between calcite and dolomite in thin section. Some thin sections examined in this study were stained after the method of Warne (1962). Calcite appears red in stained thin sections compared to dolomite which remains unstained (photo 2.8).

2.3.2 Phlogopite

Marble containing the assemblage calcite, dolomite, phlogopite ± quartz (figure 2.4) occurs throughout the field area. Phlogopite typically forms subhedral to euhedral hexagonal crystals, up to 5 cm in diameter. It is generally pale brown and weathers to a light, gold or silver colour. Phlogopite occurs as fine grains within discrete layers (photo 2.9a) or as coarse grained clots within coarse-grained marble. It is more abundant in marble east of the Clayton Lake shear zone. In thin section, basal sections display bird's eye extinction and first order interference colours. Elongate crystals exhibit a single cleavage and high second or third order inference colours (photo 2.9b). It is distinguished from muscovite and biotite by its pale yellow to brown pleochroism and small optic angle.

2.3.3 Quartz

Quartz is present both as recrystallized cherty layers within marble and as discrete rounded to sub-angular clastic grains and aggregates. Cherty layers vary in thickness from 1-5 cm up to 20 cm or greater. In thin section (photo 2.9b), quartz layers are composed of either individual grains with varying degrees of recrystallized grain

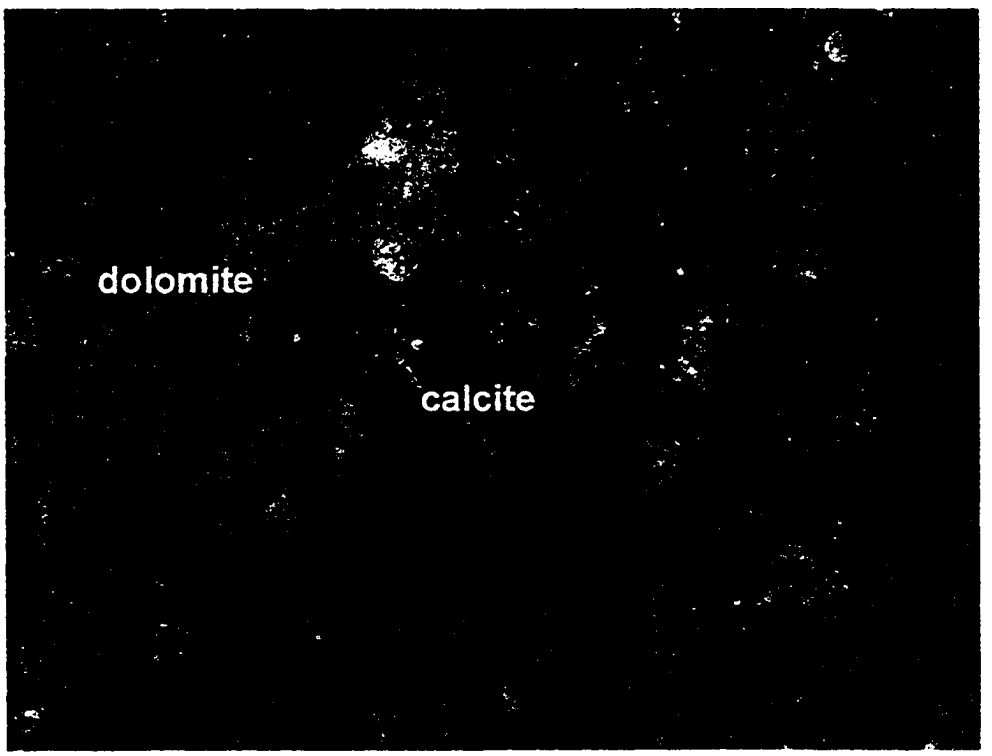

Photo 2.8 Photomicrograph of stained marble thin section under plane polarized light. Calcite appears red. (UTM coordinates 903 852) Field of view = 3.6 mm, ppl

Phlogopite-Quartz-Dolomite

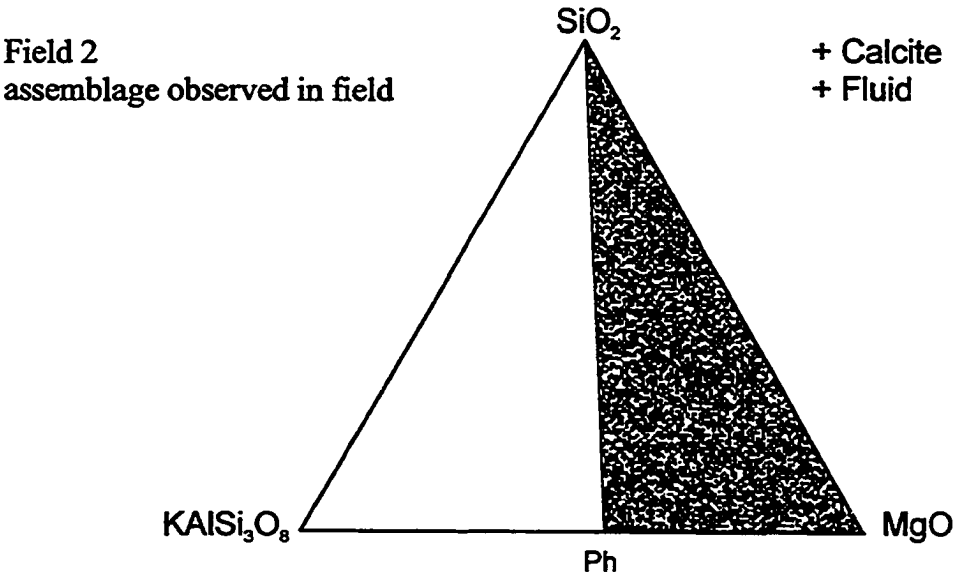

Figure 2.4 Ternary diagram displaying the assemblage calcite-dolomite-phlogopite-quartz-fluid. This assemblage corresponds to field 2 on the T-X_{co2} diagram (see figures 4.9, 4.10, and 4.11).

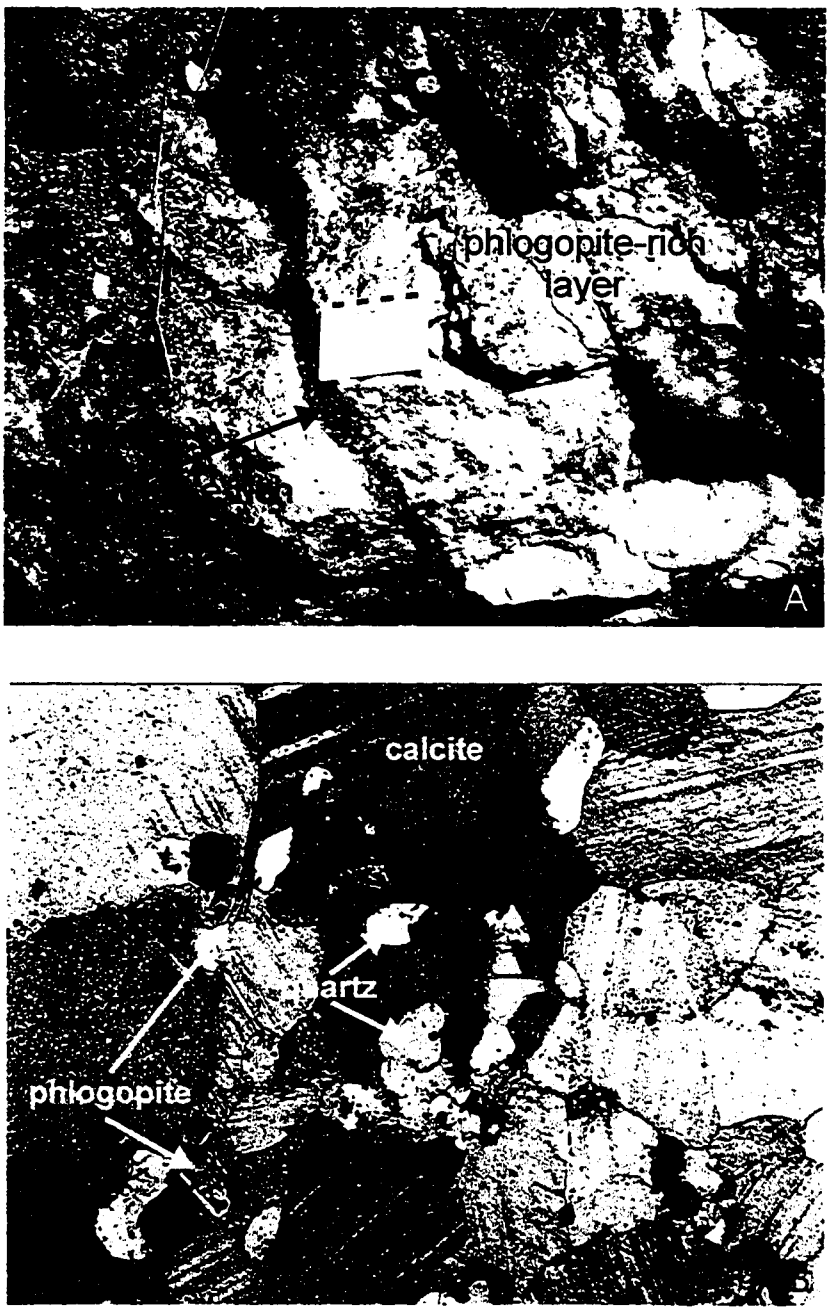

Photo 2.9 A) Coarse-grianed grey-white marble containing phlogopite-rich layers and cross-cutting veins of phlogopite (UTM coordinates 953 983). B) Photomicrograph of marble thin section (UTM coordinates 906 910) containing calcite, quartz, and phlogopite. Graphite appears as small black patches throughout the thin section. Field of view = 5mm, xpl

boundaries to veins of quartz with no grain boundaries visible. Quartz is distinguishable from potassium feldspar by its undulose extinction and uniaxial positive interference figure. Calc-silicate minerals such as tremolite or diopside may contain inclusions of quartz. Quartz was identified in all of the aforementioned assemblages with the exception of the forsterite-bearing marbles.

2.3.4 Talc

A limited number of talc-bearing assemblages were identified. Calcite, dolomite, talc, phlogopite ± tremolite, quartz comprises the typical mineral assemblage (figure 2.5). Rocks containing primary talc without tremolite are uncommon. Assemblages containing talc + tremolite are restricted to a small number of marble outcrops west of the Clayton Lake shear zone, namely within and around the Tatlock quarry in the northwest corner of the Carleton Place map sheet, a small region to the west of Clayton and Tatlock Lakes, and adjacent to the Clayton Lake shear zone in the southern portion of the map sheet. Primary talc was also reported near Dalhousie and Bennett Lakes, southwest of the map area (Abercrombie, 1983). Secondary talc is present in variable amounts throughout the map area as an alteration mineral of tremolite or diopside.

Talc was identified in the field based on its white to buff colour, miceous habit, characteristic hardness and greasy texture. Grain size ranges from < 1 cm to ~5 cm in diameter. In outcrops near the southern exposure of the Clayton Lake shear zone, talc and tremolite are aligned in a moderately developed foliation. Talc displays high order interference colours and an elongate habit with one cleavage (photo 2.10a). Talc is

Talc-Phlogopite-Quartz or
Talc-Phlogopite-Tremolite

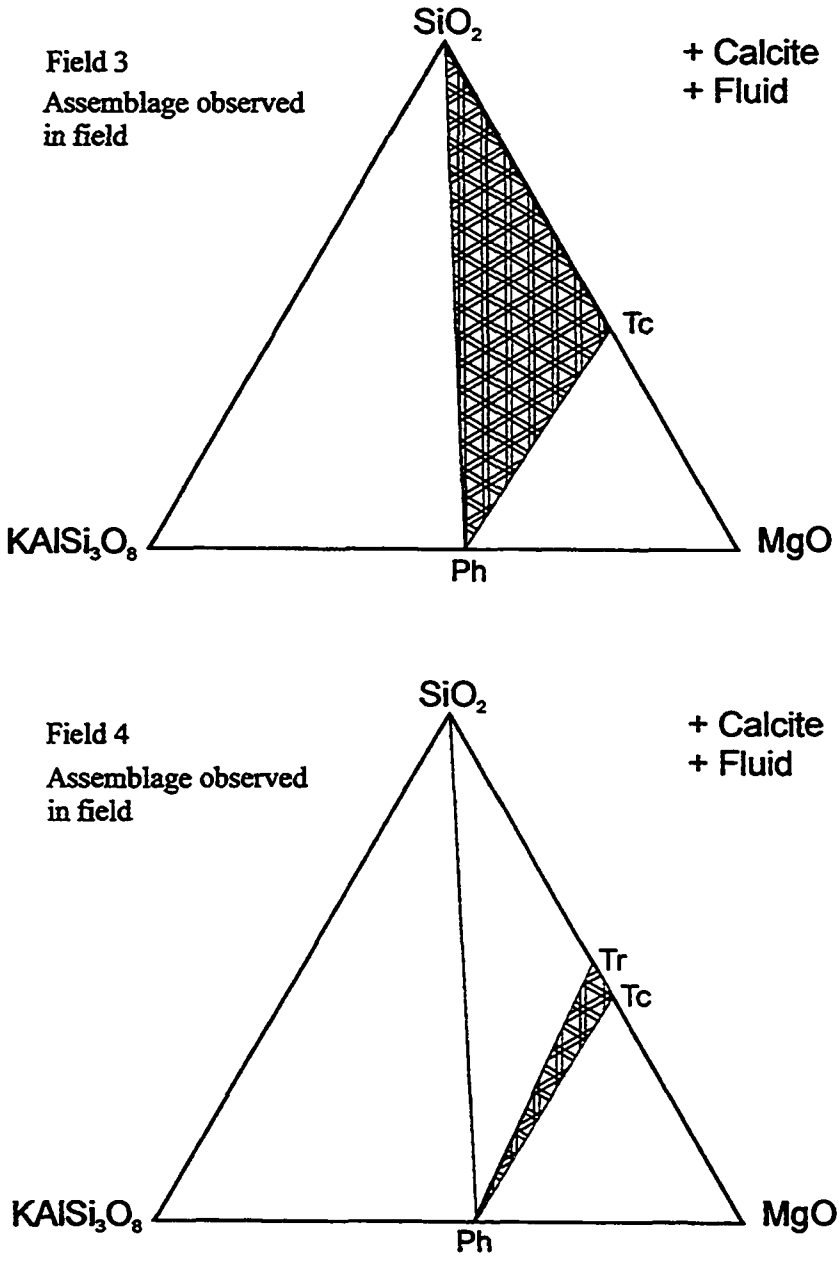

Figure 2.5 Ternary diagrams displaying talc-bearing assemblages identified in the field. Field numbers correspond to fields on figures 4.9, 4.10, and 4.11.

Photo 2.10 A) Photomicrograph of talc-bearing calcite marble. Talc is randomly oriented (UTM coordinates 851 046). Field of view = 3.6 mm, xpl

B) Talc alteration of tremolite (UTM coordinates 870 842). Field of view = 1.5 mm, xpl

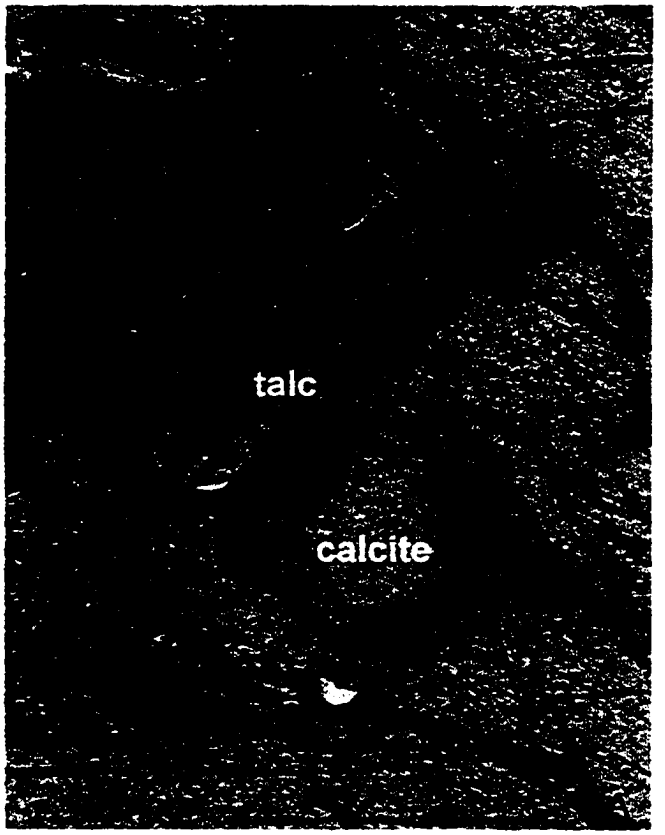

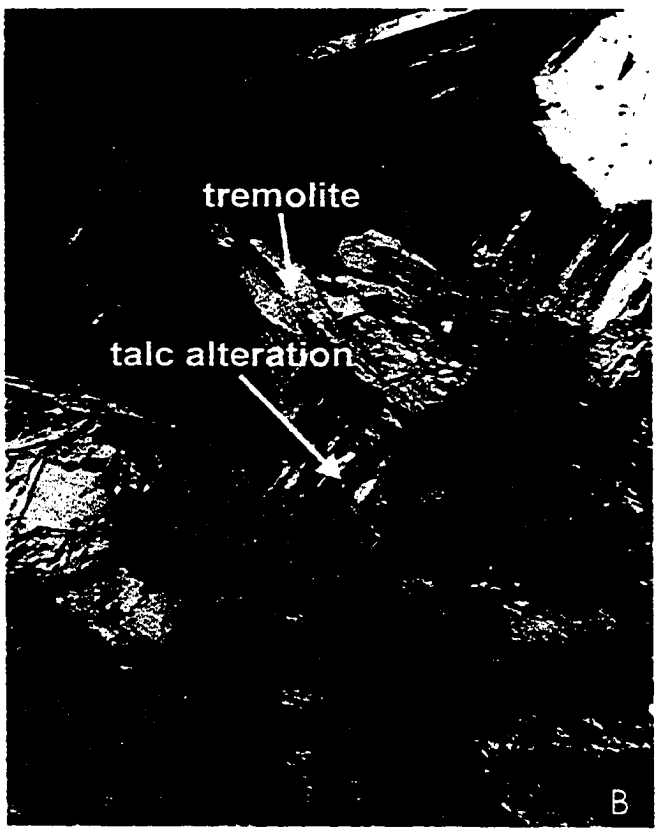

difficult to distinguish from muscovite in thin section and definitive identification may require microprobe analysis. Finely crystalline aggregates of talc as pseudomorphs after tremolite (photo 2.10 b) are abundant.

2.3.5 Tremolite

Tremolite occurs in a variety of coexisting mineral assemblages (figure 2.6). The most common tremolite-bearing assemblages contain calcite, dolomite, phlogopite, and tremolite or calcite, dolomite, quartz, and tremolite. Tremolite-bearing marble containing potassium feldspar was less common and was only identified in thin section.

Tremolite shows considerable variation in its form, colour and habit within marbles across the field area. The colour varies between a characteristic white colour to green, blue, or brown. Tremolite crystals are present as fibrous radiating aggregates (photo 2.11a) or elongate, blocky crystals (photos 2.11b and c). Individual crystals range between 1 and 8 cm in length and may be aligned into a lineation along foliation surfaces. Locally, tremolite laths appear to be broken.

In thin section, tremolite is distinguishable from the other calc-silicate minerals by its characteristic amphibole cleavage, diamond-shaped cross-section (photos 2.12a and b), second order interference colours and radiating habit (photo 2.12c). A few thin sections contain zoned tremolite or polysynthetic twinning. Tremolite may contain inclusions of quartz or calcite. Talc or fine-grained masses of sericite are the commonest alteration products.

Tremolite-bearing Assemblages

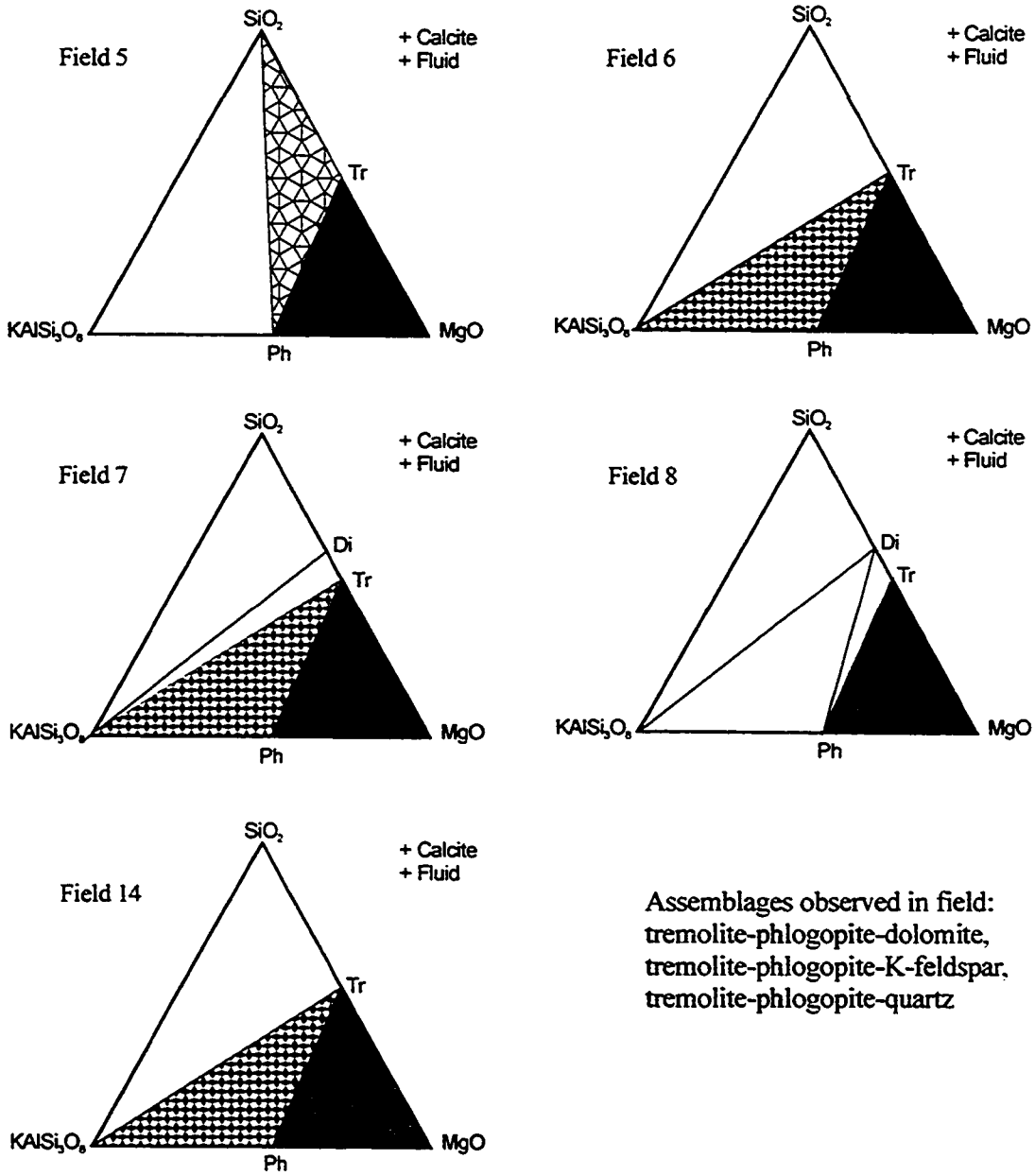

Assemblages observed in field:
tremolite-phlogopite-dolomite,
tremolite-phlogopite-K-feldspar,
tremolite-phlogopite-quartz

Figure 2.6 Ternary diagrams displaying tremolite-bearing assemblages identified in the field. Field numbers correspond to fields on figures 4.9, 4.10, and 4.11.

Photo 2.11 A) Radiating sprays of tremolite in grey-white coarse-grained marble (UTM coordinates 874 849). Marble also contains talc. Pen is 13.5 cm long.

B) Elongate and broken tremolite crystals in marble (UTM coordinates 875 848). Pen is 13.5 cm long.

C) Large, blocky tremolite crystals in marble (UTM coordinates 902 926). The tremolite crystals are more resistant to weathering than the surrounding carbonate matrix. Hammer grip is 15 cm long.

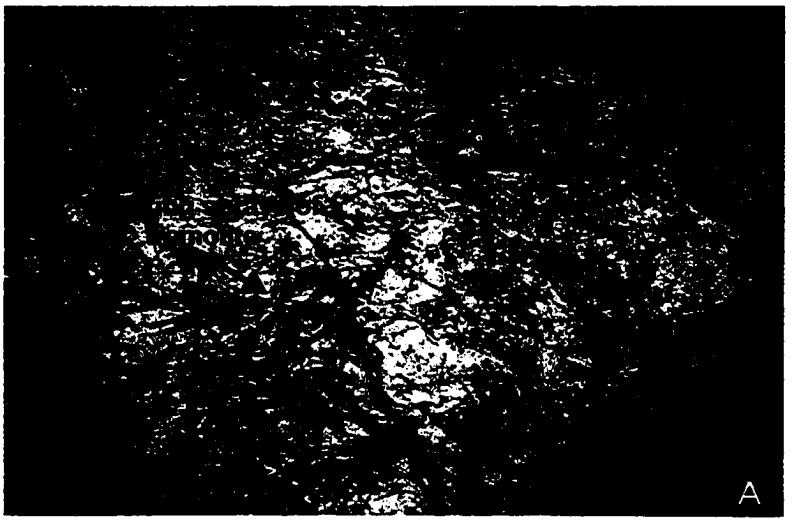

Photo 2.12 A) Photomicrograph of calcite marble containing tremolite, quartz, and phlogopite (UTM coordinates 915 931). Tremolite displays characteristic amphibole cleavage. Phlogopite has been kinked. Field of view = 3.6 mm, xpl

B) Partially resorbed tremolite marble in calcite marble (UTM coordinates 851 046). Tremolite and phlogopite are aligned in a foliation. Field of view = 3.6 mm, xpl

C) Radiating spray of tremolite in marble (UTM coordinates 923 024a). The tremolite crystals are more resistant to weathering than the surrounding carbonate matrix. Field of view = 3.6 mm, xpl

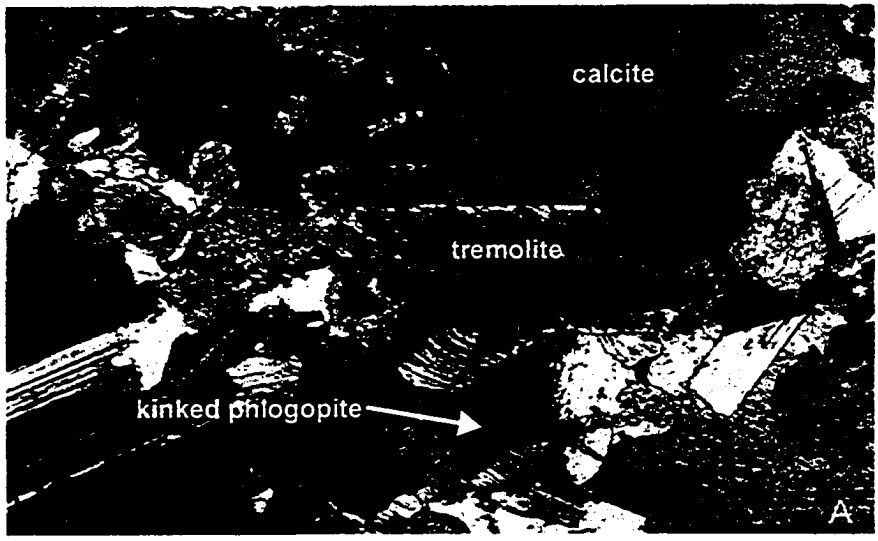

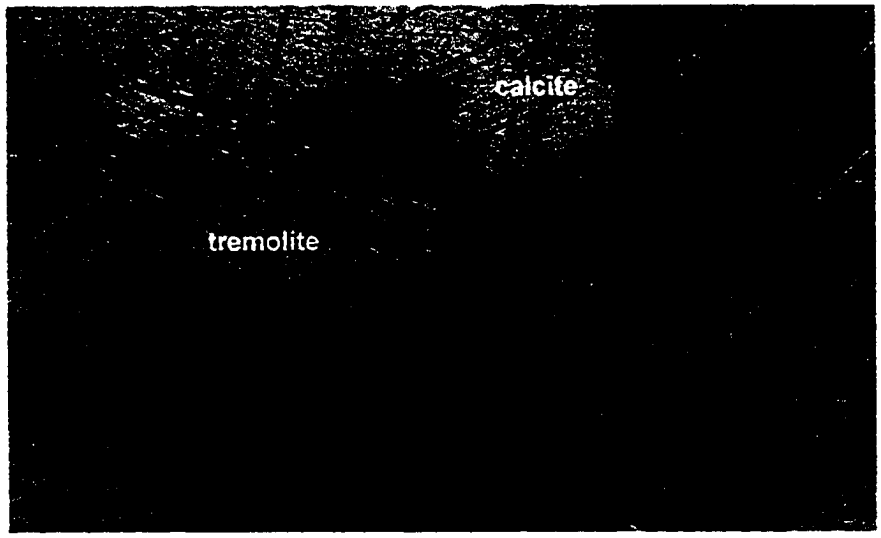

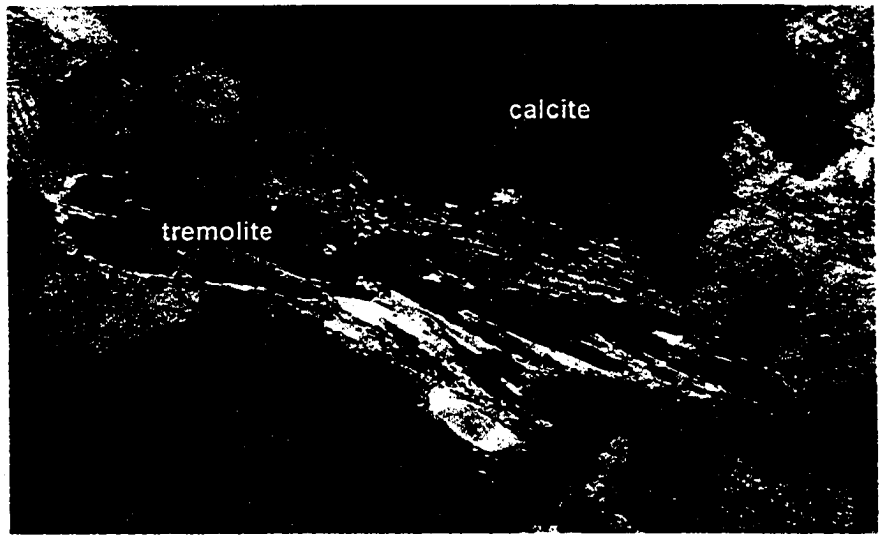

2.3.6 Potassium Feldspar

Potassium feldspar was present in a few thin sections of marble from the study area. Typically, it has been completely replaced by phlogopite. It formed small sub-rounded to blocky grains with no discernible cleavage. It is distinguishable from quartz in thin section by its slightly higher relief, cloudy appearance and biaxial interference figure.

2.3.7 Diopside

Diopside is present in three different mineral assemblages. It usually occurs with calcite, dolomite, phlogopite ± tremolite (figure 2.7), although assemblages containing calcite, dolomite, phlogopite, and diopside were identified in thin section.

Diopside is seen in the field as either stubby crystals up to 1.5 cm in length or as small rounded crystals. It is usually dark green in colour but it is locally pale green or bluish green in colour. When present it may compose up to 30-35% of the mineralogy of a particular horizon or outcrop (photos 2.13a and b). It is typically more resistant to weathering than the surrounding carbonates but may show less relief where it has been pseudomorphed by sepentine.

Diopside generally forms large, sub-rounded, blocky crystals in thin section (photos 2.14a and b). It is easily distinguishable from tremolite by its habit, pyroxene cleavage and strong dispersion. It may contain inclusions of tremolite, calcite, or quartz and typically alters to sepentine.

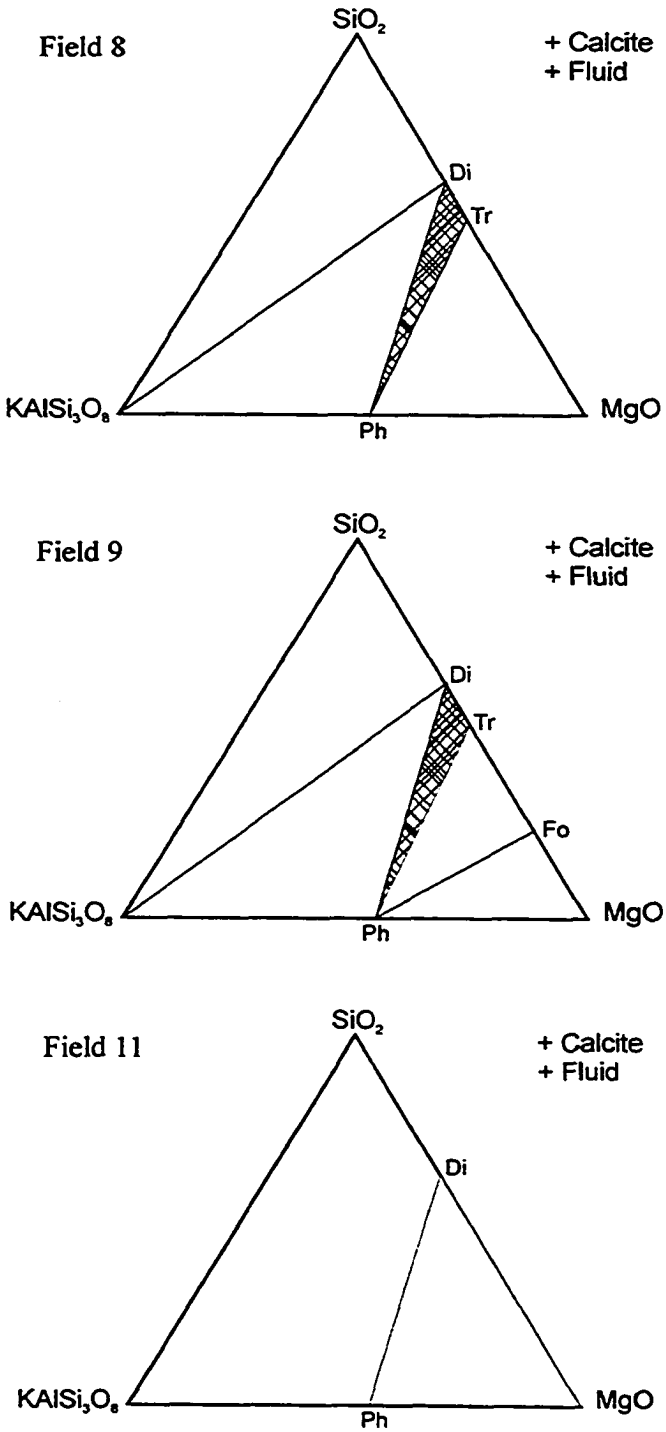

Figure 2.7 Ternary diagrams displaying diopside-bearing assemblages identified in the field. Field numbers correspond to fields on figures 4.9, 4.10, and 4.11.

Photo 2.13 A) Diopside-bearing marble in contact with amphibolite exposed along Tatalock Road (County Road 9; UTM coordinates 915 931). Diopside is concentrated in layers and is more abundant adjacent to the contact. Hammer is 40 cm long.

B) Diopside-bearing marble (UTM coordinates 0265 972). Diopside has been partially replaced by serpentine and chlorite, producing the mottled green patches. Hammer is 40 cm long.

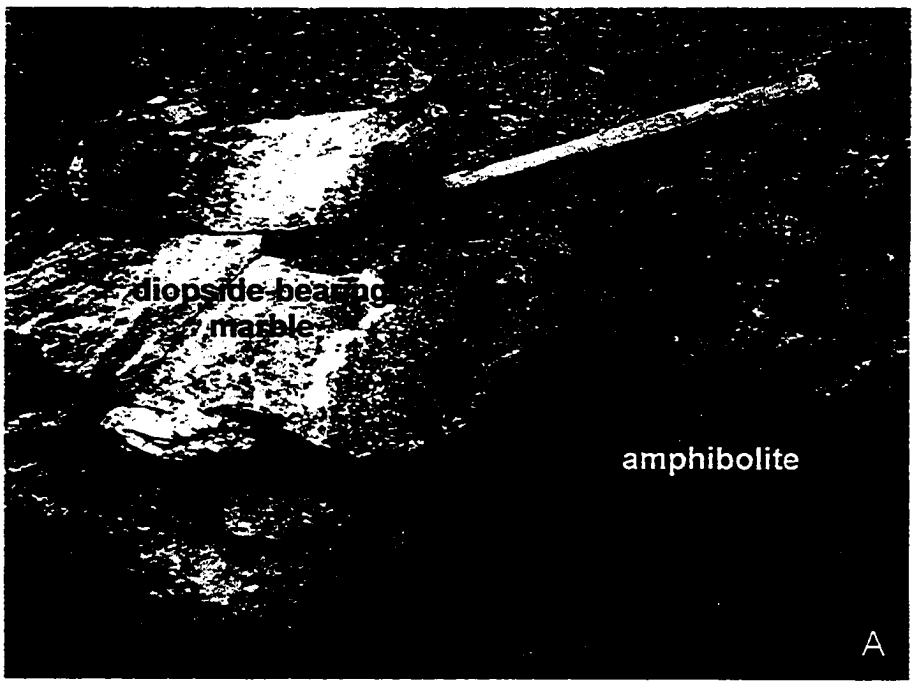

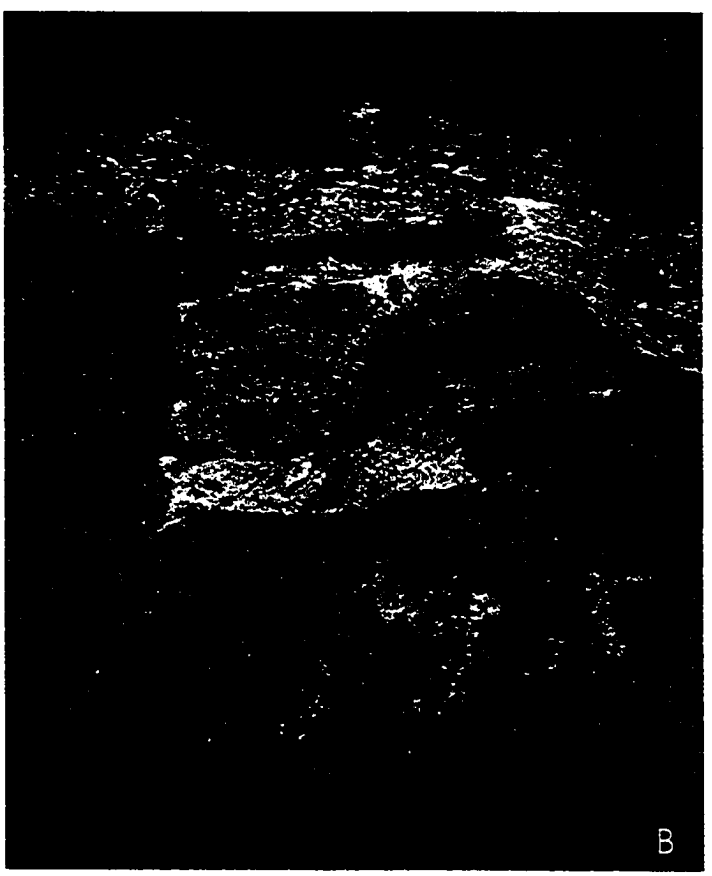

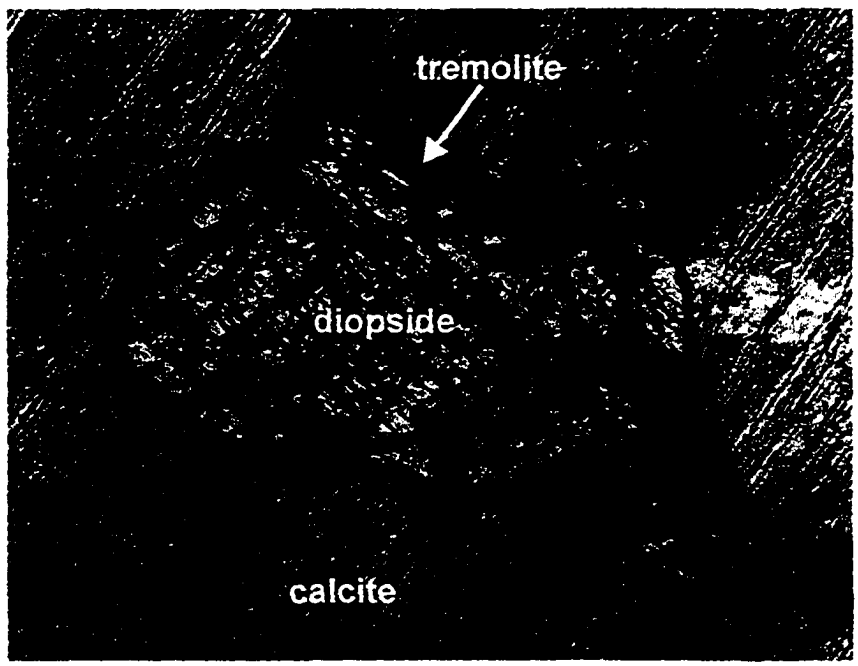

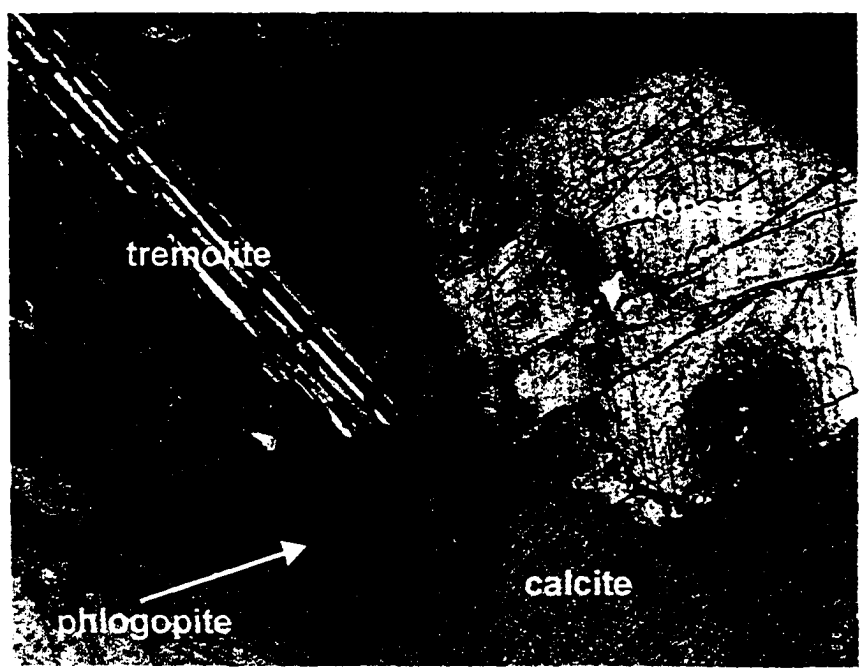

Photo 2.14 A) Photomicrograph of diopside-bearing calcite marble (UTM coordinates 932 933). Diopside displays characteristic pyroxene cleavage. Diopside crystal is in contact with tremolite along upper edge. Field of view = 3.6 mm, xpl
B) Diopside, tremolite, and phlogopite in calcite marble (UTM coordinates 931 013). Phlogopite displays two phases of growth. Tremolite exhibits polysynthetic twinning. Field of view = 3.6 mm, xpl

2.3.8 Forsterite

Forsterite was not identified in the field. Two distinct forsterite-bearing mineral assemblages were identified in thin section (figure 2.8), namely calcite-dolomite-phlogopite-tremolite-forsterite and calcite-dolomite-phlogopite-diopside-forsterite. In thin section, it forms small relict cores within rounded masses of cloudy sepentine. It is distinguishable from diopside by its higher birefringence, lack of cleavage and rounded crystal outline pseudomorphed by sepentine.

2.4 Evidence for a Tremolite-Grade Overprinting Metamorphism

Some marbles within the narrow high-grade zone west of the trace of the Clayton Lake shear zone and enclosing the Wolf Grove Structure display evidence of a second metamorphic event or possibly continued metamorphic mineral growth on the retrograde path. Altered diopside crystals appear in the cores of fresher-looking tremolite crystals (photos 2.15a and b) in a number of samples. In a sample from Galbraith Road (UTM coordinates 921 037), diopside is partially enclosed by "teeth" of tremolite and an embayment in a diopside crystal is filled by a euhedral tremolite crystal. There are no other tremolite crystals apparent in the thin section suggesting diopside may have formed prior to tremolite.

In other samples, small, euhedral tremolite crystals are replacing altered tremolite crystals (photos 2.16a, b, and c). Altered tremolite also occurs surrounded by fresher appearing tremolite. Talc and tremolite-bearing marbles from Sheridan Rapids Road west (e.g. UTM coordinates 874 848) of Lanark display two forms of tremolite in

Forsterite-Phlogopite-Dolomite

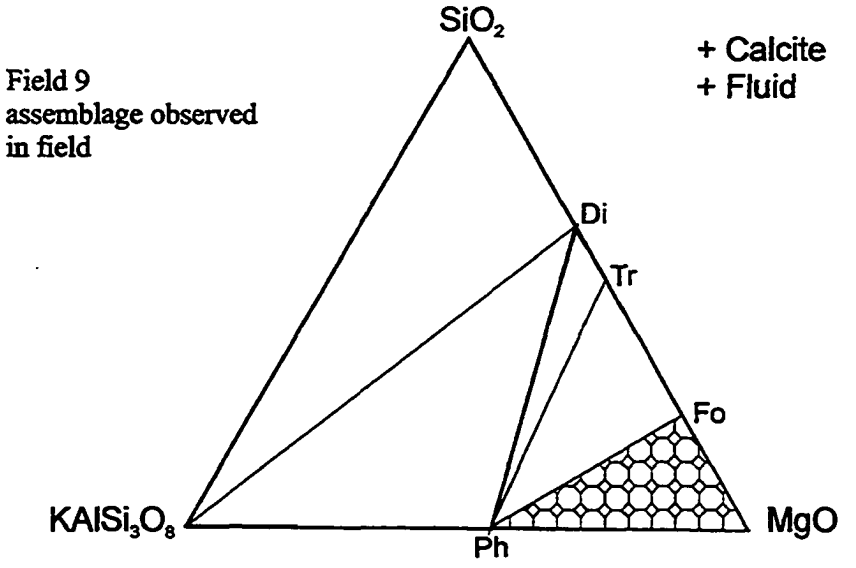

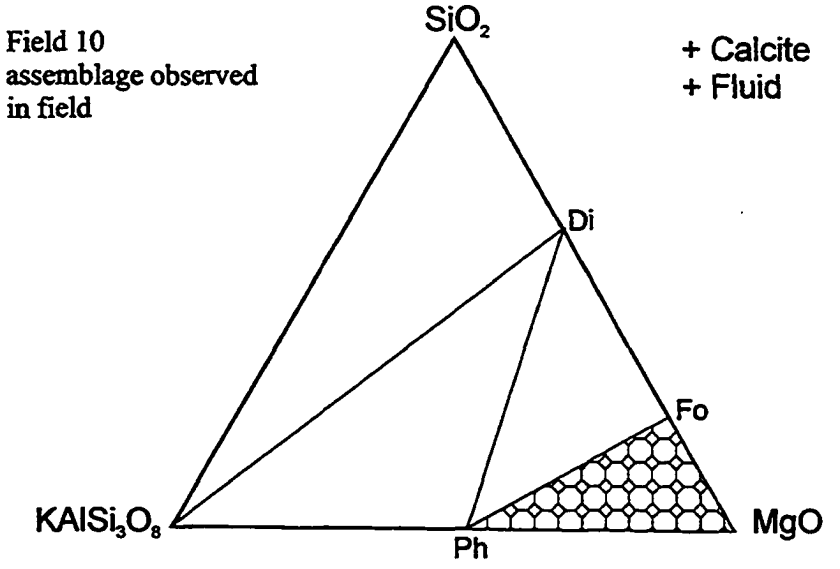

Figure 2.8 Ternary diagrams displaying forsterite-bearing assemblages identified in the field. Field numbers correspond to fields on figures 4.9, 4.10, and 4.11.

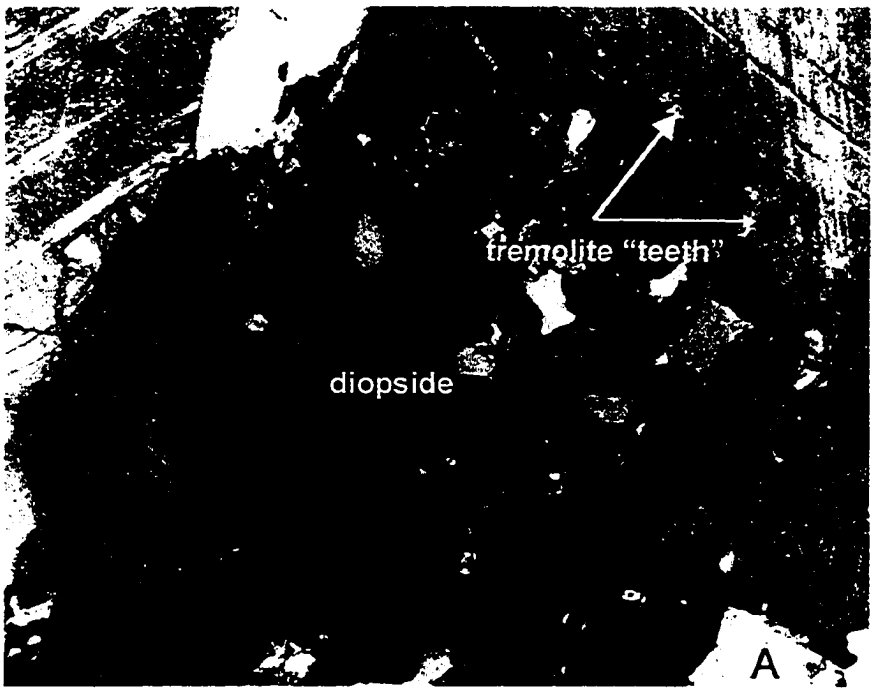

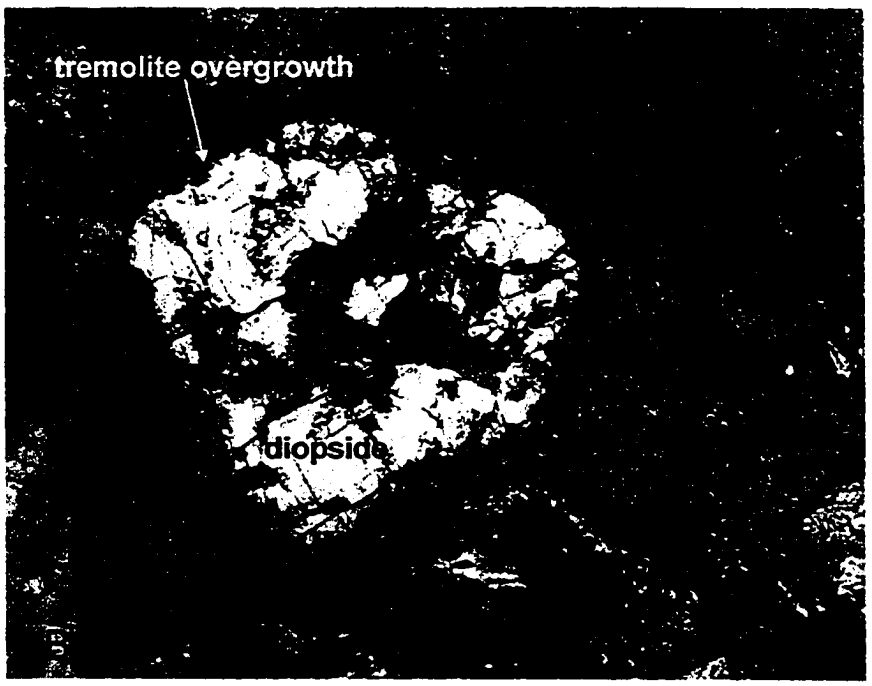

Photo 2.15 A) Photomicrograph of diopside-bearing calcite marble (UTM coordinates 921 037). Diopside with "tremolite teeth". Field of view = 3.6 mm, xpl B) Diopside displays secondary growth of tremolite crystals (UTM coordinates 963 999). Field of view = 3.6 mm, xpl

Photo 2.16 A) Photomicrograph of tremolite-bearing calcite marble. Two phases of tremolite growth are visible. (UTM coordinates 900 968). Field of view = 3.6 mm, xpl

B) Tremolite crystal with mantle of secondary tremolite. Tremolite core contains inclusion of quartz in lower right. (UTM coordinates 923 006b). Field of view = 3.6 mm, xpl

C) Tremolite "teeth" replacing elongate tremolite crystal. (UTM coordinates 923 006a). Field of view = 3.6 mm, xpl

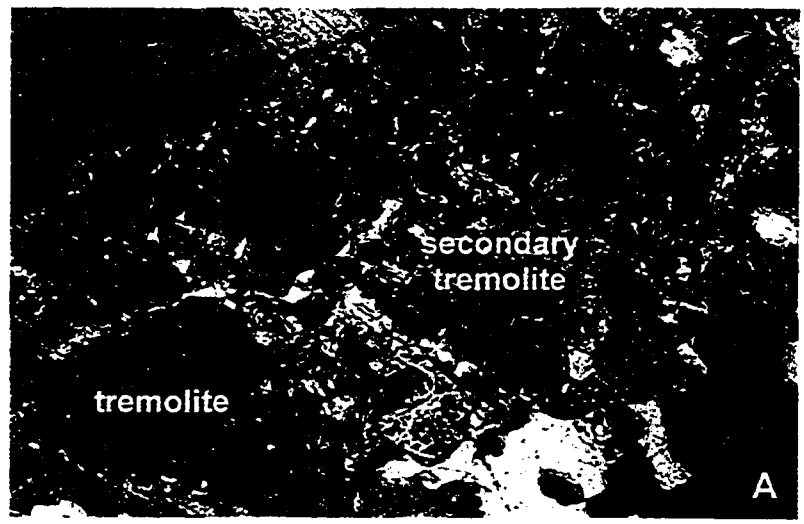

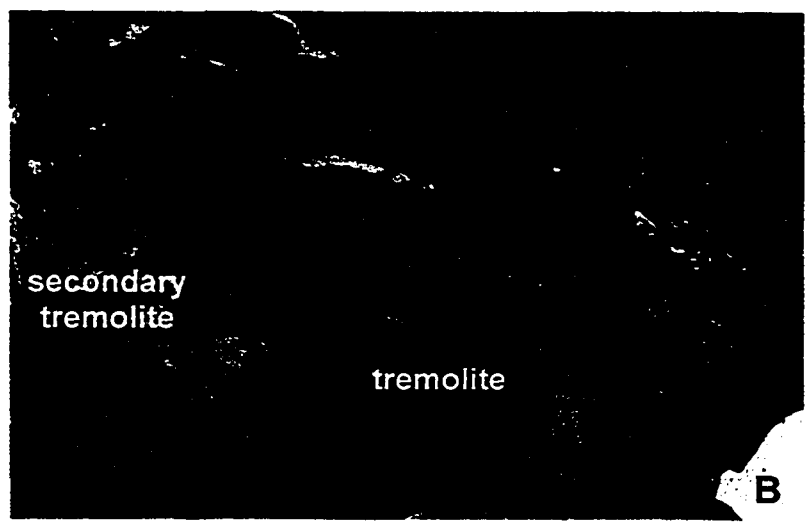

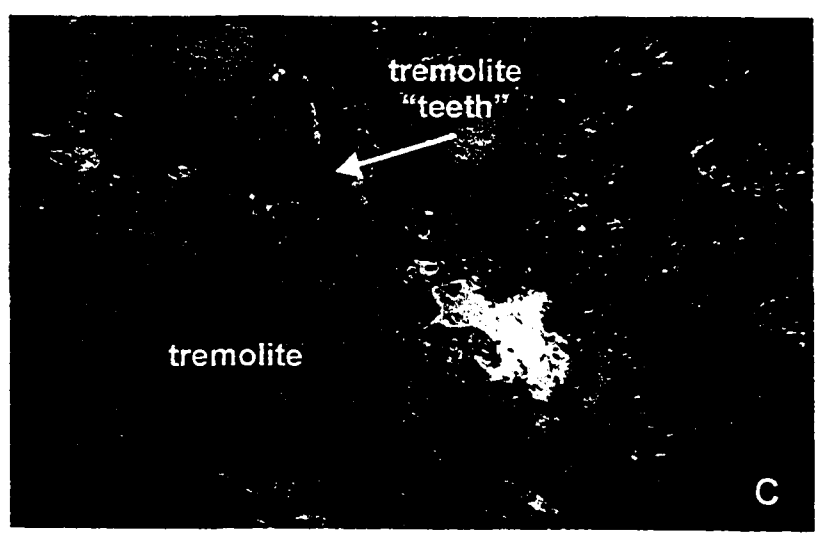

outcrop. Long, broken needles of tremolite are aligned into the regional foliation. The marble also contains radiating sprays of tremolite which display no preferential alignment.

2.5 Relationship of Mineralogy to Metamorphic Grade

Unmetamorphosed limestones can range from very pure sediments to limestones with a high percentage of detrital grains and diagenetic dolomite. Very pure limestones remain relatively unchanged mineralogically, as calcite is stable under most crustal conditions. However, a variety of minerals may develop in siliceous carbonate rocks undergoing metamorphism. The sequence of mineral development in regionally metamorphosed dolomitic marbles appears to be:

(1) talc (may not be present)

(2) tremolite

(3) diopside or forsterite

(4) diopside + forsterite

Wollastonite is present at higher grades in contact and regionally metamorphosed carbonate rocks.

The appearance of these metamorphic minerals is directly related to changes in pressure, temperature and fluid composition and can be defined in terms of a number of specific reactions. Much of the previous work of marbles has focused on the experimental derivation of these reactions, e.g. Greenwood (1967), Metz and Winkler (1969), Gordon and Greenwood (1970), and Skippen (1971) and were used to construct

models for the metamorphism of carbonate rocks, e.g. Metz and Trommsdorff (1968), Skippen (1971, 1974), Slaughter et al. (1975). Comprehensive field studies of marbles, such as the classic work on regionally metamorphosed dolomitic marbles by Trommsdorff (1972) or the delineation of intersecting isograds in carbonates and pelites by Carmichael (1970), have emphasized diagnostic mineral assemblages for prograde metamorphism, In addition, these studies have highlighted the role of variation in fluid composition and thermal gradients in the sequence of mineral development. The above sequence can be used as a general guide to the metamorphic grade of siliceous carbonate rocks; natural examples of progressively metamorphosed marbles are far more complex. Thermobarometry is necessary to quantify more precisely the metamorphic conditions experienced by carbonates and associated rocks within the study area.

Chapter 3 - Geothermobarometry

3.1 Introduction

Mineral compositions can be used to quantify metamorphic conditions. Geothermobarometry is the calculation of the pressure (P) and temperature (T) conditions of equilibration, based on measured compositions of the coexisting mineral solid solutions, from which the thermodynamic activities of the solid solution end-members can be determined. The basic equation used to quantify P-T conditions of metamorphism or equilibrium is:

$$G = U + PV - TS = \sum \mu_c N_c \quad \text{(equation 1) or}$$

$$0 = dG = -SdT + VdP + \sum \mu_c dN_c$$

where G = Gibbs free energy, U = internal energy, P = pressure, V = volume, T = temperature, S = entropy, μ_c = chemical potential, and N = matter; the summation is over c components. Gibbs free energy measures only chemical energy and is constant at fixed P, T, and N. At equilibrium, the free energy of reaction must be zero. Many geochemical calculations integrate equation 1 for each component from the reference P and T of a database to the P and T of equilibrium under geological conditions.

Minerals usually exist as a solid solution of end members. The partitioning of elements such as iron and magnesium between two minerals that form a solid solution can be used to determine the equilibration temperature of the rock. Given $\mu^\circ = \Delta G^\circ_f$, the free energy per mole of an end-member at fixed P and T, it is necessary to calculate the chemical potential of the same component dissolved in a solution. The function used to

represent this relationship comes from ideal gas theory.

$0 = \mu = \mu^\circ + RT\ln X$ (equation 2) or

$0 = G = G^\circ + RT\ln K$

where μ = chemical potential, R = gas constant, T = temperature in degrees Kelvin, X = composition, and K = equilibrium constant. Solutions that are adequately described by equation 2 are called ideal solutions. However, real solutions (ie. mineral solutions) deviate from the above relationship and require an adjustment.

$0 = \mu = \mu^\circ + RT\ln a$ (equation 2a) and $a = \gamma X$ (equation 3)

where a is the activity of a component and γ is the activity coefficient.

In the traditional methods of geothermobarometry, mineral compositions are converted into activities through the application of an activity coefficient, which varies in a complex fashion with pressure, temperature and composition. The remaining thermodynamic data can be taken from internally consistent compilations (eg. Berman, 1988). These values can be substituted into a set of independent equilibria describing the free-energy balances among the mineral end-members, which are solved for pressure and temperature (figure 3.1).

The INVEQ method (Inverse Chemical Equilibrium problem: Gordon, 1992, 1998; Gordon et al., 1994; Ghent and Gordon, 2000) uses an alternative approach to the computational part of the process and calculates the amounts and compositions of phases that will coexist in a system at equilibrium given a pressure, temperature, and bulk composition. This method determines pressure and temperature by finding a best-fit hyperplane to the partial molar free energies of all phase components, given

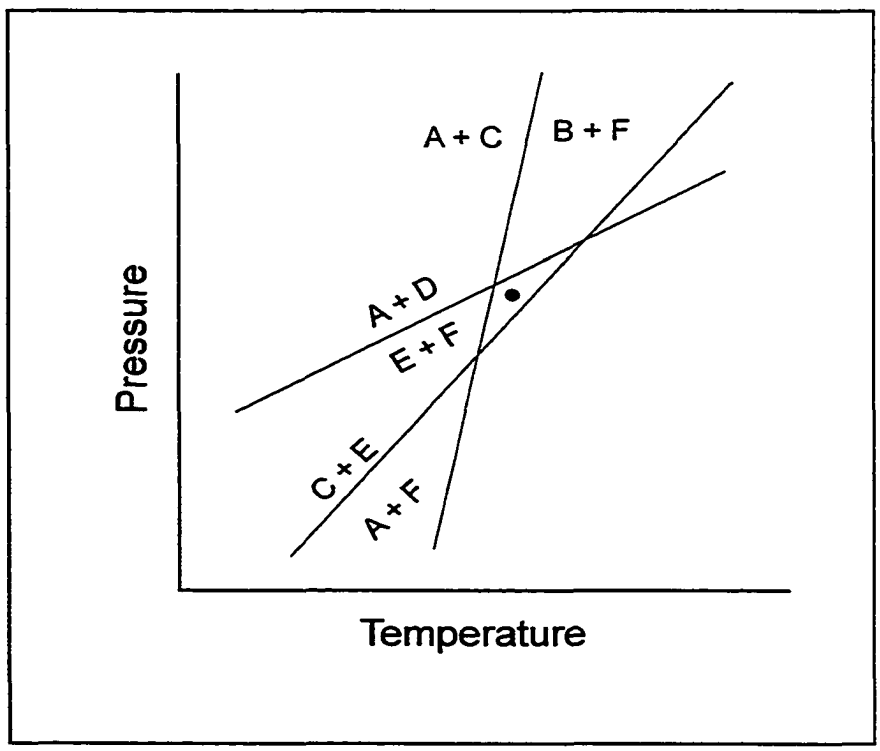

Figure 3.1 An example of "traditional" thermobarometry output. Intersection point provides pressure and temperature of rock equilibration.

measurements of their thermochemical constants and mineral compositions (figure 3.2). WEBINVEQ (world-wide web based version of INVEQ) has the advantage of providing a measure of the misfit for each individual phase component and an easily computed confidence region. A detailed explanation of the computation of error ellipses is found in Gordon et al. (1994) and Ghent and Gordon (2000).

The following activity models are utilized by INVEQ in thermobarometric calculations:

Garnet - Berman (1990)

Biotite - McMullin et al. (1991)

Amphibole - Mäder and Berman (1992)

Plagioclase - Fuhrman and Lindsley (1988)

Clinopyroxene - Newton (1983)

3.2 Analytical Techniques

Pressure and temperature conditions within the Wolf Grove Structure and the Lavant Gabbro Complex were assessed on the basis of detailed petrography, mineral composition and geothermobarometry. Eleven samples were selected for microprobe analysis based on the presence of garnet-bearing mineral assemblages for which P and T can be calculated, the lack of discernible alteration or visible mineral overgrowths suggesting retrograde metamorphism, and relatively coarse grain size. The location of the samples analysed for thermobarometry is shown in figure 3.3. UTM coordinates are given in appendix 1 along with results from thermobarometry. The 6-figure coordinates

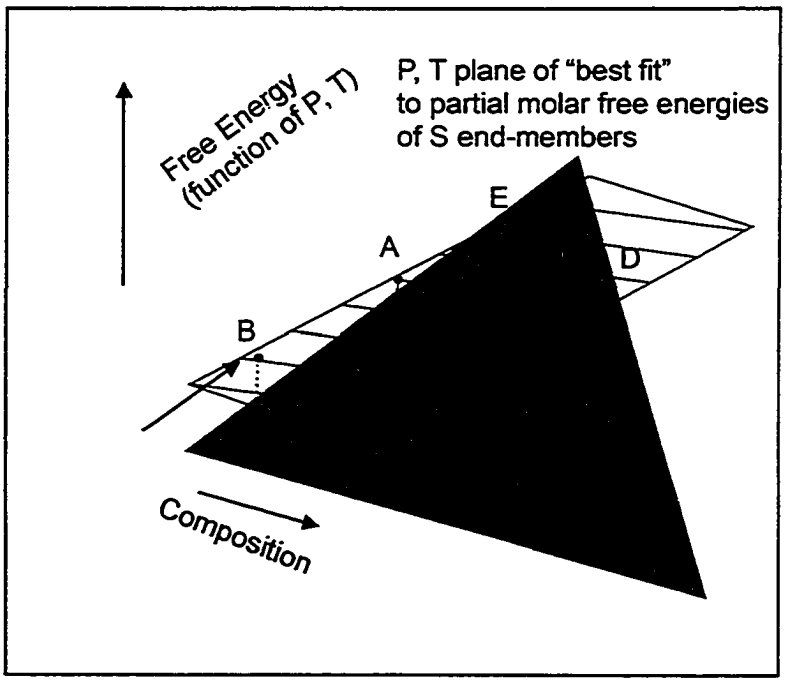

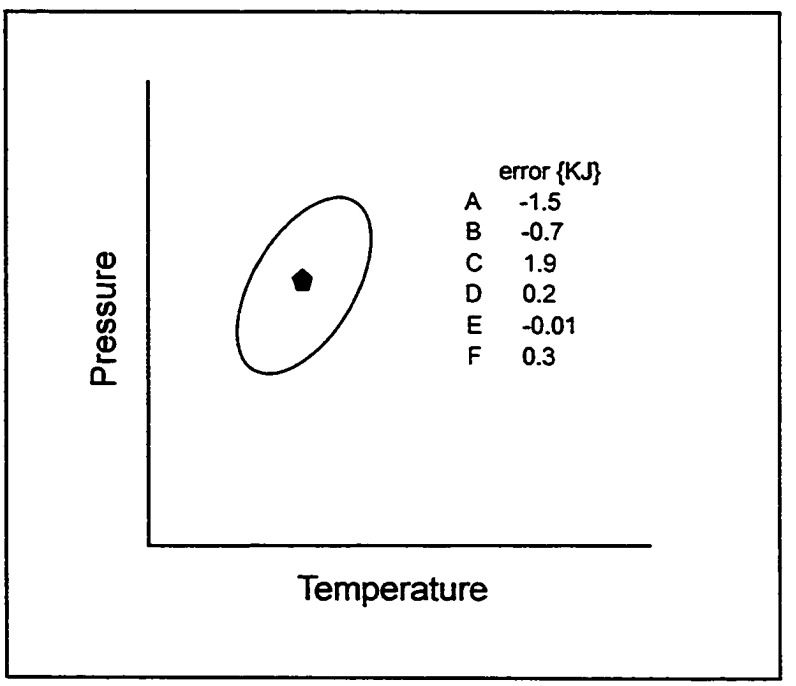

Figure 3.2 A) An example of the "best fit" hyperplane calculated by INVEQ.
B) An example of the graphical output from INVEQ. P-T graph displays confidence region and pinpoints exact P and T of equilibration. Error list reports the components position above or below the hyperplane.

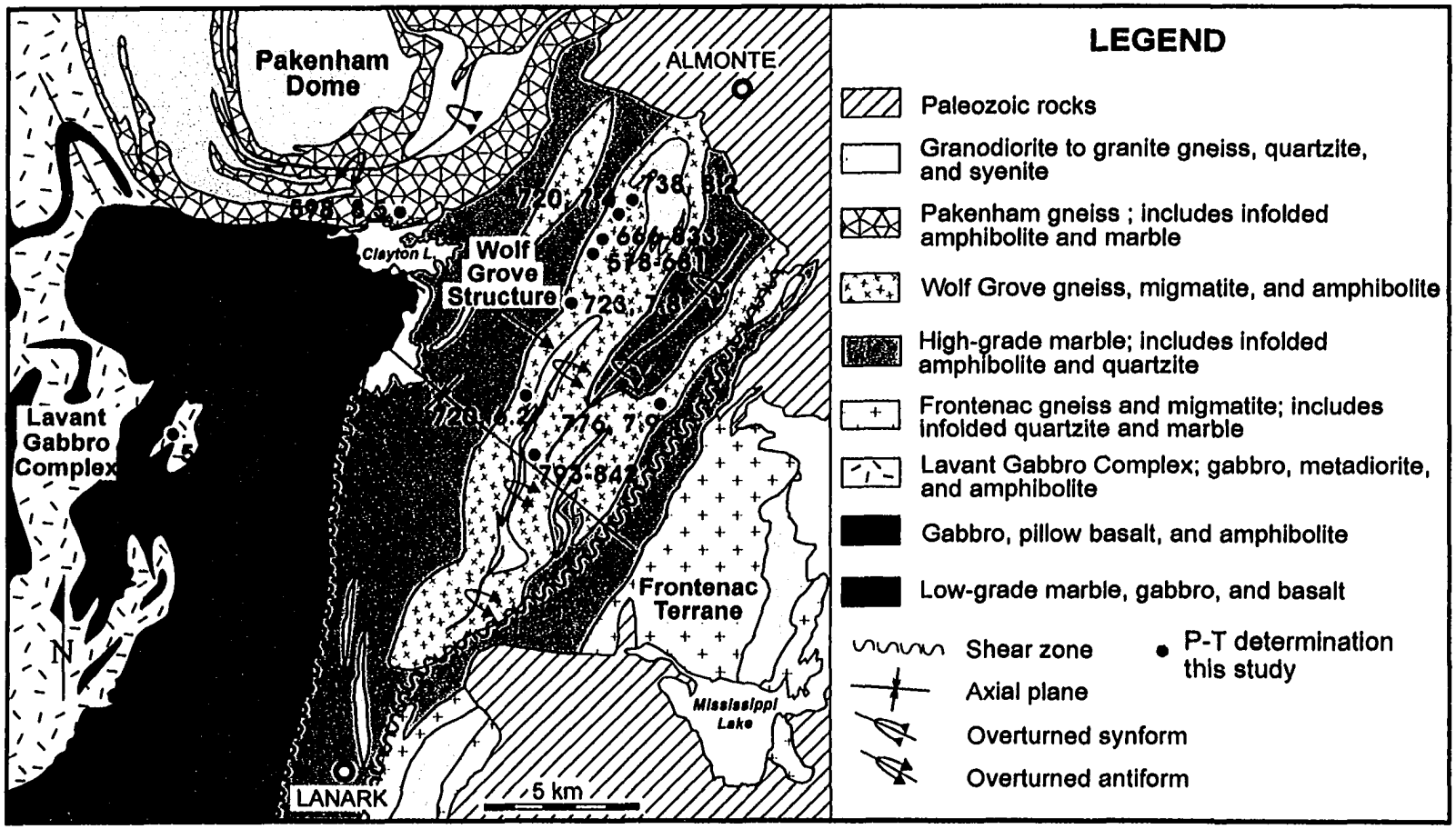

Figure 3.3 Simplified geological map of the Carleton Place area showing sample locations used for thermobarometry in this study. UTM coordinates are recorded as subsection headings throughout chapter 3. (Modified from Reinhardt and Liberty, 1973)

are found by dropping the first digit and the last two digits for the easting and the first two digits and the last two digits from the northing. For example, the full UTM reference for sample 993 007 would read as 399300 (easting) 5000700 (northing). The 6-figure grid references are considered accurate to the nearest 100m. When 7 figures are quoted, the grid references is accurate to the nearest 50m.

Electron microprobe analyses on which P-T estimates are based can be found in appendix 2. For each sample, two or more domains containing the required assemblage of minerals were analysed and used for thermobarometric calculations to ensure consistency at the thin section scale. The quoted range of P-T values for each sample reflects the variation between different domains within the thin section. It does not take into account probe error or uncertainty in thermodynamic parameters.

The samples collected contain typical middle to upper amphibolite mineral assemblages comprised of garnet, hornblende, biotite, and plagioclase. Clinopyroxene, gedrite, actinolite, and chlorite were also present in some of the samples. Eight samples were selected from the hornblende migmatite, garnet-bearing amphibolite, and garnet gneiss units of the Wolf Grove Structure. A sample of hornblende migmatite from the southern edge of the Pakenham Dome was selected. Garnet-bearing metadiorite from the Lavant Gabbro Complex and migmatitic gneiss from the Lyndhurst area were also analysed. For each sample, descriptions of the thin section and thermobarometric results are presented.

Mineral chemistry was determined on an automated 4 spectrometer Camabax MBX scanning electron microprobe by the wavelength dispersive x-ray analysis method

(WDX) at Carleton University, in Ottawa, Ontario. Operating conditions; 15 kV accelerating potential, and a beam current of 20 nano-amperes (nA) for silicates. Peak counting times for each analysed element were: 15-40 seconds or 40,000 accumulated counts. Background measurements were made at 50% peak counting time on each side of the analysed peak. Raw x-ray data were converted to elemental weight % by the Cameca PAP matrix correction program. Well characterised natural and synthetic minerals and compounds were used as calibration standards. For plagioclase, the electron beam was rastered over a 40×40 μm area to minimize loss of sodium. Analyses are accurate to 1-2% relative for major elements and 3-5% relative for minor elements (< 1 wt%).

Digital BSE (back-scattered electron) images were collected at 512 x 512 resolution with a Lamont 4 element solid state BSE detector and BSE Quad Summing Amplifer interfaced to a 4Pi Analysis Inc. digital imaging system and a Power Macintosh computer.

3.3 Problems with Geothermobarometry in High-Grade Rocks

A basic assumption of geothermobarometry is that the mineral compositions used to calculate P-T conditions represent equilibrium coexistence. Complete equilibrium is characterized by chemically homogeneous crystals and all crystals of a given phase having the same composition (Fitzsimons and Harley, 1994). This is rarely achieved by natural metamorphic mineral assemblages. Careful petrographic observation can help evaluate the degree of chemical equilibrium within a rock sample.

The detection of chemical zoning has important implications in the interpretation

of geothermobarometric results. Growth zoning reflects changes in the composition of material supplied to the surface of a growing crystal (Tracy, 1982). Growth zoning in garnet is typically lost in garnets that have attained temperatures greater than 600 °C (Tuccillo et al., 1990). Diffusion zoning, or the transport of matter driven by a chemical potential gradient can occur during retrograde re-equilibration of mineral compositions during cooling, uplift or overprinting by subsequent metamorphic events (Spear,1992; Spear and Florence, 1992; Fitzsimons and Harley, 1994). Homogenization is believed to be caused by diffusion (Tracy, 1982). If zoning is revealed, one must decide which part of the zoned mineral is in equilibrium with the other minerals. In general, core compositions of zoned minerals are usually chosen to represent peak metamorphic conditions. Unzoned minerals such as biotite, which has a large Fe-Mg diffusion coefficient allowing it to rapidly change composition compared to garnet, are usually assumed to approach peak equilibrium compositions if the mineral is present in large proportion and if the mineral composition is consistent throughout the thin section (Ferry and Spear, 1978; Spear, 1991).

3.4 Mineral Chemistry

High-grade garnets display zoning profiles that are the reverse of those resulting from growth zoning. Zoning profiles of garnets which have experienced homogenization and retrograde zoning are characterized by a core to rim increase in Mn, a decrease in Mg and a flat Ca profile. Growth zoning is usually characterized by bell-shaped Mn profiles and an increase in Mg from core to rim (Tuccillo et al., 1990). Garnet zoning profiles

were obtained for garnets within each sample by analysing an average of 5-15 points across each crystal. The resulting profiles are relatively flat and appear to have been homogenized as expected in high-grade garnets. Garnets in this study are typically almandine rich with lesser amounts of grossular, pyrope and spessartine. Garnet from sample 954 051, a migmatite collected from the edge of the Pakenham Dome, is noticeably enriched in Fe and Mg with negligible amounts of Ca and Mn compared to the other samples. These garnets are similar in chemistry to garnet in sample 97RME-0023B-1 from the Westport area (Buckley et al., 1997). The garnet composition with the highest Mg/(Fe+Mg) ratio was used in the thermobarometry calculations to estimate peak metamorphic conditions (Spear, 1991; Florence and Spear, 1991). This point typically corresponds to the inner rim or core composition of the garnet.

Biotite compositions are relatively consistent. Mg#s (100Mg/(Fe+Mg)) range from 25-40 and Ti contents range from 3-3.5 wt.%. Biotite from sample 954 051 has higher Mg#s ranging from 60-68 and lower Ti contents which average 1.3 wt.%. Plagioclase compositions are generally albitic with two exceptions. Feldspar from samples 050 008 and 993 004 are dominantly anorthitic. Amphibole is generally present as hornblende but gedrite, and actinolite were also identified in some samples.

3.5 Thermobarometry Results - Wolf Grove Structure

3.5.1 Sample 993 007

Sample 993 007 is a hornblende migmatite collected on Tatlock Road. The sample contains plagioclase, biotite, potassium feldspar, garnet, quartz, and iron oxides.

Mineralogy of this unit shows strong compositional layering. Garnet may vary from less than 1 % to up to 20 % within an outcrop. Garnet tends to be present in more siliceous layers and hornblende is more commonly associated with plagioclase and biotite, although garnet and hornblende do occur together. Garnet is anhedral to subhedral, fractured and contains few inclusions of biotite, quartz or plagioclase. Biotite is medium- to coarse-grained with strongly pleochroic reddish brown colour and is commonly surrounded by iron oxides. The bulk of the sample is composed of mortar texture feldspars and quartz with a few larger porphyroblasts of plagioclase and quartz. Layers of mortar texture quartz and feldspar are aligned sub-parallel to the weak fabric defined by biotite alignment. Plagioclase shows considerable alteration with many grains containing fussy brown cores. Apatite and zircon comprises > 1% of the sample.

Garnet-biotite thermometry yielded a temperature range of 793 - 842 °C.

3.5.2 Sample 012 043b

Sample 012 043b was collected from a garnet-rich layer within amphibolite from Wolf Grove Road. It contains plagioclase, biotite, garnet, potassium feldspar, and quartz. Garnet displays subhedral, rounded texture with abundant fracturing. Garnet appears to have overgrown biotite. Biotite is aligned in a poorly developed foliation and also occurs as inclusions within garnet. Plagioclase displays comb-style twinning and variable degrees of alteration. More altered grains contain small elongate laths of muscovite. Equilibrium is assumed, based on the presence of sharp, 120° grain boundaries. Chlorite has formed around some of the garnets suggesting limited retrograde metamorphism.

Two garnet-biotite pairs within this sample were used for temperature estimation. Temperature ranges of 578 - 637 °C and 632 - 681 °C were obtained from garnet-biotite thermometry.

3.5.3 Sample 017 048a

Sample 017 048a is garnet-bearing leucosome from hornblende migmatite, exposed along Wolf Grove Road. The sample contains plagioclase, biotite, quartz, garnet, potassium feldspar, iron oxides and minor chlorite. Reddish-brown biotite forms subhedral to euhedral laths, which define a well-developed foliation. The fabric appears to wrap around some garnets. Garnets vary from anhedral to euhedral crystals and are generally fractured. Biotite and plagioclase are present as inclusions within garnet. Mortar texture feldspar and quartz are unevenly distributed within the thin section and some areas appear to be recrystallized. Plagioclase is altered with some grains replaced by mats of very fine-grained sericite. Antiperthitic spots are also visible within the plagioclase.

Three garnet-biotite pairs were used for thermometry. The resulting temperatures range from 666 °C to 833 °C.

3.5.4 Sample 024 054a

This sample was collected from the hornblende migmatite unit exposed along Wolf Grove Road. Plagioclase, hornblende, biotite, garnet, quartz and iron oxides are present. Sample 024 054a exhibits both foliation and moderately developed gneissic

texture. Biotite and amphibole are aligned into the foliation. Some biotite is kinked suggesting intense deformation accompanied metamorphism. Hornblende is concentrated into distinct layers. Garnet is also layer controlled and is found in contact with hornblende and within more felsic layers.

Garnet displays two forms within the sample. Small (< 2 mm) garnets are nearly euhedral with no inclusions, whereas larger garnets (> 3 mm) are anhedral and typically fractured. Both forms are typically enclosed feldspar and may be in contact with biotite and hornblende. It is possible that these forms are the result of either two separate metamorphic events, represent a change in prevailing conditions during an extended period of metamorphism, or a change of growth mechanism during metamorphism. Two distinct garnet sizes are present throughout this unit, on both the northwestern and eastern margins of the Wolf Grove Structure.

Plagioclase contains exosolution lamellae and displays shadowy or comb-style twinning. Feldspar cores show minor alteration. Grain boundaries are mostly smooth 120° boundaries suggesting equilibrium. A few sutured boundaries between adjacent plagioclase or quartz grains are still visible.

Two garnets were analysed in contact with biotite in addition to hornblende and plagioclase. One garnet is small, anhedral and partially surrounded by biotite, displaying no preferential alignment. The second garnet is larger, slightly less anhedral and contains inclusion trails which are aligned with the cleavage of the surrounding biotite. Chemically, the garnets are very similar; the smaller garnet is lower in SiO_2, FeO, MgO and MnO than the larger garnet. Pressure and temperature conditions were calculated for

the following mineral combinations: garnet-biotite-hornblende-plagioclase, garnet-biotite-plagioclase, garnet-hornblende-plagioclase, and garnet-hornblende. Conditions were also calculated using only hornblende. Thermobarometry results are in table 3.1 and selected graphical WEBINVEQ results are shown in figure 3.4. The mean temperature and pressure for sample 025 054a is 720 °C and 7399 bars, based on 18 analyses with standard deviations of 45.6 and 1203.6. The temperatures range from 646-775 °C and pressure varies between 5587 and 9460 bars.

Table 3.1	024 054a A	024 054a B	024 054a C
gt-hb-bt-plag	762 °C, 9.0 kbars	646 °C, 6.5 kbars	745 °C, 8.8 kbars
gt-hb-bt	757 °C, 6.2 kbars	669 °C, 7.4 kbars	742 °C, 5.6 kbars
gt-hb-plag	775 °C, 9.4 kbars	666 °C, 6.8 kbars	771 °C, 9.3 kbars
gt-hb	762 °C, 6.7 kbars	668 °C, 7.4 kbars	758 °C, 6.7 kbars
hornblende	688 °C, 6.8 kbars	702 °C, 7.4 kbars	688 °C, 6.8 kbars

3.5.5 Sample 025 055a

Sample 025 055a was collected approximately 100 m northeast of 024 054a along Wolf Grove Road. It is also a hornblende migmatite. It displays similar textures to the sample described above. Sample 025 055a comprises of plagioclase, hornblende, biotite, garnet, and iron oxides. Quartz forms less than 2% of the sample. Garnets range in size and crystal form. The most euhedral grains are less than 2 mm. The larger garnets are fractured and contain inclusions of biotite and plagioclase. Garnet appears to have overgrown biotite. Biotite is aligned in a moderately developed foliation and is kinked in

Figure 3.4 WEBINVEQ results for sample 024 054a from the Wolf Grove Structure. Mineral assemblages used for the calculations are as follows A = garnet-biotite-hornblende-plagioclase, B = garnet-biotite-hornblende, C = garnet-hornblende-plagioclase, D = garnet-hornblende, and E = hornblende.

The error ellipses for all samples described in section 3.5 were calculated by WEBINVEQ using linear approximations to the free energy functions for the end-members. This is an adequate approximation over ~200 degrees and ~2 kilobars around the T and P of the solutions. If the problem is exactly determined (e.g. hornblende only phase used), the solid ellipse is the uncertainty in T and P as determined by error propagation using the uncertainties entered (ie. 1). If the problem is overdetermined (e.g. multiple phases), the two ellipses are approximate contours of constant sum-of-squares.

If the errors in the free energy estimates are independent and normally distributed with zero means, then:

If the uncertainties supplied are the actual standard deviations of the errors, th solid ellipse is approximately a 68% confidence region for P and T. This calculation follows Press et al. (1992). The solid ellipse thus depends on the supplied uncertainties and the linear dependence of the compositions of the end-members. It does not depend on the size of the residuals (errors) resulting from misfit of the hyperplane.

If the uncertainties supplied are relative standard deviations, ie .known up to multiplication by a constant, the dotted ellipse is approximately a 68.3% confidence region for P and T. This calculation follows Seber and Wild (1989). The dotted ellipse thus depends on the supplied uncertainties, the linear dependence of the compositions of the end-members, and the sum of squares of the residuals and the difference between the number of end members and the rank of the composition matrix.

Therefore, both ellipses represent 68.3% confidence levels. The solid ellipse depends on the supplied uncertainties (1) and the dotted ellipse estimates the uncertainties from the residuals (misfit). If the residuals are small the dotted ellipse will fall inside the solid ellipse and if the errors are large, the dotted ellipse will fall outside the solid ellipse.

For a more detailed explanation of the calculation of the errors by WEBINVEQ, see Gordon et al. (1994) and Ghent and Gordon (2000).

Sample 024 054a

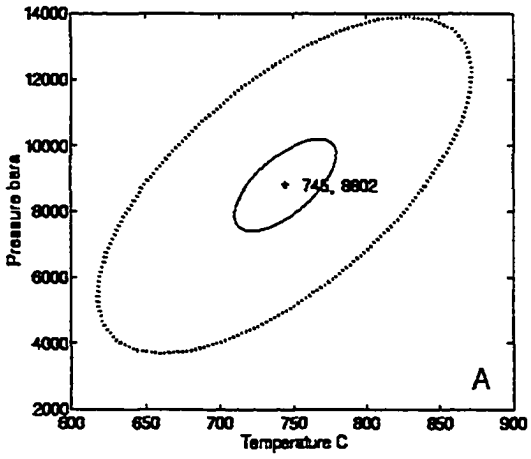

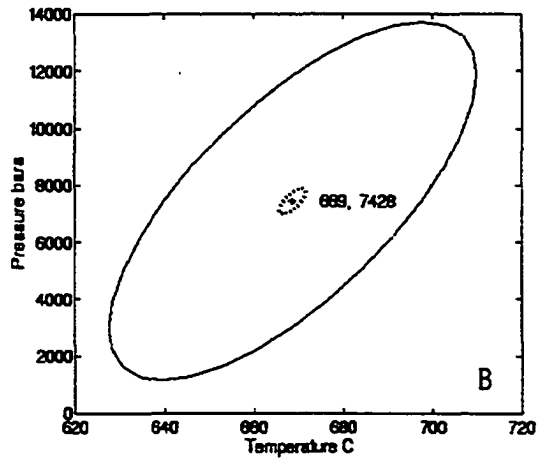

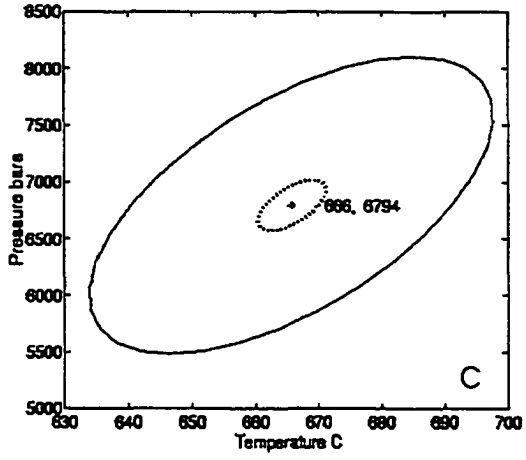

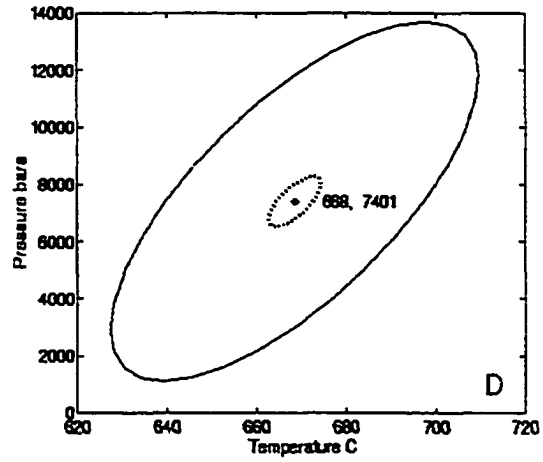

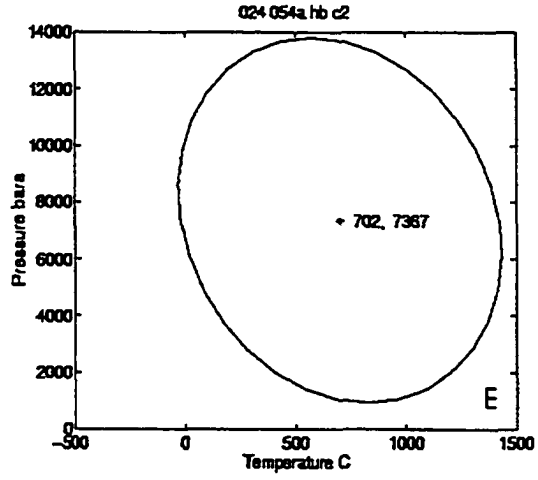

some areas. Plagioclase also shows evidence of strain with shadowy or comb-style twinning. Some biotite appears aligned at a nearly 90° to the dominant foliation. This supports the evidence from garnet of possible multiple or prolonged metamorphism and deformation events. However, the presence of 120° grain boundaries suggests equilibrium conditions have been obtained.

Two garnets were analysed, in addition to several biotite, hornblende and plagioclase grains. Pressure and temperature conditions were calculated for the following mineral combinations: garnet-biotite-hornblende-plagioclase, garnet-biotite-hornblende, garnet-hornblende-plagioclase, and garnet-hornblende. Conditions were also estimated using only hornblende. Selected thermobarometry results are in table 3.2 and selected graphical WEBINVEQ results are shown in figure 3.5. A mean temperature and pressure of 738 °C and 8221 bars was obtained from 14 different analyses. The standard deviations are 37.8 and 1434.7. Overall, temperature ranged from 678 to 789 °C and pressure ranged from 6290 to 9894 bars.

Table 3.2	025 055a A	025 055a B	025 055a C
gt-hb-bt-plag	735 °C, 6.3 kbars		
gt-hb-bt	721 °C, 6.3 kbars	788 °C, 9.5 kbars	
gt-hb-plag	734 °C, 9.1 kbars	789 °C, 9.8 kbars	
gt-hb	721 °C, 6.4 kbars	786 °C, 9.2 kbars	
hornblende	678 °C, 6.4 kbars	751 °C, 9.3 kbars	723 °C, 8.2 kbars

Figure 3.5 WEBINVEQ results for sample 025 055a from the Wolf Grove Structure. Mineral assemblages used for the calculations are as follows A = garnet-biotite-hornblende-plagioclase, B = garnet-biotite-hornblende, C = garnet-hornblende-plagioclase, D = garnet-hornblende, and E = hornblende.

Sample 025 055a

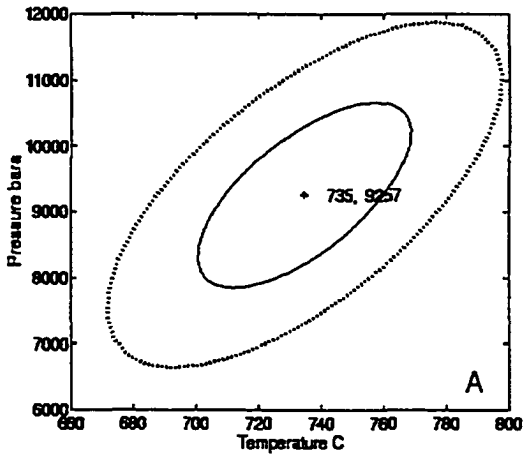

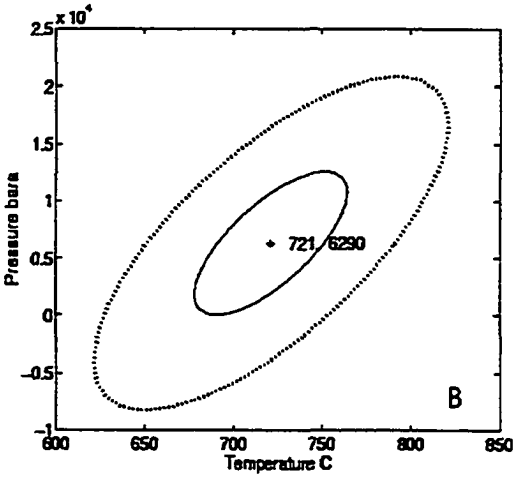

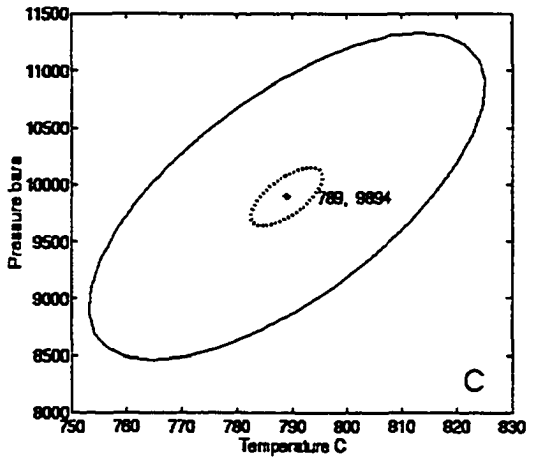

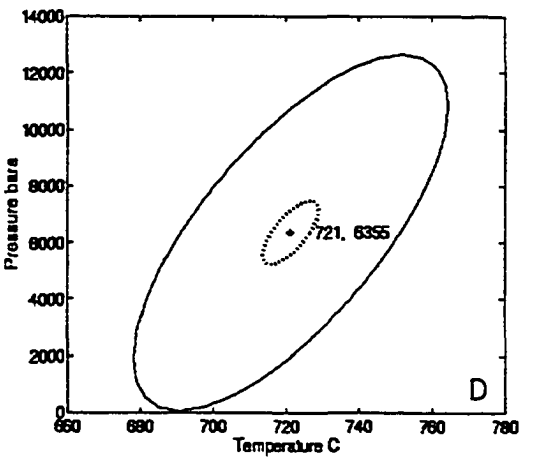

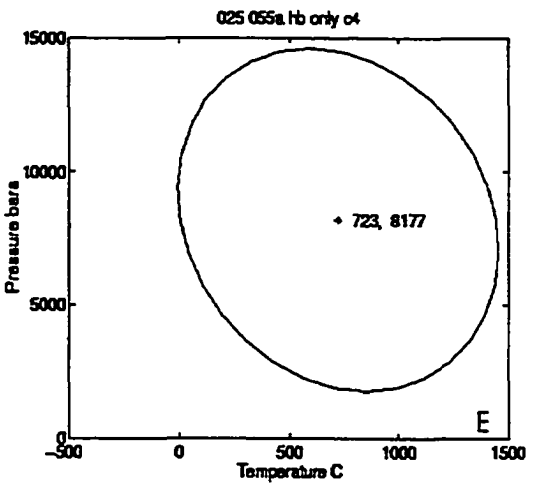

3.5.6 Sample 050 008

Sample 050 008 is a garnet amphibolite collected from outcrop exposed near Quarry Road on the east side of the Wolf Grove Structure. This sample contains plagioclase, hornblende, clinopyroxene, garnet, biotite, and quartz. Chlorite is present as an alteration product in the cores of the amphibole and clinopyroxene. A small amount of cloudy chlorite also appears to be overgrowing biotite and garnet. The garnets in sample 050 008 are very large and range from 2-5 mm across. They are typically subhedral with slightly ragged grain boundaries and few inclusions of plagioclase, quartz or altered biotite. The presence of amphibole, pyroxene, biotite and chlorite indicates that equilibrium may not have be achieved by this sample.

Pressure-temperature estimates were produced for sample 050 008 using the following mineral combinations; garnet-biotite-hornblende-clinopyroxene-plagioclase, garnet-hornblende-clinopyroxene-plagioclase, garnet-biotite-hornblende-plagioclase, garnet-biotite-hornblende, garnet-hornblende-plagioclase, and garnet-hornblende. Conditions were also calculated using only hornblende. Thermobarometry results are in table 3.3 and selected graphical WEBINVEQ results are shown in figure 3.6. 14 analyses yielded a mean temperature and pressure of 776 °C and 7906 bars with standard deviations of 76.1 and 1374.9. Temperature varied between 668 and 891 °C and pressure ranged from 5560-9900 bars.

Sample 050 008

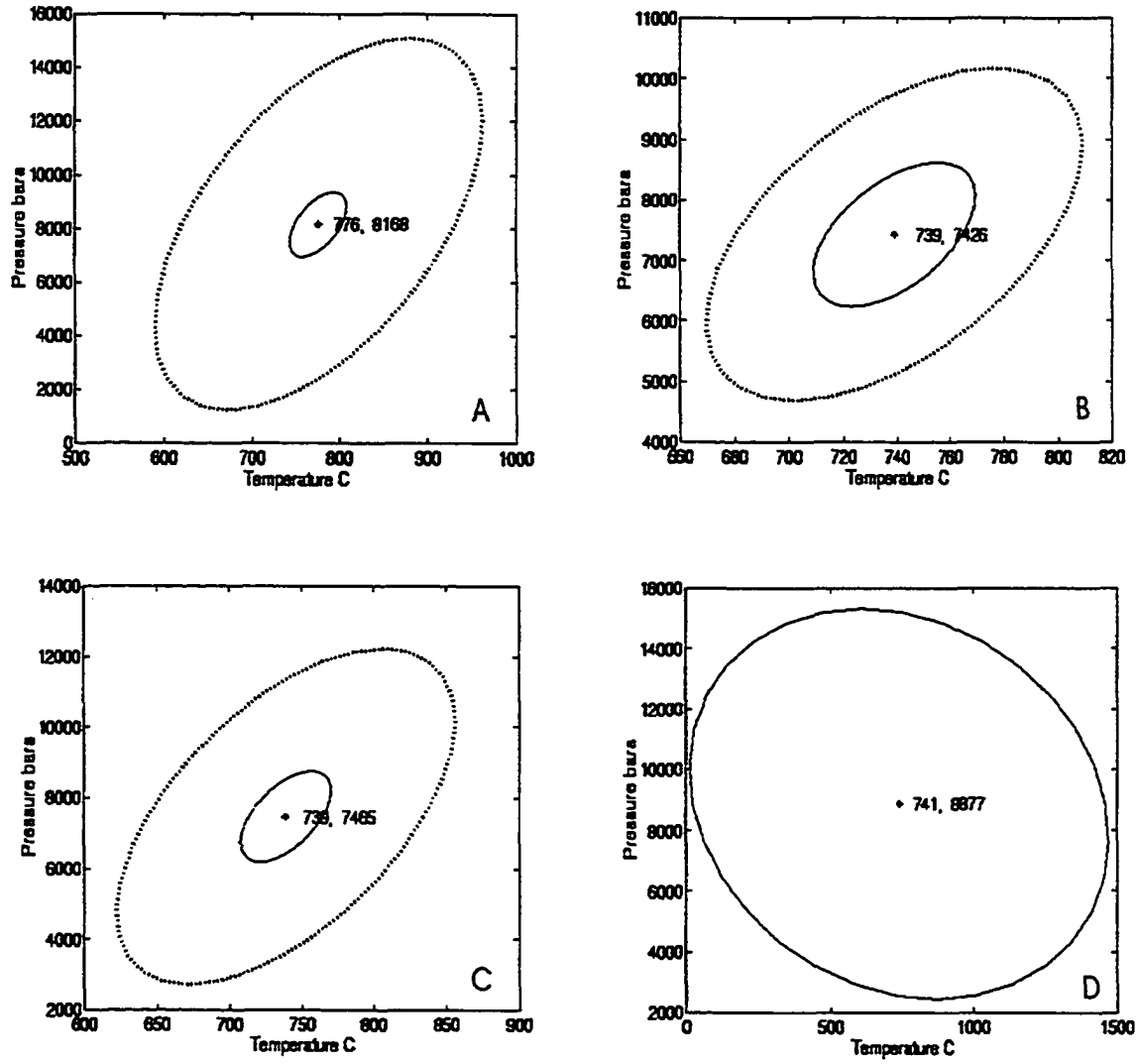

Figure 3.6 WEBINVEQ results for the sample 050 008 from the Wolf Grove Structure. Mineral assemblages used for the calculations are as follows: A = garnet-biotite-clinopyroxene-hornblende-plagioclase, B = garnet-clinopyroxene-hornblende-plagioclase, C = garnet-hornblende-plagioclase, and D = hornblende.

Table 3.3	050 088 A	050 008 B	050 008 C
gt-hb-bt-plag	670 °C, 5.7 kbars	813 °C, 9.9 kbars	812 °C, 9.4 kbars
gt-hb-bt			891 °C, 9.1 kbars
gt-hb-plag	749 °C, 7.5 kbars		
gt-hb			884 °C, 8.5 kbars
hornblende			741 °C, 8.9 kbars
gt-hb-cpx-bt-plag	668 °C, 5.6 kbars	776 °C, 8.2 kbars	761 °C, 7.3 kbars
gt-hb-cpx-plag	739 °C, 7.4 kbars		749 °C, 9.4 kbars

3.5.7 Sample 995 0035b

This sample is a garnet amphibolite collected from a large outcrop along Tatlock Road. Plagioclase, biotite, hornblende, quartz, garnet, chlorite and iron oxides comprise the mineral assemblage. Matrix plagioclase and quartz retains some very fine-grained mortar texture which has partially annealed. Amphibole and biotite occur as fine-grained laths aligned into a moderately developed foliation. Chlorite has replaced both hornblende and biotite and displays anomalous blue interference. Garnets range from 1-3 mm in diameter and are generally anhedral. The garnets contain multiple inclusions of quartz, plagioclase, biotite, and hornblende. One diamond-shaped hornblende inclusion, associated with quartz shows evidence of zoning along the rim. Garnets are surrounded by circular zones of coarser plagioclase and quartz which may also contain biotite and amphibole.

Three domains within the thin section were analysed. Pressure and temperature conditions were calculated for the following mineral combinations: garnet-biotite-

hornblende-plagioclase, garnet-biotite-hornblende, garnet-hornblende-plagioclase, and garnet-hornblende. Conditions were also estimated using only hornblende. Thermobarometry results are presented in table 3.4 and selected graphical WEBINVEQ results are shown in figure 3.7. Results from sample 995 0035b fall into two groups. The first group has a mean temperature of 723 °C and a mean pressure of 7799 bars. These data were obtained from 7 different analyses with standard deviations of 22.4 and 264.0. For this group the temperature ranges from 701 to 744 °C and pressure ranges from 7562 to 8050 bars. The second group yielded pressures which are significantly lower than the first group. The mean temperature of the second group is 663 °C and a pressure of 2464 bars. This is based on 9 analyses with standard deviations of 59.9 and 640.8. Temperature shows a larger range (584-720 °C) than group one. Pressure varied between 1800 and 3195 bars.

Table 3.4	995 0035b A	995 0035b B
gt-hb-bt-plag	701 °C, 7.6 kbars	741 °C, 8.0 kbars
gt-hb-bt	680 °C, 1.8 kbars	720 °C, 2.9 kbars
gt-hb-plag	707 °C, 7.6 kbars	744 °C, 8.0 kbars
gt-hb	681 °C, 1.9 kbars	720 °C, 3.0 kbars
hornblende	584 °C, 2.0 kbars	595 °C, 3.2 kbars

3.5.8 Sample 989 988

This sample was collected from a garnet amphibolite outcrop exposed along Miller Road, near the center of the Wolf Grove Structure. This sample exhibits similar

Sample 995 0035b

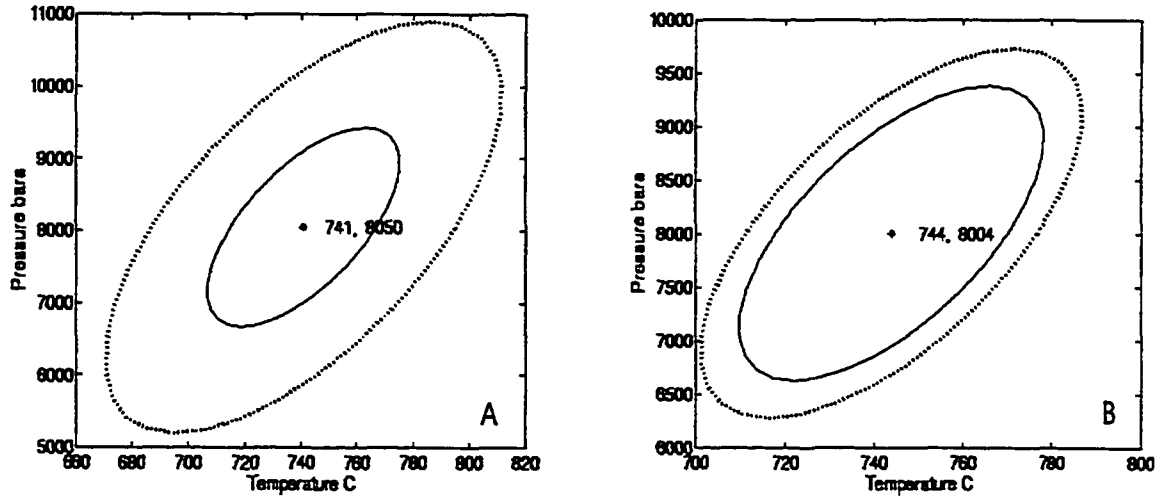

Figure 3.7 WEBINVEQ results for the sample 995 0035b from the Wolf Grove Structure. Mineral assemblages used for the calculations are as follows: A = garnet-biotite-hornblende-plagioclase, B = garnet-hornblende plagioclase.

textures and mineralogy to the sample above. In 989 988, the mortar texture plagioclase and quartz have been more completely recrystallized into large grains with undulose extinction. Twinning is not visible in the feldspars. Amphibole forms ragged to subhedral diamonds. Hornblende is mostly pleochroic in shades of green and brown but a few grains are bluish green to green. Biotite shows little preferential orientation and is intergrown with hornblende. Garnet is divisible into two size categories. Small garnets ($\leq$0.5 mm) are typically euhedral with no inclusions. Larger, anhedral to subhedral garnets range in size from 2-5 mm and contain many inclusions of plagioclase, quartz, biotite and hornblende. Many of the larger garnets are fractured and are aligned in a weak foliation.

Four domains containing garnet, hornblende, ± biotite and plagioclase were analysed within sample 989 988. Thermobarometry results are in table 3.5 and selected graphical WEBINVEQ results are shown in figure 3.8. 14 of 19 thermobarometry calculations using the following mineral combinations: garnet-biotite-hornblende-plagioclase, garnet-biotite-hornblende, garnet-hornblende-plagioclase, garnet-hornblende and hornblende yielded results which fall within two distinct ranges. The first group yielded higher temperatures and pressures, although there is overlap with the temperature range of the second group which displays lower pressures. The mean temperature of group 1 is 720 °C at a pressure of 6165 bars for 8 analyses with standard deviations of 23.3 and 862.1. Temperature ranged from 695-758 °C and pressure varied between 5383 and 7646 bars. Average temperature and pressure for the second group is 675 °C and 2094 bars, calculated using 6 analyses with standard deviations of 90.4 and 168.0.

Sample 989 988

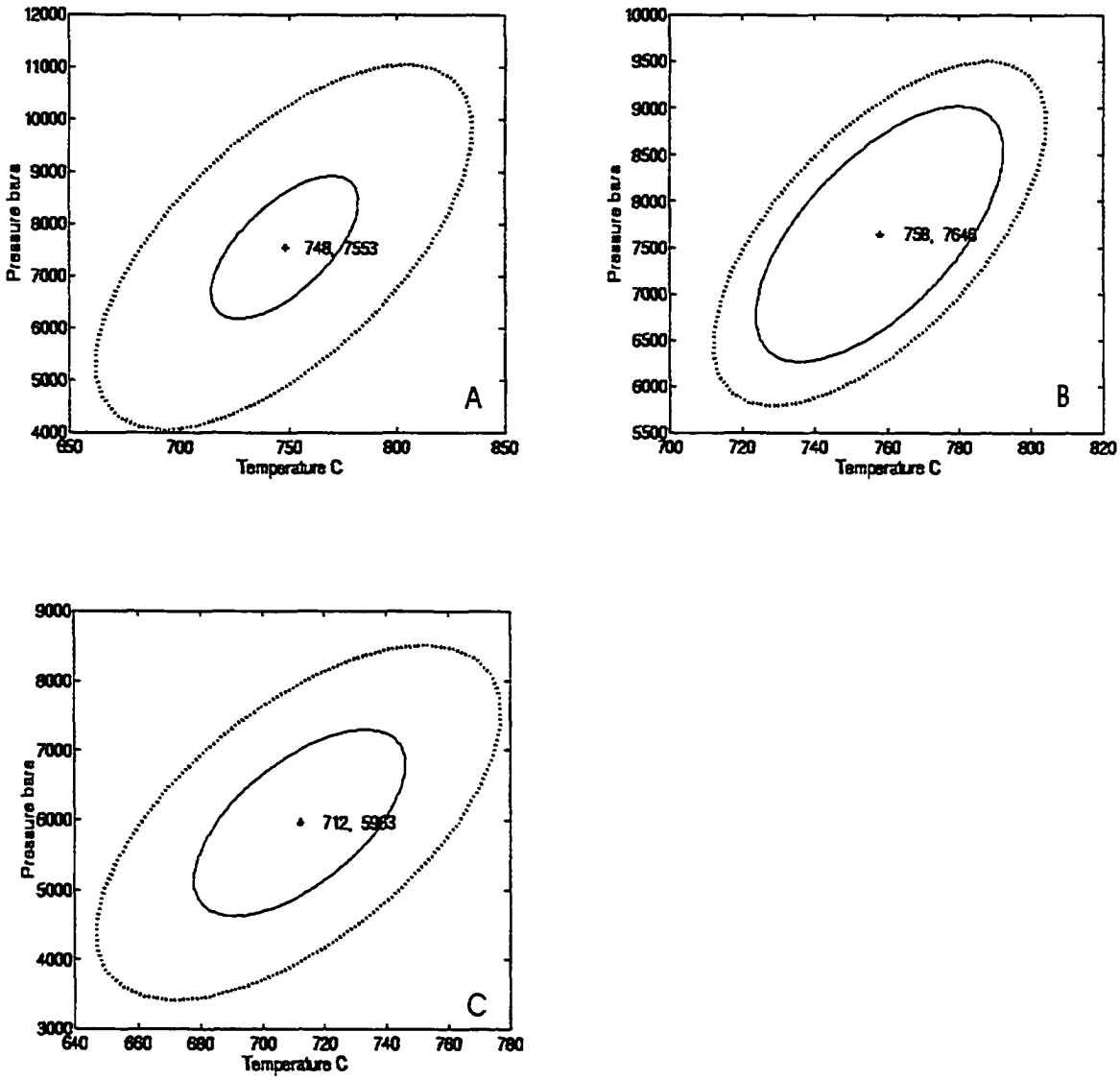

Figure 3.8 WEBINVEQ results for the sample 989 988 from the Wolf Grove Structure. Mineral assemblages used for the calculations are as follows: A = garnet-biotite-hornblende-plagioclase, B = garnet-hornblende-plagioclase, and C = garnet-biotite-hornblende-plagioclase.

Temperature and pressure ranged from of 571 to 728 °C and 1934 to 2269 bars for group 2.

Table 3.5	989 988 A	989 988 B	989 988 C
gt-hb-bt-plag	712 °C, 6.0 kbars	724 °C, 5.9 kbars	
gt-hb-bt		728 °C, 2.0 kbars	
gt-hb-plag	715 °C, 6.0 kbars	758 °C, 7.6 kbars	695 °C, 5.4 kbars
gt-hb		727 °C, 1.9 kbars	
hornblende		571 °C, 2.3 kbars	

3.6 Thermobarometry Results - Pakenham Dome

3.6.1 Sample 954 051

Sample 954 051 is a migmatitic amphibolite, collected from the edge of the Pakenham Dome, north of Clayton Lake along Tatlock Road. This sample is comprised of plagioclase, quartz, biotite, amphibole, and garnet. Unlike the previous samples analysed the amphibole is gedrite (orthoamphibole) which displays a needle-like crystal form ≥ 2 cm in length and parallel extinction. Gedrite and biotite define the well developed foliation. Gedrite contains inclusions of plagioclase and quartz and appears to have overgrown some biotite. The garnets in sample 954 051 are very large (≤ 5 mm) and contain multiple inclusions of quartz, plagioclase, and biotite. They exhibit rounded subhedral to euhedral shapes and are commonly fractured. Biotite appears to both wrap around some garnets and be overgrown by garnet. Plagioclase and quartz are strained and retain shadowy evidence of previous crystal outlines. Feldspar shows minor sericite alteration. Chlorite alteration is present along the edges of some biotite laths. Grain

boundaries generally intersect at 120 ° angles indicating equilibrium among the phases present.

One very large garnet (<5 cm in diameter) and two smaller garnets (> 1 cm) were analysed, in addition to biotite, amphibole and plagioclase. Pressure and temperature conditions were calculated for the following mineral combinations: garnet-biotite-gedrite-plagioclase, garnet-biotite-hornblende, garnet-gedrite-plagioclase, garnet-gedrite and gedrite. Selected thermobarometry results are in table 3.6 and selected graphical WEBINVEQ results are shown in figure 3.9. 22 P-T results fall within two groups similar to samples 995 0035b and 989 988 of the Wolf Grove Structure but with overall lower temperatures for both groups. The mean temperature and pressure for group 1 is 598 °C and 8513 bars, based on 13 calculations with standard deviations of 31.2 and 320.2. Temperature ranges from 530 to 762 °C and pressure ranges from 6344 to 9706 bars for group 1. 508 °C and 2285 bars is the average P-T result calculated for the second group. This is based on 9 analyses with standard deviations of 10.8 and 440.5. 496-520 °C is the temperature range and 1466-2659 bars is the pressure range for group 2.

Table 3.6	954 051 A	954 051 B	954 051 D
gt-hb-bt-plag		501 °C, 2.4 kbars	500 °C, 2.3 kbars
gt-hb-bt	530 °C, 9.3 kbars	539 °C, 8.2 kbars	531 °C, 6.3 kbars
gt-hb-plag	496 °C, 2.2 kbars	516 °C, 2.7 kbars	520 °C, 2.7 kbars
gt-hb	532 °C, 9.5 kbars	539 °C, 8.2 kbars	545 °C, 8.2 kbars
hornblende	748 °C, 9.1 kbars	711 °C, 7.7 kbars	711 °C, 7.7 kbars

Sample 954 051

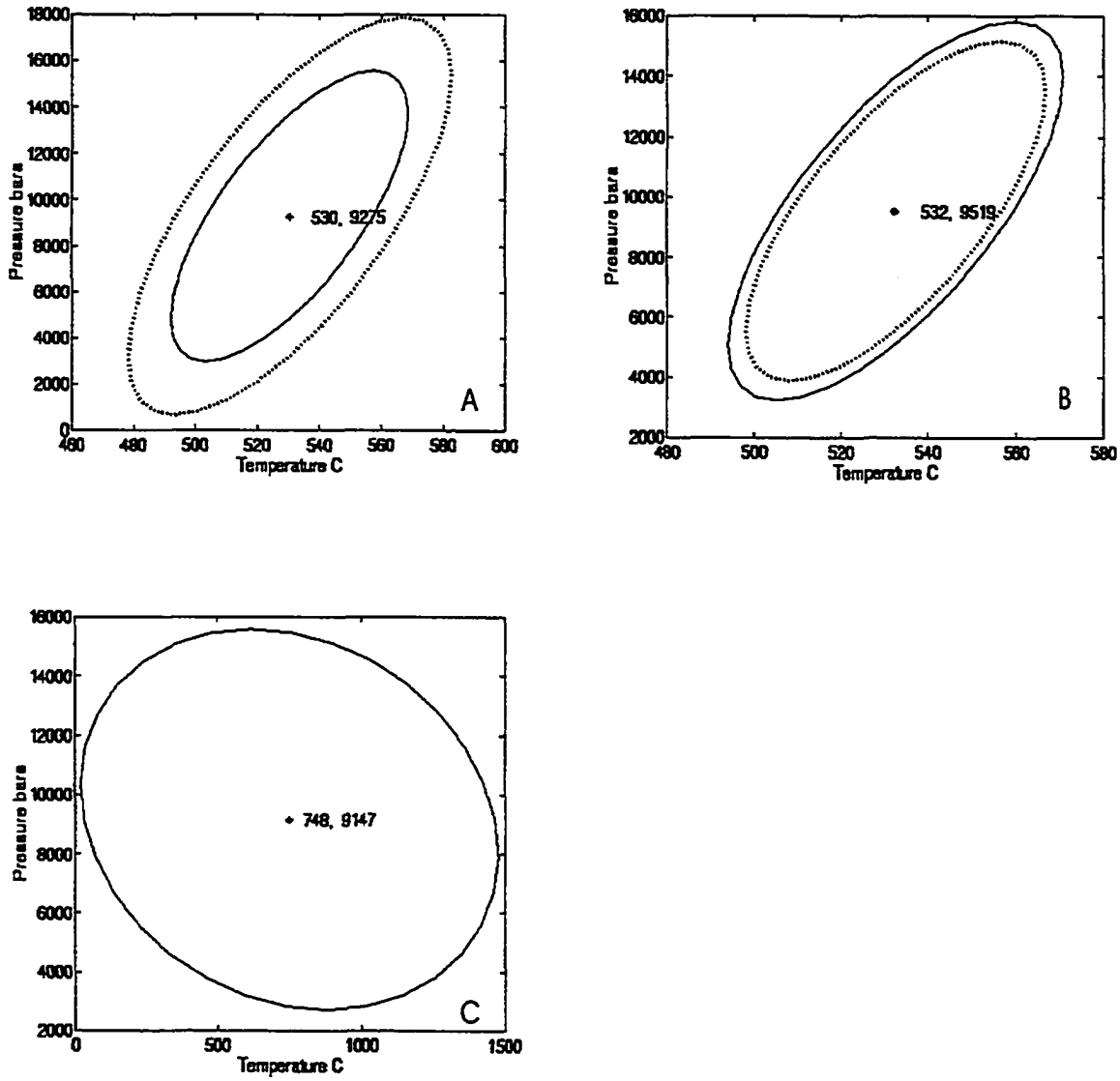

Figure 3.9 WEBINVEQ results for the sample 954 051 from the Pakenham Dome. Mineral assemblages used for the calculations are as follows: A = garnet-biotite-hornblende, B = garnet-hornblende, and C = hornblende

3.7 Thermobarometry Results - Lavant Gabbro Complex

3.7.1 Sample 859 004

This sample is a garnet-bearing metadiorite from the northeastern corner of the field area. It was collected from an outcrop exposed on Wark's Road and represents an intermediate phase of the Lavant Gabbro Complex. Plagioclase, hornblende, biotite, garnet are present in the sample with trace amounts of quartz and iron oxides. The sample exhibits a very poorly developed foliation defined by the sub-parallel alignment of biotite. Some biotite laths are aligned at an acute angle to the main foliation. Hornblende forms ragged edged anhedral grains which are pleochroic in shades of green and bluish-green. Larger grains contain cores of biotite. Plagioclase crystals are strained with shadowy to absent twinning and possible core to rim zoning. Garnets are anhedral to subhedral, range in size from 0.5-2 mm and contain inclusions of plagioclase, quartz, biotite, and iron oxide. Most garnets are fractured. Grain boundaries between phases are generally sharp and straight indicating equilibrium conditions.

Garnet, biotite, hornblende, and plagioclase were analysed for thermobarometry. The following mineral combinations were used to calculate pressure and temperature conditions: garnet-biotite-hornblende-plagioclase, garnet-biotite-hornblende, garnet-hornblende-plagioclase, garnet-hornblende and hornblende alone. Selected thermobarometry results are in table 3.7 and selected graphical WEBINVEQ results are shown in figure 3.10. 554 °C and 3321 bars is the mean P-T result for sample 859 004 based on 21 calculations with standard deviations of 59.9 and 1587.6. This is significantly lower in temperature and pressure than the majority of results obtained for

Sample 859 004

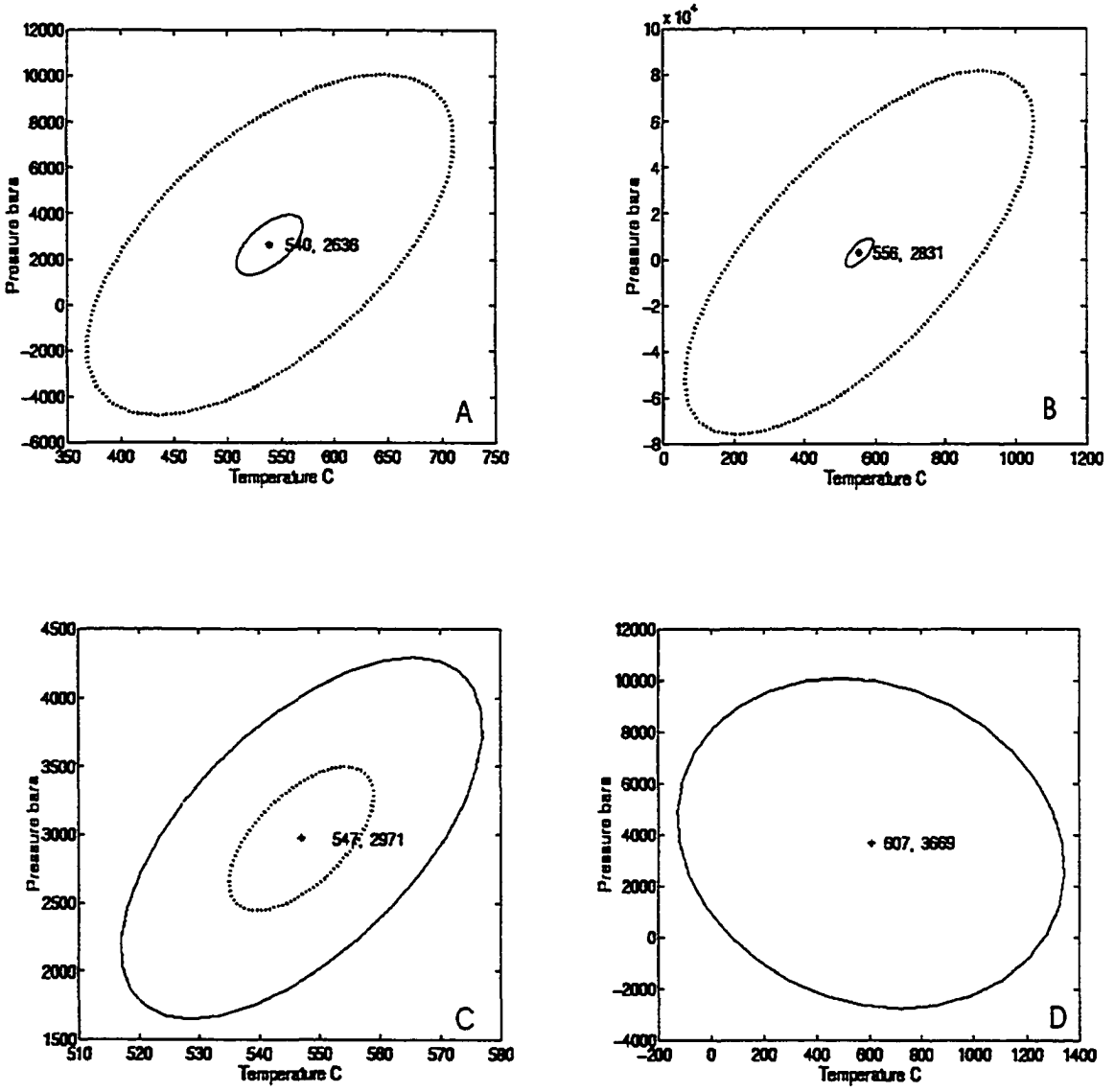

Figure 3.10 WEBINVEQ results for the sample 859 004 from the Lavant Gabbro Complex. Mineral assemblages used for the calculations are as follows: A = garnet-biotite-hornblende-plagioclase, B = garnet-biotite-hornblende, C = garnet-hornblende-plagioclase, and D = hornblende.

the Wolf Grove Structure. The temperature ranges from 355 to 665 °C and pressure varies between 1000 and 6052 bars.

Table 3.7	859 004 A	859 004 B	859 004 D
gt-hb-bt-plag	546 °C, 4.4 kbars	501 °C, 2.4 kbars	540 °C, 2.6 kbars
gt-hb-bt	355 °C, 4.9 kbars	539 °C, 8.2 kbars	556 °C, 2.8 kbars
gt-hb-plag	531 °C, 2.5 kbars	516 °C, 2.7 kbars	590 °C, 4.1 kbars
gt-hb	547 °C, 3.0 kbars	539 °C, 8.2 kbars	599 °C, 6.0 kbars
hornblende	550 °C, 3.8 kbars	711 °C, 7.7 kbars	665 °C, 5.9 kbars

3.8 Thermobarometry Results - Frontenac terrane - Lyndhurst Area

3.8.1 Sample 070 304

Sample 070 304 is a garnet-hornblende gneiss collected from the Lyndhurst area of the Westport map sheet. It is the only unquestionable sample from the Frontenac terrane. The sample is comprised of plagioclase, biotite, hornblende, quartz, garnet, minor chlorite and iron oxides. Garnets in this sample are small, anhedral and display ragged grain boundaries. Garnet and hornblende both appear to be overgrowing biotite. Hornblende is deep green with serrated grain edges. Plagioclase is strained and exhibits minor alteration limited to the cores of crystals.

Garnet, biotite, hornblende, and plagioclase were analysed for thermobarometry. Pressure-temperature conditions were calculated using both core and rim compositions of hornblende. The following mineral combinations were used to calculate pressure and temperature conditions: garnet-biotite-hornblende-plagioclase, garnet-biotite-hornblende,

garnet-hornblende-plagioclase, garnet-hornblende and hornblende alone. Selected thermobarometry results are in table 3.8 and selected graphical WEBINVEQ results are shown in figure 3.11. The results are divisible into two groups with some overlap in temperature but very different pressure conditions. The higher pressure group yielded a mean temperature and pressure of 71 °C and 7522 bars, from 20 calculations with standard deviations of 23.1 and 1322.9. Temperature and pressure ranges for group 1 are 657-748 °C and 5335-9328 bars, respectively. Calculated average temperature and pressure conditions for the second group are 663 °C and 2641 bars. This is based on 9 results with standard deviations of 61.9 and 693.9. Temperature and pressure ranges for group 2 are 569-719 °C and 1942-3499 bars, respectively.

Table 3.8	070 304 A	070 304 C	070 304 E
gt-hb-bt-plag	710 °C, 7.9 kbars	698 °C, 8.1 kbars	713 °C, 7.0 kbars
gt-hb-bt	698 °C, 5.3 kbars	686 °C, 1.9 kbars	744 °C, 9.8 kbars
gt-hb-plag	711 °C, 8.0 kbars	716 °C, 8.3 kbars	738 °C, 7.4 kbars
gt-hb	700 °C, 5.5 kbars	687 °C, 2.0 kbars	
hornblende	657 °C, 5.6 kbars	569 °C, 2.2 kbars	677 °C, 6.4 kbars

3.9 Discussion

Peak metamorphic pressure and temperature conditions calculated by WEBINVEQ for samples collected within the Wolf Grove Structure produced results (figure 3.3) consistent with those previously reported by Buckley et al. (1997; figure 3.12). The mean temperature and pressure of peak metamorphism for rocks within the

Figure 3.11 WEBINVEQ results for sample 070 304, a gneiss from the Lyndhurst area. Mineral assemblages used for the calculations are as follows A = garnet-biotite-hornblende-plagioclase, B = garnet-hornblende-plagioclase, C = garnet-hornblende-plagioclase, D = garnet-hornblende and E = hornblende.

Sample 070 304

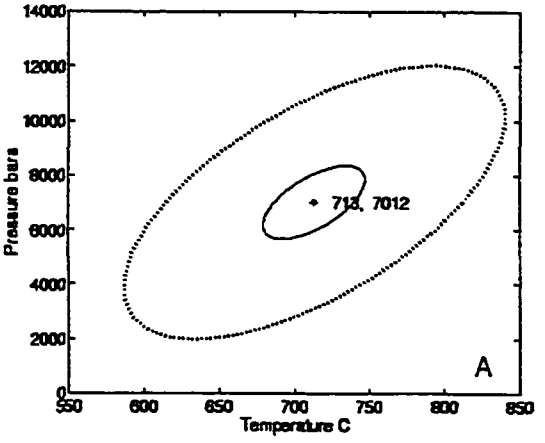

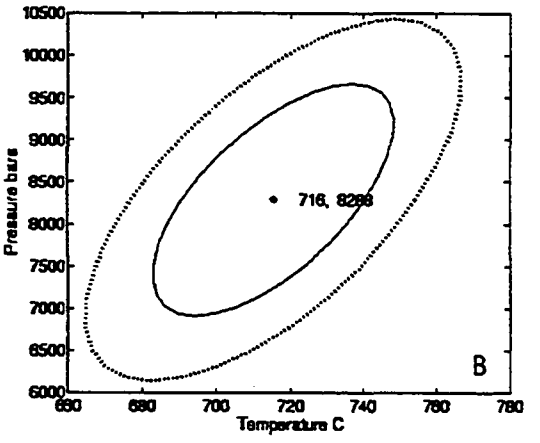

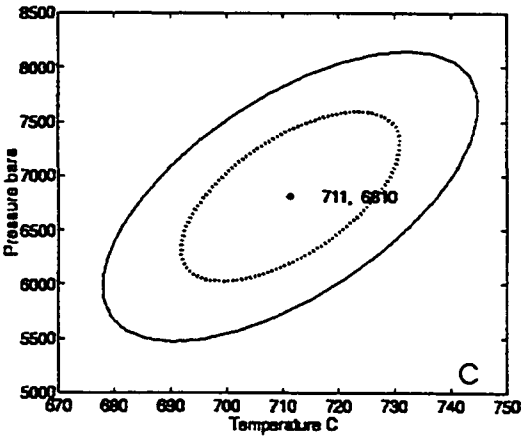

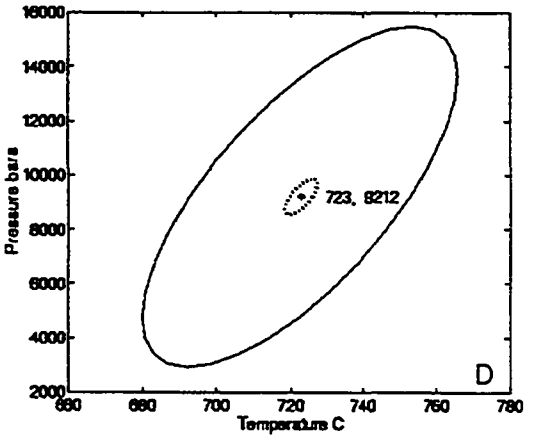

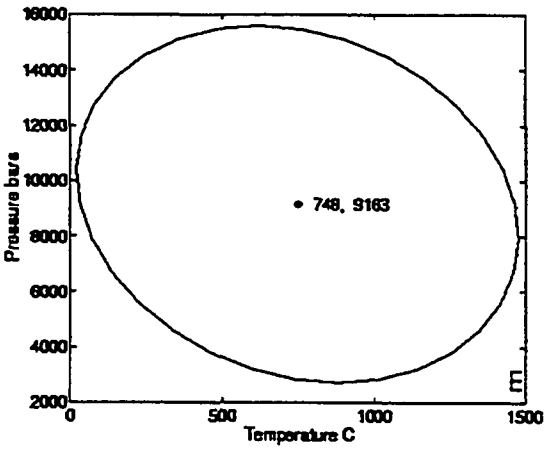

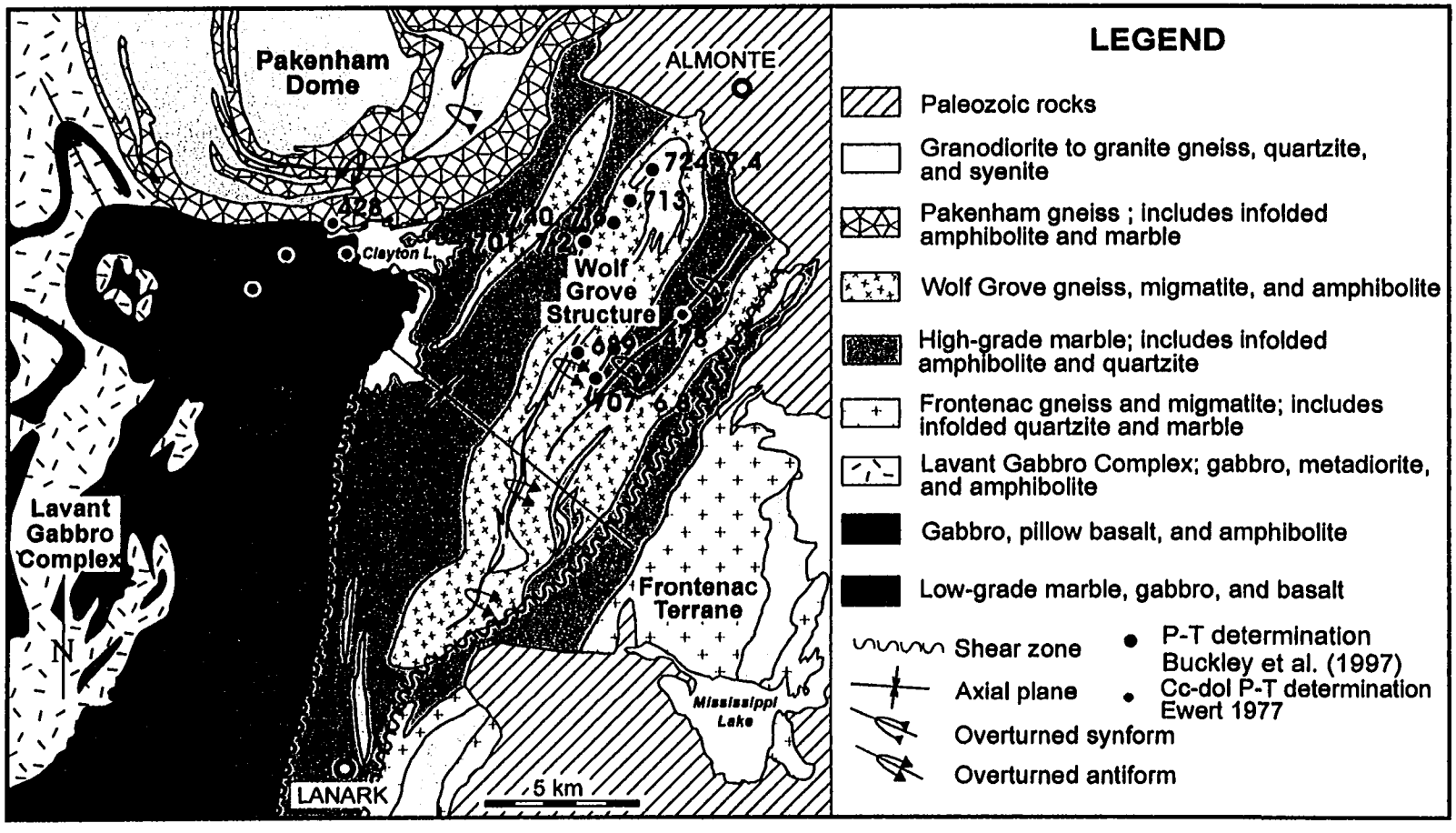

Figure 3.12 Simplified geological map of the Carleton Place area showing thermobarometry sites and results from two previous studies (Ewert, 1977; Buckley et al., 1997). (Modified from Reinhardt and Liberty, 1973)

structure is 713 °C at 7.8 kbars with results from the low pressure group excluded. This is based on 57 calculations with standard deviations of 82.7 and 1314.9. These conditions are in agreement with the assigned upper amphibolite grade based on mineralogy and petrography for rocks within the Wolf Grove Structure. Buckley et al. (1997) reported average metamorphic pressure and temperature conditions of 7.2 kbars at 718 °C for the Wolf Grove Structure. The consistency of P-T conditions for the different units within the structure indicates they were part of the structure during metamorphism. Geochronological work by Corfu and Easton (1997) resulted in an age of ~ 1168 Ma for this event.

Results from the Pakenham Dome indicate lower temperature and higher pressure conditions (598 °C and 8.5 kbars) prevailed within this structure compared to the data from the Wolf Grove Structure. However, the overall range in P-T conditions overlaps those recorded by the Wolf Grove Structure. Field and petrographic evidence from the migmatitic and gneissic units within the structure are indistinguishable from those within the Wolf Grove Structure.

Buckley et al. (1997) reported a roughly 2 kbar and 50 °C difference between P-T conditions for the Westport and Carleton Place areas. Results for Lyndhurst, from this study, suggest higher pressures similar to those recorded by the Wolf Grove Structure were experienced in the Westport area. The Lyndhurst sample also yielded low pressure results comparable to the Carleton Place rocks. However, as this is based on only one thin section, additional thermobarometry is needed to characterize the P-T conditions within the Frontenac terrane.

Pressure-temperature conditions calculated for the metadiorite sample from the Lavant Gabbro Complex are much lower than those of the Wolf Grove Structure. Thermobarometry yielded an average temperature of 554 °C at 3.3 kbars pressure. As the complex is a composite intrusion (Easton, 1992; Easton and Davidson, 1997), this low pressure-high temperature metamorphism is likely a result of contact metamorphism during emplacement of the various phases of the intrusion. Thermobarometry closer to the Clayton Lake shear zone is required to determine the extent of syn-Lavant metamorphism and the western limit of the ~1168 Ma event characteristic of the Wolf Grove Structure and the Frontenac terrane.

Based on the results obtained from thermobarometry, rocks in the Wolf Grove Structure and possibly the Pakenham Dome experienced either a prolonged metamorphic event or multiple events under variable pressure-temperature conditions. This is supported by the field and petrographic evidence, including relict mineral assemblages, variations in the size and form of garnets, and presence of biotite both aligned in the regional foliation and randomly oriented. Similarity of the results between rocks of the Carleton Place area and the Frontenac terrane implies a possible link between the two areas. However, the difference in pressure conditions suggests that the Wolf Grove Structure represents a different structural level (Buckley et al., 1997).

The very low pressure results from the Wolf Grove and Pakenham Structures may be consistent with a limited greenschist-facies metamorphism reported by Buckley et al. (1997) and Praamsma et al. (2000). Praamsma et al. (2000) concluded that ca. 1113 Ma U-Pb ages from titanite of the Pakenham granodiorite records the timing of either

greenschist-facies metamorphism and/or fluid infiltration, as the titanite preserves textural and isotopic evidence of a secondary origin by breakdown of Fe-Ti oxides. In addition, amphibolite from the Wolf Grove Structure with a greenschist-facies overprint contains titanite with a U-Pb age of ca. 1123 Ma (Corfu and Easton, 1997). Buckley et al. (1997) noted anthophyllite overgrowths on hornblende and the presence of relict clinopyroxenes.

Chapter 4 – Petrology of Siliceous Dolomitic Marbles

4.1 Introduction

Minerals or phases in metamorphosed siliceous carbonate rocks are composed of various combinations of components within the CaO-MgO-SiO_2-CO_2-H_2O system. Marbles with clay present in the protolith require one additional component, $KAlSi_3O_8$. As discussed in chapter 2, co-existing mineral assemblages in this system can be represented on MgO-SiO_2-$KAlSi_3O_8$ ternary diagrams projected from $CaCO_3$, H_2O, and CO_2, provided these phases are present in excess. The stability of these assemblages in marbles changes with variations in fluid composition as well as pressure and temperature.

The Gibb's phase rule ($f = c + 2 - \phi$) relates the number of phases and components within a rock to the number of equations constraining these phases; where f = degrees of freedom which is defined as the difference between the number of variables: pressure, temperature, and chemical potential of each component and the number of equations that constrain these variables, c = number of components (i.e. independently variable chemical entities such as CaO or $KAlSi_3O_8$), and ϕ = number of phases or minerals + fluid.

Various types of phase diagrams may be used to represent the stability of coexisting mineral assemblages in siliceous marbles. Isobaric or isothermal T-X_{CO2} phase diagrams are commonly used in the interpretation of the metamorphic history of siliceous marbles. A disadvantage of this approach is that the influence of a key metamorphic variable either temperature or pressure is obscured (Connolly and Trommsdorff, 1991).

A polybaric T-X_{CO2} section (figure 4.1) for aluminous, siliceous marbles was calculated by Flowers and Helgeson (1983). The polybaric T-X_{CO2} section has been produced with pressure increasing as a function of temperature according to a field gradient recorded in rocks of the Lepontine Alps in Switzerland and northern Italy (Turner, 1968: figure 4.2). Table 4.1 lists the reactions corresponding to the curves on figure 4.1. The assemblages constituting points I, II, III, IV, and V are also listed in table 4.1.

Figure 4.1 displays the stable relationships among the minerals calcite, dolomite, quartz, K-feldspar, phlogopite, talc, tremolite, diopside, and forsterite. Curves in the five component system CaO-MgO-SiO_2-CO_2-H_2O involve five phases and are divariant (f = 2). Divariant relations correspond to the fields on figure 4.1. Points such as I, III, and V are univariant (f = 1) and plot as a curves in P-T space. These assemblages appear as points (figure 4.1) on the T-X_{CO2} section because a degree of freedom is used in construction of the diagram to specify P as a function of T. In T-X_{CO2} space, they are referred to as isobaric invariant points. Each curve omits one of the minerals or fluid around the isobaric invariant point. Points II and IV belong to the six component system CaO-MgO-$KAlSi_3O_8$-SiO_2-CO_2-H_2O. The number of curves around these isobaric invariant points is reduced because of degeneracy. In these cases, both K-feldspar and phlogopite are omitted.

Several authors have projected the trace of one or more isobaric invariant points onto the P-T plane including Connolly and Trommsdorff (1991; figure 4.3) and Carmichael (1991; figure 4.4). Connolly and Trommsdorff suggest that P-T projections

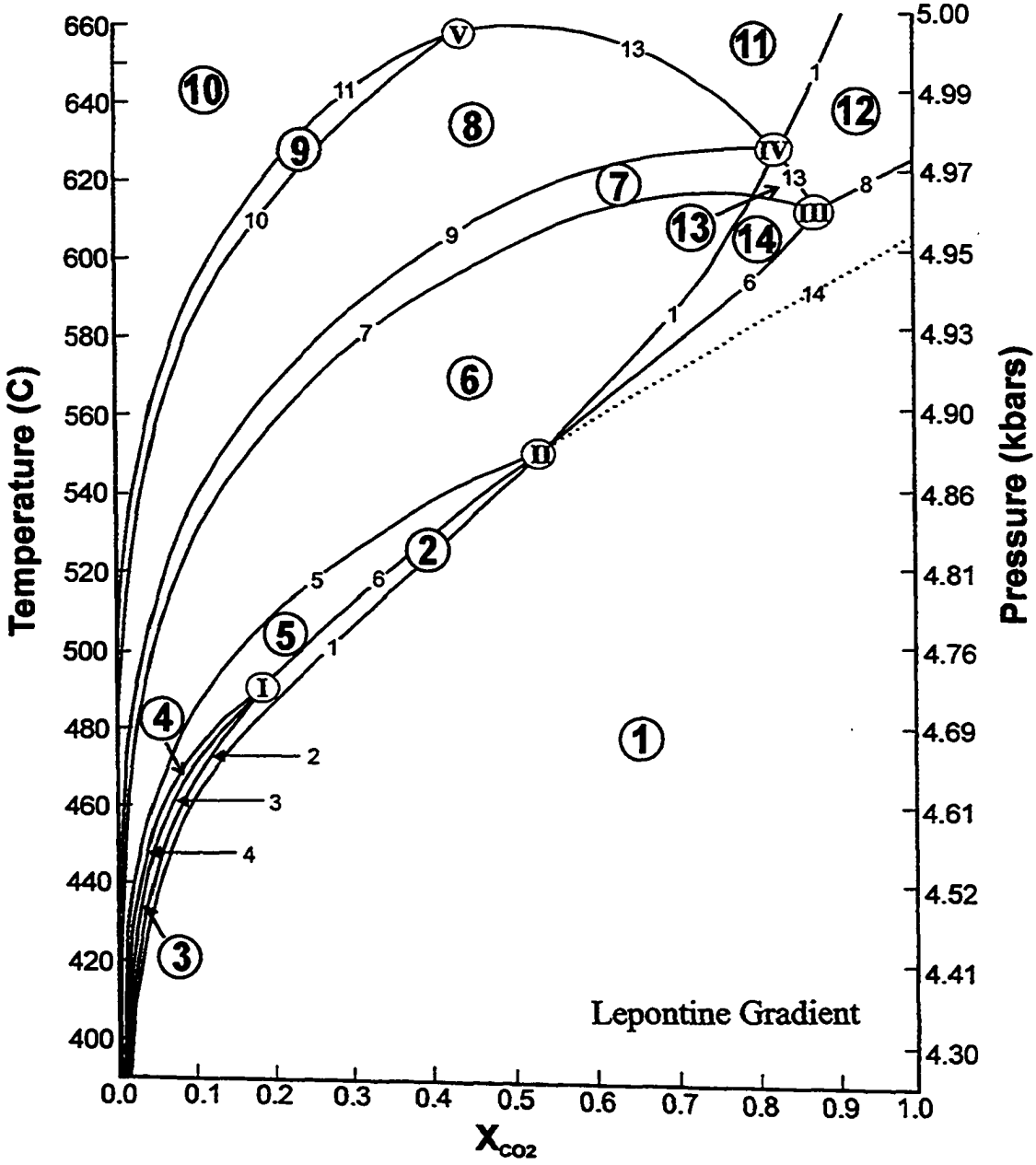

Figure 4.1 Polybaric T-X_{co2} diagram for siliceous marbles calculated using a field gradient from rocks of the Lepontine Alps (Turner, 1968). After Flowers and Helgeson (1983). Curve 14 is dashed as it is only observed in magnesite-bearing carbonates.

Table 4.1 T-X_{CO2} diagram reaction list for the Lepontine Alps, Lavant Gabbro and Wolf Grove (1) gradients

(1) K-feldspar + 3 dolomite + H_2O = phlogopite + 3 calcite + 3 CO_2

(2) 3 dolomite + 4 quartz + H_2O = talc + 3 calcite + 3 CO_2

(3) 5 talc + 6 calcite + 4 quartz = 3 tremolite + 6 CO_2 + 2 H_2O

(4) 2 talc + 3 calcite = tremolite + dolomite + H_2O + CO_2

(5) 24 quartz + 6 calcite + 5 phlogopite = 3 tremolite + 5 K-feldspar + 2 H_2O + 6 CO_2

(6) 5 dolomite + 8 quartz + H_2O = tremolite + 3 calcite + 7 CO_2

(7) tremolite + 3 calcite + 2 quartz = 5 diopside + 3 CO_2 + H_2O

(8) dolomite + 2 quartz = diopside + 2 CO_2

(9) 3 tremolite + 6 calcite + K-feldspar = 12 diopside + phlogopite + 6 CO_2 + 2 H_2O

(10) tremolite + 11 dolomite = 8 forsterite + 13 calcite + 9 CO_2 + H_2O

(11) 3 tremolite + 5 calcite = 11 diopside + 2 forsterite + 3 H_2O + 5 CO_2

(12) diopside + 3 dolomite = 2 forsterite + 4 calcite + 5 CO_2

(13) tremolite + 3 calcite = dolomite + 4 diopside + H_2O + CO_2

Point I = calcite-dolomite-quartz-talc-tremolite-fluid

Point II = calcite-dolomite-quartz-phlogopite-K-feldspar-tremolite-fluid (Di)

Point III = calcite-dolomite-quartz-tremolite-diopside-fluid (Ksp, Phl)

Point IV = calcite-dolomite-phlogopite-K-feldspar-tremolite-diopside-fluid (Q)

Point V = calcite-dolomite-tremolite-diopside-forsterite-fluid

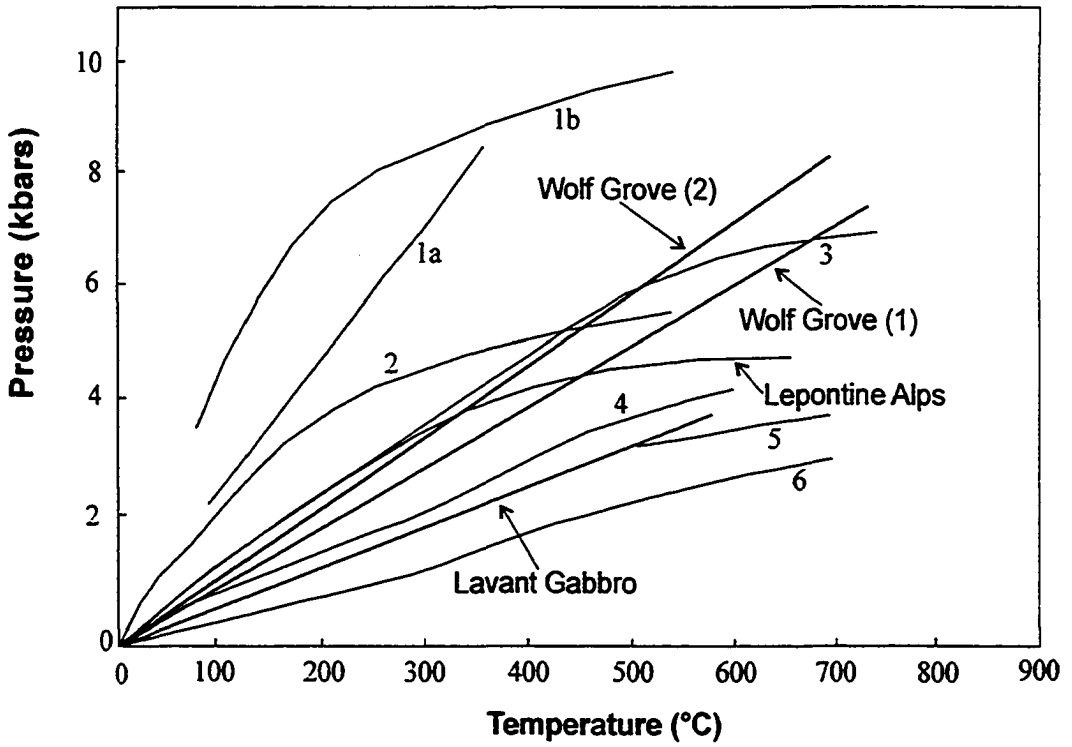

Figure 4.2 P-T diagram displaying examples of various field gradients. Field gradients calculated for this study and for the Lepontine Laps are as marked. The remaining gradients are from the following locations: 1a = glaucophane schist, Japan, 2 = Alpine schist belt, New Zealand, 3 = southeastern Dalradian Scotland (Barrow's zones), 4 = New Hampshire and Vermont, 5 = amphibolite-granulite, northwestern Adirondacks, and 6 = New Hampshire and Vermont. After Turner (1968).

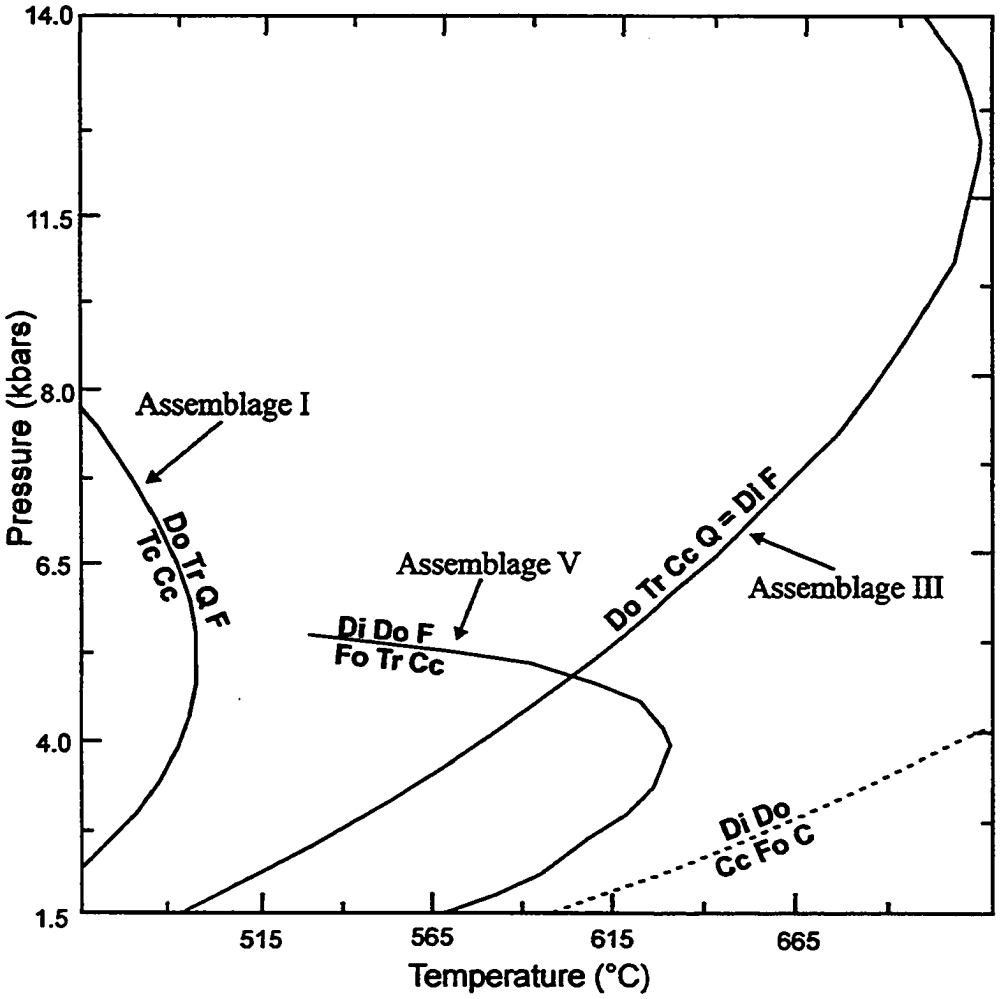

Figure 4.3 P-T diagram displaying the univariant curves relevant to the Carleton Place area. After Connolly and Trommsdorff (1991).

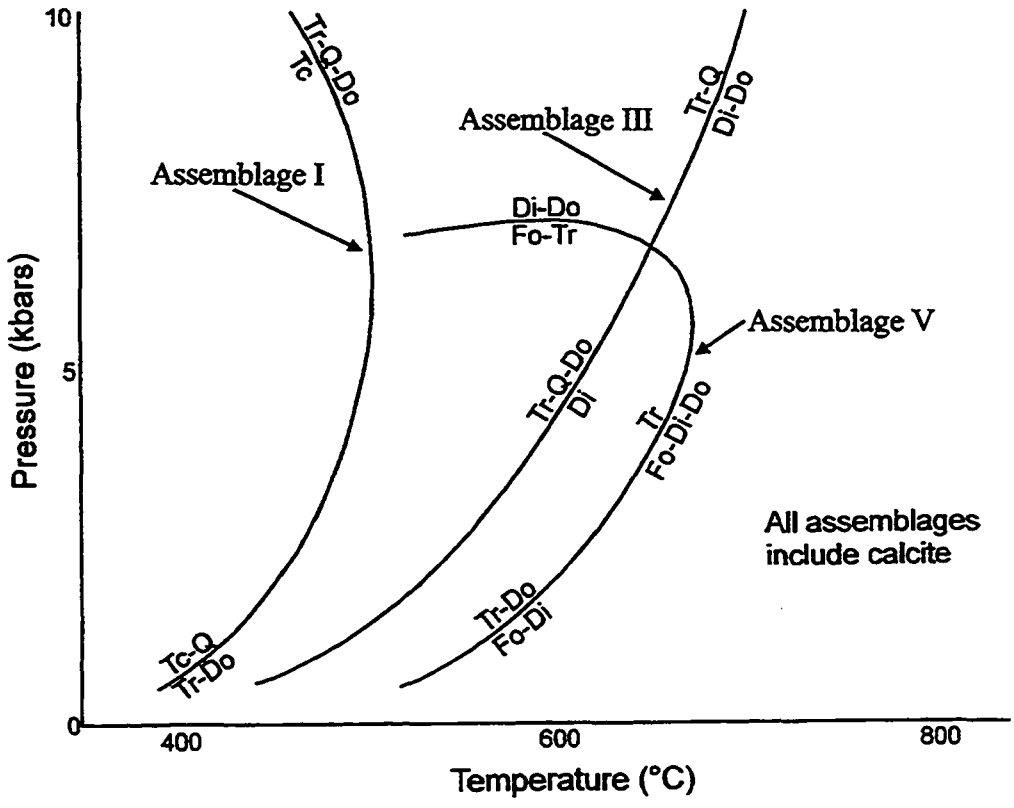

Figure 4.4 P-T diagram displaying the univariant curves relevant to the Carleton Place area. After Carmichael (1991).

have the advantage of defining the absolute stability of mineral assemblages with or without a co-existent fluid phase. Carmichael suggests that such diagrams have a greater utility in the mapping of isograds in the field compared to isobaric T-X_{CO2} sections. Similar to the method proposed by Skippen (1974) in which the isobaric invariant point is bracketed by mineral assemblages above and below the point, Carmichael suggests that identifying the divariant assemblages above and below the univariant curve on the P-T projection is sufficient to map the trace of the isobaric invariant point in the field, based on the work of Ewert (1977).

The P-T diagrams shown in figures 4.3 and 4.4 have been simplified to display curves applicable to the marbles in the Carleton Place area. The curves correspond to the three invariants, namely I, III, and IV (see table 4.1). Comparison of the figures indicates the trajectories of the curves are similar but their upper and lower P-T limits are different. These variations may be a reflection of the different databases employed by the authors in the calculation of the P-T projections. Connolly and Trommsdorff (1991) used data from Berman (1988), Kerrick and Jacobs (1981) and Connelly et al., (1992). Carmichael (1991) employed thermochemical data from Helgeson et al. (1978), H_2O fugacities from Helgeson and Kirkham (1974), CO_2 fugacity coefficients from Burnham and Wall (Carmichael, personal communication). These P-T diagrams are of limited usefulness in phlogopite- and K-feldspar-bearing marbles as data for these phases are not included.

In order to determine whether the T-X_{CO2} diagram of Flowers and Helgeson (1983) is appropriate for the metamorphic conditions of the siliceous marbles within the Carleton Place area, field gradients were calculated using thermobarometry data from the

gneissic and meta-igneous rocks associated with the marbles in the study area.

4.2 Field Gradients

The minerals within metamorphic rocks are an important record of the pressure-temperature history of the rocks. A metamorphic field gradient is obtained by fitting a line to a plot of the peak pressure-temperature conditions for rocks in an area that have experienced a common metamorphic history.

Field, petrographic, and thermobarometric evidence from the rocks within the Carleton Place area indicate that uniform metamorphic conditions did not exist across the whole of the field area. The western section of the field area is dominated by poorly to moderately foliated marbles, which have been intruded by plutonic rocks of the Lavant Gabbro Complex. Typical mineral assemblages consist of calcite + dolomite + phlogopite + tremolite ± talc suggesting metamorphic grade is low. In contrast, the eastern portion of the field area is characterized by marbles, quartzites, and gneissic rocks. Both the marbles and the gneisses display well-developed foliation and are commonly tightly- to isoclinally folded. Metamorphic grade is higher than in the western half of the field area based on mineralogy within the gneisses and the marbles. The gneissic rocks contain garnet, biotite, hornblende, feldspars and clinopyroxene. Migmatitic textures are common. Marbles generally are composed of calcite + dolomite + phlogopite + tremolite ± diopside or forsterite. A shear zone west of Clayton Lake (Easton and Hildebrand, 1994) forms the boundary between these two sections of the field area and is marked by a zone of marble breccia.

Thermobarometric data from the Lavant Gabbro Complex in the west and gneissic rocks of the Wolf Grove Structure in the east also suggest different metamorphic conditions prevailed on either side of the Clayton Lake shear zone. Rocks from the Lavant Gabbro Complex yielded average P-T conditions of 554 °C and 3.3 kbars. Gneissic rocks from the Wolf Grove Structure recorded higher temperatures and pressures with an average of 735 °C and 7.6 kbars.

Based on this evidence, field gradients were calculated for both the western and eastern sections of the Carleton Place area, namely the Lavant Gabbro Block and the Wolf Grove Block.

4.2.1 Calculation of Field Gradient for the Lavant Gabbro Block

Thermobarometry data from rocks of the Lavant Gabbro Complex were plotted on a pressure-temperature (P-T) diagram (figure 4.5). Anomalously high or low values were excluded prior to the calculation of the field gradient. The anomalously low values were produced using averaged mineral composition data for each mineral (i.e. garnet, biotite, amphibole and plagioclase). Recalculation of these analyses using the garnet composition with the highest Mg/(Fe+Mg) ratio (Spear, 1991; Florence and Spear, 1991; Ford, 2002) and rim or core compositions of the remaining minerals produced P-T conditions consistent with adjacent domains within the samples. Anomalously high values for pressure and temperature were obtained from equilibria within amphibole only. P-T conditions obtained using only amphibole data may be unreliable due to the uncertainties in the database and activity models used.

Figure 4.5 P-T diagram displaying thermobarometric data from the Lavant Gabbro block of the western portion of the Carleton Place area. Estimated field gradient is ~ 47° C/km.

Lavant Gabbro Block
field gradient

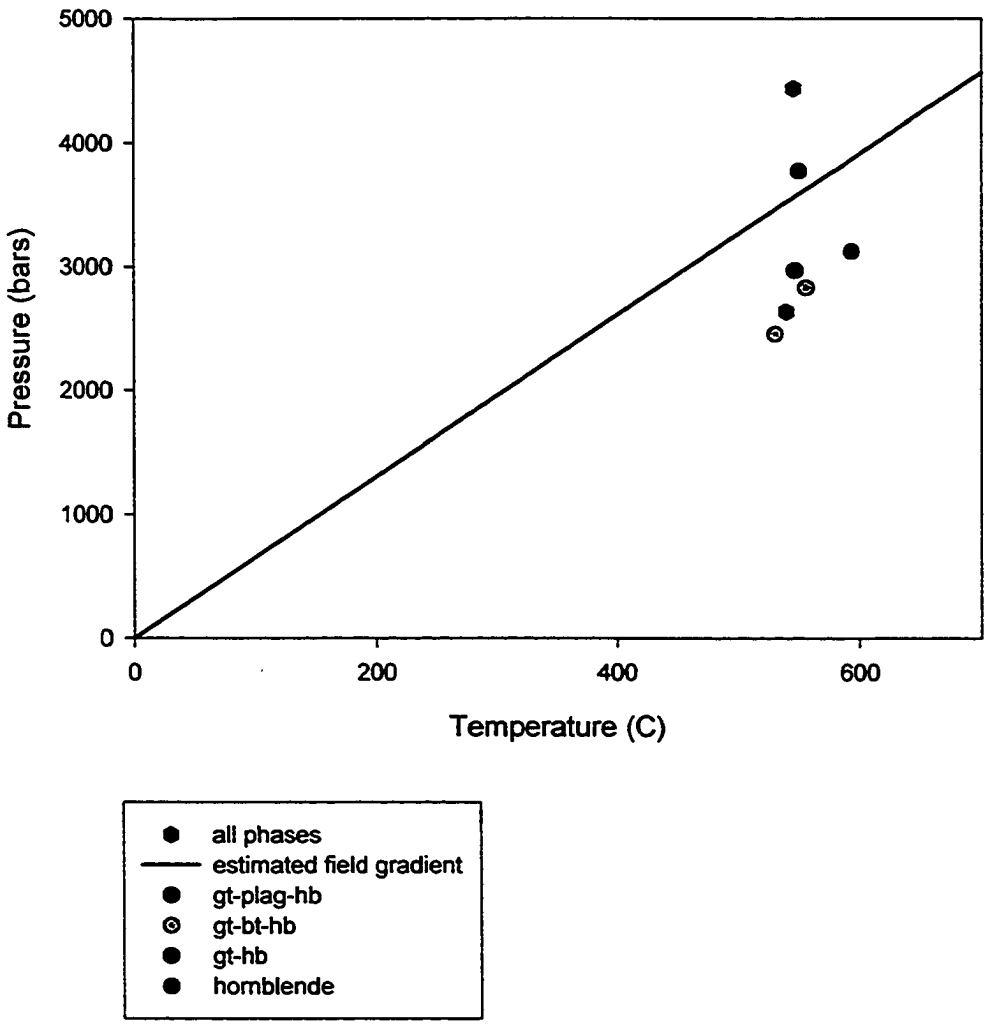

A field gradient was determined by calculation of a regression line forced through the origin; as rocks in the present study area do not retain a complete record of the P-T conditions and the field gradient must begin at surface pressures and temperatures. The Lavant Gabbro Block data produced a field gradient of ~47 °C/km. This gradient is consistent with the contact metamorphic conditions experienced by the rocks of the western portion of the field area. It is also steeper than the gradient recorded by the Lepontine Alps (Turner, 1968).

4.2.2 Calculation of Field Gradient for the Wolf Grove Block

Thermobarometry data for gneisses in the eastern section of the field area were plotted on a P-T diagram (figure 4.6). Analyses which appeared to be anomalously high or low were excluded before the calculation of the field gradient.

Anomalously high values for the Wolf Grove Block have a lower pressure limit of 8.4 kbars. Average pressure for samples within the Wolf Grove Structure is 7.6 kbars. Some of these values may reflect preservation of an earlier granulite-facies metamorphism. Samples which produced high pressure values contain two distinct forms of garnet. One form is larger (≤ 2 cm across) with irregular grain boundaries, multiple inclusions, and appears partially resorbed. The smaller garnets (≥0.5 cm across) are mainly euhedral with sharp grain boundaries and no inclusions. This implies the preservation of two phases of metamorphic mineral growth. Migmatitic rocks 500 m north along strike also display textures consistent with polymetamorphism.

Easton and Davidson (1997) described similar gneissic and/or migmatitic rocks

Figure 4.6 P-T diagram displaying thermobarometric data from the Wolf Grove block of the eastern portion of the Carleton Place area. This gradient (Wolf Grove 1) was calculated without the high pressure data. Estimated field gradient is ~ 32° C/km.

Wolf Grove Block
field gradient (1)

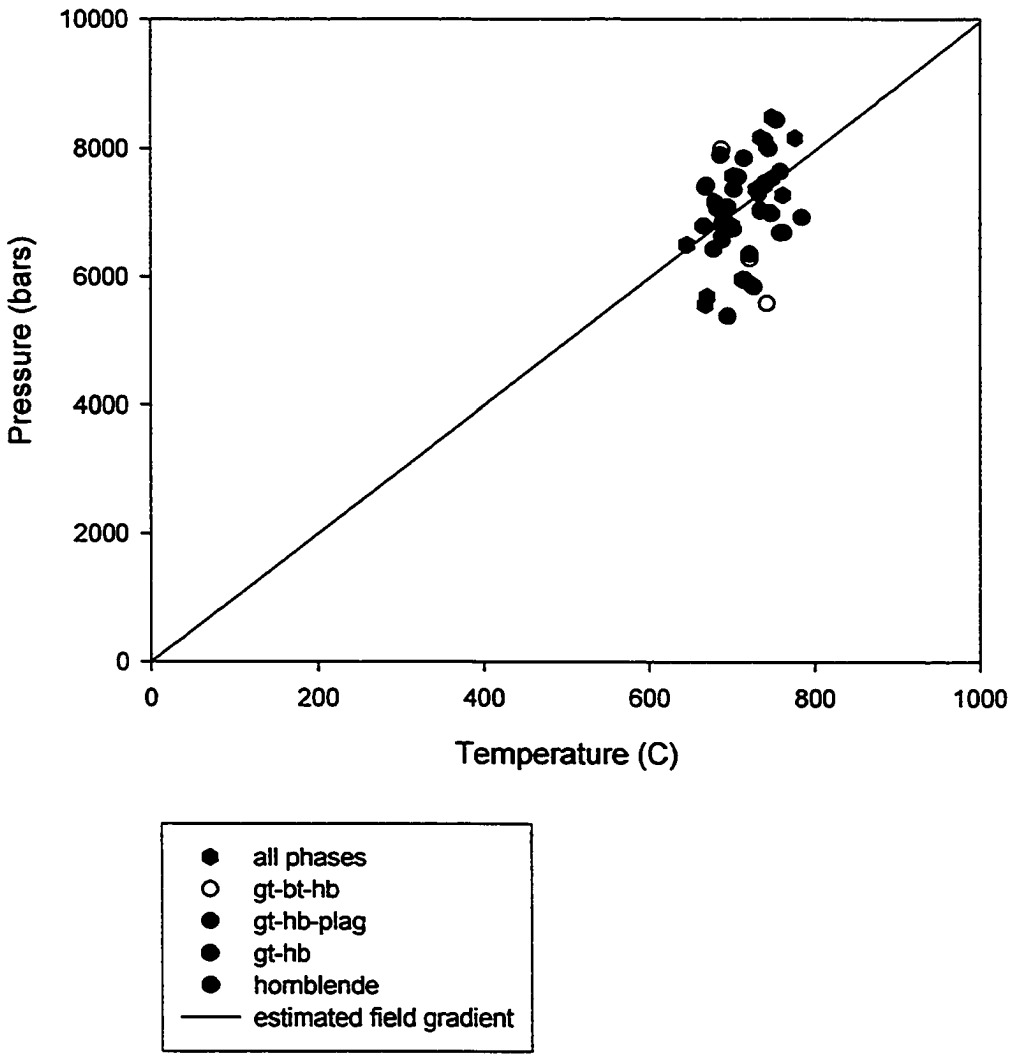

which contain quarter-sized garnet pseudomorphs composed of a mixture of garnet, biotite, and quartz. The authors stated that these textures and the presence of relict high-grade mineral parageneses in the migmatites suggest an earlier high-temperature metamorphism prior to the preserved metamorphic conditions, which developed at ~1168 Ma (Corfu and Easton, 1997) and which yield P-T conditions of 718 °C and 7.2 kbars (Buckley et al., 1997).

Three of the high-pressure values were based on P-T conditions calculated using amphibole alone. As discussed in the previous section, uncertainties within the activity models and databases for amphiboles affect the reliability of metamorphic conditions based solely on hornblende.

The anomalously low values from the Wolf Grove gneisses may be related to a greenschist-facies metamorphic event (Buckley et al., 1997; Praamsma et al., 2000), which also affected the marbles enclosing the Wolf Grove Structure and exposed along the trace of the Clayton Lake shear zone. Within the marbles this event corresponds to tremolite overgrowths and tremolite "sun bursts" (see photos 2.11 a and 2.16 a-c). The age of this event is unknown. The sample which produced the low P-T results outcrops less than 1 km from marble containing tremolite overgrowths.

Two field gradients were calculated for the Wolf Grove block because of the possible preservation of at least two metamorphic events in the Wolf Grove gneisses or the possibility that the dominant metamorphic episode was actually a protracted metamorphic episode with the local preservation of earlier phases. In each case a line of regression was plotted on the P-T diagram and forced through the origin. The first

gradient (figure 4.6) excludes the high pressure values and the anomalously low P-T results; this yields a field gradient of ~32 °C/km for the eastern half of the field area. The second field gradient includes the high-pressure data (figure 4.7); the resulting field gradient is slightly steeper at ~26 °C/km.

4.3 Comparison with the Lepontine Alps

The polybaric T-XCO_2 diagram of Flowers and Helgeson (1983) is based on a field gradient of approximately 63 °C/km (figure 4.2). This gradient is much shallower than the field gradients calculated for either the western or eastern sections of the field area. Based on the differences in field gradients, the Flowers and Helgeson (1983) T-X_{CO2} diagram is not directly applicable to the rocks within the Carleton Place area. Therefore to accurately model the pressure, temperature, and fluid conditions within the marbles, polybaric T-X_{CO2} diagrams utilizing the calculated field gradients have been produced.

4.4 T-X_{CO2} Diagrams

Polybaric T-X_{CO2} sections specific to the field gradients calculated for the western and eastern portions of the Carleton Place area were constructed using the computer program PTAX (Brown et al., 1988). The diagrams were created by incrementing pressure as a function of temperature based on the field gradient.

The locations of the isobaric invariant points are determined by obtaining the intersection of the univariant with the field gradient on a P-T diagram (figure 4.8). This

Figure 4.7 P-T diagram displaying thermobarometric data from the Wolf Grove block of the eastern portion of the Carleton Place area. This gradient (Wolf Grove 2) was calculated with the high pressure data. Estimated field gradient is ~ 26° C/km.

Wolf Grove Block
field gradient (2)

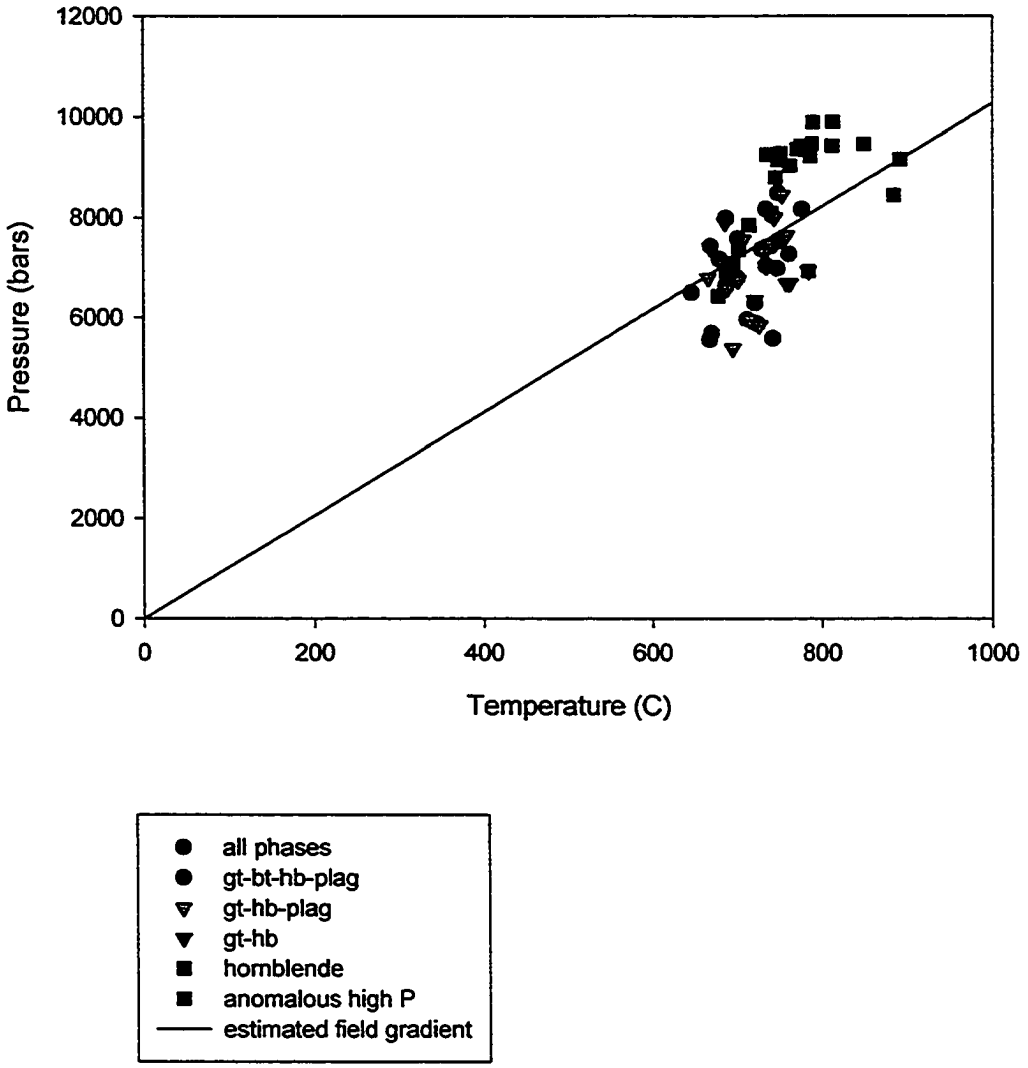

Figure 4.8 P-T diagram displaying the univariant curves I, II, III, IV, V, VI, and VII. Also shown are the field gradients calculated from the thermobarometric data produced in this study. The univariant curves for assemblages II, III, IV, VI, and VII intersect at ~ 625° C and 6.0 kbars. Symbols in parentheses indicate absent phases.

Assemblages:

Point I = calcite-dolomite-quartz-talc-tremolite-fluid
Point II = calcite-dolomite-quartz-phlogopite-K-feldspar-tremolite-fluid
Point III = calcite-dolomite-quartz-tremolite-diopside-fluid (Ksp, Ph)
Point IV = calcite-dolomite-phlogopite-K-feldspar-tremolite-diopside-fluid (Q)
Point V = calcite-dolomite-tremolite-diopside-forsterite-fluid
Point VI = calcite-dolomite-quartz-phlogopite-K-feldspar-diopside-fluid (Tr)
Point VII = quartz-phlogopite-K-feldspar-tremolite-diopside-fluid (Cc, Do, F)

Point VII is defined by the solid-solid reaction:

$$KAlSi_3O_8 + Ca_2Mg_5Si_8O_{22}(OH)_2 = 2\ CaMgSi_2O_6 + KMg_3AlSi_5O_{10}(OH)_2 + 4\ SiO_2$$

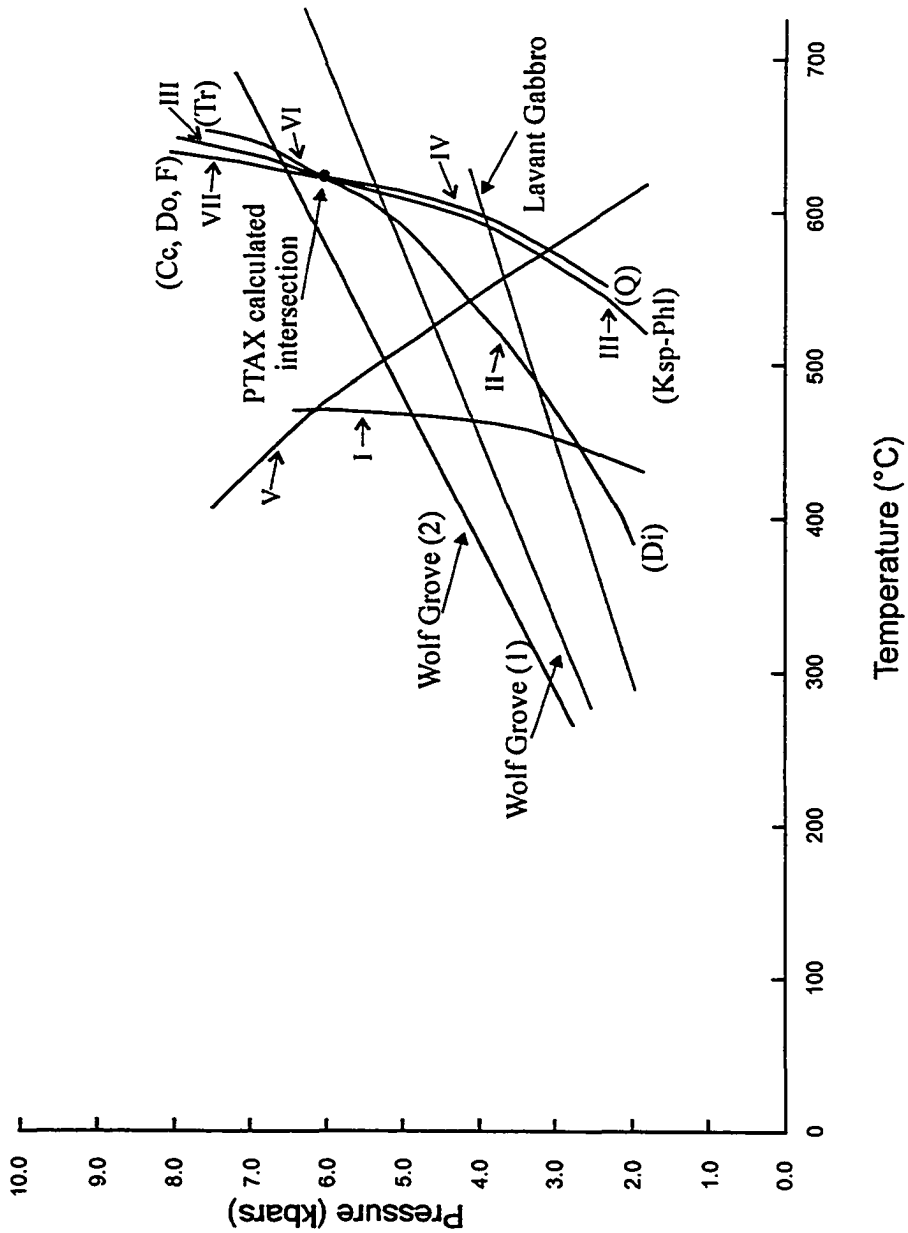

provides the pressure and temperature of the isobaric invariant point. The exact fluid composition of the invariant point can then be obtained by producing a T-X_{CO2} section at the pressure indicated by the intersection. The univariant curves can then be plotted by calculating values for temperature and composition as pressure is incrementally increased within the range of the field gradient. Positions of the isobaric invariant points determine the topology of the resulting T-X sections. Univariant curves must pass through the isobaric invariant point which involves the phases affected by the univariant reactions. For example, isobaric invariant point I involves the minerals calcite, dolomite, quartz, talc and tremolite. Therefore the reaction; 3 dolomite + 4 quartz +H_2O = talc + 3 calcite + 3 CO_2 or 5 talc + 6 calcite + 4 quartz = 3 tremolite + 6 CO_2 +2 H_2O must pass through invariant point I.

An important feature of the P-T diagram (figure 4.8) is the intersection of the univariant curves II, III, and IV, generating an invariant point in P-T space involving the eight minerals calcite, dolomite, quartz, potassium feldspar, phlogopite, tremolite, diopside, and fluid. Calculations by PTAX (Brown et al, 1988) indicate this intersection occurs at ~625 °C and 6.0 kbars. Isobaric invariant points I (talc present) and V (forsterite present) are not affected by this intersection. This intersection has a significant impact on the phase relations within siliceous marbles. Along each univariant curve radiating from the invariant point one phase must be missing. The univariant curve for assemblage II in P-T space is a diopside-absent assemblage. The univariant curve for point IV is a quartz- absent reaction. The univariant curve for point III is a degenerate reaction involving the absence of two phases, namely phlogopite and potassium feldspar.

It is stable above and below the invariant point in figure 4.8. In accordance with the Morey-Schreinmakers rule (Yardley, 1989), the univariant curves for II and IV are unstable above this point and two other phases must be absent above the invariant point. The univariant VI is a tremolite- absent curve involving the minerals calcite, dolomite, quartz, potassium feldspar, phlogopite, and diopside. The degenerate univariant VII excludes the phases calcite, dolomite, and fluid and is therefore independent of fluid composition on a T-X section.

The field gradients calculated for the Lavant Gabbro Block and the Wolf Grove Block, excluding the high pressure data (Wolf Grove 1) intersect the univariant curves for invariant points II, III, and IV below the invariant on figure 4.8. The T-X_{CO2} diagrams for these gradients include invariant points I, II, III, IV, and V. The second field gradient calculated for the Wolf Grove Block (Wolf Grove 2) passes above the invariant point on figure 4.8. The T-X_{CO2} diagram for this gradient differs significantly from the other two cases and includes invariants points I, III, V, VI, and VII. Other possible combinations of minerals are metastable.

4.4.1 Lavant Block and Wolf Grove (1) Block T-X_{CO2} Diagrams

The polybaric T-X_{CO2} diagrams for the Lavant and Wolf Grove (1) blocks produced using field gradients calculated for the western (figure 4.9) and eastern (figure 4.10) are significantly different from the diagram (figure 4.3) constructed by Flowers and Helgeson (1983). Table 4.1 lists the reactions corresponding to the univariant curves on figures 4.9 and 4.10. Although the maxima and inflection points of the univariant curves

Figure 4.9 Polybaric T-X_{CO2} diagram for the Lavant block of the Carleton Place area using a field gradient of 47 °C/km. Numbers within the circles refer to the unique set of trivariant assemblages that are possible within each area. These numbers correspond to the CaO-MgO-SiO_2 diagrams shown in chapter 2 and Table 5.1 in chapter 5.

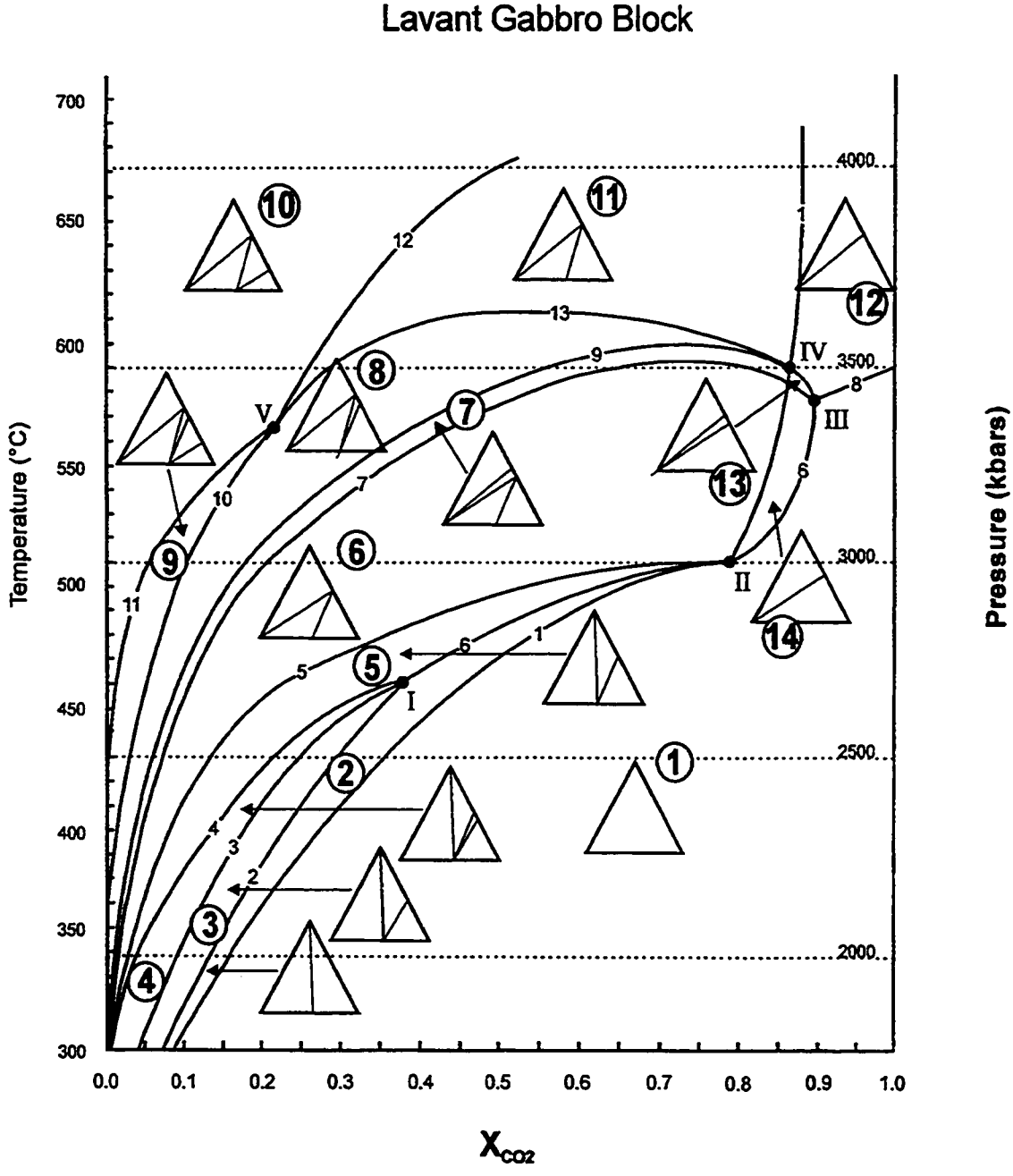

Figure 4.10 Polybaric T-X_{CO2} diagram for the Wolf Grove block of the Carleton Place area using the Wolf Grove (1) field gradient of 32° C/km. Numbers within the circles refer to the unique set of trivariant assemblages that are possible within each area. These numbers correspond to the CaO-MgO-SiO_2 diagrams shown in chapter 2 and Table 5.1 in chapter 5.

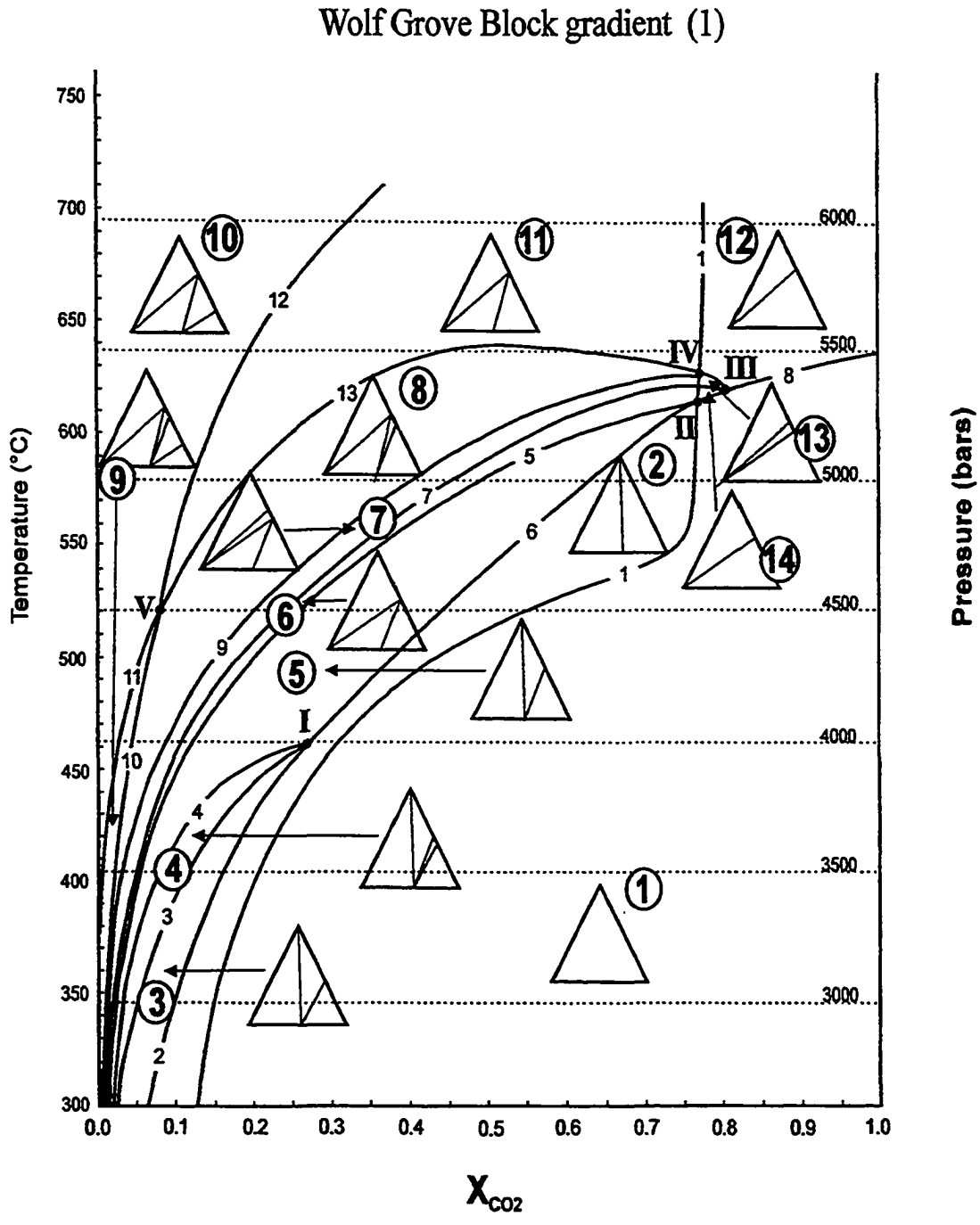

retain the same fluid composition on either isobaric or polybaric diagrams, the positions of the invariant points on these T-X_{CO2} sections have changed. In addition the size and/or shape of the stability fields of various mineral assemblages has changed.

Point I involves the phases calcite, dolomite, quartz, talc and tremolite. Three reactions below isobaric invariant point I control the stability of talc. Talc is not stable above invariant point I. The position of the isobaric invariant point and the size of the talc stability field is different on each of the three diagrams. Flowers and Helgeson (1983) show point I at 20% CO_2 and approximately 490 °C and 4.7 kbars with a very narrow talc stability field. The position of point I shifts towards more CO_2-rich conditions on both figures 4.9 (40 %) and 4.10 (30%). The size of the stability field is also larger. Talc should become unstable at P-T conditions of 2.7 kbars and 450 °C on the Lavant Gabbro diagram and at a pressure of 4.0 kbars and 460 °C on the Wolf Grove (1) section, which is consistent with Flowers and Helgeson (1983). According to Ewert (1977) talc may persist to up to 550 °C at 5 kbars. The pervasive presence of graphite within marbles of the Wolf Grove block is consistent with CO_2-rich fluid compositions and a lack of primary talc. The percentage of graphite in the marbles decreases as the eastern margin of the Wolf Grove Structure is approached. Near the contact with the structure, the marbles contain veins of chert suggesting the passage of water-rich fluids.

The T-X sections for the Lavant and Wolf Grove (1) gradients also contrast sharply with the isobaric T-X_{CO2} section of Ewert (1977). The T-X section of Ewert (1977) shows a double intersection of invariant point I at 5 kbars. In addition, this T-X section exhibits a greatly expanded talc field at 5 kbars. This appears to agree with

observations of Metz and Trommsdorff (1968), Trommsdorff (1972), and Puhan and Hoffer (1973) but contradicts findings of Slaughter et al. (1975) who suggest that the talc field decreases at higher pressures. The T-X sections of Flowers and Helgeson (1983) and this study support the later. Based on the P-T diagram of Connolly and Trommsdorff (1991), the back bending character of the calcite + dolomite + quartz + talc + tremolite + fluid curve (invariant I) suggests that the thermal stability of talc increases with pressure up to a maximum of 5 kbars, thereafter decreasing with pressure. In each case, talc is restricted to relatively water-rich conditions at low pressures and temperatures.

Isobaric invariant points III and IV are in similar locations on the T-X sections for the Lepontine Alps and the Lavant Gabbro block. Compared to figure 4.3, point II is shifted towards CO_2-rich conditions (~ 80%) on both the Lavant Gabbro and Wolf Grove (1) diagrams. In the case of the Wolf Grove (1) diagram points II, III, and IV cluster very close together, reflecting the proximity of the field gradient to the intersection of these curves on the P-T diagram (figure 4.8). All indicate relatively high CO_2 conditions. As a consequence of the proximity of the isobaric invariant points, the fields 13 and 14 are greatly restricted in size compared to the T-X section for the Lepontine Alps. Identification of the corresponding mineral assemblages would be very useful for the determination of the pressure and temperature conditions in the field. However, the very small stability fields mean it is extremely unlikely that these assemblages would occur.

The location of isobaric invariant point V varies considerably among the three diagrams. On the Lepontine diagram (figure 4.3), point V requires moderately water-rich conditions (60%) and high P-T conditions as it occurs above isobaric invariant point IV.

The Lavant Gabbro diagram indicates lower P-T conditions and more water-rich conditions. Point V is also located below points III and IV. Extremely water-rich conditions (90+ %) are required for point V on the Wolf Grove (1) diagram. It also occurs below points II, III, and IV. Isobaric invariant point V occurs at 550 °C and 3.3 kbars on figure 4.9 and 525 °C and 4.5 kbars on figure 4.10.

The T-X section calculated by Ewert (1977) shows that over a wide range of CO_2-rich conditions forsterite should form prior to diopside, based on the relative positions of the reactions responsible for the first formation of diopside (i.e. reaction 7; tremolite + 3 calcite + 2 quartz = 5 diopside + 3 CO_2 + H_2O) and forsterite (i.e. reaction 12; tremolite + 11 dolomite = 8 forsterite + 13 calcite + 9 CO_2 + H_2O). Skippen (1971) found that at total pressures of 2 kbars and less, reaction 7 occurs before reaction 12 indicating that at low pressures diopside should form before forsterite. Skippen (1974) suggested that at pressures equaling 3 kbars the two reactions intersect and at still higher pressures the curves may cross allowing forsterite to form before diopside, which is consistent with Ewert (1977). On the polybaric T-X section of Flowers and Helgeson (1983), formation of forsterite prior to diopside could only occur over a small range of H_2O-rich conditions. This is supported by the relative positions of the two reactions on both the Lavant Gabbro and Wolf Grove (1) sections.

4.4.2 Wolf Grove (2) Block T-X_{CO2} Diagram

The second Wolf Grove block field gradient (~26 °C/km) intersects the univariant curves above the invariant point in P-T space (figure 4.11). As a result the univariant

Figure 4.11 Polybaric T-X_{CO2} diagram for the Wolf Grove block of the Carleton Place area using the Wolf Grove (2) field gradient of 26 °C/km. Numbers within the circles refer to the unique set of trivariant assemblages that are possible within each area. These numbers correspond to the CaO-MgO-SiO_2 diagrams shown in appendix 4.

Wolf Grove Block gradient (2)

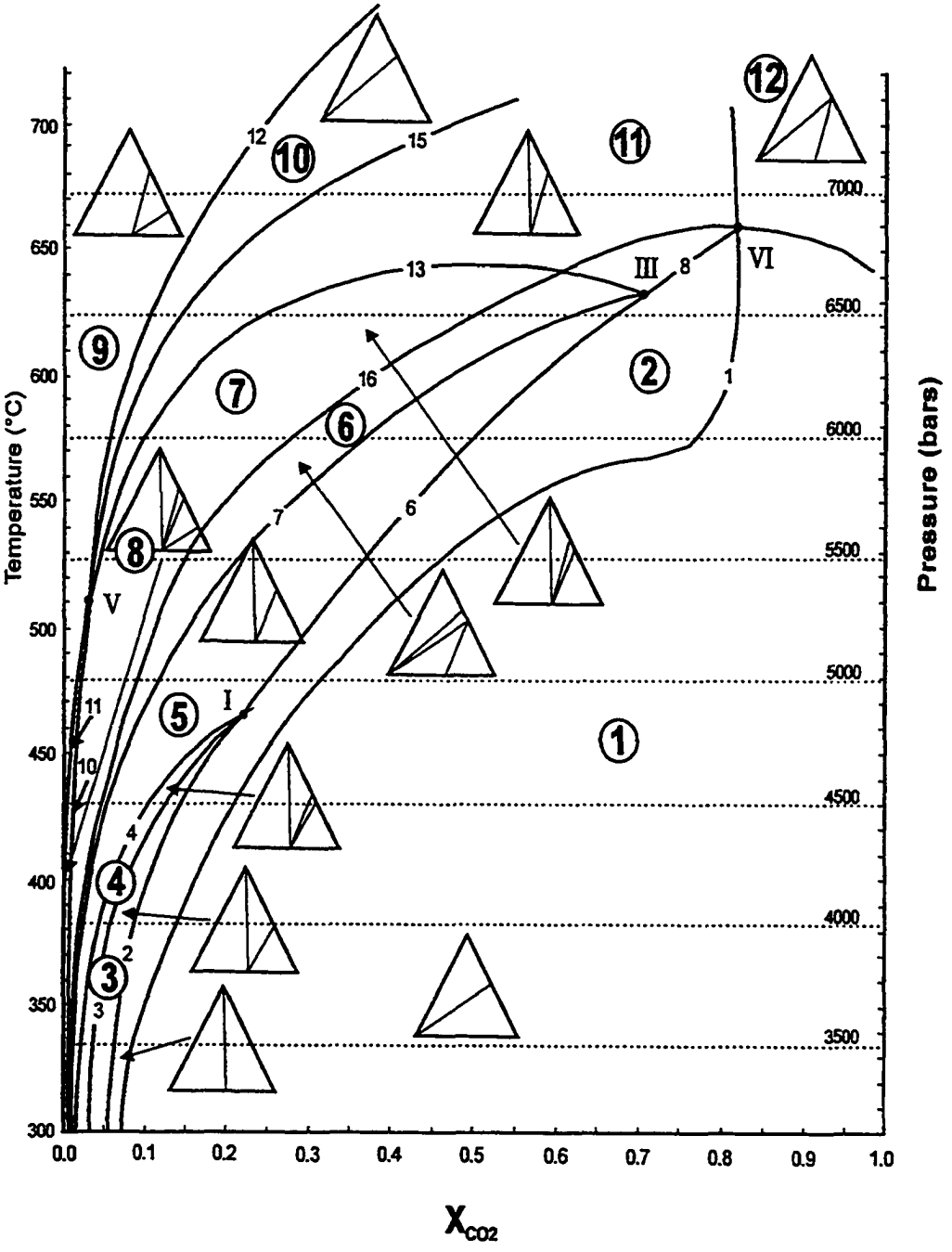

Table 4.2 T-X_{CO2} diagram reaction list for the Wolf Grove (2) gradient

(1) K-feldspar + 3 dolomite + H_2O = phlogopite + 3 calcite + 3 CO_2

(2) 3 dolomite + 4 quartz + H_2O = talc + 3 calcite + 3 CO_2

(3) 5 talc + 6 calcite + 4 quartz = 3 tremolite + 6 CO_2 + 2 H_2O

(4) 2 talc + 3 calcite = tremolite + dolomite + H_2O + CO_2

(6) 5 dolomite + 8 quartz + H_2O = tremolite + 3 calcite + 7 CO_2

(7) tremolite + 3 calcite + 2 quartz = 5 diopside + 3 CO_2 + H_2O

(8) dolomite + 2 quartz = diopside + 2 CO_2

(10) tremolite + 11 dolomite = 8 forsterite + 13 calcite + 9 CO_2 + H_2O

(11) 3 tremolite + 5 calcite = 11 diopside + 2 forsterite + 5 CO_2 + 3 H_2O

(12) diopside + 3 dolomite = 2 forsterite + 4 calcite + 5 CO_2

(13) tremolite + 3 calcite = dolomite + 4 diopside + H_2O + CO_2

(14) 5 dolomite + 4 tremolite = 13 diopside + 6 forsterite + 10 CO_2 + 4 H_2O

(15) 3 calcite + phlogopite + 6 quartz = K-feldspar + 3 diopside + 3 CO_2 + H_2O

(16) K-feldspar + tremolite = 4 quartz + phlogopite + 2 diopside

Point I = calcite-dolomite-quartz-talc-tremolite-fluid

Point III = calcite-dolomite-quartz-tremolite-diopside-fluid (Ksp, Phl)

Point V = calcite-dolomite-tremolite-diopside-forsterite-fluid

Point VI = calcite-dolomite-quartz-phlogopite-K-feldspar-diopside-fluid (Tr)

Point VII (not shown; metastable) = quartz-phlogopite-K-feldspar-tremolite-diopside-fluid (Cc, Do, F)

curves II and IV are metastable and the corresponding isobaric invariant points do not appear on the T-X section. Two phases are absent at point III. As a result, this is a degenerate reaction and the univariant curve is stable above and below the invariant point in P-T space (figure 4.8). Points I and V are unaffected by the crossing of the univariant curves and therefore appear on the T-X_{CO2} section. Isobaric invariant points II and IV are replaced by VI and VII. Point VI involves the phases calcite, dolomite, K-feldspar, phlogopite, quartz, and diopside. Point VII involves the phases quartz, K-feldspar, phlogopite, tremolite, and diopside. This significantly changes the geometry of the T-X section compared to previous diagrams. Fourteen independent reactions define the phase relations related to this steeper field gradient. Table 4.2 lists the reactions corresponding to the univariant curves on figure 4.11 and the assemblages present at the isobaric invariant points.

Isobaric invariant point VII does not involve the phases calcite, dolomite and fluid is therefore independent of fluid composition on the T-X section. Based on field and petrographic evidence fluid is assumed to be present in the study area. Isobaric invariantpoint VII and the reactions related to it do not appear on the T-X section (figure 4.11) as they are metastable where fluid is present.

As described previously, talc is stable below isobaric invariant point I. The talc stability field is very restricted and indicates very H_2O-rich conditions (~80-100%). Similar to the lower Wolf Grove gradient, talc is absent above 450 °C.

The location of isobaric invariant point III is shifted towards the H_2O axis with the steeper field gradient. This is consistent with the pattern observed from figures 4.3, 4.9,

and 4.10. The mineral assemblage tremolite-phlogopite-dolomite is unstable above point III and has an expanded stability field on figure 4.11.

The position of isobaric invariant point V occurs at a slightly lower temperature but approximately 0.75 kbars higher pressure than the lower Wolf Grove field gradient. Point V moves towards the H_2O axis as the gradient becomes steeper. Mineral assemblages containing both forsterite and tremolite or forsterite and diopside are restricted to very water-rich fluid conditions. The stability field of the assemblage tremolite-forsterite-phlogopite is extremely narrow and can only occur with nearly pure H_2O fluids. As suggested by Connolly and Trommsdorff (1991), this assemblage is limited to relatively low pressure (< 5 kbars) and is rare in regionally metamorphosed carbonates.

Isobaric invariant point VI occurs on the CO_2-rich side of the T-X section. This point indicates very high pressure and temperature conditions of 6.8 kbars and ~650 °C.

4.5 Unique Mineral Assemblages Above and Below the P-T Invariant Point

Due to the differences in the T-X_{CO2} diagrams, there are a limited number of assemblages which can be used to identify whether the metamorphic assemblages present in marbles of the eastern block formed along a field gradient above or below the invariant point on the P-T section (figure 4.8). Comparison of the SiO_2-$KAlSi_3O_8$-MgO ternary diagrams for the fields of figures 4.10 and 4.11 indicates that the same mineral assemblages are present in fields 2, 3, 4, and 5 of both diagrams. The sequence of ternary diagrams around each invariant point varies for fields above field 5; however, the mineral

assemblages possible are largely the same.

There are differences between the T-X sections such as the stability of the assemblage calcite + potassium feldspar + diopside + phlogopite. This assemblage is stable over a wide range of conditions on figure 4.10. On figure 4.11 this assemblage is restricted to a single field at very high pressure and temperature conditions. It requires very CO_2-rich fluids of ~80 % or higher, whereas the same assemblage is present at fluid conditions of 0-75 % CO_2 on figure 4.10. Similarly, the assemblages calcite + diopside + phlogopite+ potassium feldspar or calcite + dolomite + diopside + phlogopite correspond to fluid conditions which are less than 75% CO_2 on figure 4.10. On figure 4.11 the same assemblages require higher pressure and temperatures and a fluid containing 80 % CO_2 or greater.

The mineral assemblage calcite + dolomite + potassium feldspar + quartz is the only assemblage which does not appear on the Wolf Grove (2) T-X section (figure 4.11). This assemblage corresponds to unmetamorphosed carbonates. Ewert (1977) identified the unreacted assemblage quartz + dolomite across the field area. These unreacted assemblages were not identified in the field area during this study.

The only unique trivariant mineral assemblage for the Wolf Grove (2) T-X section is diopside + phlogopite + quartz corresponding to field 11 on figure 4.11. It occurs over a wide range of pressure, temperature, and fluid conditions on figure 4.11 and is not a stable assemblage for rocks which were metamorphosed along the shallower Wolf Grove (1) gradient. Identification of this assemblage in rocks of the eastern block would indicate the steeper gradient is applicable.

Examination of petrographic evidence from the marbles indicates that at least 11 samples from the eastern Wolf Grove block contain calcite, dolomite, diopside, phlogopite, and quartz. However, in each of the samples tremolite is also present and there is also evidence of tremolite overgrowths in four of the samples. This assemblage is compatible with fields 8 and 9 (diopside + tremolite + phlogopite) from figure 4.10 and could mark the transition from field 11 (diopside + phlogopite + dolomite or diopside + potassium feldspar + quartz) to field 8. This would suggest that the lower field gradient is appropriate. Ewert (1977) concluded the tremolite+diopside-bearing samples indicated invariant point IV (calcite-dolomite-quartz-tremolite-diopside) has been reached and he mapped the corresponding isograd in three locations in the Carleton Place area.

The assemblage diopside, tremolite, phlogopite, and quartz could be a transitional assemblage from field 11 (diopside +phlogopite + quartz) to field 7 (diopside + tremolite + phlogopite) on figure 4.11, which would be compatible with the steeper field gradient. The presence of tremolite overgrowths and relict diopside in the cores of tremolite crystals suggest that such a reaction could be taking place. However it does not preclude the transition from field 11 to field 8 on figure 4.10.

The most common mineral assemblage found in the field area is that containing tremolite, phlogopite, and calcite. This assemblage occurs over a wide range of metamorphic conditions on both of the T-X_{CO2} diagrams. The lack of potassium feldspar in the various mineral assemblages may provide some additional support for the rocks having formed along the steeper field gradient. The gneissic rocks associated with the marbles indicate a prolonged period of regional metamorphism or multiple events at

relatively high P-T conditions, similar to that found in the marbles (see chapter 2). As the majority of the samples do not provide unequivocal evidence for the steeper field gradient and the main metamorphic event appears to be at the slightly lower pressures and temperatures, the shallower field gradient (Wolf Grove 1) is assumed to be generally applicable to the eastern portion of the Carleton Place area.

Chapter 5 - Isograds within the Siliceous Dolomitic Marbles

5.1 Prograde Sequence of Metamorphic Mineral Development in Carbonates

The general prograde sequence of mineral development in dolomitic marbles was first described by Eskola (1922) and refined by Bowen (1940). Bowen concluded that the progressive metamorphism of siliceous dolomitic marbles is a decarbonation process involving 13 steps and the appearance of 10 distinct mineral phases:

(1) tremolite
(2) forsterite
(3) diopside
(4) periclase
(5) wollastonite
(6) monticellite
(7) akermanite
(8) spurrite
(9) merivinite
(10) larnite

Later research by Tilley (1951) led to the recognition of talc as the mineral first formed at the lowest grade and the addition of tilleyite and rankinite among the higher temperature phases. Of the above listed mineral sequence, numbers 6 -10, tilleyite and rankinite are normally restricted to the contact metamorphic aureoles adjacent to igneous intrusive bodies.

The sequence of mineral appearance isograds encountered in this study is typical (Yardley, 1989) for regionally metamorphosed siliceous dolomitic marbles:

(1) talc or phlogopite

(2) talc + tremolite

(3) tremolite

(4) tremolite + diopside

(5) diopside or forsterite

(6) diopside + forsterite

Forsterite first appears in marbles at very similar temperature and pressure conditions as diopside (Yardley, 1989). Variations in bulk rock composition and fluid composition dictate which mineral appears first. This also applies to the first appearance of talc or phlogopite.

5.2 Effect of Fluid Composition Variations on Isograd Development

Isograds in marbles are influenced by a combination of local P-T conditions and variations in fluid composition. In the case of carbonates, the first appearance of a mineral could be accomplished by several reactions; therefore it is necessary to base the mapping of an isograd on a specific reaction. These reactions correspond to univariant curves on isobaric T-X_{CO2} sections, such as figures 4.9 , 4.10, and 4.11. Such isograds are not isothermal and the first appearance of a given mineral may occur at different temperatures across the field area, depending on fluid composition defined by the relationship, $P_{Total} = P_{CO2} + P_{H2O}$. CH_4 and H_2 are required to account for graphite-bearing mineral assemblages; however, due to the relatively small concentrations of these fluid components $X_{CO2} + X_{H2O} \approx 1$ is considered adequate (Flowers and Helgeson, 1983).

Three types of isograds may develop in siliceous marbles depending on the relationship of fluid composition to peak metamorphic conditions.

5.2.1 Case 1: Regionally Uniform Fluid Composition

Case 1 involves a regionally uniform fluid which is analogous to the assumption of pure H_2O fluids in aluminous rocks. All the rocks at a specific P and T in a field area have a consistent fluid composition that is either fixed or varies uniformly with metamorphic grade over the entire area. Isograds in marbles and other rock types are parallel to each other and to the isotherms and isobars. The isograd marks a sharp boundary separating assemblages that fall below and above the related isobaric univariant curve. In this case, the isobaric invariant is not seen along the field gradient because the required fluid composition generally does not occur.

5.2.2 Case 2: Internally Buffered Fluid Composition

Case 2 isograds develop when the composition of the fluids is controlled by reactions occurring within the rock (ie. internal buffering). As the marble is heated, a reaction begins to convert the low-grade assemblage stable below the isograd to the higher grade assemblage stable above the isograd. The composition of the fluid phase is held to the divariant reaction until one of the reactants is totally consumed. Rather than a linear isograd that can be mapped as a line separating two metamorphic zones (case 1), internal buffering of the fluid results in a zone containing both the reactant and product assemblages across a range of metamorphic grade. The P-T curve on a diagram such as Connolly and Trommsdorff (1991; see figure 4.3) gives the limiting P-T conditions for this case (ie. either maximum or minimum P-T depending on the specific isograd).

5.2.3 Case 3: Fluid Gradient and Intersecting Isograds

Case 3 occurs when a fluid gradient develops at an angle to the regional P-T gradient. The fluid composition varies across the field area due to fluid infiltration or as a result of carbon dioxide production during decarbonation of marble. This is an example of external fluid control and can result in intersecting isograds between aluminous rocks and marbles (see Carmichael, 1970 and 1991). In this case, the first appearance of a given mineral or assemblage occurs at different P-T conditions across the area. The resulting isograd is at an angle to isotherms and isobars. Such isograds on a map resemble the T-X section with the isobaric invariant reduced to a point and the isograds related to the univariant curves radiating outwards from the invariant.

Skippen (1974) highlighted the importance of these points for describing the distribution of metamorphic grade. It is typically not possible to locate these points directly but their locations can be inferred by mapping the distribution of three- and four-mineral assemblages below and above the isobaric invariant point, resulting in the bracketing of such points in relation to temperature. Intersecting isograds within marbles were mapped by Ewert (1977) and Carmichael (1970).

5.3 Isograds in the Field

Results from detailed outcrop-scale mapping and petrographic analysis of co-existing mineral assemblages for marbles throughout the study area were used in combination with the T-X_{CO2} diagrams (figures 4.9 and 4.10) to identify the location of isograds (figure 5.1) within the siliceous dolomitic marbles of the Carleton Place area.

Figure 5.1 Simplified geological map of the Carleton Place area showing the location of isograds and isobaric invariant points mapped in this study. (Geology after Reinhardt and Liberty, 1973)

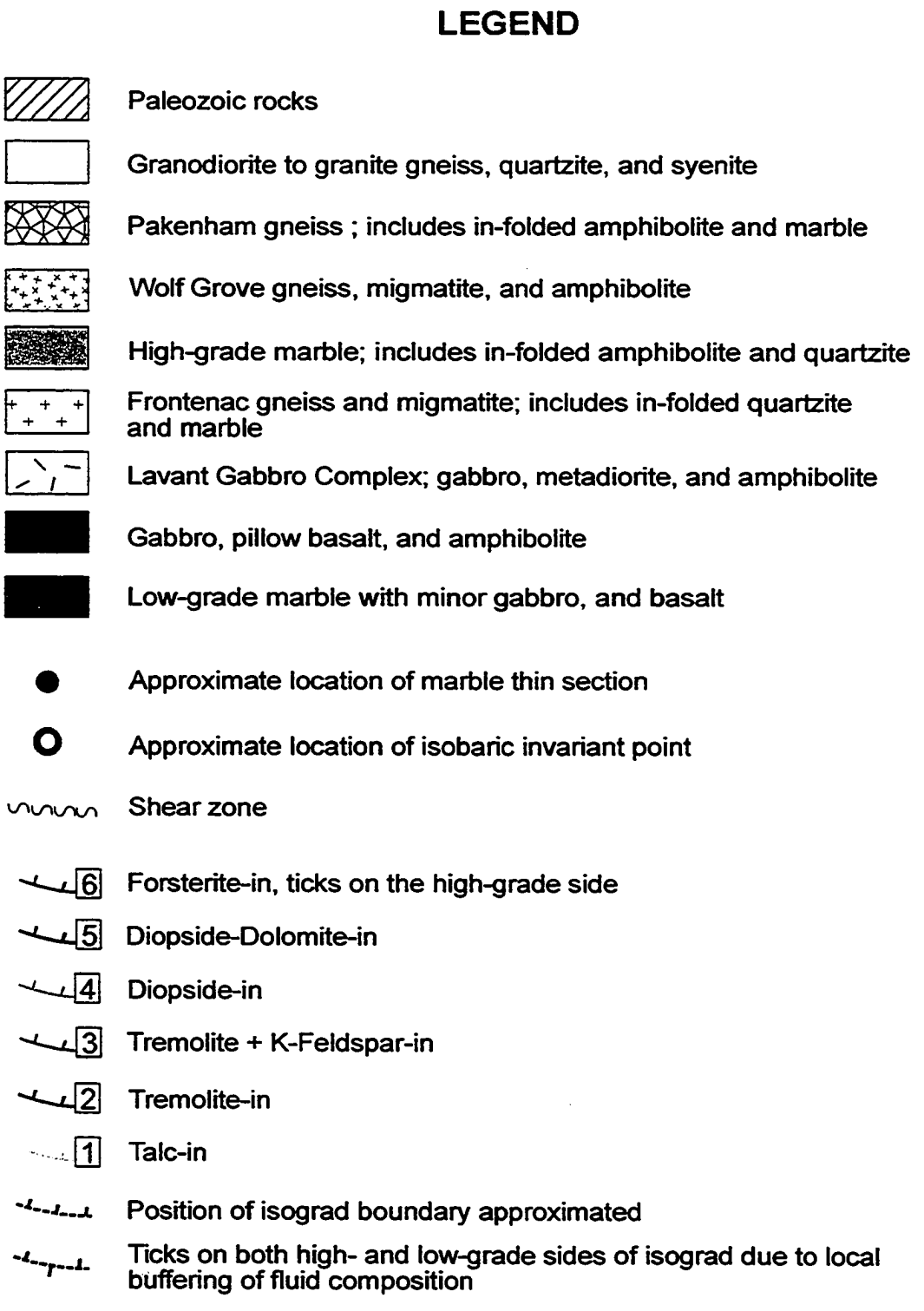

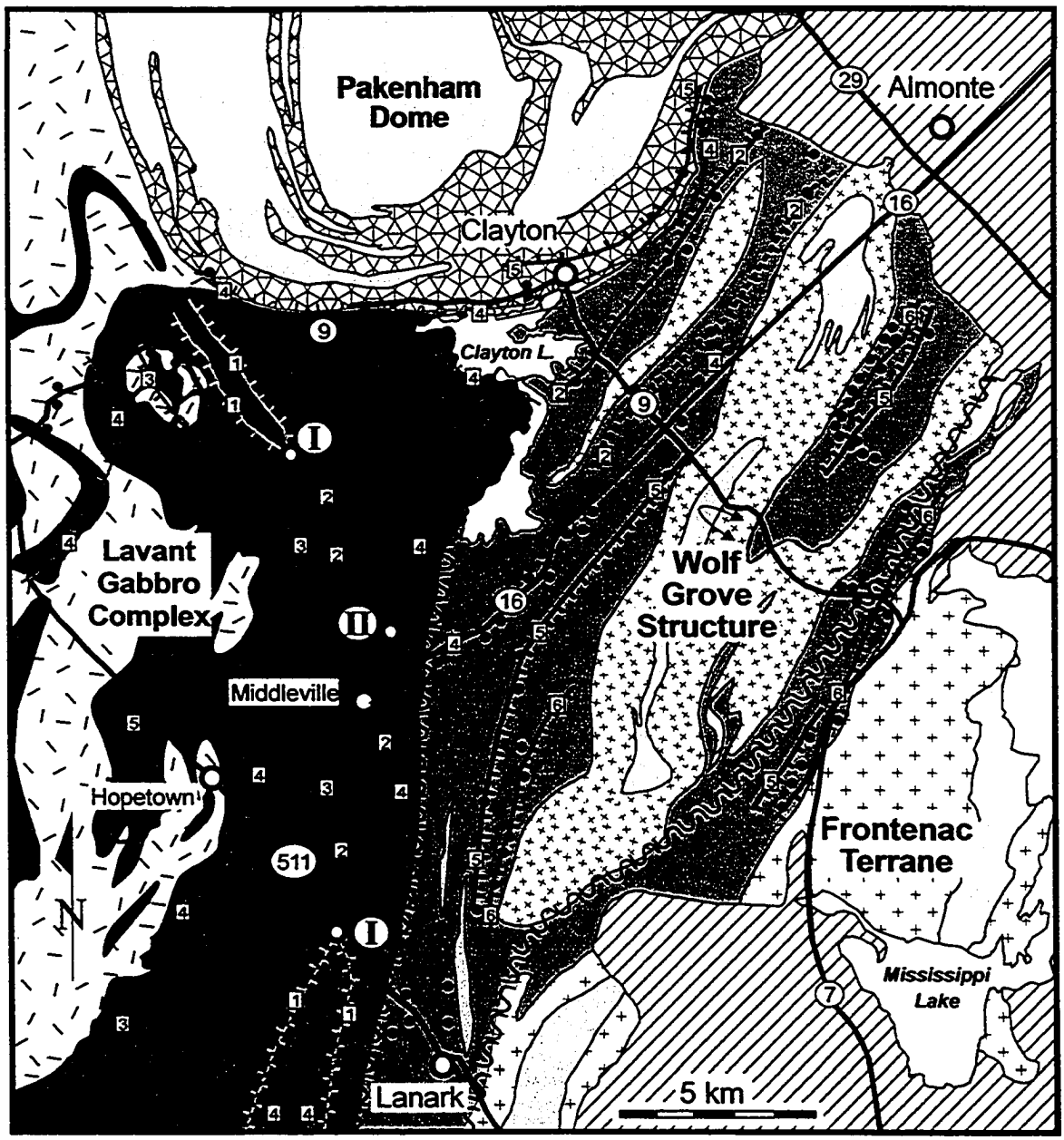

UTM coordinates and mineral assemblages of marble samples used to delineate the isograds are listed in appendix 3. The six-figure coordinates are found by dropping the first digit and the last two digits for the easting and the first two digits and the last two digits from the northing. For example, the full UTM reference for 869 924 from photo 2.1 A would read as 386900 (easting) 4992400 (northing). The six-figure grid references are considered accurate to the nearest 100m. When seven figures are quoted, the grid references is accurate to the nearest 50m.

Isograds were mapped by identifying the coexisting mineral assemblages in each sample and plotting the assemblage on ternary diagrams for the CaO-MgO-$KAlSi_3O_8$-SiO_2-CO_2-H_2O system (table 5.1). Table 5.1 illustrates the stable trivariant mineral assemblages possible with increasing metamorphic grade starting with field 1 of the T-X_{CO2} diagram (figures 4.9 and 4.10). The assemblages may be stable in either a single field or in multiple fields on a T-X_{CO2} diagram. Transition from one field to another allows the identification of the univariant reaction curve. Isograds corresponding to the following univariant reaction curves were mapped:

1 Talc-out: 2 talc + 3 calcite = tremolite +dolomite + H_2O + CO_2

2 Tremolite-in: 5 dolomite + 8 quartz +H_2O = tremolite +3 calcite + 7 CO_2

3 Tremolite + K-feldspar-in: 24 quartz + 6 calcite + 5 phlogopite = 3 tremolite + 5 K-feldspar + 2 H_2O + 6 CO_2

4 Diopside-in: tremolite + 3 calcite + 2 quartz = 5 diopside + 3 CO_2 + H_2O

5 Diopside-Dolomite-in: tremolite + 3 calcite = dolomite + 4 diopside + H_2O + CO_2

Table 5.1 Trivariant assemblages corresponding to fields 1-14 on the T-X_{CO2} diagrams

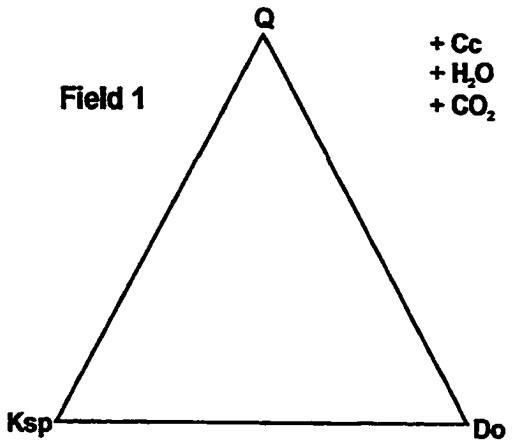

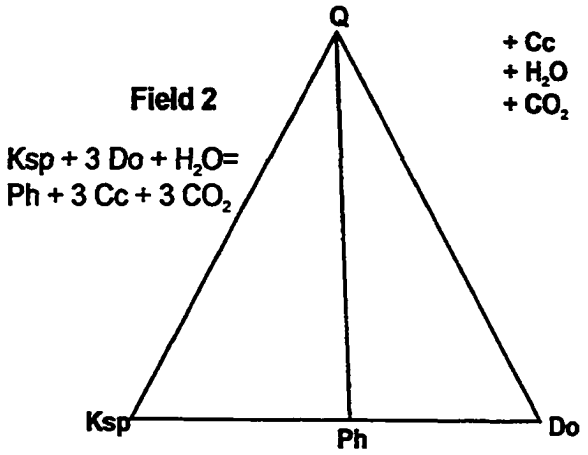

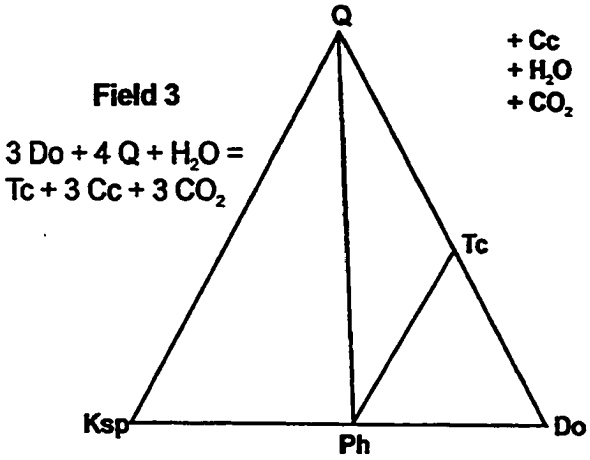

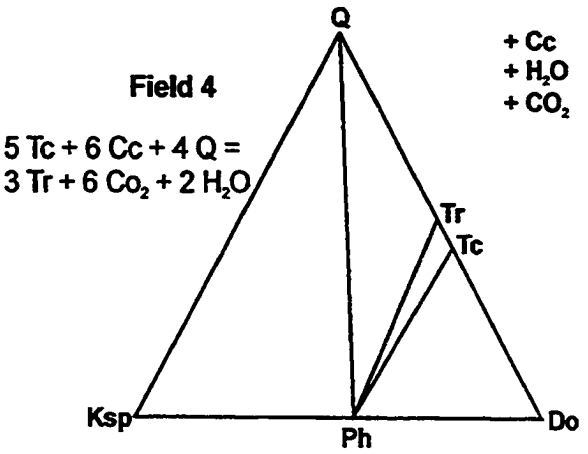

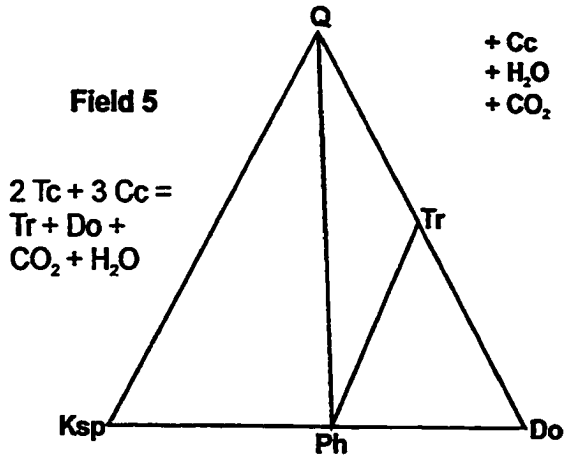

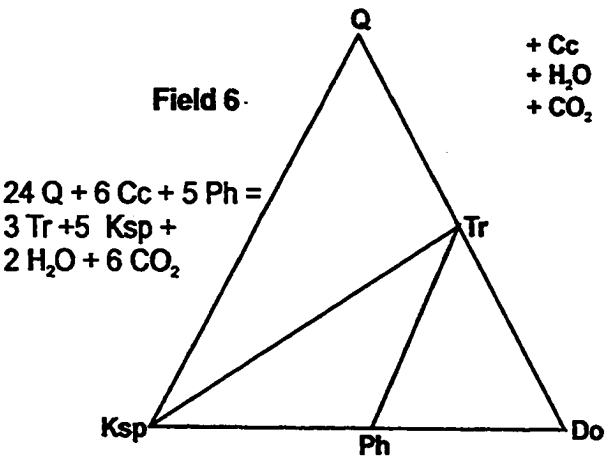

Table 5.1 (cont.) Trivariant assemblages corresponding to fields 1-14 on the T-X_{CO2} diagrams

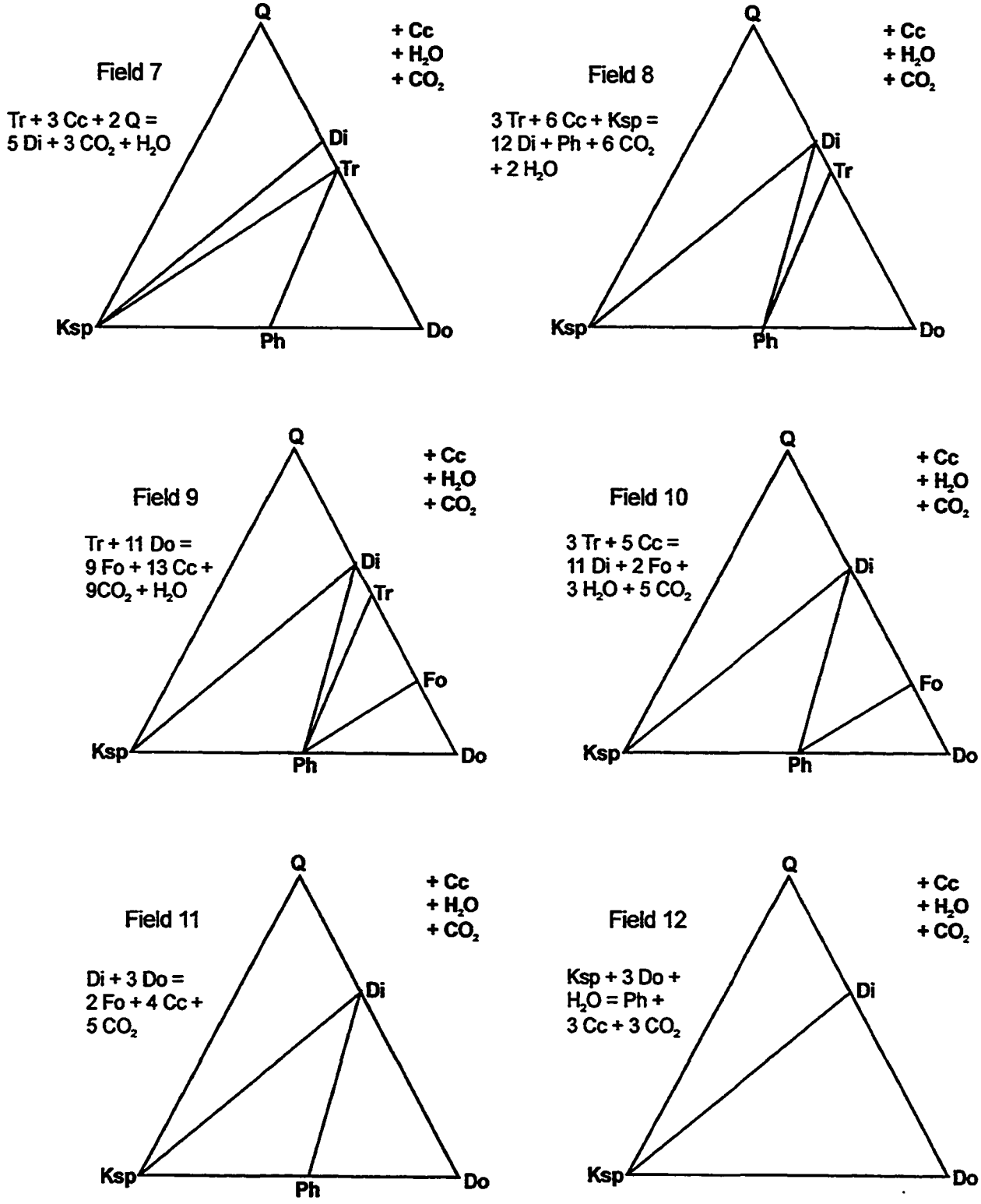

Table 5.1 (cont.) Trivariant assemblages corresponding to fields 1-14 on the T-X_{CO2} diagrams

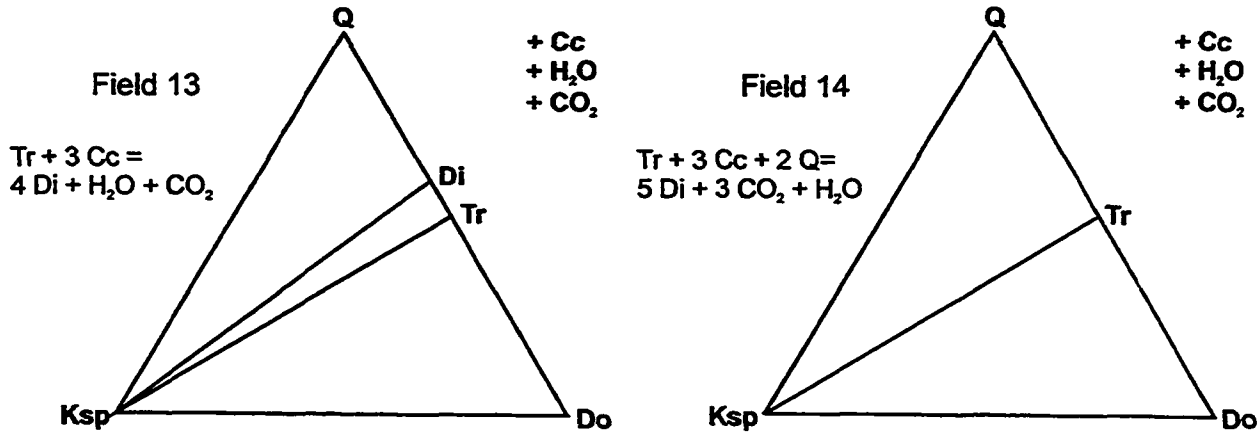

6 Forsterite-in: tremolite + 11 dolomite = 8 forsterite + 13 calcite + 9 CO_2 + H_2O

The position of these isograds relative to the isobaric invariant points and fluid composition is shown in table 5.2. Isograds corresponding to the above univariant reaction curves were mapped using position of the reactant and product assemblages of the various isograds. For example, talc-bearing marble is above the talc-in isograd (figure 5.1) and corresponds to mineral assemblages stable in fields 3 and 4 of the T-X_{CO2} diagram (figures 4.9 and 4.10) and is below the talc-out isograd. Both these isograds occur on the water-rich side of table 5.2.

The locations of two isobaric invariant points were mapped by bracketing them in the manner suggested by Skippen (1974). Isobaric invariant point I, corresponding to the assemblage calcite-dolomite-quartz-talc-tremolite-fluid, appears twice in the Lavant Gabbro Block. Isobaric invariant point II , corresponding to the assemblage calcite-dolomite-quartz--phlogopite-K-feldspar-tremolite-fluid is located near the central margin of the western marble unit.

Careful examination of both the field and petrographic evidence suggests that at least two metamorphic events or possibly one prolonged metamorphic event with mineral development on the retrograde path have been recorded by both the marbles and the gneissic rocks in portions of the field area. The location of one isograd (diopside-in, along the western margin of the Wolf Grove Structure) is based on the peak metamorphic assemblage overprinted by later, possibly retrograde, mineral growth.

Table 5.2 Relationship of mapped isograds to fluid composition and isobaric invariant points

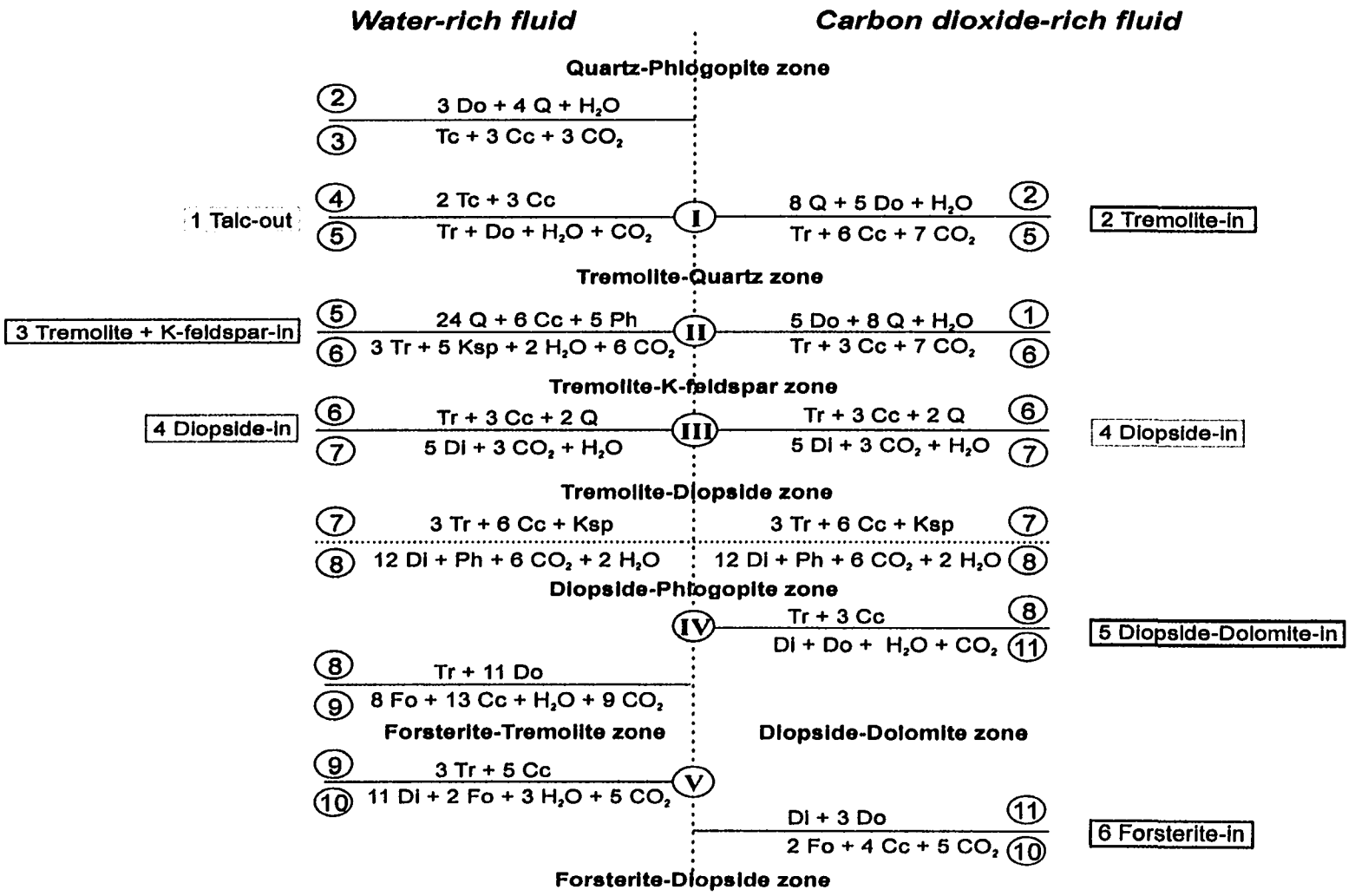

5.3.1 Isograd distribution in the Lavant Gabbro Block

Isograd patterns within the siliceous marble of the Lavant Gabbro Block form an antiformal pattern. Metamorphic grade is low in the "central" portion of the block and increases to the east and west. The lowest grade is characterized by talc- and talc-tremolite-bearing marbles in the northwest and along the southeastern margin. The areas of high metamorphic grade occur along the contact with the Lavant Gabbro Complex, the margin of the Pakenham Dome, and along the Clayton Lake shear zone. Traverse lines across the isograds of the block are shown in figure 5.2. The mineral assemblages present above and below the isograds and their corresponding fields are shown in the T-X_{CO2} diagram for the Lavant Gabbro Block (figure 5.3) and in table 5.1.

Internal buffering of the fluid composition, as described in case 2, appears to have controlled mineral development within the "central" low of the Lavant Gabbro Block marbles. South of the line E-I on figure 5.2, isograd 2 or the tremolite-in isograd does not occur as a sharp boundary. Locally in a zone roughly one kilometre-wide between the inferred location of isobaric invariant points I and II, marbles in closely spaced outcrops contain mineral assemblages consistent with both the product and reactant assemblages of the tremolite-in reaction. Reactant assemblages are comprised of calcite, dolomite, quartz, and phlogopite. Product assemblages contain calcite, quartz, phlogopite, and tremolite ± dolomite. These assemblages correspond to fields 2 and 5 in figure 5.3 and table 5.1. The presence of mineral assemblages from above and below the isograd indicates the fluid composition within the marble has been controlled by the reaction: 5 dolomite + 8 quartz +H_2O = tremolite +3 calcite + 7 CO_2 (reaction 6, figure 5.3).

Figure 5.2 Simplified geological map of the Carleton Place area showing the location of isograds and isobaric invariant points mapped in this study. Traverse lines correspond to lines on T-X_{co2} diagrams 5.3 and 5.4 (Geology after Reinhardt and Liberty, 1973)

LEGEND

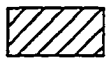
Paleozoic rocks


Granodiorite to granite gneiss, quartzite, and syenite

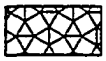
Pakenham gneiss ; includes in-folded amphibolite and marble


Wolf Grove gneiss, migmatite, and amphibolite


High-grade marble; includes in-folded amphibolite and quartzite

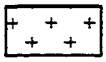
Frontenac gneiss and migmatite; includes in-folded quartzite and marble

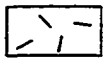
Lavant Gabbro Complex; gabbro, metadiorite, and amphibolite


Gabbro, pillow basalt, and amphibolite


Low-grade marble with minor gabbro, and basalt


Approximate location of marble thin section


Approximate location of isobaric invariant point


Shear zone

Forsterite-in, ticks on the high-grade side

Diopside-Dolomite-in

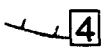

Diopside-in

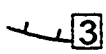

Tremolite + K-Feldspar-in

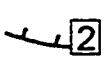

Tremolite-in

Talc-in

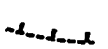
Position of isograd boundary approximated


Ticks on both high- and low-grade sides of isograd due to local buffering of fluid composition

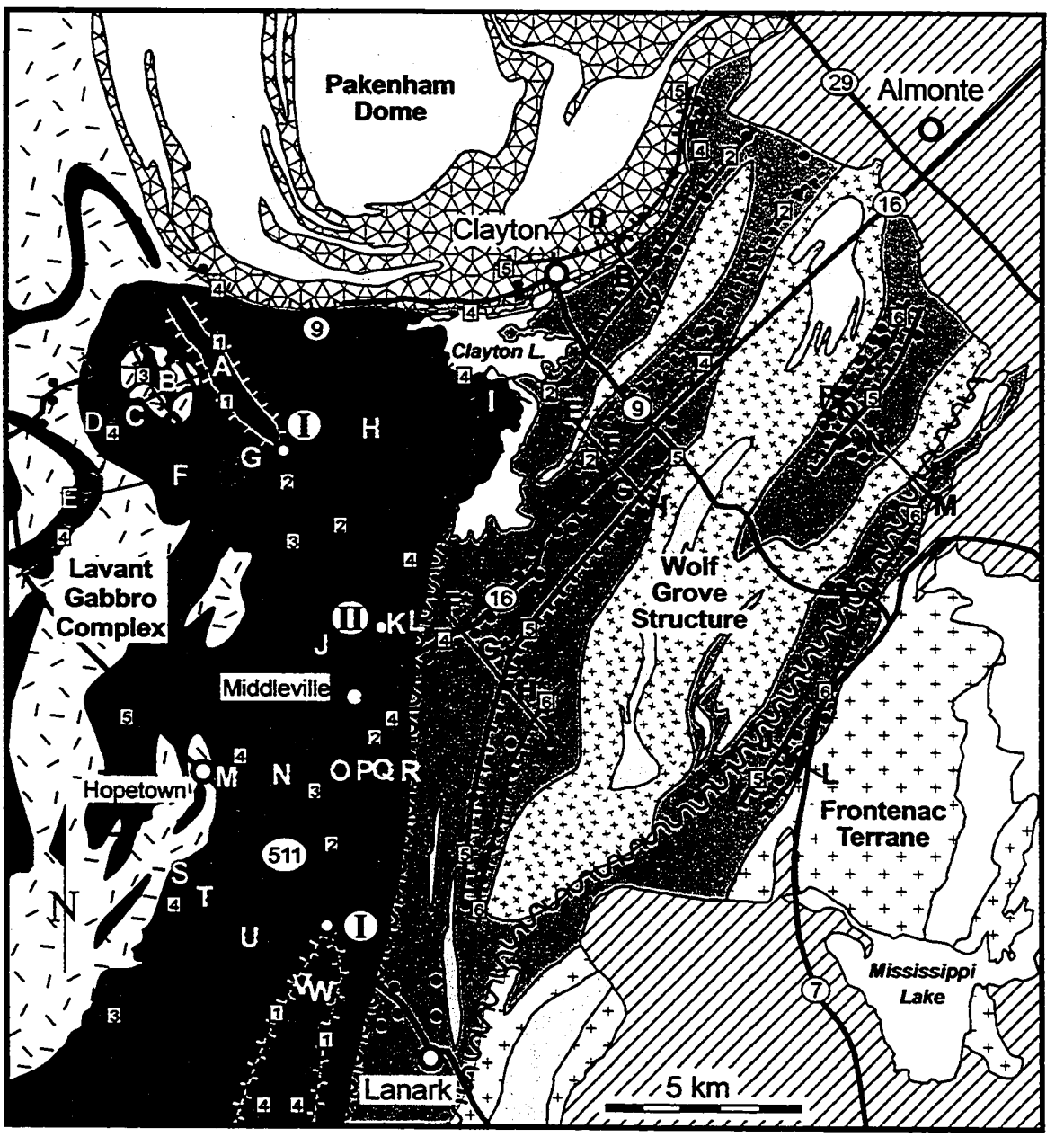

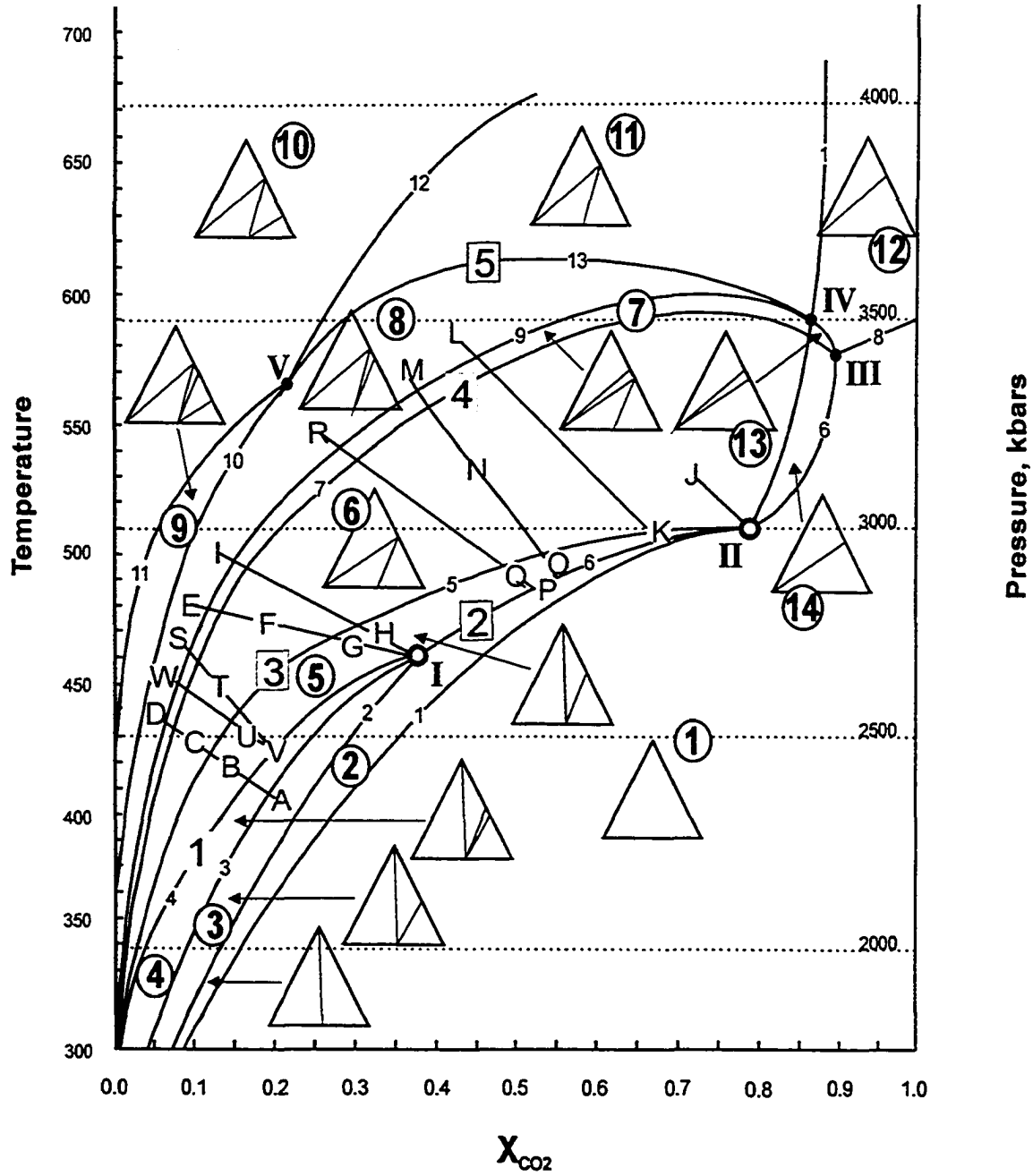

Figure 5.3 T-X_{co2} diagram displaying alphabetically-labelled lines corresponding to traverse lines on figure 5.2. Letters are within fields which correspond to the trivariant mineral assemblages identified by petrography. Circled numbers refer to the field number. Table 5.1 contains labelled CaO-SiO_2-MgO diagrams corresponding to the fields shown here. The lines are numbered by reaction and the reactions are listed in table 4.1.

A second zone of internally buffered marble is located south of the isobaric invariant point II. Line M-R on figure 5.2 crosses this zone and exemplifies the change in metamorphic grade within the Lavant Gabbro Block from west to east. At M near the contact with the Lavant Gabbro Complex, the marble is above isograd 4 (diopside-in) and is at the highest grade along the line. The mineral assemblages present are consistent with fields 8, and 9 of the T-X_{CO2} section (figure 5.3) and table 5.1. Marble located between isograds 4 and 3 (tremolite + K-feldspar-in), labelled N, contain trivariant mineral assemblages from field 6 of figure 5.3 and table 5.1. Mineral assemblages consistent with field 7 were not identified in the field which is the assemblage predicted to occur first above the tremolite + K-feldspar-in isograd. However, field 7 is restricted to a rather narrow band between fields 6 and 8 on the T-X_{CO2} section (figure 5.3) making identification of this assemblage in the field less likely. Marble at O falls between isograds 3 and 2 (tremolite-in) and contains mineral assemblages consistent with field 5 of figure 5.3. Along isograd 2, assemblages from both above and below (fields 2 and 5) the isograd are present (P on figure 5.3) indicating the fluid composition has been internally buffered. At Q, the metamorphic grade rises as the Clayton Lake shear zone is approached. The rocks are above isograd 2 but lack sufficient potassic phases to delineate isograd 3 in this area. Diopside-bearing marbles at R indicate the rocks are above isograd 4 (diopside-in). Isograd 4 is truncated by the Clayton Lake shear zone just below R.

Evidence of internal buffering is also present along line S-W to the northwest of Lanark (figure 5.2). Between points U and V along this line, the talc-out isograd (isograd

1) is crossed. However, as described above, marbles containing assemblages above and below the isograd are present, indicating that fluids were buffered along reaction 4 (figure 5.3) to isobaric invariant point I. Mineral assemblages consistent with fields 3 , 4, and 5 are found in close proximity locally defining a narrow zone. As demonstrated by figure 5.3 and table 5.2, the presence of talc indicates water-rich fluid conditions (>60%).

Between points V and W along line S-W, the diopside-in isograd (isograd 4) is crossed. At W, marble contains mineral assemblages corresponding to field 8 (figure 5.3 and table 5.1). The close proximity of talc-bearing and diopside-bearing marbles in this area may reflect increased permeability of the marbles. This area is within the marble breccia zone of the Clayton Lake shear zone and does show evidence of deformation in outcrop. The increased permeability of possibly sheared or deformed marbles may allow reactions to progress more rapidly than in massive marble.

Line A-D crosses three isograd boundaries which appear to be more typical of case 1 than the lines discussed above. Each isograd north of isobaric invariant point I is marked by a distinct change in mineral assemblage over a short distance. Point A is below the talc-out boundary and the marble contains minerals consistent with fields 3 and/or 4 below the isograd. Marble at B contains tremolite and is within field 5 of figure 5.3. Marble at point C is above the tremolite + K-feldspar isograd (isograd 3) and the mineral assemblage corresponds to field 6. Point D is above the diopside-in isograd (isograd 4) and corresponds to field 8. Mineral assemblages specific to field 7 were not identified.

The locations of the isobaric invariant points I and II were determined by the

bracketing of the points with assemblages above and below the points and the intersection of the isograds. The intersection of isograds at isobaric invariant points in the field indicate that a fluid gradient at an angle to the regional thermal gradient existed as described in case 3.

Isobaric invariant point II appears only once within the Lavant Gabbro Block; however, this does not mean that the peak metamorphic conditions occurred at point II (see line J-L). Isobaric invariant point II is likely repeated in a similar manner to point I. However, the mineral assemblages above point II corresponding to fields 13 and 14 (figure 5.3 and table 5.1) were not identified in the field. In each case, the assemblages contain K-feldspar and as has been noted above, potassic phases are less common within the marbles as the Clayton Lake shear zone is approached.

A local occurrence of CO_2-rich fluids is implied by the presence of diopside-dolomite-bearing marbles within an embayment of the Lavant Gabbro Complex approximately 2 kilometres west of Hopetown (figures 5.1 and 5.2). The marble contains the mineral assemblage calcite-dolomite-diopside-phlogopite (field 11, figure 5.3 and table 5.1) indicates conditions above isograd 5 (diopside-dolomite-in). This assemblage is stable in fluid conditions at or above ~25% CO_2.

5.3.2 Isograd Distribution within the Wolf Grove Block

Isograds parallel the Wolf Grove Structure and the trend of the Maberly shear zone within the Wolf Grove Block. Metamorphic grade is highest near the margins of the

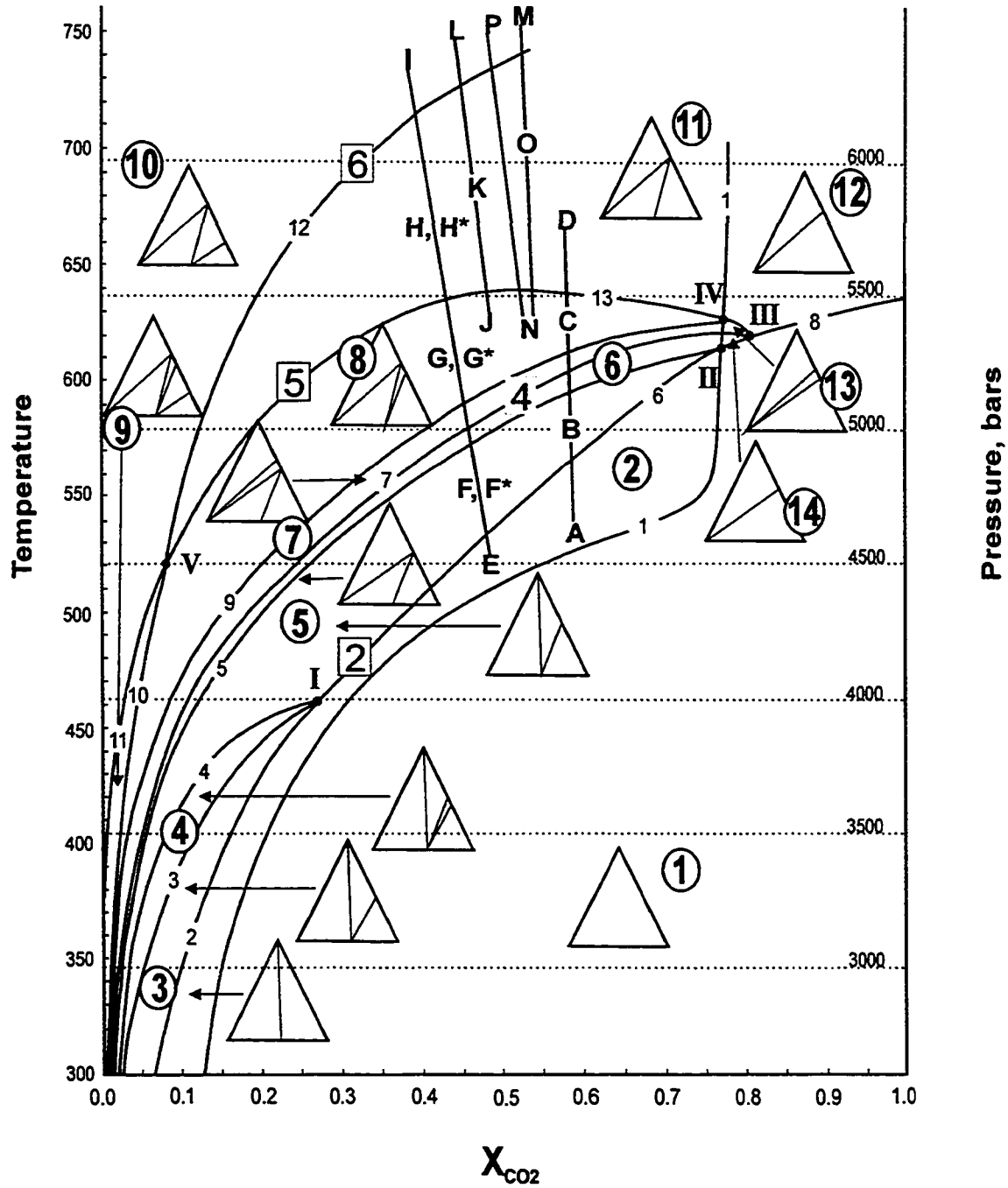

Figure 5.4 T-X_{co2} diagram displaying alphabetically-labelled lines corresponding to traverse lines on figure 5.2. Letters are within fields correspond to the trivariant mineral assemblages identified by petrography.

Pakenham Dome, Wolf Grove Structure and the Frontenac gneisses. An area of low grade marble (below isograd 2 - tremolite-in) outcrops between the main body of the Wolf Grove Structure and the eastern edge of the Pakenham Dome. The low grade marble encloses a narrow body of amphibolite and migmatite. Traverse lines across the isograds are shown in figure 5.2. The mineral assemblages present above and below the isograds and their corresponding fields are shown in the T-X_{CO2} diagram for the Wolf Grove Block (figure 5.4) and in table 5.1.

The lines A-D, E-H and F*-I demonstrate the increase in metamorphic grade within the marbles as the two gneissic structures are approached. At A, the marble contains the mineral assemblage calcite-dolomite-phlogopite-quartz, corresponding with field 2 of figure 5.4 and table 5.1. Metamorphic grade increases to the northwest and at B the tremolite-in isograd has been crossed. The assemblage at B falls within field 5 of figure 5.4. The diopside-in isograd roughly coincides with the margin of the Pakenham Dome. The marble at C is above the isograd 4 and is comprised of calcite-dolomite-phlogopite-tremolite-diopside±quartz. At point D, marble in-folded with gneisses of the Pakenham Dome are above isograd 5 (diopside-dolomite-in) and contain mineral assemblages corresponding to field 11 of figure 5.4 and table 5.1. Between isograds 2 and 4, isograd 3 (tremolite + K-feldspar-in) must have be crossed. However, the lack of K-feldspar within these marbles prohibits the delineation of this isograd.

A similar pattern of increasing metamorphic grade occurs along lines E-H and F*-I. The mineral assemblages at F -F*, G-G*, and H-H* are the same, allowing the two segments to be discussed as one continuous line. The metamorphic grade at E is low and

below the tremolite-in isograd (field 2 of figure 5.4 and table 5.1). At F and F*, the metamorphic grade has increased and the mineral assemblage is comprised of calcite-dolomite-phlogopite-tremolite±quartz, corresponding to field 5 (figure 5.4 and table 5.1). Marble at G and G* has crossed above isograd 4 (diopside-in). The marble is composed of calcite-dolomite-phlogopite-tremolite-diopside, equivalent to field 8. Fields 6 and 7 must have been crossed with increasing P and T. However, these fields are stable over a very narrow range of temperature conditions on figure 5.4 which reduces the likelihood of identifying these assemblages in the field. Grade continues to increase at H-H* and the diopside-dolomite-in isograd (isograd 5) has been crossed. This isograd is mapped on the basis of the peak metamorphic assemblage. The samples used to outline this isograd display tremolite overgrowths on diopside (see photos 2.15 and 2.16), indicating a second period of metamorphic mineral growth subsequent to peak conditions. Isograd 6 is crossed between points H-H* and I. Marble at I is composed of forsterite-bearing assemblages consistent with field 10 of figure 5.4 and table 5.1. This is the highest metamorphic grade identified within the Wolf Grove Block.

Isograds 2-6 west of the Wolf Grove Structure are all sharp boundaries suggesting a relatively uniform fluid composition, as described in case 1. Isograds 4, 5, and 6 are truncated by the Wolf Grove Structure which suggests a slight gradient in fluid composition to P-T conditions may have existed. Isograd 4 is also truncated by the Clayton Lake shear zone.

On the east side of the Wolf Grove Structure, metamorphic grade increases towards the margins of both the Wolf Grove Structure and the Frontenac gneisses, as

shown by line M-P (figures 5.2 and 5.4). The lowest metamorphic grade within the marbles falls between the two structures (see N) and corresponds to field 8 (figure 5.4 and table 5.1). Between N and M, isograd 6 (diopside-forsterite-in) is crossed. Isograd 5 must also have been crossed. However, this isograd could not be continued along the trace of the Maberly shear zone from line J-L due to a lack of exposure or the truncation of isograd 5 by the shear zone. In addition, the intense deformation of rocks within the Wolf Grove Block complicates the tracing of particular assemblages along strike.

On the east side of the structure, the isograds are sharp boundaries with no apparent evidence of internal buffering which is common within the Lavant Gabbro Block.

Fluid composition within the Wolf Grove Block appears to be CO_2-rich (figure 5.4 and table 5.2). The marble contains abundant graphite and phlogopite. Talc and sepentine are present only as retrograde alteration products. This suggests that significantly different fluid regimes were present on either side of the Clayton Lake shear zone.

Chapter 6 - Metamorphic and tectonic history of the Carleton Place area

6.1 Tectonic significance of the Wolf Grove Structure and the surrounding siliceous marbles

Two fundamental questions were addressed by this study regarding the nature of the relationship between the siliceous marbles and the various gneissic and plutonic rocks of the Carleton Place area:

1) Do the siliceous marbles share the same metamorphic history as the Wolf Grove Structure or are the marbles related to the Lavant Gabbro Complex (i.e. what is the terrane assignment of the gneissic Wolf Grove Structure and the marbles)?

2) Where do the siliceous marbles and the Wolf Grove Structure fit into the tectonic models proposed for the Carleton Place area?

Three hypothetical tectonic models will be described first along with existing evidence which either supports or contradicts the model. Evidence from this study will then be discussed and integrated into a revised tectonic model.

6.2 Proposed tectonic models for the Sharbot Lake-Frontenac terrane boundary

Easton and Davidson (1997) proposed three hypotheses to explain the juxtaposition of rocks from the Wolf Grove Structure and the siliceous dolomitic marbles. Figure 6.1 is a schematic representation of the possible tectonic relationships between the gneissic rocks and the marbles as suggested by the various models. In each of the three hypotheses, the Maberly shear zone represents the boundary between the

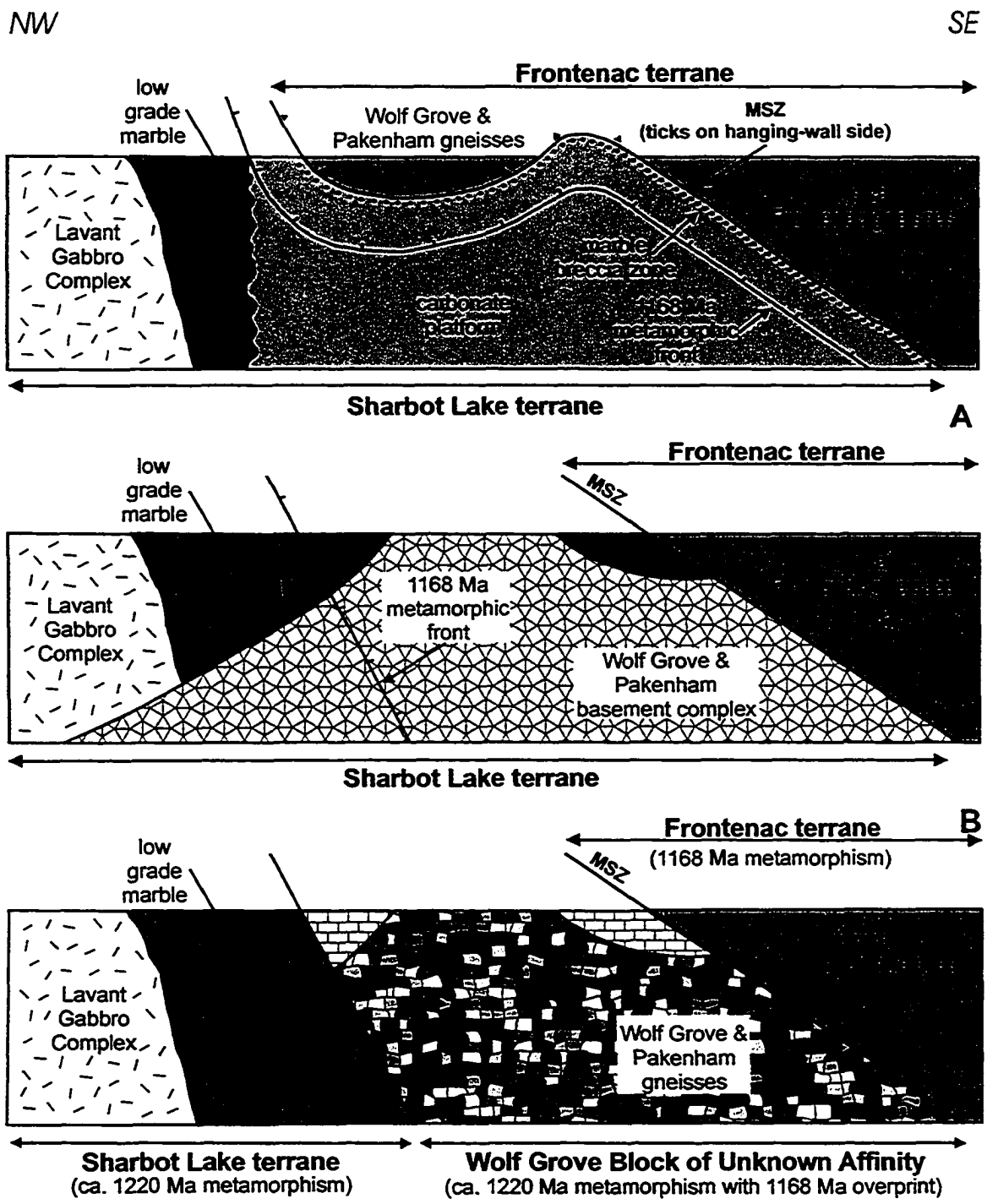

Figure 6.1 Cross -sections showing three interpretations of the relationships between the major rock units within the Carleton Place area. Section A represents the regional thrust model of Hildebrand and Easton (1995). Section B represents the Sharbot Lake basement model of Easton and Davidson (1997). Section C represents the Wolf Grove Block model of Easton and Davidson (1997). CLSZ = Clayton Lake shear zone; MSZ = Maberly shear zone. After Easton and Davidson (1997).

Sharbot Lake and Frontenac terranes. Each of the three proposed models is outlined below.

6.2.1 Regional thrust model

Hildebrand and Easton (1995) suggested that a majority of the existing evidence supported a regional thrust interpretation for the rocks of the Carleton Place area. The basis for this model (figure 6.1 A) is the development of a major suture in the southern Central Metasedimentary Belt at ~1161 Ma, after the intrusion of the Frontenac suite of plutonic rocks. An allochthon consisting of high-grade metamorphic rocks (including the Wolf Grove and Pakenham Dome structures) and the Frontenac plutonic suite was thrust northwestwards over the lower grade footwall rocks (dominantly marbles) of the Sharbot Lake terrane. Subsequent to thrusting, the hangingwall was then isoclinally folded and coaxially refolded before the intrusion of ~1160 Ma diabase dykes.

Hildebrand and Easton (1995) suggested that only one highly folded marble contact is traceable throughout the area and the contact between the high-grade Frontenac terrane and the low-grade Sharbot Lake terrane is distinguished by marble breccia implying a tectonic contact (figure 6.2 B). The authors also stated that there is no evidence of intrusive contacts between marbles and the Frontenac suite of plutons. Titanite ages from carbonates within the Frontenac terrane range from ca. 1178 to 1157 Ma (Mezger et al., 1993), overlapping the range of plutonism of the Frontenac suite. This was interpreted by Hildebrand and Easton (1995, 1997) to be the result of dynamothermal metamorphism during emplacement of the hot allochthon.

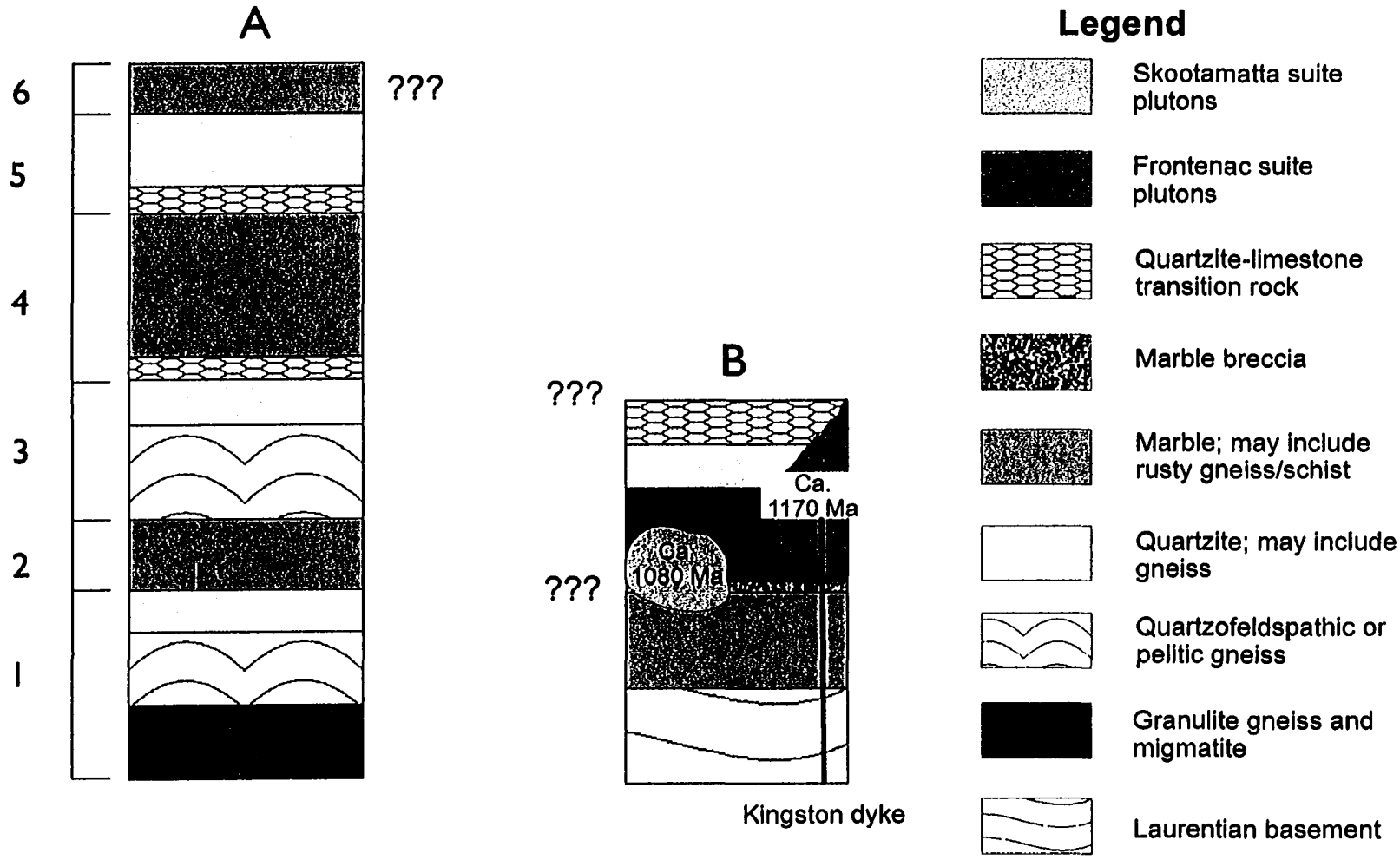

Figure 6.2 Simplified stratigraphic columns. Column A is the hypothetical stratigraphy proposed by Wynne-Edwards (1967 a). Column B represents the stratigraphy proposed by the regional overthrust model of Hildebrand and Easton (1995). (After Hildebrand and Easton, 1995)

This model is based on the following interpretations of geological realtions:

1.) Rocks of the Frontenac plutonic suite and the enclosing gneisses are restricted to the hangingwall and the marbles to the footwall.

2.) Marbles within the boundaries of the Frontenac terrane (east of the Maberly shear zone) represent windows into the footwall and were metamorphosed to high grade by dynamothermal metamorphism related to thrusting.

3.) Rocks above and below the thrust contact have been subjected to different plutonic, metamorphic and structural histories.

There are several lines of evidence which appear to support the regional thrust model.

Results from a geochemical study of the marbles from both the Sharbot Lake and Frontenac terranes (Easton, 1995) indicate marble from the contact with the Lavant Gabbro Complex to the Maberly shear zone (within the boundaries of the Sharbot Lake terrane) has similar signatures to marble from the Lyndhurst area of the Frontenac terrane. Marble breccia from the Frontenac terrane has a distinctive geochemistry, characterized by high REE abundances, no correlation between REE abundance and Al_2O_3 content and enrichment in Ba, Sr, Zr, and Ti relative to Grenville marbles. This is consistent with the restriction of the marble to the footwall as proposed by Hildebrand and Easton (1995).

Geochronological studies by Corfu et al. (1995) and Corfu and Easton (1997) yielded two generations of titanite at 1159 Ma and 1153 Ma from marble breccia within the Frontenac terrane. According to Corfu and Easton (1997), the titanite ages from marble breccia may date the metamorphic crystallization of the marble matrix following

tectonic juxtaposition of the gneiss-quartzite assemblage during or following the ~1168 Ma metamorphic event.

In addition, age data for migmatite and gneisses of the Wolf Grove Structure and metasedimentary rocks from east of the Maberly shear zone (figure 6.3; Corfu and Easton, 1997) show that the main phase of metamorphism, migmatization and granitic plutonism ranges between ca. 1169-1166 Ma and overlaps the main period of intrusion of the Frontenac suite (van Breemen and Davidson, 1988; Marcantonio et al., 1990; Wasteneys, 1994; Davidson and van Breemen, 2000). The Sharbot Lake terrane shows no apparent evidence of metamorphism at 1168 Ma. Corfu and Easton (1997) consider the ca. 1168 Ma event within the Wolf Grove Structure as diagnostic of the Frontenac terrane, as 1168-1160 Ma metamorphic and plutonic activity along the Frontenac terrane boundary was also a major event throughout the terrane.

Metamorphic lows with unreacted quartz + dolomite or K-feldspar + dolomite assemblages were documented by Ewert (1977) and suggest the regional metamorphic grade of the Lavant Gabbro Complex and the adjacent marbles is low. The preservation of primary sedimentary features indicates the marbles have undergone only one prograde metamorphic event (Kornik, 1986; Easton, 1992). Mapping by Ewert (1977; figure 6.4) suggested that metamorphic grade increases within the marbles as the Wolf Grove Structure and Pakenham Dome are approached and isograds are oblique to the structure which suggests "that metamorphism of the carbonate rocks was decoupled from the metamorphic events that produced the Wolf Grove and Pakenham gneisses (Easton, p.28 in Easton and Davidson, 1997). The gneisses document metamorphic conditions ranging

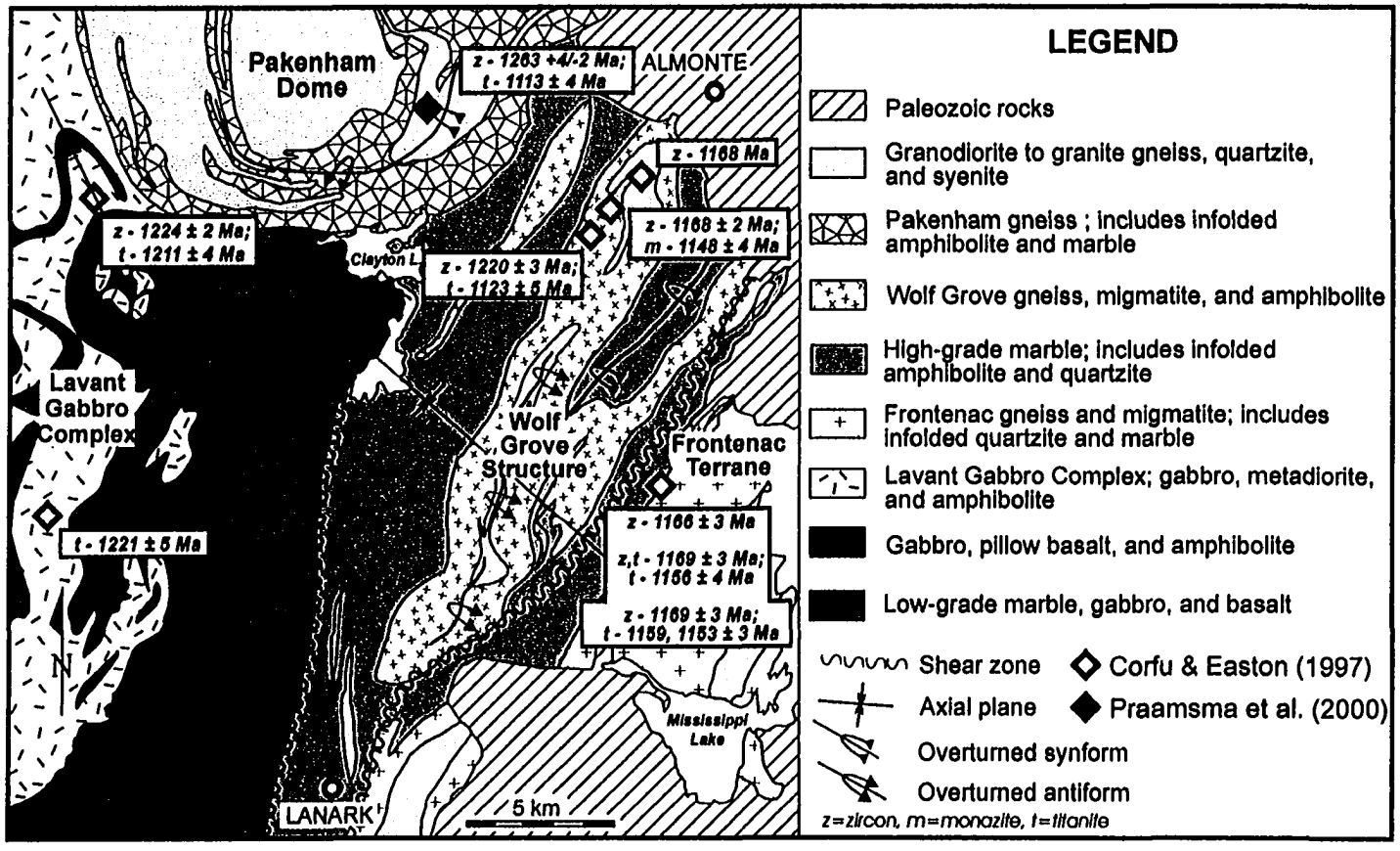

Figure 6.3 Simplified geological map of the Carleton Place area displaying locations of U-Pb geochronology samples from Corfu and Easton (1997) and Praamsma et al. (2000). Geology modified from Reinhardt and Liberty (1973).

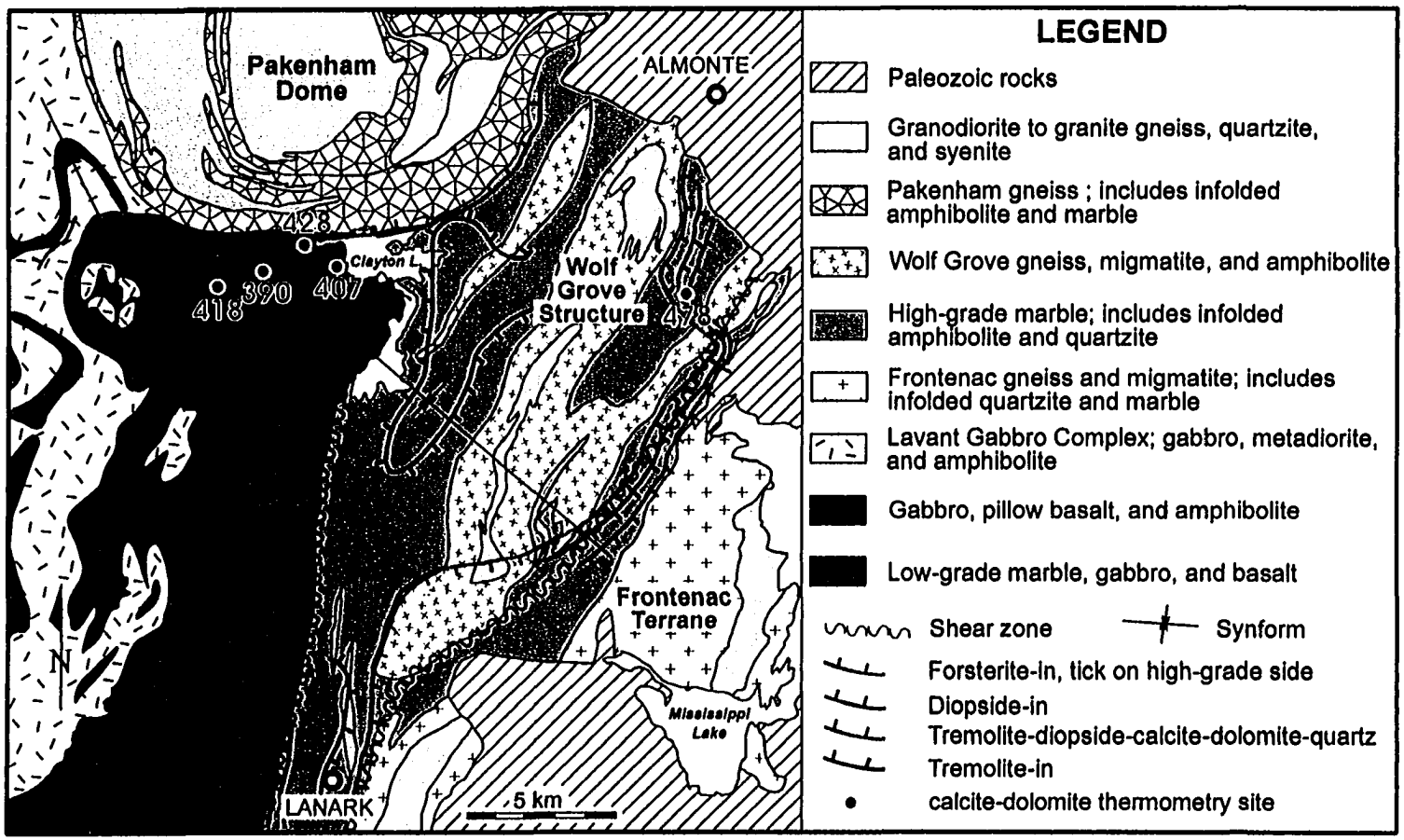

Figure 6.4 Simplified geological map of the Carleton Place area displaying locations of isograds as mapped by Ewert (1977). Geology modified from Reinhardt and Liberty (1973).

from upper amphibolite facies to locally granulite facies (Easton, 1992; Buckley et al., 1997). Relict mineral assemblages in migmatitic gneiss from the Wolf Grove Structure implies either multiple metamorphic events or protracted high-grade metamorphism within the gneisses.

Based on these observations, Hildebrand and Easton (1995) and Corfu and Easton (1997) suggested that the marble and the gneisses did not share common metamorphic and structural histories which is consistent with the regional thrust model.

Davidson and Carmichael (1997) put forth several objections to the regional thrust model. The stratigraphy proposed by Wynne-Edwards (1967 a; figure 6.2 A) suggests more than one marble unit is present and quartzite both overlies a lower marble unit as well as faces toward and grades into marble. Existing geological maps also show that quartzite lies concordantly between gneiss and the main marble unit (Wynne-Edwards, 1967 b). Davidson and Carmichael (1997) suggest that if the Hildebrand and Easton (1995) model is correct, the thrust sheet must have been overturned during emplacement.

Contrary to the contention that the marble was metamorphosed at low grade by the emplacement of the thrust sheet, the marble contains diopside, forsterite and chondrodite indicating high-grade metamorphism. The marble is commonly enclosed by granulite-facies pelitic gneisses (Wynne-Edwards, 1967 a) and these assemblages are far removed from silicate gneisses and plutonic rocks of the overriding upper plate. According to Davidson and Carmichael (1997) the metamorphic and geochronological evidence does not support the model of a hot upper plate overthrusting a cool carbonate platform.

The Lyndhurst pluton (ca. 1166 Ma; Marcantonio et al, 1990) was placed within the upper plate along with the pelitic gneisses and quartzites of the country rocks (Hildebrand and Easton, 1995). The authors considered the granite to be part of a "pluton-dominated klippe". Davidson (in Easton and Davidson, 1997) presented evidence that plutons of the Frontenac suite are in intrusive contact with marble from the proposed lower plate implying that the marble is part of the country rock and not within the footwall of the thrust. Detailed mapping by Davidson (in Easton and Davidson, 1997) demonstrates that the pluton truncates a steeply dipping, folded sequence of gneiss, quartzite and marble. This succession is in agreement with the stratigraphic sequence proposed by Wynne-Edwards (1967 a). Mapping also revealed a second phase of folding which has also been crosscut by the granite suggesting that deformation occurred before the emplacement of the pluton. There is no evidence of regional metamorphism or deformation after ca. 1166 Ma as predicted by the regional thrust model (Hildebrand and Easton, 1995).

U-Pb titanite ages in the same range or slightly younger than the age range of the Frontenac suite (Mezger et al., 1993; Corfu and Easton, 1997) imply that peak regional metamorphism in both the Sharbot Lake and Frontenac terranes preceded the emplacement of the Frontenac suite plutons (Davidson and Carmichael, 1997; Davidson and van Breemen, 1997; Davidson in Easton and Davidson, 1997). The ages indicate that the terranes had cooled below the titanite blocking temperature ($\leq$ 600 °C; Davidson and van Breemen, 2000) at the same time as plutonism and have not been reset by later events, such as regional scale folding and metamorphism related to the emplacement of a

thrust sheet. The presence of granulite-facies assemblages in plutons deformed by the Maberly shear zone may be the result of emplacement in a zone of active compression (Davidson and van Breemen, 1997; Davidson and van Breemen, 2000).

Frontenac suite plutons near the Maberly Shear Zone and its subsidiary shear zones in the northwest section of the Frontenac terrane are deformed and recrystallized (Easton, 1992; Davidson in Easton and Davidson, 1997). Davidson and van Breemen (2000) concluded that emplacement in an actively compressing shear zone was responsible for the fabric development in the plutons rather than post-plutonic tectonism in the boundary zone, based on the similarity of U-Pb titanite ages (Mezger et al., 1993; Corfu and Easton, 1997) from metamorphic rocks from the region southeast of the Robertson Lake Shear Zone, within the Maberly Shear Zone and the age of the Frontenac suite (Davidson and van Breemen, 2000). Easton (in Easton and Davidson, 1997) acknowledges that the Frontenac suite of plutons argue against significant displacement of the ca. 1160 Ma suture, unless they are considered as stitching plutons linking the Sharbot Lake and Frontenac terranes.

6.2.2 Sharbot Lake basement model:

The second model proposed by Easton and Davidson (1997 ;figure 6.1 B) suggests that the rocks of the Wolf Grove Structure and the Pakenham Dome are basement to the marbles of the Sharbot Lake terrane, which has been intruded by the Lavant Gabbro Complex and overprinted by ca. 1168 Ma metamorphism. An alternative possibility is that the two gneissic bodies represent the deeper structural level of a gabbro-

tonalite complex related to the Lavant suite, which has been overprinted by ca. 1168 Ma metamorphism during the thrust emplacement of the Frontenac terrane along the Maberly shear zone. In either case, the marble unit and associated metavolcanics overlie the Wolf Grove Structure and the Pakenham Dome. Marble also may be part of the overriding plate comprising the Frontenac terrane.

Age data from the Wolf Grove amphibolite appear to support a link to the Lavant Gabbro complex (figure 6.2; Corfu and Easton, 1997). The Lavant Gabbro Complex yielded an age range between ca. 1224 Ma and ca. 1211 Ma based on titanite, monazite, and zircon analyses, with a lack of a ca. 1168 Ma metamorphic overprint. Age data from zircons in the amphibolite represent either magmatic crystallization or metamorphism at ca. 1220 Ma (Corfu and Easton, 1997). Geochemical analysis of the amphibolite (Corfu and Easton, 1997) suggests this unit is indistinguishable from the tholeiitic gabbroic sills which intruded the marbles prior to the emplacement of the Lavant suite, which is typically calc-alkalic. Corfu and Easton (1997) indicate that the amphibolite could be a chemically distinct tholeiitic member of the gabbro complex or an older part of a gabbroic or basaltic unit within the marbles affected by syn-Lavant metamorphism. Both of these interpretations place the amphibolite within the Sharbot Lake terrane, consistent with the basement model.

Mapping of the Wolf Grove Structure (Reinhardt and Liberty, 1973) indicates a close connection between the amphibolite and the Wolf Grove gneisses metamorphosed at ca. 1168 Ma and assigned to the Frontenac terrane. Corfu and Easton (1997) conclude that the amphibolites and gneisses must have been structurally juxtaposed during the

waning stages of the ca. 1168 Ma event, as the amphibolites show no evidence of polymetamorphism.

Foliated granite and granodiorite from the core of the Wolf Grove Structure possess geochemical similarities to both migmatitic gneiss within the structure and monzogranites of the Lavant suite. Discordant U-Pb zircon age data from the granite range from ca. 1258 Ma to 1181 Ma and ca. 1171 to 1166 Ma (Corfu and Easton, 1997). The younger age range overlaps that obtained for the migmatite. Easton (in Easton and Davidson, 1997) contends that the older ages could be the result of inheritance and that formation of the migmatite and granite was coeval. However, the older age range may date magmatic crystallization of the granite, with the younger ages representing metamorphism of the structure during emplacement of the Frontenac terrane.

Geochronological work on foliated granodiorite from the Pakenham Dome by Praamsma et al. (2000) appears to support linkage of the intrusion to the Sharbot Lake terrane and expands the known age range for Elzevirian magmatism in the terrane. A U-Pb zircon age of 1263 +4/-2 Ma (figure 6.3) was obtained and interpreted as the crystallization age of the granodiorite.

Praamsma et al. (2000) suggest the marble and mafic volcanic sequence, which characterize the terrane, were deposited upon an Elzevir-type basement including the ca. 1263 Ma Pakenham intrusion. This sequence was intruded by the Lavant Gabbro Complex at ca. 1224 Ma (Corfu and Easton, 1997), which possibly represented the subvolcanic magma chamber for the earlier mafic volcanics associated with the marble (Easton, 1988 b). An alternative explanation is that both the Pakenham granodiorite and

the Lavant Gabbro Complex intruded the marble and mafic volcanic sequence. Praamsma et al. (2000) favour the first possibility, citing the contrasting structural and metamorphic histories of the Pakenham intrusion and the marble package and the suggestion by Corfu and Easton (1997) that felsic components of the Lavant Gabbroic Complex were produced by the partial melting of or strongly contaminated by sialic crust underlying the Sharbot Lake terrane. Both models are consistent with the basement model of Easton and Davidson (1997).

The presence of ca. 1258 Ma zircon in the Wolf Grove granite (Corfu and Easton, 1997) indicates a possible link to the ca. 1263 Ma Pakenham granodiorite. As the intrusions cross cut fabric within gneisses of both structures, it suggests that migmatization occurred significantly earlier than the ca. 1168 Ma time frame of the Hildebrand and Easton (1995) regional thrust model. The ca. 1168 Ma metamorphism recorded by the Wolf Grove Structure reflects overprinting during the emplacement of the Frontenac terrane (Easton and Davidson, 1997). The lack of any evidence for metamorphism at ca. 1168 Ma by the Pakenham intrusion may be the result of confinement of high-grade metamorphism to the immediate hanging wall of the Maberly shear zone (Praamsma et al., 2000).

An alternative explanation is offered by Davidson and van Breemen (2000). They contend that closure and thrusting between the Sharbot Lake and Frontenac terranes may have occurred as early as ca. 1220 Ma and the ca. 1168 Ma metamorphism is related to renewed compressional deformation along the Maberly shear zone and intrusion of the Frontenac suite of plutons.

6.2.3 Wolf Grove block model:

The third tectonic model proposed by Easton and Davidson (1997; figure 6.1 C) suggests that the rocks in and around the Wolf Grove Structure and the Pakenham Dome are related to neither the Sharbot Lake nor Frontenac terranes. The two structures are separated from the Sharbot Lake terrane by a shear zone exposed along Clayton Lake (Easton and Hildebrand, 1994; Clayton Lake shear zone, this study) and from the Frontenac by the Maberly shear zone (Davidson and Ketchum, 1993). The block between the shear zones has been affected by metamorphism at ca. 1220 Ma with an ca. 1168 Ma overprint but the rocks within have an unknown terrane affinity. This model places all the low grade marble west of the Clayton Lake shear zone within the Sharbot Lake terrane. Marble associated with the Pakenham and Wolf Grove Structures is also of unknown affinity. Marble east of the Maberly shear zone is then assigned to the Frontenac terrane as suggested by Wynne-Edwards (1967 a and b; figure 6.2 A). Age data obtained from rocks within the block are the result of metamorphism occurring during or after amalgamation of the separate blocks.

As has been noted above, there appear to be numerous links between the marbles and the gneissic structures to both the Sharbot Lake and Frontenac terranes suggesting that the rocks enclosed by the Clayton Lake and Maberly shear zones do not form a block of unknown affinity but may comprise a complex mix of rocks from both terranes.

6.3 Evidence from mapping and petrology

Detailed mapping within the Carleton Place area combined with petrographic and

petrological examination of the siliceous marble indicates that two marble units are present. The two units are juxtaposed along the Clayton Lake shear zone and experienced different metamorphic and deformational histories.

Marble to the west of the Clayton Lake shear zone is typically massive to weakly foliated. The tight to isoclinally folding which is characteristic of rocks east of the shear zone is largely absent. Metamorphic grade varies across the Lavant Gabbro Block. The highest grade marbles are located near the Lavant Gabbro Complex, the edge of the Pakenham Dome, and along the trace of the Clayton Lake shear zone. Low grade talc-tremolite-bearing marbles are present in the center of the block. Marbles near the Lavant Gabbro Complex display textural and mineralogical evidence of contact metamorphism. The remainder of the block appears to have experienced low-grade regional metamorphism, possibly related to emplacement of the composite Lavant Gabbro Complex.

The fluid composition shows evidence of internal buffering within the core of the block based on the close proximity of reactant and product assemblages at the isograd boundary. However, apart from locally CO_2-rich fluids within an embayment of the gabbro, the fluids are dominantly H_2O-rich indicated by the presence of talc ($X_{CO2} < 0.40$, figure 5.3) and chondrodite ($X_{CO2} < 0.50$; Bourne 1974).

A roughly 1-2 km wide zone of higher grade (diopside-bearing), brecciated and tightly folded marble follows the trace of the Clayton Lake shear zone. Deformation increases as the shear zone is approached. This zone may represent the limit of the ca. 1168 Ma metamorphism typically associated with the Frontenac terrane. The diopside-in

isograd outlining the shear zone is truncated by it (figure 5.1).

East of the Clayton Lake shear zone, marble is strongly foliated or banded and is frequently tightly to isoclinally folded and boudinaged. The metamorphic grade is higher than within the Lavant Gabbro Block and marble typically contains tremolite, diopside, and forsterite. The ubiquitous presence of graphite and phlogopite, a lack of primary talc, and the trivariant mineral assemblages present in marble of the Wolf Grove block indicates CO_2-rich fluids dominated the eastern portion of the map area. Isograds nearly parallel the Wolf Grove Structure and the Frontenac gneisses and the isograds are truncated by the Clayton Lake shear zone (figure 5.1).

Hildebrand and Easton (1995) and Corfu and Easton (1997) suggested that marble isograds at an oblique angle to the gneissic rocks (figure 5.1) or apparently cross-cutting the structure indicated a "decoupling" of the marble and gneisses, supporting the interpretation that marbles were absent in the hangingwall. Local variations in fluid composition could result in the isograds being oblique to the gneisses as the development of metamorphic minerals within carbonates is strongly controlled by the fluid composition. Due to a lack of exposure, it was not possible to continue the trace of isograds around the Wolf Grove Structure. In addition, Davidson (in Easton and Davidson, 1997) indicated that marble within the boundaries of the Frontenac terrane is in contact with plutonic rocks such as the Lyndhurst pluton which supports the presence of marble within the hangingwall.

The existence of two marble units is also compatible with the interpretations of the other models proposed by Easton and Davidson (1997; figure 6.1 B and C). Marble

overlies the Wolf Grove and Pakenham basement complex in the Sharbot Lake basement model (figure 6.1 B). The two marble units could represent different structural levels juxtaposed by the Clayton Lake shear zone but still encompassed by the Sharbot Lake terrane. In the case of the Wolf Grove Block model (figure 6.1 C) the two marble units would be separated by the two shear zones present in the Carleton Place area. The lower grade marble west of the Clayton Lake shear zone would belong to the Sharbot Lake terrane and the high-grade marble would overlie the Wolf Grove and Pakenham gneisses and could be a possible correlative to the Flinton Group sediments (Moore and Thompson, 1972). Both these models would require another marble unit east of the Maberly shear zone as Davidson and Carmichael (1997) and Davidson (in Easton and Davidson, 1997) has shown that marble must be present within the Frontenac terrane.

Easton and Hildebrand (1994) identified three major folding events in the Carleton Place area and contended that only the youngest F_3 folding event is recorded by the marbles. Northeast-trending refolded folds were observed in marble east of the Clayton Lake shear zone and the marble appears to be complexly in-folded with the gneissic rocks and amphibolites of the Wolf Grove Structure. As indicated by Easton and Hildebrand (1994), only the northwest-trending folds appear to have affected the entire map area. Primary igneous textures are preserved in units comprising the Lavant Gabbro Complex and pillow basalts were identified within 2 km of the shear zone. This suggests that the marble and gneissic rocks were juxtaposed prior to deformation in the Wolf Grove block and share a common structural history.

Thermobarometry data obtained from the various gneissic and plutonic rocks

associated with the marbles also suggest different metamorphic conditions prevailed on either side of the Clayton Lake shear zone. Relatively high temperature and low pressure conditions existed in the west (554 °C, 3.3 kbars). The approximate thermal gradient calculated from for the Lavant Gabbro Block is ~ 47 ° C/km. This gradient is consistent with either contact metamorphism or low-pressure regional metamorphism. The polybaric T-X_{CO2} diagram for this block (figure 4.9) shows that pressure-temperature conditions within the low-grade core of the block ranged from ~ 300-500 °C and ~ 1.5-3.0 kbars. Near the contact with the Lavant Gabbro Complex the P-T conditions exceeded 3.5 kbars and 600 °C which is comparable to conditions recorded by a garnet-bearing dioritic phase of the complex and reflects the increase in grade as the gabbro and the Pakenham Dome are approached.

High temperature and high pressure regional metamorphism are suggested by the data from the Wolf Grove block with average P-T conditions of 724 °C and 7.4 kbars. This corresponds to data obtained from the Westport area of the Frontenac terrane from both this study (706 °C, 7.2 kbars) and results reported by Buckley et al. (1997; 770 °C, 5.2 kbars), although pressures are lower,suggesting a link with the Frontenac terrane. This data produced approximate field gradients of ~ 26 °C/km-32 °C/km. Based on the polybaric T-X_{CO2} diagram for the Wolf Grove Block (figure 4.10), P-T conditions within the marbles ranged between 450-700+ °C and 4.0-6.0+ kbars. The pressure-temperature conditions predicted by figure 4.11 show a greater similarity to the thermobarometry data and suggest a range of ~ 470-700+ °C and 5.0-7.0+ kbars. The trivariant mineral assemblage unique to figure 4.11 was not identified, however, evidence from both the

field and thermobarometry indicates this higher field gradient could be applicable to the Wolf Grove Block.

In addition, there is evidence that at least two phases of metamorphism or a single prolonged metamorphic event are preserved by biotite-hornblende migmatite and garnet-biotite gneiss. Large (quarter-sized) garnets have been replaced by a mixture of garnet and biotite or tow forms of garnet are present within a single layer. Adjacent marble also locally displays textures consistent with either a protracted metamorphic event or a second metamorphic event. Some marbles contain a mineral assemblage with overgrowths of tremolite on diopside or tremolite. In the field, tremolite aligned in the regional foliation coexists in the same outcrop as randomly oriented tremolite sprays. This implies that the marble east of the Clayton Lake shear zone and rocks of the Wolf Grove Structure share a common metamorphic history.

Regional metamorphism within the Wolf Grove Block is likely related to movement along the Clayton Lake shear zone and/or the Maberly shear zone, possibly as early as ca. 1220 Ma and the emplacement of the Frontenac suite of plutons (ca. 1175-1152 Ma; Carr et al., 2000; Davidson and van Breemen, 2000).

Hildebrand and Easton (1995) and Corfu and Easton (1997) maintained a tectonic contact separates marble of the Sharbot Lake terrane and the amphibolite and gneisses of the Wolf Grove Structure. Examination of the contacts between marbles and the units within the Wolf Grove Structure and the Frontenac gneisses does not suggest a tectonic contact. Quartzofeldspathic-biotite schist occurs as pods and layers within marble to the east of the Clayton Lake shear zone. Similar units occur in the Perth and Westport areas

and are interpreted by Wynne-Edwards (1967 a) as representing original silty or sandy beds within limestone. These pods were not identified within marble of the Lavant Gabbro block.

Contacts between marble and amphibolite vary between gradational and sharp. Gradational contacts are characterized by interlayering of marble and amphibolite the contact. Foliation in both units is parallel to the contact and there is no visible evidence of grain size reduction or mylonization along the contact. Marble locally displays an increase in the amount of phlogopite adjacent to the amphibolite. Amphibolite frequently contains discontinuous layers, pods or veins of carbonate, which decrease in abundance away from the contact. Sharp contacts between marble and amphibolite exhibit no changes in grain size or mineralogy at the contact. Foliation in each unit is parallel to the contact.

Blocks and layers of amphibolite within marble are common within the Wolf Grove block. The amphibolite is often complexly folded and boudinaged within marble which may or may not display similar deformation. This may be interpreted as evidence of a tectonic breccia forming the contact between the two units. An alternate interpretation is that the marble has recrystallized more readily than the more rigid amphibolite during changes in regional deformation conditions.

Corfu and Easton (1997) favoured an igneous protolith for the amphibolite and suggested it may be related to the Lavant Gabbro Complex or the metavolcanics of the Sharbot Lake terrane, based on its geochemistry and ages from U-Pb dating of zircons. As the marble and amphibolite units are interlayered, Corfu and Easton (1997) concluded

that these rocks were part of the Sharbot Lake terrane and are overlain along a thrust contact by the gneisses and migmatites of the Frontenac terrane. In the northwestern quarter of the map area, amphibolite is in close association with both the Lavant Complex and the Pakenham Dome. However, deformation related to folding and shearing obscures the exact nature of the contacts between units.

The amphibolite exhibits compositional layering and is closely associated with both garnet amphibolite and garnet gneiss. Contacts between amphibolite and these units is typically gradational or interlayered. Amphibolite and garnet amphibolite are only distinguishable by the amount of garnet present and the existence of a well-developed gneissosity. In addition, along contacts with marble, the amphibolite contains more abundant calc-silicate minerals. This suggests that a portion of the amphibolite may have a calc-silicate protolith and is part of a metasedimentary sequence which varied between carbonate-rich and siliceous sediments.

Biotite-hornblende migmatite (photo 6.1a and b) is frequently interlayered with amphibolite and garnet amphibolite. Migmatitic rocks are also in contact with quartzite (photo 6.2a) and quartzofeldspathic-gneiss (photo 6.2b) within the Wolf Grove Structure. Locally, the migmatitic rocks become richer in quartz near the contact with quartzite. Quartzite is considered a characteristic rock type of the Frontenac terrane. The presence of quarzite within the Wolf Grove Structure supports the linkage of this package of gneisses with the Frontenac terrane.

Both these units strongly resemble quartzite and migmatite east of the Maberly shear zone. Easton (in Easton and Davidson, 1997) proposed the lack of migmatization

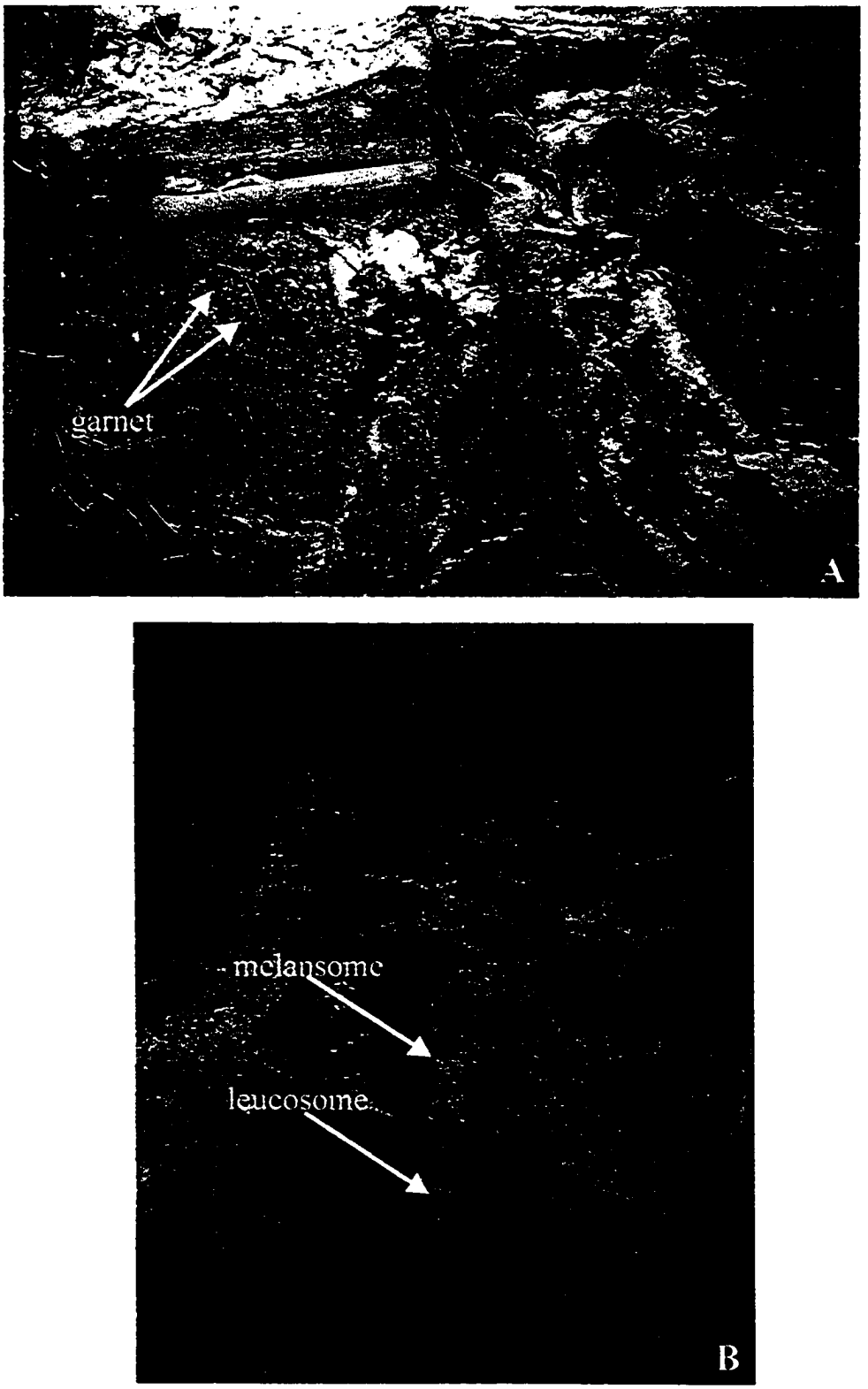

Photo 6.1 A) Migmatitic garnet-biotite gneiss. Mafic layers contain up to 20% garnet. Leucosome may be foliation parallel or cross-cutting. Hammer is 30 cm long.
B) Typical migmatite of the Wolf Grove Structure. Dark melansome is visible along margins of leucosome. Hammer is 40 cm long.

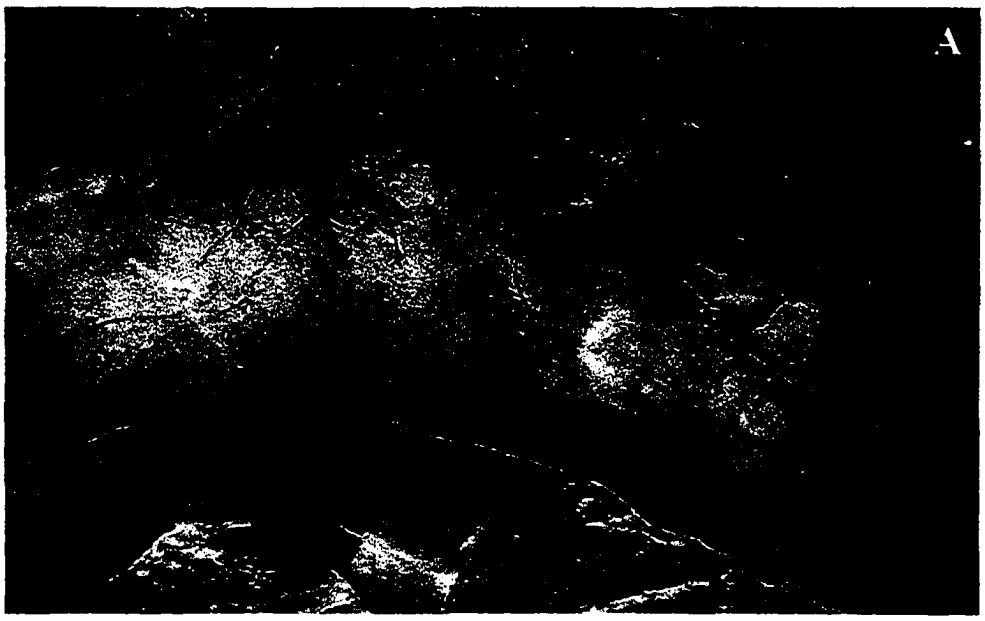

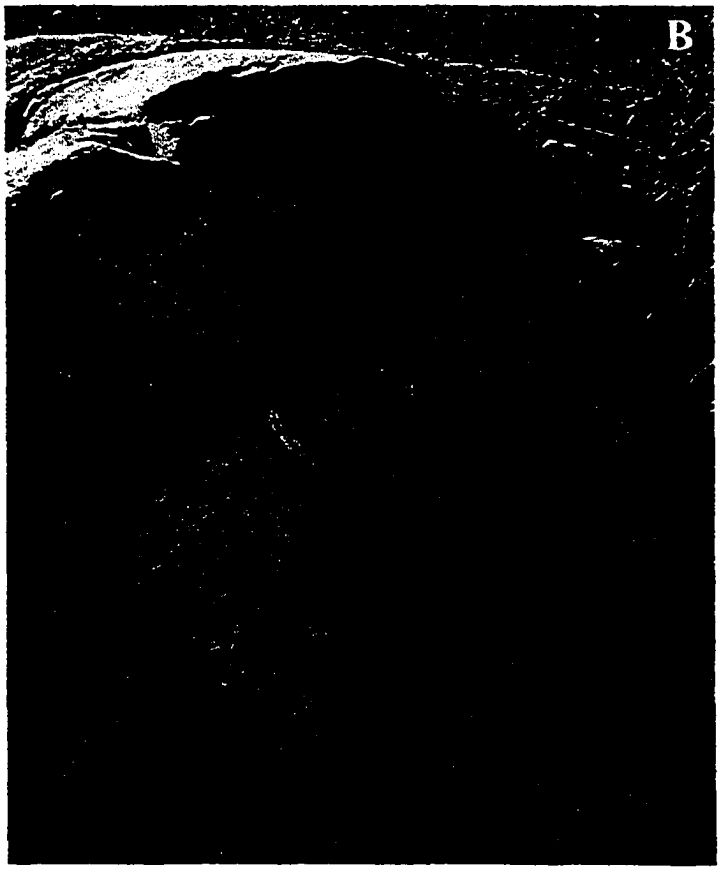

Photo 6.2 A) Pure, massive, white-grey quartzite within the Wolf Grove Structure. Quartzite is mainly located within the core of the structure. Hammer is 40 cm long.
B) Quartzofeldspathic gneiss exposed along Wolf Grove Road. Hammer is 30 cm long.

of rocks in contact with the hornblende-biotite migmatite could be a result of compositional differences. The amphibolites do not contain sufficient quartz to permit melting of the quartzofeldspathic component, unlike the migmatitic gneisses which contain up to 20-30% quartz and feldspar.

6.4 Revised tectonic model for the Carleton Place area

A revised tectonic model for the Carleton Place area is necessary to incorporate the results of this study. The revised model shares elements of the regional thrust model of Hildebrand and Easton (1995) and the tripartite stratigraphy of Wynne-Edwards (1967a). A schematic cross-section (figure 6.5) outlines the major elements of this new model. Key elements of this model are the recognition of two different marble units which have been juxtaposed by the Clayton Lake shear zone and the dissimilar structural and metamorphic histories on each side of the shear zone.

In this model, the Frontenac terrane has been thrust over the Sharbot Lake terrane along the Clayton Lake shear zone rather than the Maberly shear zone. The Sharbot Lake side of the boundary is characterized by low-grade metamorphism at ca. 1220 Ma. In contrast, the overriding Frontenac terrane experienced high-grade metamorphism over a prolonged period from approximately ca. 1220 Ma to ca. 1125 Ma with a major event at ca. 1168 Ma. Rocks within the overriding plate have been structurally repeated by both isoclinal folding and movement along the Maberly shear zone.

Based on this model, marbles west of the Clayton Lake shear zone are assigned to the Sharbot Lake terrane and form the footwall to the thrust. The marbles are intercalated

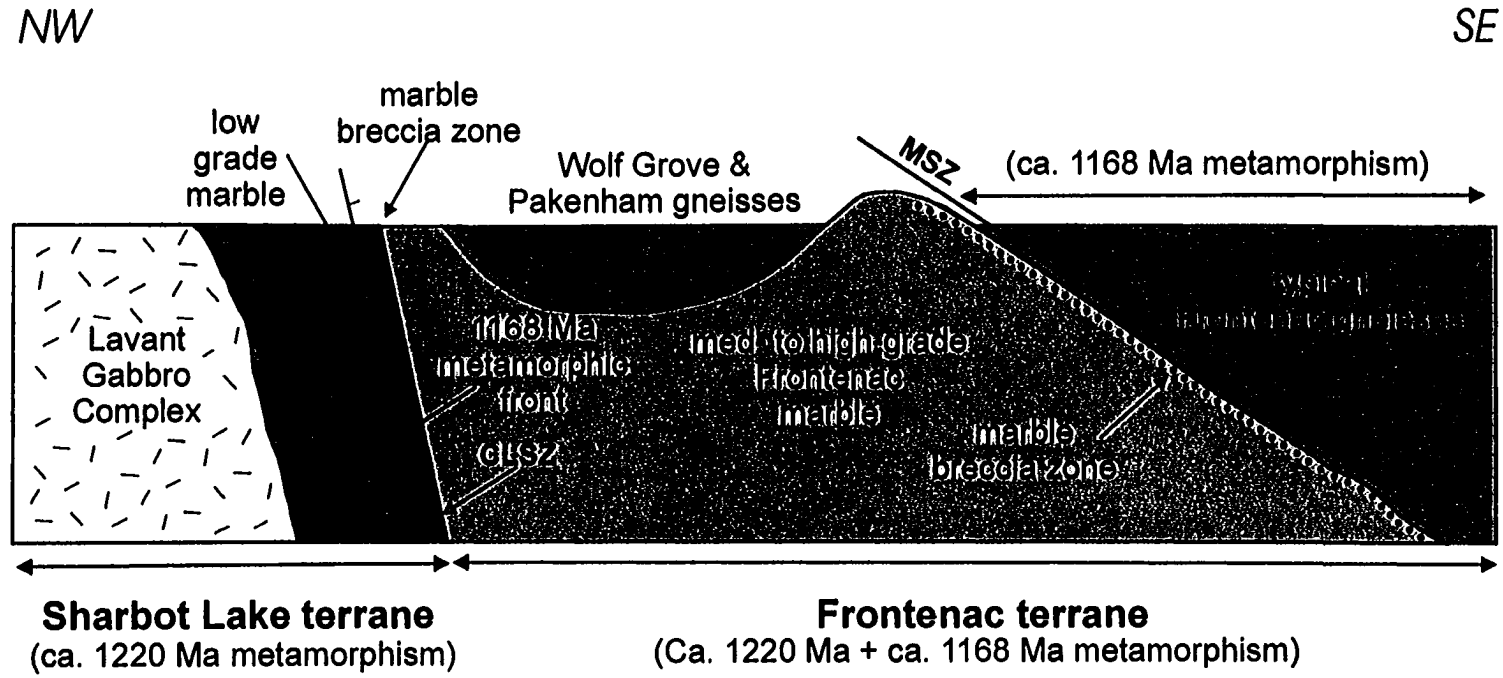

Figure 6.5 Hypothetical cross-section across the Carleton Place area showing the relationships of the Lavant Gabbro Complex, the western marble unit, the eastern marble unit, and the Wolf Grove Structure to the CLSZ (Clayton Lake) and MSZ (Maberly) shear zones. After Easton and Davidson, 1997.

with mafic metavolcanics and both are intruded by the Lavant Gabbro Complex. These rocks experienced a relatively shallow field gradient related to contact and regional metamorphism in the presence of H_2O-rich fluids.

Hildebrand and Easton (1995) predicted metamorphism of the cool platformal marbles by the hot, overriding thrust sheet with tectonic breccias marking the shear zone and metamorphic grade decreasing away from the contact. A marble tectonic breccia is present along the Maberly shear zone, however, metamorphic grade remains relatively high on either side of the Wolf Grove Structure. The Clayton Lake shear zone is marked by a roughly 2 km-wide zone of deformed and brecciated marbles. Metamorphic grade is high adjacent next to the boundary and decreases progressively away from the shear zone as expected in the regional thrust model. Metavolcanics just west of the shear zone retain primary igneous features such as pillows and diabasic textures. Therefore the location of the terrane boundary is the Clayton Lake shear zone.

Basement to the Sharbot Lake terrane is unknown. Praamsma et al. (2000) suggested that the Pakenham intrusion could form the basement of the marble-metavolcanic sequence. A U-Pb zircon age of 1263 +4/-2 Ma appears to support linkage of the structure to the terrane (Praamsma et al., 2000). Thermobarometric data from this study indicates the structure experienced slightly higher temperatures and pressures (750-800 °C and 5.5 kbars) than the Lavant Gabbro Complex. A possible interpretation of this data is that the Pakenham Dome does represent a lower structural level or basement of the Sharbot Lake terrane. An alternative explanation for the differences in pressure and temperature conditions between the Wolf Grove Structure and the Frontenac gneisses is

that the rocks are an older, structurally lower part of the Frontenac terrane which have been exhumed during movement along either the Clayton Lake or Maberly shear zones.

All rocks east of the Clayton Lake shear zone are assigned to the Frontenac terrane including the Wolf Grove Structure and the enclosing marbles. The marbles form an integral part of a metasedimentary package including various gneisses and quartzite, as suggested by the stratigraphy of Wynne-Edwards (1967a). The interlayered contacts between marble, gneisses, and amphibolite, similarity of deformation, and consistency of metamorphic grade across the marbles and the gneisses supports the conclusion that marbles are presence within the hangingwall, as suggested by Davidson and Carmichael (1997) and Davidson and van Breemen (2000).

Evidence for a limited ca. 1220 Ma metamorphic event within the Wolf Grove Structure and possibly the Pakenham Dome indicates the two terranes could have been juxtaposed during this intrusive event or have been in close proximity to each other. The higher pressure and temperature conditions and relict mineral assemblages within the gneisses may be related to this event. The dominant ca. 1168 Ma metamorphism could coincide with either amalgamation of the Sharbot Lake and Frontenac terranes or could be a response to renewed movement along the Maberly shear zone.

Davidson and van Breemen (2000) indicate that U-Pb titanite ages of ca. 1180-1150 Ma from metasedimentary gneisses overlap the emplacement of the Frontenac suite. The prservation of these ages and $^{40}Ar/^{39}Ar$ hornblende ages of ca. 1125 Ma suggest that regional cooling occurred very slowly. Metamorphism could have continued on the retrograde path leading to the preservation of the higher P-T assemblages in addition to

the dominant ca. 1168 Ma results. The secondary mineral growth displayed by both the gneisses within the Wolf Grove Structure and the marbles east of the Clayton Lake shear zone could have taken place during the cooling and uplift of the leading edge of the Wolf Grove block subsequent to juxtaposition against the Sharbot Lake terrane.

6.5 Suggestions for future research

The following list includes some of the possible research suggested by this study:

1) Mapping and sample collection of marbles surrounding the Wolf Grove Structure to determine whether the isograds continue around the structure.

2) Additional geochronology of both the marbles and the gneisses within the Carleton Place area, in particular to pinpoint the age of movement along the Clayton Lake shear zone and age of the metavolcanics.

3) Detailed structural mapping and analysis of the Clayton Lake shear zone.

4) Thermobarometry of gneisses of the Wolf Grove Structure, Pakenham Dome, Lavant Gabbro Complex, metavolcanics, and mafic dykes which intrude marble of the Wolf Grove Block.

5) Mineral chemistry of the garnets in gneisses with two or more generation of mineral growth. Similar work is required for tremolite within marbles displaying evidence of prolonged metamorphism.

6) Mapping and geochemistry of amphibolite and mafic dykes within the Carleton Place area to determine whether the amphibolite unit includes rocks with both igneous and sedimentary protoliths and the relationship of the amphibolite to the dykes. As some of

the dykes are metamorphosed and some retain igneous textures, can they be related to mafic dykes of known age.

7) Stable isotope and further geochemistry of the marbles.

8) Analysis of fluid inclusions from rocks throughout the Carleton Place area.

Chapter 7 - Conclusions and Contributions to Knowledge

1) An invariant point involving the phases calcite, dolomite, quartz, K-feldspar, phlogopite, tremolite, diopside, and fluid exists in pressure-temperature space. The computer program PTAX (Brown et al., 1988) calculated the temperature and pressure values at the intersection to be ~ 625 °C and 6.0 kbars. Univariant curves II (diopside absent) and IV (quartz absent) are unstable above this point and are replaced by univariant VI (a tremolite absent curve involving calcite-dolomite-quartz-potassium feldspar-diopside) and univariant VII involving the phases quartz-potassium feldspar-tremolite-diopside. Isobaric invariant point VII does not appear on the T-X_{CO2} diagram (figure 4.11) as it is only applicable in fluid absent conditions.

2) The following isograds were mapped in the Carleton Place area, a region approximately 40 km by 40 km:

1 Talc-out: 2 talc + 3 calcite = tremolite +dolomite + H_2O + CO_2

2 Tremolite-in: 5 dolomite + 8 quartz +H_2O = tremolite +3 calcite + 7 CO_2

3 Tremolite + K-feldspar-in: 24 quartz + 6 calcite + 5 phlogopite = 3 tremolite + 5 K-feldspar + 2 H_2O + 6 CO_2

4 Diopside-in: tremolite + 3 calcite + 2 quartz = 5 diopside + 3 CO_2 + H_2O

5 Diopside-Dolomite-in: tremolite + 3 calcite = dolomite + 4 diopside + H_2O + CO_2

6 Forsterite-in: tremolite + 11 dolomite = 8 forsterite + 13 calcite + 9 CO_2 + H_2O

3) Isograds form a simple antiformal pattern within the Lavant Gabbro block, west of the Clayton Lake shear zone. Metamorphic grade is relatively low within the central portion of the block and increases as the western, northern, and eastern margins are approached. A rapid increase of grade in the southeastern corner of the Lavant Gabbro block from talc-bearing assemblages to diopside-grade marble, may have resulted from increased permeability of marble due to deformation related to the shear zone.

4) Two isobaric invariant points (I; talc present and II; tremolite present) were mapped in the Lavant Gabbro Block by bracketing the isobaric invariant points with assemblages above and below the points and through the intersection of isograds.

5) Isograds within the western block exhibit evidence of internal buffering, as some isograds are marked by zones containing mineral assemblages both above and below the isograd. The intersection of isograds indicates that a fluid gradient to the P-T conditions existed during prograde metamorphism.

6) Prograde talc-bearing assemblages are confined to 2 areas west of the Clayton Lake shear zone and are indicative of water-rich conditions as shown on the T-X_{CO2} diagrams (figures 4.8, 4.9, and 4.10). Retrograde talc is present in rocks adjacent to the northwestern margin of the Lavant Gabbro Complex.

7) Isograds with the Wolf Grove block, east of the Clayton Lake shear zone nearly

parallel the margins of the Pakenham Dome, Wolf Grove Structure, and the Frontenac gneisses. Metamorphic grade increases as the gneissic bodies are approached. The isograds may have been folded with the structure but could not be traced around the southern edge of the Wolf Grove Structure do to lack of good exposure. The lowest metamorphic grade was observed between the Pakenham and Wolf Grove Structures. Two isograds from the eastern block are truncated by the Clayton Lake shear zone.

8) East of the Clayton Lake shear zone, CO_2-rich conditions are prevalent based on the abundance of phlogopite and graphite with evidence of later retrograde metamorphism dominated by water-rich fluids as shown by talc alteration of tremolite and sepentine alteration of forsterite.

9) Thermobarometry data obtained from gneissic and plutonic rocks associated with the marbles of the study area suggest different metamorphic conditions prevailed on either side of the Clayton Lake shear zone. Relatively high temperature and low pressure conditions existed in the west and area consistent with mineralogical and textural evidence from the marble that indicate both contact metamorphism associated with emplacement of the Lavant Gabbro Complex and a low-grade regional metamorphism. A prolonged high pressure and high temperature regional metamorphism is indicated by the data from the Wolf Grove Block.

10) Presumed peak metamorphic pressure and temperature conditions calculated by

WEBINVEQ (Gordon, 1998) for samples collected within the Wolf Grove Structure produced a mean temperature and pressure of equilibration of 713 °C at 7.7 kbars. Results from the Pakenham Dome imply lower temperature and higher pressure conditions (598 °C and 8.5 kbars) prevailed within this structure. However, the overall range in P-T conditions overlaps those recorded by the Wolf Grove Structure. Buckley et al. (1997) reported average metamorphic pressure and temperature conditions of 7.2 kbars at 718 °C for the Wolf Grove Structure. In contrast, pressure-temperature conditions calculated for the sample from the Lavant Gabbro Complex are much lower than those of the Wolf Grove Structure. Thermobarometry yielded an average temperature of 554 °C at 3.3 kbars pressure. A sample collected from the Lyndhurst area of the Frontenac terrane yielded an average temperature and pressure of 706 °C and 7.2 kbars, comparable to values obtained for the Wolf Grove Structure.

11) Detailed mapping and petrological examination of the siliceous dolomitic marbles of the Carleton Place area indicated that two marble units are present in the map area. They are distinguishable on the basis of mineralogy, metamorphic grade, degree of deformation, and associated rock types. The Clayton Lake shear zone is boundary between the two units. The western marble unit (Lavant Gabbro Block) is characterized by low metamorphic grade (talc and tremolite-bearing marbles are most common), poorly developed to absent regional foliation, and intrusive contacts with both mafic metavolcanic rocks and felsic to mafic metaplutonic rocks of the Lavant Gabbro Complex. This marble shows evidence of both contact and low-grade regional

metamorphism in the presence of water-rich fluids. The eastern marble unit is characterized by a higher metamorphic grade with tremolite + diopside- and forsterite-bearing assemblages dominating, displays a well developed regional foliation which is complexly folded, and forms an integral part of a metasedimentary package containing quartzofeldspathic gneisses and quartzites. The eastern marble and the associated metasediments experienced prolonged deformation and metamorphism with metamorphism outlasting deformation. The fluid composition is dominantly CO_2-rich based on the abundance of phlogopite and graphite.

12) The Clayton Lake shear zone was previously mapped by (Easton and Hildebrand, 1994) and was named in this study based on its exposure along the edge of Clayton Lake. The age of the shear zone is unknown but it may be related to the Maberly shear zone (Davidson and Ketchum, 1993). The shear is usually steep (75-90° dip) and is marked by a 1-2 km wide zone of tectonically brecciated marbles. A zone of high grade tremolite+diopside-bearing marbles along the western margin of the Clayton Lake shear zone may represent the extent of the metamorphic front associated with ~1168 Ma metamorphism characteristic of the Wolf Grove Structure and the Frontenac terrane. These marbles are folded and brecciated unlike the majority of carbonates west of the shear zone which are dominantly massive.

13) Marble east of the shear zone locally exhibits tremolite overgrowths on diopside and tremolite, and broken, aligned tremolite laths and radiating sprays of tremolite crystals

within the same outcrop. This implies either a prolonged metamorphic event with mineral growth on the retrograde path or a second distinct metamorphism. Gneissic rocks within the Wolf Grove Structure also contain evidence of multiple metamorphic events or protracted metamorphism. The gneisses contain large garnet pseudomorphs replaced by a mixture of garnet, biotite, quartz and/or feldspar. Some samples display two forms of garnet and biotite crystals both aligned into the foliation and randomly oriented crystals.

14) Thermobarometric data from the gneissic rocks were used to calculate approximate thermal gradients for the marbles within the field area. The Clayton lake shear zone was considered to be the boundary between the high temperature-low pressure metamorphism of the Lavant Gabbro Complex and the high temperature-pressure metamorphism characterized by the eastern half of the field area. Calculations yielded a thermal gradient of 47 °C/km for the Lavant block. Due to experimental uncertainty in the data from the Wolf Grove block, two field gradients were calculated. The resulting gradients for this block are steeper than those calculated for the Lavant block or the Lepontine Alps (Turner, 1968). The first gradient excludes the highest P-T conditions corresponding to pressures exceeding 9 kbars and is 32 °C/km. The second gradient excludes data with pressures under 5 kbars and is 26 °C/km. The range in the thermobarometric data for these units of the Wolf Grove block may be the result of prolonged metamorphism or a second metamorphic event as indicated in (13).

15) Polybaric T-X_{CO2} diagrams specific to the Carleton Place field gradients were

calculated using the computer program PTAX. Invariant points in T-X_{CO2} space are univariant curves in P-T space. Univariant curves in P-T space are reduced to isobaric invariant points in the T-X_{CO2} section. The exact fluid composition of the isobaric invariant points in T-X_{CO2} space was located by the intersection of two or more curves calculated using PTAX.

16) Two polybaric T-X_{CO2} diagrams were calculated for the eastern portion of the study area as it was determined that the higher field gradient intersected above the crossing point of univariant curves II, III, and IV in P-T space at approximately 625 °C and 6.0 kbars.

17) The polybaric T-X_{CO2} diagram calculated for the marbles of the eastern half of the map area using the lower regional field gradient was used for mapping the isograds based on the coexisting minerals assemblages identified in the marbles and the widespread preservation of the lower P-T conditions in the gneisses associated with the marbles.

18) Some of the amphibolite within the Wolf Grove Structure is inferred to have a metasedimentary, calc-silicate protolith, based on its characteristic compositional layering and stratigraphic relationships to the enclosing marbles and the gneisses within the structure. A combination of both para-amphibolite and ortho-amphibolite present in the structure may explain why amphibolite textures are preserved in close contact with migmatitic gneisses.

19) Marble, (amphibolite), migmatite, gneiss and quartzite east of the Clayton Lake shear zone are considered to be a sedimentary sequence intruded by granitic and granodioritic plutons and structurally repeated by folding. The stratigraphic sequence represents a change in sedimentation from dominantly carbonate to siliciclastic. These units appear to be very similar to gneissic units east of the Maberly shear zone and have been assigned to the Frontenac terrane. Rocks to the west of the shear zone belong to the Sharbot Lake terrane. The Sharbot Lake-Frontenac terrane boundary is assigned to the Clayton Lake shear zone, a possible splay of the Maberly shear zone. The two terranes were juxtaposed along the shear zone either prior to the ca. 1220 Ma emplacement of the Lavant Gabbro Complex or at ca. 1168 Ma. This is consistent with the tectonic model of Hildebrand and Easton (1995).

References

Abercrombie, H., 1983. Partitioning of fluorine between tremolite, talc, and phlogopite. Unpublished M.Sc. thesis, Carleton University, Ottawa, Ontario, 153 p.

Berman, R. G., 1988. Internally-consistent thermodynamic data for minerals in the system Na_2O- K_2O- CaO- MgO- FeO-Fe_2O_3- Al_2O_3- SiO_2- TiO_2- H_2O- CO_2. Journal of Petrology **29**, pp. 445-522.

Berman, R. G., 1990. Mixing properties of Ca-Mg-Fe-Mn garnets. The American Mineralogist, **75**, p. 328-344.

Berman, R. G., 1991. Thermobarometry using multiequilibrium calculations: a new technique with petrologic applications. Canadian Mineralogist, **29**, pp. 833-855.

Bourne, J. H., 1974. The petrogenesis of the humite group minerals in regionally metamorphosed marbles of the Grenville Supergroup. Unpublished Ph.D. thesis, Queen's University, Kingston, Ontario, 159 p.

Bowen, N. L., 1940. Progressive metamorphism of siliceous limestone and dolomite. Journal of Geology, **48**, pp. 225-274.

Brown, T .H., Berman, R. G., and Perkins, E. H., 1988. PTAX; Software for the calculation and display of pressure-temperature-activity phase diagrams. Computers and Geosciences, **14**, pp. 279-289.

Buckley, S. G., Easton, R. M. and Ford, F. D., 1997. P-T conditions, metamorphic history, and Sharbot Lake-Frontenac Terrane relationships in the Carleton Place and Westport map areas, Grenville Province. Summary of Field Work and Other Activities, 1997, Ontario Geological Survey Miscellaneous Paper 168, pp. 100-108.

Carmichael, D. M., 1970. Intersecting isograds in the Whetstone Lake area, Ontario. Journal of Petrology, **11**, p. 147-181.

Carmichael, Dugald M., 1991. Univariant mixed-volatile reactions: pressure-temperature phase diagrams and reaction isograds. Canadian Mineralogist, **29**, pp. 741-754.

Carmichael, D. M., Moore, J. M., Jr., and Skippen, G. B., 1978. Isograds around the Hastings metamorphic "low". Toronto '78, Field Trips Guidebook, editors, A. L. Currie and W. O. Mackasey, Geological Association of Canada, pp. 325-346.

Carmichael, D. M., Helmstaedt, H. H., and Thomas, N., 1987. A field trip in the Frontenac Arch with emphasis on the stratigraphy, structure and metamorphism.

Field trip guidebook, Kingston, Ontario, Friends of the Grenville, 24 p.

Carr, S. M., Easton, R. M., Jamieson, R. A., and Culshaw, N. G., 2000. Geologic transect across the Grenville orogen of Ontario and New York. Canadian Journal of Earth Sciences, **37**, pp. 193-216.

Connolly, J. A. D. and Trommsdorff, V., 1991. Petrogenetic grids for metacarbonate rocks: pressure-temperature phase-diagram projection for mixed-volatile systems. Contributions to Mineralogy and Petrology, **108**, pp. 93-105.

Corfu, F. and Easton, R. M. 1995. U-Pb geochronology of the Mazinaw terrane, an imbricate segment of the Central Metasedimentary Belt, Grenville Province, Ontario, Canadian Journal of Earth Sciences, **32**, pp. 959-976.

Corfu, F. and Easton, R. M. 1997. Sharbot Lake terrane and its relationships to Frontenac terrane, Central Metasedimentary Belt, Grenville Province: new insights from U-Pb geochronology. Canadian Journal of Earth Sciences, **34**, pp. 1239-1257.

Corfu, F., Easton, R. M., and Hildebrand, R S., 1995. Late Mesoproterozoic history of the Sharbot Lake, Frontenac and Adirondack Lowland terranes, Grenville Province. Geological Society of America, Abstracts with Programs, **27**, no. 6, p. A160-A161.

Cosca, M. A., Sutter, J. F., and Essene, E. J., 1991. Cooling and inferred uplift/erosion history of the Grenville Orogen, Ontario: Constraints from $^{40}Ar/^{39}Ar$ thermochronology. Tectonics, **10**, pp. 959-977.

Daly, J. S. and McLelland, J. M., 1990. Crustal growth in the SW Grenville Province. Geological Society of America, Abstracts with Programs, **22**, no. 2, p. 10.

Davidson, A., 1998. An Overview of Grenville Province Geology, Canadian Shield; Chapter 3. *in* Geology of the Precambrian Superior and Grenville Provinces and Precambrian Fossils in North America, co-ordinated by S. B. Lucas and M. R. St-Onge, Geological Survey of Canada, Geology of Canada, no. 7, pp. 205-270.

Davidson, A. and Carmichael, D. M., 1997. An 1161 Ma suture in the Frontenac terrane, Ontario segment of the Grenville orogen: Comment and Reply, Geology, **25**, pp. 88-90.

Davidson, A. and Ketchum, J. W. F., 1993. Observations on the Maberly shear zone, a terrane boundary within the Central Metasedimentary Belt, Grenville Province, Ontario. Current Research, Part C, Geological Survey of Canada, Paper 93-1C, pp. 265-269.

Davidson, A. and van Breemen, O., 1997. Age of plutonism constrains tectonic activity

along the Maberly shear zone, Central Metasedimentary Belt, Grenville Province, southeastern Ontario. Geological Association of Canada, Program with Abstracts, A 35.

Davidson, A. and van Breemen, O., 2000. Age and extent of the Frontenac plutonic suite in the Central Metasedimentary Belt, Grenville Province, southeastern Ontario. Geological Survey of Canada, Current Research 2000-F4; Radiogenic Age and Isotopic Studies, Report 13, 15 p.

Easton, R. M., 1988 a. Regional mapping and stratigraphic studies, Grenville Province with some notes on mineralization environments. Summary of Field Work and Other Activities, 1988, Ontario Geological Survey Miscellaneous Paper 141, pp. 300-308.

Easton, R. M., 1988 b. Precambrian Geology of the Darling area, Frontenac and Renfrew Counties. Ontario Geological Survey, Open File Report, 5693, 208 p.

Easton, R. M., 1992. The Grenville Province and the Proterozoic History of Central and Southern Ontario. Geology of Ontario, Ontario Geological Survey, Special Volume 4, Part 2, pp. 714-904.

Easton, R. M., 1995. Regional geochemical variation in Grenvillian carbonate rocks:

Implications for mineral exploration. Project Unit 91-08, 92-05 and 94-07, Summary of Field Work and Other Activities, Ontario Geological Survey Miscellaneous Paper 164, pp. 6-18.

Easton, R. M. and Davidson, A., 1994 a. Terrane boundaries and lithotectonic assemblages within the Grenville province, eastern Ontario. Waterloo, Ontario, Geological Association of Canada Field Trip Guidebook A 11, 9 p.

Easton, R. M. and Davidson, A., 1994 b. Terrane boundaries and lithotectonic assemblages within the Grenville Province. Geoscience Canada, 21, pp. 30-34.

Easton, R. M. and Davidson, A., 1997. Frontenac-Sharbot Lake relationships: evaluation of a provocative hypothesis concerning the tectonics of the Central Metasedimentary Belt, Ontario. Friends of the Grenville, Annual Field Excursion, Guidebook, 26-28 September 1997, 70 p.

Easton, R. M. and Ford, F. D., 1991. Geology of the Mazinaw area. Summary of Field Work and Other Activities, 1991, Ontario Geological Survey, Miscellaneous Paper 157, pp. 95-106.

Easton, R. M. and Hildebrand, R.S., 1994. Sharbot Lake-Frontenac terrane relationships in the Carleton Place map area, Grenville Province. Summary of Field Work and Other Activities, 1994, Ontario Geological Survey Miscellaneous Paper 163, pp.

52-55.

Eskola, P., 1922. On contact phenomena between gneiss and limestone in western Massachusetts. Journal of Geology, **30**, pp. 265-294.

Ewert, W. D., 1977. Metamorphism of siliceous carbonate rocks in the Grenville Province of southeastern Ontario. unpublished Ph.D. thesis, Carleton University, Ottawa, Ontario, 276 p.

Ferry, J. M. and Spear, F. S., 1978. Experimental calibration of the partitioning of Fe and Mg between biotite and garnet. Contributions to Mineralogy and Petrology, **66**, pp. 113-117.

Fitzsimons, I. C. W. and Harley, S. L., 1994. The influence of retrograde cation exchange on granulite P-T estimates and a convergence technique for the recovery of peak metamorphic conditions. Journal of Petrology, **35**, part 2, pp. 543-576.

Florence, F. P. and Spear, F. S., 1991. Effects of diffusional modification of garnet growth zoning on P-T path calculations. Contributions to Mineralogy and Petrology, **107**, pp. 487-500.

Flowers, G. C. and Helgeson, H. C., 1983. Equilibrium and mass transfer during

progressive metamorphism of siliceous dolomites. American Journal of Science, **283**, pp. 230-286.

Ford, D. F., 2002. Progressive metamorphism of Flinton Group Pelitic Schists Grenville Province, southeastern Ontario. Unpublished PhD thesis, Carleton University, Ottawa, Ontario, pp. 292.

Fuhrman, M. L. and Lindsley, D. H., 1988. Ternary- feldspar modeling and thermometry. American Mineralogist, **73**, pp. 201-216.

Ghent, E. D. and Gordon, T. M., 2000. Application of INVQ to the geothermobarometry of metamorphic rocks near a kyanite-sillimanite isograd, Mica Creek, British Columbia. American Mineralogist, **85**, pp. 9-13.

Gordon, T. M.,1992. Generalized thermobarometry; Solution of the inverse chemical equilibrium problem using data for individual species. Geochimica et Cosmochimica Acta, **56**, pp. 1793-1800.

Gordon, T. M.,1998. WEBINVEQ thermobarometry: An experiment in providing interactive scientific software on the World Wide Web. Computers and Geosciences, **24**, pp. 43-49.

Gordon, T. M., Aranovich, L. Ya., and Fed'kin, V. V., 1994. Exploratory data analysis in thermobarometry: an example from the Kisseynew Sedimentary Gneiss Belt, Manitoba, Canada. American Mineralogist, **79**, pp. 973-982.

Gordon, T. M. and Greenwood, H. J., 1970. The reaction dolomite + quartz + H_2O = talc + calcite + CO_2. American Journal of Science, 268, pp. 225-242.

Greenwood, H. J., 1967. Mineral equilibria in the system MgO-SiO_2-H_2O-CO_2. *in* Abelson, P. H., editor, Researches in Geochemistry. John Wiley and Sons, New York, pp. 542-567.

Helgeson, H. C. and Kirkham, D. H., 1974. Theoretical prediction of the thermodynamic behavior of aqueous electrolytes at high pressures and temperatures. *in* Summary of the thermodynamic/electrostatic properties of the solvent. American Journal of Science, v. **274**, pp. 1089-1198.

Helgeson, H. C., Delany, J. M., Nesbitt, H. W., and Bird, D. K., 1978. Summary and critique of the thermodynamic properties of rock forming minerals. American Journal of Science, v. **278-A**.

Hildebrand, R. S. and Easton, R. M., 1995. An 1161 Ma suture in the Frontenac terrane, Ontario segment of the Grenville orogen. Geology, **23**, pp. 917-920.

Hildebrand, R. S. and Easton, R. M., 1997. An 1161 Ma suture in the Frontenac terrane, Ontario segment of the Grenville orogen: Comment and Reply, Geology, **25**, pp. 88-90.

Kerrick, D. M. and Jacobs, G. K., 1981. A modified Redlich-Kwong equation for H_2O, CO_2 mixtures at elevated pressures and temperatures. American Journal of Science, v. **281**, pp. 735-767.

Kinsman, A. E., 1990. Geochronology of detrital zircons from quartzites in the Elzevir and Frontenac terranes, Central Metasedimentary Belt, Grenville Province. Unpublished B.Sc. thesis, Carleton University, 46 p.

Kinsman, A. E. and Parrish, R. R., 1990. Geochronology of detrital zircons from five quartzites in the Central Metasedimentary Belt of the Grenville Province. Programs with Abstracts, Geological Association of Canada, **15**, p. A70.

Kornik, W. D., 1986. Delineation of metamorphic isograds in siliceous dolomitic marble west of Almonte. Unpublished B.Sc. thesis, Carleton University, Ottawa, Ontario, 36 p.

Korzhinskii, D. S., 1959. Physiochemical basis of the analysis of the paragenesis of minerals. Consultants Bureau Inc., New York, 142 p.

Lonker, S., 1980. Conditions of metamorphism in high-grade pelitic gneisses from the Frontenac Axis, Ontario, Canada. Canadian Journal of Earth Sciences, **17**, pp. 1666-1684.

Lumbers, S. B., Heaman, L. M., Vertolli, V. M., and Wu, T. W., 1990. Nature and timing of Middle Proterozoic magmatism in the Central Metasedimentary Belt, Ontario. *in* Mid-Proterozoic Laurentia-Baltica. Edited by C.F. Gower, T. Rivers, and B. Ryan, Geological Association of Canada, Special Paper 38, pp. 243-276.

Mäder, U. K., and Berman, R. G., 1992. Amphibole thermobarometry: a thermodynamic approach. in Current Research, Part E. Geological Survey of Canada Paper 92-1E, pp. 393-400.

Marcantonio, F., McNutt, R. H., Dickin, A. P. and Heaman, L. M., 1990. Isotopic evidence for the crustal evolution of the Frontenac Arch in the Grenville Province of Ontario, Canada. Chemical Geology, 83, pp. 297-314.

McLelland, J., Daly, S., and Chiarenzelli, J., 1993. Sm-Nd and U-Pb isotopic evidence of juvenile crust in the Adirondack lowlands implications for the evolution of the Adirondack Mts. Journal of Geology, **101**, pp. 97-105.

McMullin D., Berman R. G., Greenwood H. J., 1991. Calibration of the SGAM

thermobarometer for pelitic rocks using data from phase equilibrium experiments and natural assemblages. Canadian Mineralogist, **29**, pp. 889-908.

Metz, P. and Trommsdorff, V., 1968. On phase equilibria in metamorphosed siliceous dolomites. Contributions to Mineralogy and Petrology, **18**, pp. 305-309.

Metz, P. and Winkler, H. G. F.., 1969. Equilibrium reaction on the formation of talc and tremolite by metamorphism of siliceous dolomite. Naturwiss., **55**, pp. 225-226.

Mezger, K., Essene, E. J., van der Pluijm, B. A., and Halliday, A. N., 1993. U-Pb geochronology of the Grenville Orogen of Ontario and New York: constraints on ancient crustal tectonics. Contributions to Mineralogy and Petrology, **114**, p. 13-26.

Moore, J. M., 1986. Introduction: The "Grenville Problem" Then and Now. *in* The Grenville Province, edited by J. M. Moore, A. Davidson, and A. J. Baer, Geological Association of Canada Special Paper 31, pp. 1-11.

Moore, J. M., 1992. Stratigraphy and tectonics of the Grenville orogen in eastern Ontario. 1982 Grenville Workshop, Rideau Ferry, Abstracts, p. 7.

Moore, J. M. and Thompson, P. H., 1972. The Flinton Group, Grenville Province,

eastern Ontario. 24th International Geological Congress, Proceedings, section 1, pp. 221-229.

Newton, R. C., 1983. Geobarometry of high-grade metamorphic rocks. American Journal of Science, 283-A, pp. 1-28.

Pauk, L., 1989. Geology of the Lavant area. Ontario Geological Survey, Report, 253, 61 p.

Percival, J. A., Bleeker, W., Cook, F. A., Rivers, T., Ross, G., and van Staal, C., 2004. Panlithoprobe Workshop IV: Intraorogen correlations and comparative orogenic anatomy. Geoscience Canada, 31, pp. 23-39.

Praamsma, T., Wodicka, N., and Easton, R. M., 2000. Evidence for magmatism of Elzevirian age in the Sharbot Lake domain, Central Metasedimentary Belt, Grenville Province of Ontario. Geological Survey of Canada, Current Research 2000-F6; Radiogenic Age and Isotopic Studies, Report 13, 8 p.

Press, W. H., Teukolsky, S. A., Vetterling, W. T., and Flannery, B. P. (1992) Numerical Recipes in Fortran. The Art of Scientific Computing. Second Edition. Cambridge University Press. Cambridge, 963 p.

Puhan, D. and Hoffer, E., 1973. Phase relations of talc and tremolite in metamorphic calcite - dolomite sediments in the southern portion of the Damara Belt (Southwest Africa). Contributions to Mineralogy and Petrology, v. **40**, pp. 207-214.

Reinhardt, E. W. and Liberty, B. A., 1973. Geology, Carleton Place, Ontario. Geological Survey of Canada, Map 1362A, scale 1:50,000.

Rivers, T., Martignole, J., Gower, G. F., and Davidson, A., 1989. New tectonic divisions of the Grenville Province, southeast Canadian Shield. Tectonics, **8**, pp. 63-84.

Seber, G. A. F. and Wild, C. J. (1989) Nonlinear Regression. John Wiley and Sons. New York, 768 p.

Sheih, Y-N., 1985. High-^{18}O granitic plutons from the Frontenac Axis, Grenville Province of Ontario, Canada. Geochimica et Cosmochimica Acta, 49, pp. 117-124.

Skippen, G. B., 1971. Experimental data for reactions in siliceous marbles. Journal of Geology, **79**, pp. 451-481.

Skippen, G. B., 1974. An experimental model for low pressure metamorphism of

siliceous dolomitic marble. American Journal of Science, **274**, pp. 487-509.

Skippen, G. B., 1997. Metacarbonate rocks from the Grenville Province of eastern Ontario. Geological Association of Canada, Abstract Volume, v. **22**, p. A138.

Slaughter, J., Kerrick, D. M.., and Wall, V. J., 1975. Experimental and thermodynamic study of equilibria in the system CaO-MgO-SiO_2-H_2O-CO_2. American Journal of Science, **275**, pp. 148-182.

Spear, F. S., 1991. On the interpretation of peak metamorphic temperatures in light of garnet diffusion during cooling. Journal of Metamorphic Geology, **9**, pp. 379-388.

Spear, F. S., 1992. Thermobarometry and P-T paths from granulite-facies rocks: an introduction. Precambrian Research, **55**, pp. 201-207.

Spear, F. S. and Florence, F. P., 1992. Thermobarometry in granulites: pitfalls and new approaches. Precambrian Research, **55**, pp. 209-241.

Tilley, C. E., 1951. A note on the progressive metamorphism of siliceous limestone and dolomites. Mineralogical Magazine, **88**, pp. 175-178.

Tracy, R. J., 1982. Compositional zoning and inclusions in metamorphic minerals. *in* Ferry, J. M. ed., Characterization of Metamorphism through Mineral Equilibria, Mineralogical Society of America Review in Mineralogy, **10**, pp. 355-397.

Trommsdorff, V., 1972. Change in T-X during metamorphism of siliceous dolomitic rocks of the Central Alps. Schweiz Mineral Petrographie Mitt, 52, pp. 1-4.

Tuccillo, M. E., Essene, E. J., and van der Pluijm, B. A., 1990. Growth and retrograde zoning in garnets from high-grade metapelites: Implications for pressure-temperature paths. Geology, **18**, pp. 839-842.

Turner, F. J., 1968. Metamorphic Petrology: Mineralogical and Field Aspects. McGraw-Hill Inc., pp. 359.

van Breemen, O. and Davidson, A., 1988. U-Pb zircon ages of granites and syenites in the Central Metasedimentary Belt, Grenville Province, Ontario. Radiogenic age and isotopic studies: Report 2, Geological Survey of Canada, Paper 88-2, pp. 45-50.

Warne, S. S. J., 1962. A quick field or laboratory staining scheme for the differentiation of the major carbonate minerals. Journal of Sedimentary Petrology, **32**, pp. 29-38.

Wasteneys, H. A., 1994. U-Pb geochronology of the Frontenac terrane, Central Metasedimentary Belt, Grenville Province, Ontario. Geological Association of Canada, Program with Abstracts, **19**, p. A118.

Wilson, M. E., 1918. The subprovincial limitations of Precambrian nomenclature in the St. Lawrence Basin. Journal of Geology, **26**, pp. 325-333.

Wilson, M. E., 1925. The Grenville Precambrian Subprovince. Journal of Geology, **33**, pp. 389-407.

Wolff, J. M., 1982. Geology of the Long Lake area. Ontario Geological Survey, Report 216, 76 p.

Wolff, J. M., 1985. Geology of the Sharbot Lake area. Ontario Geological Survey, Report 228, 70 p.

Wyllie, P. J., 1962. The effect of "impure" pore fluids on metamorphic dissociation reactions. Mineralogical Magazine, **33**, pp. 9-25.

Wynne-Edwards, H. R., 1963. Brockville-Mallorytown map area, Ontario. Geological Survey of Canada, Map 7-1963, scale 1:63,360.

Wynne-Edwards, H. R., 1965. Geology of the Tichbourne area. Geological Survey of Canada, Paper 64-56, 5 p.

Wynne-Edwards, H. R., 1967 a. Westport map area with special emphasis on the Precambrian rocks. Geological Survey of Canada, Memoir 346, 142 p.

Wynne-Edwards, H. R., 1967 b. Geology, Westport, Ontario. Geological Survey of Canada, Map 1182A.

Wynne-Edwards, H. R., 1972. The Grenville Province. *in* Variations in tectonic styles in Canada. R. A. Price and R J. W. Douglas, editors. Geological Association of Canada, Special Paper 11, pp. 263-334.

Yardley, Bruce W. D., 1989. An Introduction to Metamorphic Petrology. Longman Scientific & Technical, New York, 248 p.

Appendix 1: Summary of thermobarometry results from PTAX and WEBINVEQ

sample UTM	domains	gt-bt-plag	gt-hb-bt-plag	gt-hb-bt	gt-hb-plag
Wolf Grove Structure					
012 043b	043b A	578-637°C			
	043b B	632-681°C			
017 048	048a A	666-714°C			
	048a B	757-807°C			
	048a C	782-833°C			
993 007		793-842°C			
024 054a	054a A		762°C 9039 bars	757°C 6216 bars	775°C 9460 bars
	054a B		646°C 6502 bars	669°C 7428 bars	666°C 6794 bars
	054a C		745°C 8802 bars	742°C 5587 bars	771°C 9361 bars
025 055a	055a A		735°C 9257 bars	721°C 6290 bars	734°C 9132 bars
	055a B			788°C 9478 bars	789°C 9894 bars
	055a C				
	055a D				
050 008	008 A		670°C 5691 bars		749°C 7455 bars
	008 B		813°C 9900 bars		
	008 C		812°C 9433 bars	891°C 9161 bars	
995 0035b	0035b A		701°C 7580 bars	680°C 1800 bars	707°C 7562 bars
	0035b B		741°C 8050 bars	720°C 2949 bars	744°C 8004 bars
989 988	988 A		712°C 5963 bars		715°C 5956 bars
	988 B		724°C 5876 bars	728°C 2048 bars	758°C 7646 bars
	988 C				695°C 5383 bars
Pakenham Dome					
954 051	051*			549°C 8889 bars	
	051 A			530°C 9275 bars	496°C 2224 bars
	051 B		501°C 2422 bars	539°C 8176 bars	516°C 2655 bars
	051 C				519°C 1466 bars
	051 D		500°C 2286 bars	531°C 6344 bars	520°C 2659 bars
Lavant Gabbro Complex					
859 004	004 A		546°C 4436 bars	537°C 1003 bars	564°C 5072 bars
	004 B		355°C 4929 bars	531°C 2455 bars	547°C 2971 bars
	004 C				552°C 1576 bars
	004 D		540°C 2636 bars	556°C 2831 bars	590°C 4118 bars
Lyndhurst area					
070 304a	304 A (hb rim)		710°C 7929 bars	698°C 5335 bars	711°C 7951 bars
	304 B (hb core)		694°C 6587 bars	716°C 8222 bars	711°C 6810 bars
	304 C (hb rim)		698°C 8081 bars	686°C 1942 bars	716°C 8288 bars
	304 D (hb core)		723°C 8997 bars	713°C 2888 bars	747°C 9328 bars
	304 E		713°C 7012 bars	744°C 9816 bars	738°C 7402 bars

Appendix 1 (cont.): Summary of thermobarometry results from PTAX and WEBINVEQ

sample UTM	domains	gt-hb	hornblende only	gt-hb-cpx-bt-plag	gt-hb-cpx-plag
Wolf Grove Structure					
012 043b	043b A				
	043b B				
017 048	048a A				
	048a B				
	048a C				
993 007					
024 054a	054a A	762°C 6691 bars	688°C 6821 bars		
	054a B	668°C 7401 bars	702°C 7367 bars		
	054a C	758°C 6690 bars	688°C 6821 bars		
025 055a	055a A	721°C 6355 bars	678°C 6430 bars		
	055a B	786°C 9223 bars	751°C 9290 bars		
	055a C		723°C 8177 bars		
	055a D		690°C 6904 bars		
050 008	008 A			668°C 5560 bars	739°C 7426 bars
	008 B			776°C 8168 bars	
	008 C	884°C 8451bars	741°C 8877 bars	761°C 7275 bars	849°C 9470 bars
995 0035b	0035b A	681°C 1892 bars	584°C 1967 bars		
	0035b B	720°C 2982 bars	595°C 3195 bars		
989 988	988 A				
	988 B	727°C 1934 bars	571°C 2269 bars		
	988 C				
Pakenham Dome					
954 051	051*		762°C 9706 bars		
	051 A	532°C 9519 bars	748°C 9147 bars		
	051 B	539°C 8186 bars	711°C 7727 bars		
	051 C	515°C 521 bars	526°C 505 bars		
	051 D	545°C 8161 bars	711°C 7727 bars		
Lavant Gabbro Complex					
859 004	004 A	556°C 3185 bars	593°C 3125 bars		
	004 B	550°C 3774 bars	607°C 3669 bars		
	004 C	549°C 1000 bars	539°C 1017 bars		
	004 D	599°C 6052 bars	665°C 5925 bars		
Lyndhurst area					
070 304a	304 A (hb rim)	700°C 5527 bars	657°C 5621 bars		
	304 B (hb core)	723°C 9212 bars	748°C 9163 bars		
	304 C (hb rim)	687°C 1996 bars	569°C 2178 bars		
	304 D (hb core)	719°C 3342 bars	603°C 3499 bars		
	304 E		677°C 6407 bars		

Appendix 2 - Mineral Chemistry

Garnet analyses ***Wolf Grove Structure***

Sample 012 043b									
analysis	**SiO_2**	**AL_2O_3**	**TiO_2**	**Cr_2O_3**	**FeO**	**MnO**	**MgO**	**CaO**	**TOTAL**
043B-1	36.62	20.56	0.03	0.02	35.09	4.96	0.76	2.81	100.85
043B-2	36.91	20.76	0	0	36.23	3.62	1.13	2.52	101.17
043B-3	36.48	20.99	0	0.02	36.74	3.15	1.25	2.47	101.1
043B-4	37.04	20.67	0	0.03	36.97	2.99	1.35	2.44	101.49
043B-5	36.71	20.36	0	0.06	35.84	4.26	0.98	2.39	100.6
043B-6	36.86	20.41	0.02	0	35.27	2.67	1.4	3.43	100.06
043B-7	36.68	20.82	0	0.03	35.74	2.86	1.61	2.69	100.43
043B-8	37.13	20.82	0.03	0	36.21	2.66	1.64	2.47	100.96
043B-9	36.62	20.54	0	0.09	36.17	2.26	1.88	2.52	100.08
043B-10	37.15	20.35	0.02	0.01	34.96	2.28	1.65	3.17	99.59
043B-11	36.86	20.78	0.02	0.05	35.49	3.08	1.05	3.1	100.43
043B-12	36.85	20.2	0	0.02	36.18	2.5	1.54	2.4	99.69
043B-13	36.97	20.67	0	0	36.97	2.73	1.46	2.56	101.36
043B-14	36.55	20.73	0	0.01	35.95	3.55	0.7	2.47	99.96
043B-15	36.61	20.31	0.02	0	35.94	3.39	0.81	2.51	99.59
043B-16	36.73	20.58	0	0.06	35.92	2.59	1.43	2.41	99.72
043B-17	37.58	20.79	0	0.03	34.93	2.73	1.12	3.6	100.78
Sample 017 048a									
048A-1	37.21	20.34	0.02	0	23.96	13.91	0.8	3.72	99.96
048A-2	37.24	20.01	0.04	0.04	27.51	9.75	1.86	3.51	99.96
048A-3	37.34	20.01	0	0.05	27.37	10	1.86	3.63	100.26
048A-4	36.82	19.74	0.26	0	23.35	13.86	0.78	4.66	99.47
048A-5	38.09	20.01	0.06	0	23.15	14.19	0.62	4.72	100.84
048A-6	36.84	19.76	0.03	0.02	27.14	10.49	1.59	3.69	99.56
048A-7	36.94	19.87	0	0	27.03	10.8	1.53	3.68	99.85
048A-8	36.55	19.89	0.03	0	24.42	13.53	0.87	4.05	99.34
048A-9	36.69	19.95	0	0.06	24.09	13.39	0.99	3.9	99.07
048A-10	36.86	19.65	0	0	27.7	9.7	1.96	3.36	99.23
048A-11	37.07	19.79	0	0.03	28.9	8.8	2.3	3.31	100.2
048A-12	37.23	19.94	0.03	0.02	26.88	9.82	1.94	3.77	99.63
048A-13	37.18	19.61	0.02	0	28.64	8.35	2.46	3.53	99.79
048A-14	37.47	19.85	0.01	0	27.97	8.9	2.33	3.4	99.93
048A-15	37.04	19.61	0.03	0	28.05	8.95	2.13	3.34	99.15
048A-16	37.41	19.74	0.03	0.02	28.77	8.71	2.15	3.38	100.21
048A-17	36.53	19.45	0	0	24.64	12.92	1.02	3.79	98.35
048A-18	37.2	20.01	0.03	0.03	24.98	11.99	1.24	4.1	99.58
048A-20	37.06	19.9	0.03	0.04	27.86	9.08	2.06	3.66	99.69
048A-21	37.52	19.94	0.03	0	27.77	8.87	2.24	3.53	99.9
048A-22	37.12	19.39	0.01	0	27.07	11.13	1.57	3.59	99.88
Sample 993 007									
007-1	36.53	20.79	0.03	0.01	26.12	8.33	1.43	7.16	100.4
007-2	37.15	21.02	0.02	0.01	26.45	7.6	2.28	5.53	100.06

Appendix 2 - Mineral Chemistry (cont.)

Garnet analyses ***Wolf Grove Structure***

Sample 993 007									
analysis	**SiO_2**	**AL_2O_3**	**TiO_2**	**Cr_2O_3**	**FeO**	**MnO**	**MgO**	**CaO**	**TOTAL**
007-3	37.44	21.3	0.03	0	26.88	8.07	2.36	5.36	101.44
007-4	37.07	20.94	0.15	0	27.22	7.78	2.34	5.41	100.91
007-5	37.02	20.9	0.02	0.01	26.39	8.09	2.29	5.15	99.87
007-6	37.07	20.71	0.19	0.06	27.21	8.03	2.11	5.68	101.06
007-7	37.25	20.81	0.03	0	25.44	9.59	1.26	5.73	100.11
007-8	38.86	21.53	0.05	0.04	25.91	8.13	1.85	5.64	102.01
007-9	37.25	20.71	0	0	25.16	7.27	1.91	7.27	99.57
007-10	37.06	21.01	0.02	0.01	27.23	7.58	2.29	5.68	100.88
007-11	39.41	22.24	0	0.02	25.73	7.3	2.28	5.61	102.59
007-12	37.82	21.61	0.01	0.02	26.29	7.47	2.22	5.43	100.87
007-13	36.9	20.73	0.01	0	25.57	7.85	1.63	6.97	99.66
Sample 024 054a									
054A G1 1	36.8	20.33	0.25	0.02	28.66	2.05	4.35	6.71	99.17
054A G1 2	36.75	20.45	0.12	0.01	29.32	2.17	4.65	6.71	100.18
054A G1 3	36.69	20.5	0.17	0	29.39	2.19	4.67	6.65	100.26
054A G1 4	36.75	20.48	0.18	0.01	29.15	2.08	4.47	6.83	99.95
054A G1 5	36.54	20.37	0.19	0.03	29.58	2.03	4.09	7	99.83
054A G1 6	36.79	20.91	0.08	0	31.85	1.69	5.32	4.09	100.73
054A G1 7	36.85	20.87	0.07	0.02	31.47	1.59	5.29	4.5	100.66
054A G2 1	36.75	21.17	0.06	0	30.13	1.58	4.76	5.52	99.97
054A G2 2	37.03	20.84	0.05	0.03	30.24	1.77	4.08	6.67	100.71
054A G2 3	37.58	20.78	0.05	0.05	29.5	2.08	4.29	6.59	100.92
054A G2 4	37.02	20.98	0.02	0	29.31	2.14	4.21	6.62	100.3
054A G2 5	37.24	20.84	0.05	0	29.3	2.08	4.09	6.47	100.07
054A G2 6	36.67	20.65	0.06	0	29.49	2.04	4.03	6.73	99.67
054A G2 7	36.71	20.53	0.13	0	30.04	1.78	3.99	7.11	100.29
054A G2 8	37.02	21.11	0	0.02	29.73	1.88	3.65	6.87	100.28
054A G2 9	37.81	21.54	0.02	0	29.92	1.62	4.01	6.49	101.41
Sample 025 055a									
055A-1	38.17	20.87	0.06	0.04	30.69	3.28	1.33	7.63	102.07
055A-2	37.53	21.03	0.14	0	30.67	3.29	1.38	7.5	101.54
055A-3	37.71	20.89	0.08	0.03	31.22	3.57	1.44	7.29	102.23
055A-4	37.77	21.25	0.07	0.02	31.16	3.33	1.54	7.29	102.43
055A-5	37.86	20.73	0	0	31.23	3.29	1.36	7.19	101.66
055A-6	37.88	20.87	0,13	0.03	30.03	4.71	1	7.15	101.8
055A-7	37.49	20.69	0.05	0.04	29.62	5.16	0.91	6.93	100.89
055A-8	37.42	20.69	0.12	0.05	30.9	3.54	1.42	7.33	101.47
055A-9	37.45	20.93	0.05	0.04	31.58	3.65	1.22	6.82	101.74
055A-10	37.86	20.67	0.08	0.07	31.18	3.4	1.53	6.89	101.68
055A-11	37.84	20.85	0.09	0.02	31.06	3.71	1.51	6.91	101.99
055A-12	37.31	20.64	0.06	0.03	30.75	3.69	1.58	6.9	100.96

Appendix 2 - Mineral Chemistry (cont.)

Garnet analyses ***Wolf Grove Structure***

Sample 025 055a									
055A-13	37.15	20.23	0.09	0	29.87	5.45	0.94	7.19	100.92
055A-14	36.96	20.77	0.08	0.02	31.41	3.58	1.5	6.73	101.05
055A-15	37.51	20.79	0.07	0.05	30.07	4.22	1.14	7.09	100.94
055A-16	36.98	20.55	0.12	0.03	28.7	6.12	0.71	7.94	101.15
055A-17	37.71	21	0.06	0.08	31.11	3.36	1.42	6.95	101.69

Sample 050 008									
analysis	**SiO_2**	**AL_2O_3**	**TiO_2**	**Cr_2O_3**	**FeO**	**MnO**	**MgO**	**CaO**	**TOTAL**
008-2G1	37.87	21.65	0.05	0.01	28.16	4.3	1.27	7.33	100.64
008-2G2	38	21.44	0.07	0.02	28.42	4.34	1.31	7.08	100.68
008-2G3	37.74	21.5	0.03	0	27.26	4.42	1.35	7.66	99.96
008-2G4	37.94	21.77	0.06	0	26.79	4.42	1.17	8.21	100.36
008-2G5	37.97	21.75	0.12	0	26.99	4.49	1.15	8.31	100.78
008-2G6	38.04	21.68	0.11	0	27.13	4.59	1.17	8.12	100.84
008-2G7	38.15	21.4	0.1	0	27.59	4.42	1.38	7.67	100.71
008-2G8	37.82	21.7	0.14	0	28.48	4.4	1.5	7.04	101.08
008-2G9	37.55	20.76	0.04	0.02	28.44	4.3	1.41	7.02	99.54
008-2G10	37.55	21.45	0.07	0.02	29.03	4	1.46	7.18	100.76
008-2G11	37.92	21.07	0.05	0	30.27	3.45	0.87	7.36	100.99
008-1G1	37.51	20.99	0.08	0.08	29.49	2.78	0.91	8.9	100.74
008-1G2	37.88	21.38	0.01	0.03	28.56	3.96	1.72	7.16	100.7
008-1G3	37.82	21.61	0.06	0	28.36	3.94	1.81	7.47	101.07
008-1G4	37.94	21.43	0.1	0.05	28.2	3.96	1.76	7.94	101.38
008-1G5	37.89	21.45	0.06	0	27.81	3.71	1.64	7.86	100.42

Sample 989 988									
988-G1	37.24	20.56	0.03	0.04	33.58	1.08	2	6.91	101.44
988-G2	37.11	20.61	0.02	0.02	33.69	1.19	2.33	6.77	101.74
988-G3	36.84	20.54	0.02	0	33.95	1.24	2.38	6.68	101.65
988-G4	37.45	20.32	0.03	0	32.44	1.15	2.15	6.66	100.2
988-G5	37.29	20.32	0.03	0	32.09	1.11	2.03	7.14	100.01
988-G6	37.44	20.67	0	0	30.88	0	0	6.87	95.86
988-G6	36.98	20.7	0	0.06	30.79	1.08	2.05	6.94	98.6
988-G7	37.05	20.89	0	0	30.52	1.2	2.08	6.89	98.63
988-G8	37.03	20.74	0	0.03	33.32	1.16	2.14	6.84	101.26
988-G9	36.93	20.65	0	0	33.31	1.25	2.1	6.78	101.02
988-G10	37.57	20.97	0	0.02	32.26	1.18	2.11	7.3	101.41
988-G11	37.5	20.75	0	0	32.51	1.08	2.1	7.28	101.22
988-G12	37.23	20.71	0	0	32.79	1.16	2.27	6.91	101.07
988-G13	37.11	20.6	0	0	33.1	1.13	2.35	6.82	101.11
988-G14	37.09	20.78	0	0	33.88	1.18	2.15	6.82	101.9
988-G15	37.45	20.77	0	0	32.78	1.03	2.46	7.15	101.64
988-G16	37.39	20.92	0.01	0	32.58	0.97	2.6	7.58	102.05
988-G17	37.03	20.58	0.03	0	33.52	1.08	2.26	6.65	101.15

Appendix 2 - Mineral Chemistry (cont.)

Garnet analyses		***Wolf Grove Structure***							
Sample 989 988									
analysis	**SiO_2**	**AL_2O_3**	**TiO_2**	**Cr_2O_3**	**FeO**	**MnO**	**MgO**	**CaO**	**TOTAL**
988-G18	37.24	20.64	0.04	0	33.91	1.09	2.4	6.79	102.11
988-G19	36.71	20.52	0.04	0	33.58	1.12	2.36	6.5	100.83
988-G20	37.25	20.74	0.03	0	33.99	1.12	2.49	6.66	102.28
988-G21	37.33	20.66	0.07	0	33.78	1.09	2.37	6.72	102.02
988-G22	37.06	20.89	0.25	0.13	33.19	1.33	2.7	7.29	102.84
988-G23	36.36	20.56	0.26	0.11	33.36	1.46	2.42	7.05	101.58
988-G24	36.96	20.83	0.05	0.03	29.88	1.13	2.2	9.76	100.84
988-G25	36.72	20.43	0.05	0.03	30.96	1.15	2.06	8.66	100.06
988-G26	36.85	19.92	0.07	0.02	32.68	1.22	2.16	8.15	101.07
988-G28	36.69	20.32	0.02	0.02	33.16	1.24	2.42	7.08	100.95
0035B G1	37.0	20.67	0	0	29.55	2.15	4.77	6.53	100.67
0035B G2	36.99	20.62	0.01	0.01	29	2.25	4.45	7	100.33
0035B G3	37.02	20.57	0.04	0	28.69	2.4	4.38	7.42	100.52
0035B G4	36.9	20.66	0.01	0	29.53	2.49	4.37	6.35	100.31
0035B G5	37.28	20.96	0.08	0	29.61	2.56	4.54	6.22	101.25
0035B G6	37.11	20.83	0.02	0	29.56	2.7	4.43	6.38	101.03
0035B G7	36.83	20.82	0.03	0.01	29.8	2.71	4.6	6.04	100.84
0035B G8	37.32	20.94	0.01	0.01	29.17	2.52	4.2	6.96	101.13
0035B G9	37.39	20.77	0.03	0.01	28.73	2.45	4.31	7.36	101.05
0035B G10	37.07	20.77	0.01	0	28.58	2.35	4.51	7.35	100.64
0035B G11	36.9	20.79	0.01	0	29.14	2.41	4.45	6.72	100.42
0035B G12	37.28	20.61	0.05	0	29.31	2.36	4.61	6.99	101.21
0035B G13	37.07	20.86	0.03	0	29.88	2.2	4.79	6.37	101.2
0035 G14	37.18	20.67	0.01	0	29.12	2.56	4.72	6.26	100.52
0035 G15	37.53	20.59	0.02	0	29.32	2.53	4.74	6.54	101.27
0035 G16	37.13	20.84	0.01	0	29.17	2.46	4.64	6.41	100.66
0035 G17	37.45	20.79	0	0	29.62	2.46	4.83	6.19	101.34
0035 G18	37.1	20.75	0	0	29.16	2.28	4.87	6.52	100.68
0035 G19	36.96	20.59	0.02	0	29.41	2.11	4.96	6.72	100.77
0035 G20	37.18	20.54	0	0	28.41	1.58	5.48	7.65	100.84
0035B G21	37.09	20.29	0.01	0.01	28.97	1.88	5.36	6.84	100.45
0035B G22	37.27	20.58	0	0.01	28.82	1.96	5.41	6.86	100.91
0035B G23	36.85	20.51	0	0.03	28.79	1.73	5.38	7.42	100.71
0035B G24	37.1	20.52	0	0.03	29.45	2.05	5.39	6.2	100.74
0035B G25	37.22	20.54	0.01	0	28.81	1.92	5.25	6.84	100.59
0035B G26	37.21	20.72	0	0	28.79	2.14	5.58	6.37	100.81
0035BG3	37.03	20.48	0	0	29.01	1.75	5.09	7.21	100.57
Garnet analyses		***Lavant Gabbro Complex metadiorite***							
Sample 859 004									
008-GA1	37.44	21.46	0.05	0	33.31	0.71	4.27	4.54	101.78
008-GA2	37.13	21.2	0.05	0	34.65	0.85	3.21	5.6	102.69
008-GA3	36.8	21.22	0.08	0	33.06	0.89	3.37	5.64	101.06

Appendix 2 - Mineral Chemistry (cont.)

Garnet analyses		*Lavant Gabbro Complex metadiorite*							
008-GA4	36.57	21.07	0.1	0.01	34.09	0.86	3.86	4.64	101.2
008-GA5	36.8	21.05	0.09	0	33.68	0.83	3.7	4.63	100.78
008-GA6	36.77	21.14	0.1	0	33.32	0.88	3.36	4.84	100.41
008-GA7	36.81	21.02	0.1	0	34.08	0.82	3.72	4.74	101.29
008-GA8	36.52	21.22	0.09	0	34.13	0.83	3.79	4.74	101.32
008-GA9	36.94	21.22	0.06	0.01	33.42	0.82	3.53	5.18	101.18
008-GA10	36.67	21.15	0.01	0.05	32.99	0.72	4.13	4.88	100.6

Garnet analyses		*Pakenham Dome gneiss*							
Sample 954 051									
analysis	**SiO_2**	**AL_2O_3**	**TiO_2**	**Cr_2O_3**	**FeO**	**MnO**	**MgO**	**CaO**	**TOTAL**
051 GA1	37.97	21.93	0.02	0	35.99	4.53	1.07	0.97	102.48
051 GA3	36.49	21.4	0.03	0.01	34.94	5.63	0.92	0.93	100.35
051 GA4	36.11	21.15	0.02	0	34.09	6.01	0.85	1	99.23
051 GA5	37.82	22.07	0	0	34.51	5.91	0.93	0.98	102.22
051 GA6	37.05	21.29	0.03	0	34.51	5.8	0.89	0.96	100.53
051 GA7	38.05	21.89	0.02	0	35.26	5.64	0.94	1.02	102.82
051 GA8	37.2	21.46	0.02	0.01	35.54	4.82	0.97	0.94	100.96
051 GB1	37.25	21.72	0.01	0	34.4	5.03	1.1	1	100.51
051 GB2	37.16	21.8	0	0	34.38	5.24	1.16	0.99	100.73
051 GB3	37.55	21.86	0.02	0	32.1	7	0.83	0.95	100.31
051 GB4	36.95	21.51	0.01	0	33.18	7.34	0.71	0.87	100.57
051 GB5	37.73	21.79	0.02	0	32.01	7.18	0.79	0.87	100.39
051 GB6	38.12	21.95	0.01	0.03	32.34	7.04	0.73	0.95	101.17
051 GB7	37.93	22.02	0	0	32.77	7	0.66	0.85	101.23
051 GB8	38.23	21.85	0	0.02	33.06	7.01	0.78	0.93	101.88
051 GB9	38.13	22.11	0.01	0.03	34.06	5.83	0.88	1.01	102.06
051 GB10	37.52	21.84	0.05	0.01	34.88	4.92	0.97	1.12	101.31
051 GC1	37.27	21.24	0.01	0	33.17	5.77	1.05	0.95	99.46
051 GC2	37.38	21.3	0	0	33.5	5.95	1.02	1	100.15
051 GC3	36.71	21.11	0	0	33.7	6.02	0.92	0.94	99.4
051 GC4	36.89	21.35	0.03	0	33.21	6.03	0.85	0.95	99.31
051 GC5	36.02	20.89	0	0	33.8	5.8	0.91	0.94	98.36
051 GC6	36.96	21.34	0.03	0	34.95	4.37	1.11	1.17	99.93
051 GC7	36.32	20.99	0.02	0	34.74	4.71	1.04	0.93	98.75
051 GC8	37.07	21.27	0.01	0	34.57	5.27	1	0.96	100.15
051 GC9	37.17	21.2	0.02	0	34.33	5.15	1.04	1	99.91
051 GC10	37.19	21.06	0	0	35.87	3.98	1.16	1.11	100.37

Garnet analyses		*Lyndhurst area gneiss*							
Sample 070 304									
analysis	**SiO_2**	**AL_2O_3**	**TiO_2**	**Cr_2O_3**	**FeO**	**MnO**	**MgO**	**CaO**	**TOTAL**
304 GA1	37.07	21.38	0.17	0	29.88	0.84	5.88	6.32	101.54
304 GA2	37.28	20.94	0.02	0	30.83	1.16	3.37	7.72	101.32

Appendix 2 - Mineral Chemistry (cont.)

Garnet analyses ***Lyndhurst area gneiss***

Sample 070 304

analysis	SiO_2	AL_2O_3	TiO_2	Cr_2O_3	FeO	MnO	MgO	CaO	TOTAL
304 GA3	37.19	20.96	0.07	0.04	30.52	1.22	3.46	7.52	100.98
304 GA4	37.13	20.9	0.01	0.03	31.24	1.23	3.49	7.65	101.68
304 GA5	37.47	20.89	0.04	0.01	31.11	1.36	3.46	7.33	101.67
304 GA6	37.35	20.71	0.06	0	30.91	1.43	3.67	7.36	101.49
304 GA7	37.28	20.66	0.14	0.02	30.96	1.41	3.78	7.22	101.47
304 GA8	37.86	21.01	0.1	0	30.94	1.41	3.68	7.28	102.28
304 GA9	37.26	20.61	0.09	0.02	30.69	1.38	3.58	7.23	100.86
304 GA10	36.96	20.65	0.12	0	31.27	1.35	3.64	7.29	101.28
304 GA11	37.15	20.65	0.13	0.04	30.36	1.41	3.59	7.37	100.7
304 GA12	37.04	20.7	0.05	0	30.88	1.17	3.37	7.06	100.27
304 GB1	37.2	20.98	0.07	0	30.48	1.07	4.81	6.52	101.13
304 GB2	37.61	20.74	0.11	0.07	30.98	1.26	2.79	7.39	100.95
304 GB3	37.01	20.92	0.14	0	30.35	1.18	2.79	8.13	100.52
304 GB4	36.92	20.64	0.12	0	30.54	1.27	3.02	8.15	100.66
304 GB5	36.97	20.79	0.05	0.01	30.56	1.25	3.08	7.89	100.6
304 GB6	37.18	20.76	0.08	0.02	30.57	1.33	2.98	7.97	100.89
304 GB7	36.99	20.62	0.09	0	30.34	1.35	2.93	7.7	100.02

Feldspar analyses **Wolf Grove Structure**

Sample 012 043b analysis	SiO_2	AL_2O_3	K_2O	CaO	Na_2O	BaO	FeO	TOTAL
043B-1	65.07	18.61	15.87	0	0.49	0.41	0.02	100.47
043B-2	64.72	18.53	15.27	0.02	0.68	0.35	0	99.57
043B-3	65.11	18.61	15.39	0.01	0.67	0.62	0	100.41
043B-4	64.72	18.61	15.7	0.01	0.61	0.69	0	100.34
043B-5	63.44	22.72	0.11	3.87	9.52	0	0	99.66
043B-6	64.49	22.65	0.19	3.3	9.87	0	0	100.5
043B-7	64.55	22.56	0.31	3.33	9.67	0	0	100.42
043B-8	65.47	22.58	0.23	3.36	9.71	0	0.02	101.37
043B-9	65.06	23.02	0.23	3.41	9.78	0	0	101.5
Sample 017 048a								
048A-1	67.57	20.29	0.07	0.84	11.7	0	0.22	100.69
048A-2	66.16	21.63	0.09	2.34	10.64	0.02	0.12	101
048A-3	65.4	22.02	0.12	2.61	10.46	0	0.04	100.65
048A-4	66.28	21.38	0.09	2.07	10.88	0	0.02	100.72
048A-5	65.47	22.39	0.12	3.23	10.25	0	0	101.46
048A-6	65.77	18.75	16.12	0	0.62	0.4	0.07	101.73
048A-7	65.68	18.71	15.77	0	0.8	0.38	0.05	101.39
048A-8	65.66	18.53	16.3	0	0.75	0.36	0.04	101.64
048A-9	65.37	18.81	15.84	0	0.87	0.44	0.05	101.38
048A-10	65.37	18.72	16.3	0.01	1.15	0.38	0	101.93
Sample 993 007								
007-1	62.58	23.19	0.13	3.86	9.66	0	0.17	99.59
007-2	67.18	20.77	0.05	0.95	11.54	0	0.32	100.81
007-3	62.46	23.74	0.13	4.8	9.12	0.02	0.08	100.35
007-4	63.95	23.14	0.02	4.1	9.63	0.06	0	100.9
007-5	65.09	18.72	15.97	0	0.58	0.64	0	101
007-6	64.67	18.75	15.38	0	0.96	0.95	0.1	100.81
007-7	63.89	18.86	15.33	0.01	1.04	0.93	0.05	100.11
Sample 024 054a								
054A P3 1	63.16	23.57	0.28	4.76	8.94	0.37	0	101.08
054A P3 2	61.68	24.16	0.25	5.5	8.36	0.12	0	100.07
054A P3 3	61.45	24.31	0.23	5.52	8.48	0.1	0	100.09
054A P3 4	59.04	23.05	0.26	5.59	7.83	1.33	0	97.1
054A P3 5	61.26	23.81	0.2	5.32	8.38	0.12	0	99.09
054A P3 6	61.38	24.18	0.21	5.59	8.33	0.11	0	99.8
054A P4 1	57.96	22.99	0.15	5.28	8.55	0.08	0	95.01
054A P4 2	56.53	22.49	0.2	5.28	8.15	0.06	0	92.71
054A P4 3	57.02	22.37	0.25	5.24	8.1	0.47	0	93.45
054A P4 5	60.92	23.84	0.11	5.27	8.47	0.3	0	98.91
054A P4 6	60.51	23.87	0.19	5.24	8.49	0.07	0	98.37
Sample 025 055a								
005A-1	64.48	23.33	0.33	4.05	9.47	0	0.34	102
005A-2	64.32	24.04	0.17	4.86	9.06	0	0.1	102.55
005A-3	66.58	18.92	15.77	0.01	0.79	0.73	0.07	102.87

Feldspar analyses **Wolf Grove Structure**

Sample 050 008 analysis	SiO_2	AL_2O_3	K_2O	CaO	Na_2O	BaO	FeO	TOTAL
008-4A7	56.08	28.31	0.16	10.4	5.64	0.23	0	100.82
008-4A8	56.04	28.26	0.15	10.45	5.81	0.04	0	100.75
008-4A9	56.92	28.18	0.14	10.05	5.88	0.19	0	101.36
008-4A10	55.81	28.09	0.18	10.39	5.79	0.04	0	100.3
008-5A9	55.83	27.54	0.15	9.67	5.92	0.26	0	99.37
008-5A10	56.32	27.61	0.17	9.86	5.98	0.11	0	100.05
008-5A11	65.29	18.18	16.65	0.03	0.68	0.1	0.04	100.97
008-5A12	65	18.32	16.68	0	0.71	0.09	0.16	100.96
Sample 989 988								
988-P1	63.35	24.14	0.01	0.25	5.23	8.65	0	101.63
988-P2	63.62	24.28	0	0.25	5.05	8.42	0.1	101.72
988-P3	62.72	24.12	0.07	0.24	5.44	8.31	0	100.9
988-P4	63.67	24.23	0.26	0.18	4.54	8.96	0.01	101.85
988-P5	62.58	24.08	0.05	0.32	5.08	8.4	0	100.51
988-P6	64.21	23.99	0.04	0.23	4.88	8.5	0.1	101.95
988-P7	64.66	23.71	0.07	0.62	4.41	8.43	0	101.9
988-P8	63.35	23.93	0	0.22	5.17	8.55	0	101.22
988-P9	63.33	23.78	0.08	0.19	4.89	8.22	0	100.49
988-P10	63.88	23.36	0.18	0.49	4.27	8.31	0	100.49
Sample 995 0035b								
0035b P1	62.12	24.63	0.02	0.2	5.59	8.69	0.11	101.36
0035b P2 rim	63.04	24.4	0.23	0.22	5.33	9.08	0.04	102.34
0035b P3	62.74	24.64	0.08	0.17	5.72	8.79	0	102.14
0035b P4	62.73	24.83	0.07	0.19	5.71	8.8	0.03	102.36
0035b P5 rim	61.6	24.76	0.39	0.18	5.74	8.5	0.03	101.2
0035b P6 rim	62.58	24.64	0.14	0.19	5.52	9.06	0	102.13
0035b P7 core	62.33	24.59	0.17	0.23	5.37	8.87	0.01	101.57
0035b P8 rim	63.03	24.19	0.26	0.21	5.08	9.14	0.13	102.04
0035b P9 core	62.86	24.33	0.08	0.2	5.42	8.85	0.01	101.75
0035b P10 rim	62.54	24.44	0.24	0.23	5.44	8.94	0.01	101.84
0035b P11	62.23	24.33	0.08	0.39	5.28	8.74	0.02	101.07
0035b P12 rim	61.97	24.37	0.2	0.21	5.39	8.92	0	101.06

Feldspar analyses **Lavant Gabbro Complex metadiorite**

Sample 859 004								
004-4A6	62.74	24.16	0.08	5.2	8.64	0.01	0	100.83
004-4A7	67.07	21.67	0.05	2.14	10.63	0.16	0	101.72
004-4A8	63.58	22.33	0.06	3.66	9.69	0.05	0	99.37
004-4A9	63.75	22.94	0.52	3.43	9.32	0.19	0	100.15
004-4A16	64.24	22.79	0.06	4.07	9.37	0.14	0	100.67
004-4A17	62.58	24.01	0.05	5.15	9	0.04	0	100.83
004-4A18	62.04	24.3	0.05	5.76	8.38	0.03	0	100.56
004-4A18	65.77	22.19	0.04	2.8	10.42	0.07	0	101.29
004-4A19	69.41	20.12	0.05	0.48	11.69	0.26	0	102.01

Feldspar analyses **Pakenham Dome gneiss**

Sample 954 051

analysis	SiO_2	AL_2O_3	K_2O	CaO	Na_2O	BaO	FeO	TOTAL
051 PL1	64.01	22.84	0.22	0.01	4.01	9.52	0	100.61
051 PL2	64.49	22.8	0.09	0.03	3.74	9.59	0	100.74
051 PL3	65.02	22.8	0	0.04	3.76	9.58	0	101.2
051 PL4	65.0	22.63	0.06	0.19	3.32	9.56	0	100.76
051 PL5	64.42	22.82	0.31	0.06	3.73	9.53	0	100.87
051 PL6	64.8	22.77	0.23	0.03	3.74	9.41	0	100.98
051 PL7	64.52	22.11	0.3	0.05	3.41	9.7	0	100.09

Feldspar analyses **Lyndhurst area gneiss**

Sample 070 304

304 FLD1	62.69	23.06	0.65	4.54	8.73	0.42	0	100.09
304 FLD2	62.06	23.55	0.21	4.99	9.04	0.09	0	99.94
304 FLD3	62.21	23.58	0.2	5.18	9.11	0.07	0	100.35
304 FLD4	61.83	23.51	0.22	5.16	9.07	0.05	0	99.84
304 FLD5	61.64	23.3	0.17	5.03	8.97	0.26	0	99.37
304 2 FLD1	63.4	23.62	0.16	4.51	9	0.21	0	100.9
304 2 FLD2	63.34	24.26	0.25	5.1	9.02	0.01	0	101.98
304 2 FLD3	64.19	23.32	0.19	4.24	9.47	0.08	0	101.49
304 2 FLD4	63.54	23.4	0.37	4.24	9.29	0.02	0	100.86
304 4 FLDa	62.65	23.73	0.19	4.87	8.92	0.19	0	100.55
304 4 FLDb	62.74	23.57	0.23	4.66	9.15	0.01	0	100.36
304 5 FLDa	63.53	18.31	16	0.01	0.65	0.05	0.58	99.13
304 5 FLDb	63.6	18.16	15.52	0	1.06	0.06	0.8	99.2

Appendix 2 - Mineral Chemistry (cont.)

Biotite analyses *Wolf Grove Structure*

Sample 012 043b														
analysis	**SiO_2**	**AL_2O_3**	**TiO_2**	**Cr_2O_3**	**FeO**	**MnO**	**MgO**	**K_2O**	**CaO**	**Na_2O**	**BaO**	**Cl**	**F**	**TOTAL**
043B-18	34.97	18.43	1.71	0	24.55	0.11	5.69	8.82	0.04	0.14	0.05	0	0.27	94.78
043B-19	34.59	18.23	1.73	0.02	24.96	0.12	5.24	9.32	0.01	0.26	0.03	0.03	0.3	94.84
043B-20	34.78	18.42	1.8	0.03	25.98	0.03	5.3	9.46	0.01	0.09	0.03	0.06	0.34	96.33
043B-21	34.76	18.24	1.61	0	26.18	0.09	5.48	9.3	0.02	0.04	0.02	0	0.34	96.08
043B-22	34.32	18.16	1.52	0	25.71	0.03	5.23	9.13	0.07	0.29	0	0.09	0.16	94.71
043B-23	34.75	18.54	1.46	0	25.17	0.13	5.58	9.12	0.06	0.16	0	0.03	0.21	95.21
043B-24	35.04	18.71	1.05	0.04	26.17	0.03	5.23	8.75	0.03	0.11	0.02	0.03	0.25	95.46
043B-25	34.84	19.31	0.57	0.01	25.32	0.11	5.57	8.74	0.03	0.09	0.01	0.01	0.31	94.92
043B-26	34.93	19.42	0.6	0	25.34	0.06	5.6	8.97	0.05	0.14	0.03	0.01	0.27	95.42
043B-27	35.25	19.37	0.62	0	25.52	0	5.36	9.35	0.03	0.05	0.02	0	0.32	95.89
043B-28	35.04	19.76	0.28	0	25.64	0.05	5.58	8.97	0.03	0.09	0	0	0.35	95.79
043B-29	35.16	19.44	0.64	0.06	25.43	0.02	5.6	9.13	0.02	0.04	0.02	0	0.31	95.87
043B-30	35.51	17.59	2.98	0	24.1	0.07	6.04	9.31	0	0.07	0.08	0.02	0.28	96.05
043B-31	35.55	17.41	3.16	0	24.23	0.09	5.96	9.28	0.04	0.09	0.09	0.07	0.3	96.27
043B-32	35.3	17.27	3.36	0	24.26	0.08	6	9.4	0.01	0.08	0.17	0.07	0.26	96.26
043B-33	35.53	17.68	3.19	0	24.72	0.04	5.82	9.33	0.01	0.07	0.11	0.07	0.27	96.84
Sample 017 048a														
048A-23	36.01	16.11	3.13	0	23.64	0.38	6.85	9.59	0.05	0.04	0	0.05	0.22	96.07
048A-24	36.45	16.1	3.07	0	23.15	0.31	7.06	9.81	0.03	0.09	0	0.05	0.14	96.26
048A-25	36.46	16.37	3.09	0.04	23.56	0.23	7.06	9.56	0	0.04	0	0.04	0.18	96.63
048A-26	36.28	17.6	1.92	0	23.62	0.23	7.5	9.57	0.08	0.05	0	0.04	0.16	97.05
048A-27	36.21	17.12	1.91	0	23.65	0.22	7.4	9.56	0.01	0.07	0.04	0.04	0.12	96.35
048A-29	35.83	16.86	2.84	0	23.45	0.54	6.65	8.47	0.01	0.08	0.07	0.05	0.17	95.02
048A-30	35.65	16.12	2.9	0	23.41	0.23	6.83	8.97	0	0	0	0.06	0.16	94.33
048A-31	35.79	16.44	3.05	0.03	23.28	0.23	6.94	9.05	0	0.01	0	0.02	0.16	95
048A-32	36.31	16.93	2.96	0	23.93	0.26	7.32	8.97	0	0.06	0	0.07	0.19	97
048A-33	38.66	15.7	2.89	0.03	21.7	0.34	6.57	8.86	0.06	0.07	0	0.06	0.2	95.14
048A-34	35.85	15.86	2.83	0.08	23.32	0.29	6.94	9.34	0	0.06	0	0.05	0.26	94.88

Appendix 2 - Mineral Chemistry (cont.)

Biotite analyses *Wolf Grove Structure*

Sample 017 048a														
analysis	**SiO_2**	**AL_2O_3**	**TiO_2**	**Cr_2O_3**	**FeO**	**MnO**	**MgO**	**K_2O**	**CaO**	**Na_2O**	**BaO**	**Cl**	**F**	**TOTAL**
048A-35	35.79	16.41	3.34	0	24.66	0.45	6.63	9.57	0	0.04	0	0.01	0.19	97.09
048A-36	35.85	16.22	3.29	0	24.61	0.28	6.37	9.62	0	0.04	0	0.07	0.17	96.52
048A-37	34.23	16.13	2.99	0.01	26.2	0.36	6.26	8.34	0	0.02	0	0.06	0.16	94.76
048A-38	35.86	16.61	3.35	0.01	24.51	0.39	6.38	9.66	0	0.03	0.05	0.29	0.06	97.2
048A-39	35.45	16.38	3.38	0	24.6	0.31	6.49	9.7	0.02	0.01	0	0	0.02	96.36
Sample 993 007														
007-15	34.92	17.22	3.49	0	24.2	0.32	7.08	9.55	0.06	0.08	0.27	0.15	0.07	97.41
007-16	34.98	17.03	3.33	0	23.46	0.25	6.96	9.63	0.04	0.07	0.07	0.16	0.17	96.15
007-17	34.24	17.12	3.57	0.01	23.86	0.21	6.21	9.53	0.06	0.11	0.24	0.14	0.1	95.4
007-18	30.97	17.48	2.07	0	26.5	0.22	7.25	6.05	0.09	0.12	0.01	0.12	0.12	91
007-18	34.54	17.28	3.12	0.02	24.16	0.2	6.25	9.61	0.04	0.14	0.07	0.19	0.22	95.84
007-19	34.08	17	3.02	0	24.05	0.18	6.35	9.2	0	0.13	0.12	0.15	0.16	94.44
007-20	34.17	17.26	2.97	0.02	25.34	0.14	6.48	8.7	0.03	0.08	0.05	0.16	0.15	95.55
007-21	35.08	17.49	3.28	0.02	24.37	0.19	5.86	9.6	0	0.11	0.28	0.21	0.17	96.66
007-22	34.58	17.35	3.15	0	25.47	0.1	6.08	8.75	0.03	0.07	0.14	0.24	0.14	96.1
007-23	33.92	17.21	3.03	0	25.7	0.13	6.26	8.5	0.01	0.1	0.1	0.18	0.16	95.3
007-24	34.07	17.17	3.06	0.01	26.06	0.09	6.1	8.57	0.06	0.04	0.26	0.16	0.12	95.77
007-25	31.34	17.67	2.56	0	27.7	0.16	6.58	6.3	0.06	0.05	0.22	0.16	0.15	92.95
007-26	34.59	17.37	3.05	0	25.83	0.13	6.17	9.13	0.05	0.06	0	0.21	0.1	96.69
007-27	35.57	17.5	3.43	0.02	25.21	0.12	5.89	9.8	0	0.07	0.36	0.22	0.15	98.34
007-28	35.25	17.33	3.4	0	24.66	0.18	5.92	9.7	0.02	0.14	0.07	0.22	0.13	97.02
Sample 024 054a														
054A B1 1	35.13	14.28	3.99	0	22.8	9.17	0.19	9.11	0.03	0.16	0	0.17	0.04	95.07
054A B1 2	35.42	14.35	4.11	0	22.79	8.84	0.14	9.01	0.03	0.16	0.14	0.22	0.03	95.24
054A B1 3	34.59	14.01	4.13	0	23.37	8.83	0.08	9.07	0.03	0.08	0.16	0.19	0.03	94.57
054A B1 4	35.02	13.85	4.22	0.07	22.67	8.69	0.13	9.11	0.05	0.12	0.24	0.25	0.05	94.47
054A B1 5	34.16	14.19	4.19	0.05	22.5	8.8	0.14	9.29	0	0.08	0.21	0.27	0.04	93.92

Appendix 2 - Mineral Chemistry (cont.)

Biotite analyses *Wolf Grove Structure*

Sample 024 054a														
analysis	**SiO_2**	**AL_2O_3**	**TiO_2**	**Cr_2O_3**	**FeO**	**MnO**	**MgO**	**K_2O**	**CaO**	**Na_2O**	**BaO**	**Cl**	**F**	**TOTAL**
054A B1 6	35.82	14.51	4.27	0	22.89	8.99	0.14	9.29	0.02	0.07	0.01	0.17	0.05	96.23
054A B1 7	35.51	14.33	4.14	0	23.31	8.85	0.09	9.11	0.01	0.13	0.26	0.28	0.06	96.08
054A B2 1	35.62	15.02	4.05	0	22.17	9.41	0.15	9.2	0.04	0.1	0.1	0.26	0.02	96.14
054A B2 2	35.16	14.74	3.97	0.04	23.13	9.03	0.1	9.1	0.05	0.07	0.05	0.17	0.03	95.64
054A B2 3	35.43	14.82	3.98	0	22.03	9.27	0.07	9.27	0	0.13	0.19	0.23	0.04	95.46
054A B2 4	35.19	14.77	4.16	0	22.16	9.41	0.12	9.26	0.01	0.11	0.24	0.33	0.02	95.78
054A B2 5	35.41	16.27	3.72	0	23.36	7.53	0.09	8.9	0.05	0.05	0.33	0.22	0.01	95.94
054A B2 6	35.19	14.82	4.24	0.07	23.79	8.02	0.06	9.14	0.02	0.09	0.02	0.18	0.02	95.66
054A B2 7	35.22	15.53	3.93	0	23.99	7.65	0.03	9.16	0.01	0.06	0.11	0.26	0.01	95.96
Sample 025 055a														
055A-18	35.12	14.94	3.68	0	28.41	0.2	5.78	9.72	0.01	0.1	0.14	0	0.29	98.39
055A-19	35.3	15.34	3.7	0	27.81	0.13	5.69	9.81	0	0.07	0.23	0	0.29	98.37
055A-22	35.14	14.89	3.47	0.03	27.68	0.3	6	9.67	0	0.06	0.32	0	0.33	97.89
055A-23	34.85	14.93	3.34	0	27.95	0.24	6.18	9.54	0.02	0.05	0.42	0	0.37	97.89
055A-26	34.55	14.68	3.4	0	28.23	0.27	5.68	9.43	0	0.07	0.25	0	0.29	96.85
055A-27	34.83	14.78	3.46	0	28.4	0.17	5.69	9.53	0	0.11	0.33	0	0.34	97.64
055A-28	35.05	14.99	3.65	0	26.93	0.2	6.38	9.88	0.02	0.08	0.15	0	0.22	97.55
055A-29	34.74	14.88	3.63	0.03	26.15	0.19	6.47	9.63	0.03	0	0.21	0	0.27	96.23
055A-30	34.09	15.08	3.47	0.03	26.64	0.22	6.53	9.66	0.02	0.08	0.25	0	0.23	96.3
055A-31	33.5	15.07	3.59	0.03	26.74	0.25	6.45	9.68	0	0	0.26	0	0.34	95.91
Sample 050 008														
008-2B1	35.8	15.33	3.81	0.02	21.24	10.22	0.02	9.35	0.11	0.05	0.09	0.24	0.19	96.47
008-2B2	35.86	14.89	3.93	0.01	20.65	10.37	0	9.76	0.06	0.03	0.07	0.43	0.2	96.26
008-2B3	35.34	14.72	3.78	0.01	20.69	10.1	0.07	9.99	0.15	0.05	0	0.34	0.23	95.47
008-2B4	34.63	14.97	4.02	0.05	22.86	8.75	0.02	9.76	0.14	0.02	0.13	0.23	0.2	95.78
008-2B5	34.92	14.93	4.2	0.07	22.28	8.85	0.04	9.88	0.08	0.03	0.2	0.23	0.22	95.93
008-2B6	35.42	15.17	3.98	0.03	22.44	8.66	0.01	9.66	0.32	0.04	0.07	0.31	0.2	96.31

Appendix 2 - Mineral Chemistry (cont.)

Biotite analyses *Wolf Grove Structure*

Sample 050 008														
analysis	**SiO_2**	**AL_2O_3**	**TiO_2**	**Cr_2O_3**	**FeO**	**MnO**	**MgO**	**K_2O**	**CaO**	**Na_2O**	**BaO**	**Cl**	**F**	**TOTAL**
008-2B7	36.12	15.08	3.4	0.02	19.95	10.82	0	9.76	0.22	0.04	0.15	0.47	0.22	96.25
008-1B1	35.45	15.26	3.52	0.03	22.04	9.66	0.06	9.85	0.06	0.06	0.03	0.34	0.26	96.62
008-1B2	35.72	15.19	3.61	0	21.77	9.85	0.05	9.53	0.1	0.06	0.11	0.39	0.25	96.63
008-1B3	35.24	15.5	3.42	0.04	22.12	9.19	0	9.59	0.06	0.07	0.01	0.27	0.23	95.74
008-1B4	35.55	15.62	3.55	0.04	22.01	9.11	0	9.58	0.18	0.05	0.11	0.29	0.24	96.33
Sample 989 988														
988-B1	34.42	14.04	5.57	0	27.9	4.42	0.12	9.14	0.05	0.05	0.21	0.15	0.07	96.14
988-B2	34.26	13.72	5.45	0	27.18	4.36	0.09	8.88	0.08	0.08	0.28	0.17	0.07	94.62
988-B3	34.35	14.29	5.18	0	28.42	4.35	0.04	9.12	0	0.05	0.38	0.15	0.04	96.37
988-B4	34.06	14.12	4.87	0	27.82	4.43	0.12	8.8	0.01	0.04	0.29	0.13	0.05	94.74
988-B5	34.37	14.09	4.81	0.01	27.43	4.46	0.08	8.87	0.1	0.05	0.19	0.2	0.06	94.72
988-B6	33.39	14.24	4.43	0.02	29.3	4.9	0.05	8.51	0.02	0.07	0.44	0.13	0.05	95.55
988-B8	33.16	13.75	4.38	0.01	28.83	4.58	0.05	8.03	0.43	0.21	0.64	0.12	0.13	94.32
Sample 995 0035b														
0035b B1	34.79	17.79	3.68	0	22.1	7.12	0.22	9.73	0.03	0.07	0	0.15	0.06	95.74
0035b B2	34.73	16.83	3.26	0.02	23.03	7.5	0.21	9.73	0.01	0.01	0.3	0.09	0.07	95.79
0035b B3	34.5	16.67	3.29	0	23.65	7.56	0.14	9.56	0.02	0.05	0.35	0.11	0.08	95.98
0035b B4	34.82	16.24	3.61	0	23.75	7.38	0.18	9.6	0.03	0.04	0.3	0.12	0.08	96.15
0035b B5	34.61	15.92	3.46	0	24.11	7.34	0.22	9.52	0.01	0.04	0.32	0.1	0.07	95.72
0035b B6	35.15	15.53	3.67	0.01	24.18	7.27	0.24	9.52	0.01	0.04	0.51	0.09	0.07	96.29
0035b B7	35.19	15.24	3.72	0.03	24.56	7.28	0.28	9.4	0	0.04	0.43	0.14	0.08	96.39
0035b B8	34.61	15.33	3.69	0.01	23.94	7.07	0.21	9.56	0.02	0.05	0.43	0.11	0.08	95.11
0035b B9	34.94	15.79	3.46	0	24.86	7.43	0.24	9.81	0	0.08	0.31	0.16	0.04	97.12
0035b B10	34.81	15.78	3.35	0	24.68	7.53	0.24	9.61	0.02	0.05	0.29	0.09	0.07	96.52
0035b B11	34.83	15.6	3.44	0	24.58	7.51	0.25	9.71	0.04	0.05	0.44	0.1	0.07	96.62
0035b B12	34.34	15.58	3.44	0	25.25	7.63	0.27	8.96	0.09	0.08	0.36	0.08	0.06	96.14
0035b B13	34.33	15.6	3.55	0	23.67	7.64	0.24	9.56	0.05	0.12	0.54	0.07	0.04	95.41

Appendix 2 - Mineral Chemistry (cont.)

Biotite analyses *Wolf Grove Structure*

Sample 995 0035b analysis	**SiO_2**	**AL_2O_3**	**TiO_2**	**Cr_2O_3**	**FeO**	**MnO**	**MgO**	**K_2O**	**CaO**	**Na_2O**	**BaO**	**Cl**	**F**	**TOTAL**
0035b B14	34.6	15.46	3.48	0	24.18	7.68	0.25	9.56	0.04	0.09	0.31	0.15	0.02	95.82
0035b B15	34.51	15.27	3.55	0	24.13	7.68	0.21	9.34	0.06	0.13	0.52	0.11	0.05	95.56
0035b B16	34.25	15.47	3.56	0	24.52	7.46	0.24	9.52	0.05	0.1	0.58	0.12	0.06	95.93

Biotite analyses *Lavant Gabbro Complex metadiorite*

Sample 859 004														
008-B 1	34.45	15.64	1.55	0	26.09	7.67	0.11	9.35	0	0.1	0.49	0.67	0.28	96.4
008-B 2	34.4	15.78	1.55	0	25.26	7.6	0	9.2	0	0.11	0.36	0.62	0.24	95.12
008-B 3	34.66	15.72	1.56	0	25.76	7.64	0.08	9.17	0.01	0.09	0.27	0.66	0.25	95.87
008-B 4	35.29	16.12	1.55	0	25.64	7.81	0.08	9.21	0.05	0.12	0.22	0.68	0.3	97.07
008-B 5	34.75	15.99	1.54	0	26.01	7.52	0.04	9.13	0.07	0.08	0.36	0.7	0.26	96.45
008-B 6	35.3	16.13	1.65	0	24.99	7.4	0.08	9.25	0	0.11	0.5	0.59	0.23	96.23
008-B 7	34.96	16.1	1.61	0	25.38	7.46	0.1	9.16	0.03	0.08	0.48	0.6	0.24	96.2
008-B 13	34.77	15.4	1.47	0.01	25.92	7.52	0.1	9.11	0.02	0.1	0	0.69	0.28	95.39
008-B 14	35.07	15.73	1.55	0	26.09	7.24	0.06	9.28	0.03	0.16	0	0.61	0.29	96.11
008-B 15	34.84	15.89	1.61	0.02	26.75	7.16	0.11	9.34	0	0.13	0	0.64	0.32	96.81

Biotite analyses *Pakenham Dome gneiss*

Sample 954 051														
051 BA1	38.22	17.68	1.23	0	13.91	15.87	0	8.99	0	0.53	0.38	0.72	0	97.53
051 BA1	37.29	17.64	1.27	0	14.42	15.49	0.02	8.82	0.01	0.4	0.12	0.54	0	96.02
051 BA2	38.03	17.63	1.28	0.01	14.26	15.51	0.01	8.8	0.01	0.39	0	0.54	0	96.47
051 BA3	37.61	17.57	1.31	0.01	14.35	15.69	0.02	8.9	0.01	0.41	0.08	0.63	0	96.59
051 BA4	37.1	17.03	1.24	0.02	13.31	15.65	0	8.6	0.06	0.44	0.11	0.6	0.1	94.26
051 BA5	37.5	17.35	1.29	0.01	13.46	15.17	0	8.65	0.04	0.65	0.06	0.62	0.08	94.88
051 BA6	37.31	17.14	1.31	0	13.79	15.1	0.02	8.59	0.01	0.56	0.03	0.61	0.09	94.56
051 BB1	37.4	16.53	1.35	0.01	15.24	14.16	0	9.32	0.01	0.27	0.14	0.6	0.07	95.1

Appendix 2 - Mineral Chemistry (cont.)

Biotite analyses ***Pakenham Dome gneiss***

Sample 954 051

051 BB2	36.67	16.52	1.08	0.05	15.03	14.3	0.06	8.94	0.04	0.38	0.16	0.72	0.08	94.03
051 BB3	37.25	16.47	1.17	0.06	14.97	14.32	0.02	9.25	0.02	0.32	0.12	0.55	0.05	94.57
051 BB4	37.32	16.66	1.11	0.03	14.95	14.46	0.04	9.08	0.01	0.28	0.15	0.56	0.05	94.7
051 BB5	36.54	16.97	1.02	0.01	15.24	14.84	0.01	8.18	0.04	0.47	0.21	0.5	0.03	94.06
051 BB6	36.73	16.58	1.13	0.07	15.59	14.29	0.05	8.82	0.03	0.38	0.18	0.64	0.09	94.58
051 BB7	36.83	16.78	1.12	0.02	15.68	14.05	0.05	9.03	0.03	0.29	0.09	0.54	0.05	94.56
051 BB8	37.37	16.69	1.14	0.05	15.66	13.88	0.04	8.92	0.03	0.3	0.09	0.59	0.07	94.83
051 BC1	37.68	17.22	1.25	0.02	13.85	15.4	0.03	8.72	0	0.42	0.16	0.69	0.07	95.51
051 BC2	38.21	17.48	1.21	0	14.09	15.02	0.01	8.69	0	0.41	0.13	0.66	0.06	95.97
051 BC3	38.21	17.31	1.18	0	13.58	15.25	0	8.65	0.02	0.53	0.12	0.7	0.03	95.58
051 BC4	34.79	17.46	1.03	0	17.11	14.47	0.01	6.78	0.08	0.41	0.06	0.45	0.05	92.7
051 BC5	37.81	16.88	1.65	0	13.97	14.74	0.09	8.54	0.03	0.44	0.16	0.63	0.08	95.02
051 BC6	35.93	16.55	1.82	0.02	16.12	14.45	0.01	7.61	0.02	0.47	0.17	0.51	0.02	93.7
051 BC7	37.36	17.14	1.22	0.03	14.36	15.61	0.05	7.97	0.19	0.45	0.13	0.58	0.07	95.16
051 BC8	37.58	17.15	1.14	0.03	14.06	15.05	0.07	8.33	0.1	0.36	0.1	0.58	0.05	94.6
051 BC9	38	16.99	1.23	0.03	13.87	15.29	0	8.66	0.09	0.5	0.11	0.64	0.05	95.46
051 BC10	37.69	17.1	1.06	0.01	14.21	15.79	0.05	8.09	0.06	0.43	0.13	0.64	0.07	95.33
051 BC11	36.61	16.97	1.15	0	14.32	15.75	0.01	7.88	0.09	0.34	0.09	0.45	0.05	93.71

Biotite analyses ***Lyndhurst area gneiss***

Sample 070 304

analysis	**SiO_2**	**AL_2O_3**	**TiO_2**	**Cr_2O_3**	**FeO**	**MnO**	**MgO**	**K_2O**	**CaO**	**Na_2O**	**BaO**	**Cl**	**F**	**TOTAL**
304 BT1	34.65	14.88	3.43	0	26.94	6.58	0.18	9.7	0	0.06	0	0.36	0.09	96.87
304 BT2	34.48	14.94	3.55	0	27.17	6.4	0.12	9.78	0	0.05	0.35	0.33	0.08	97.25
304 BT3	34.63	14.68	3.59	0.01	26.27	6.37	0.16	9.81	0	0.02	0.3	0.29	0.1	96.23
304 BT4	34.17	14.88	3.44	0.01	26.78	6.58	0.27	9.27	0.03	0.04	0.34	0.19	0.07	96.07
304 BT5	34.61	14.99	3.6	0.02	26.4	6.36	0.24	9.86	0	0.04	0.14	0.25	0.08	96.59

Appendix 2 - Mineral Chemistry (cont.)

Biotite analyses *Lyndhurst area gneiss*

Sample 070 304 analysis	**SiO_2**	**AL_2O_3**	**TiO_2**	**Cr_2O_3**	**FeO**	**MnO**	**MgO**	**K_2O**	**CaO**	**Na_2O**	**BaO**	**Cl**	**F**	**TOTAL**
304 B2B3	34.36	14.6	3.58	0.02	27.23	5.87	0.16	9.8	0.04	0.04	0.16	0.32	0	96.18
304 B2B4	34.07	14.74	3.53	0.03	27.34	6.28	0.24	8.97	0.15	0.06	0	0.31	0	95.72
304 B2B6	34.51	14.84	3.41	0.01	27.13	5.71	0.26	9.67	0.01	0.09	0.08	0.21	0	95.93
304 B2B7	34.41	14.74	3.49	0	26.7	5.89	0.15	9.52	0.02	0.06	0.15	0.37	0	95.5

Appendix 2 - Mineral Chemistry (cont.)

Amphibole analyses **Wolf Grove Structure**

Sample 024 054a													
analysis	**SiO_2**	**AL_2O_3**	**TiO_2**	**Cr_2O_3**	**FeO**	**MnO**	**MgO**	**K_2O**	**CaO**	**Na_2O**	**Cl**	**F**	**TOTAL**
054A A4 1	40.78	11.86	1.69	0.02	21.82	0.47	6.86	1.22	10.63	1.54	0.04	0.17	97.1
054A A4 2	40.91	11.57	1.9	0.01	21.74	0.49	6.79	1.44	10.67	1.57	0.03	0.1	97.22
054A A4 3	40.77	11.37	1.82	0.02	21.93	0.44	6.96	1.39	10.91	1.5	0.04	0.12	97.27
054A A4 4	40.63	11.25	2.01	0.02	21.51	0.38	6.88	1.49	10.84	1.51	0.03	0.16	96.71
054A A4 5	40.61	11.2	1.87	0.01	21.4	0.45	7.05	1.41	10.73	1.49	0.03	0.19	96.44
054A A4 6	42.16	11.53	1.84	0	21.94	0.4	7.39	1.48	10.61	1.68	0.02	0.12	99.17
054A A3 1	41.1	11.41	1.81	0.02	22.05	0.51	6.61	1.44	10.78	1.44	0.04	0.11	97.32
054A A3 2	40.31	10.99	2.09	0.02	22.64	0.6	6.53	1.45	10.65	1.63	0.05	0.1	97.06
054A A3 3	41.07	10.84	2.1	0	22.54	0.6	6.6	1.38	10.61	1.73	0.04	0.14	97.65
054A A3 4	43.2	11.27	1.57	0	21.35	0.55	6.36	1.33	10.59	1.29	0.04	0.08	97.63
Sample 025 055a													
055A-20	41.79	10.71	1.78	0	24.67	0.3	5.14	1.46	11.11	1.44	0	0.23	98.64
055A-21	41.3	11	2.09	0.02	25.5	0.41	4.87	1.5	10.54	1.63	0	0.03	98.89
055A-24	39.76	11.84	1.47	0	25.4	0.34	4.18	1.61	11.12	1.46	0	0.08	97.43
055A-25	40.42	11.2	2.11	0.05	25.41	0.39	4.43	1.67	10.96	1.55	0	0.16	98.35
055A-32	39.56	12.83	1.33	0	25.16	0.27	4.16	1.64	11.32	1.37	0	0.11	97.81
055A-33	41.22	11.39	1.76	0	24.64	0.39	4.61	1.58	10.77	1.52	0	0.14	98.05
055A-34	40.77	11.23	1.94	0	26.04	0.4	4.53	1.56	10.68	1.59	0	0.14	98.88
055A-35	37.44	13.66	0.61	0	27.39	0.43	2.62	2.27	11.17	1.37	0	0.07	97.04
055A-36	40.21	11.38	1.87	0	25.47	0.35	4.39	1.54	11.21	1.44	0	0.12	98.2
Sample 050 008													
008-1A1	40.01	13.57	1.93	0.02	19.93	0.14	6.98	2.03	11.58	1.13	0.24	0.1	97.66
008-1A3	39.77	13.29	1.9	0.06	19.41	0.22	7.02	2.11	11.54	0.99	0.24	0.08	96.63
008-1A2	46.29	8.24	0.62	0.05	17.66	0.19	10.6	0.84	11.67	0.77	0.05	0.22	97.2
008-4A3b	39.93	12.4	2.23	0.05	20.66	0.15	6.91	2.25	11.47	1.19	0.33	0.18	97.75
008-4A6	40.07	12.45	1.97	0.06	20.55	0.16	6.99	2.08	11.63	1.1	0.3	0.13	97.49
008-4A4	52.38	3.24	0.1	0.02	15.03	0.23	14.06	0.15	11.76	0.16	0	0.13	97.26
008-4A5	51.95	3.4	0.17	0.03	15.19	0.22	14.2	0.18	11.15	0.12	0	0.15	96.76

Appendix 2 - Mineral Chemistry (cont.)

Amphibole analyses **Wolf Grove Structure**

Sample 050 008													
analysis	**SiO_2**	**AL_2O_3**	**TiO_2**	**Cr_2O_3**	**FeO**	**MnO**	**MgO**	**K_2O**	**CaO**	**Na_2O**	**Cl**	**F**	**TOTAL**
008-5A1	39.62	13.05	1.88	0	20.98	0.1	6.64	2.37	11.62	1.17	0.3	0.15	97.88
008-5A2	39.86	13.34	1.54	0	20.4	0.11	6.91	2.17	11.57	0.96	0.25	0.15	97.26
008-5A3	42.39	11.66	1.17	0.01	19.87	0.16	8.24	1.47	11.5	1.1	0.08	0.23	97.88
008-5A4	41.93	12.08	0.73	0.02	19.47	0.15	8.32	1.5	11.66	1.02	0.08	0.19	97.15
008-5A6	44.76	9.97	0.5	0.04	18.02	0.15	9.85	1.2	11.47	0.94	0.04	0.13	97.07
008-5A8	53.24	3.37	0.16	0	14.81	0.2	13.89	0.17	11.15	0.17	0.03	0.16	97.35
Sample 989 988													
988-A1	39.52	12.17	2.38	0	25.17	0.13	3.75	1.73	11.19	1.48	0.11	0.12	97.75
988-A2	38.82	13.18	1.6	0	25.91	0.13	3.36	1.83	11.21	1.48	0.12	0.08	97.72
988-A2	39.71	11.45	2.23	0	25.57	0.16	3.77	1.59	11.24	1.56	0.08	0.14	97.5
988-A2	39.37	11.32	2.09	0	24.78	0.19	3.79	1.75	11.17	1.78	0.17	0.05	96.46
988-A2	38.24	12.2	1.98	0.01	24.46	0.14	3.49	2.1	11.28	2.03	0.37	0.11	96.41
988-A7	39.06	12.16	1.51	0	27.35	0.23	3.61	1.55	11.38	1.46	0.08	0.1	98.49
988-A8	39.35	12.23	1.39	0.06	27.23	0.14	3.75	1.45	11.33	1.57	0.07	0.09	98.66
988-A9	39.36	12.11	1.43	0	27.06	0.13	3.73	1.34	11.44	1.46	0.08	0.09	98.23
988-A10	39.25	13.72	0.09	0	27.13	0.2	3.69	1.56	10.96	1.4	0.02	0.18	98.2
988-A11	39.67	12.7	0.76	0.03	27.85	0.25	3.54	1.72	10.77	1.49	0.07	0.12	98.97
988-A12	39.83	12.45	1.13	0	27.75	0.22	3.62	1.76	10.89	1.44	0.07	0.1	99.26
988-A13	39.72	12.24	0.97	0.01	27.28	0.21	3.92	1.71	10.96	1.51	0.03	0.2	98.76
988-A14	38.5	11.66	2.86	0	26.7	0.11	3.53	1.73	11.24	1.53	0.09	0.07	98.02
988-A15	38.95	11.19	2.48	0	27.19	0.18	3.5	1.69	11.09	1.64	0.09	0.04	98.04
988-A16	38.99	11.16	2.44	0	27.32	0.17	3.55	1.73	10.98	1.52	0.08	0.06	98
Sample 995 0035b													
0035 A1	40.19	12.64	0.89	0	23.02	0.3	5.8	1.24	11.54	1.24	0.06	0.02	96.94
0035 A2	40.54	12.18	1.06	0	23.18	0.32	5.93	1.23	11.61	1.36	0.07	0.05	97.53
0035 A3	40.74	12.45	1.04	0	22.8	0.29	5.77	1.23	11.59	1.26	0.07	0.06	97.3
0035 A4	40.69	12.31	0.94	0	23.22	0.31	6	1.22	11.59	1.27	0.05	0	97.6

Appendix 2 - Mineral Chemistry (cont.)

Amphibole analyses **Lyndhurst area gneiss**

Sample 070 304

analysis	SiO_2	AL_2O_3	TiO_2	Cr_2O_3	FeO	MnO	MgO	K_2O	CaO	Na_2O	Cl	F	TOTAL
304 AM1	40.29	11.42	1.52	0.03	24.29	0.34	4.81	1.37	10.99	1.48	0.09	0.18	96.81
304 AM2	39.9	10.95	2.2	0.03	25.1	0.42	4.71	1.57	10.64	1.64	0.07	0.16	97.39
304 AM3	40.01	10.87	2.18	0	24.65	0.39	4.71	1.57	10.63	1.56	0.07	0.16	96.8
304 2AM1	40.27	11.25	1.69	0.03	25.51	0.27	4.5	1.49	11.11	1.37	0	0.1	97.59
304 2AM2	39.28	12.02	1.25	0	24.94	0.27	4.22	1.6	11.19	1.37	0	0.12	96.26
304 2AM3	40.39	11.53	1.32	0	25.27	0.37	4.73	1.53	11.19	1.37	0	0.19	97.89
304-4A1	40.28	12.01	1.16	0	24.63	0.47	4.88	1.46	11.15	1.37	0.08	0.23	97.72
304-4A2	40.02	11.23	2.3	0.01	25.24	0.41	4.49	1.63	10.84	1.71	0.05	0.1	98.03

Clinopyroxene analyses

Sample 050 008

analysis	SiO_2	AL_2O_3	TiO_2	Cr_2O_3	FeO	MnO	MgO	CaO	TOTAL	
008-4A1	51.62	0.95	0.08	0.03	11.98	11.24	0.32	22.97	0.3	99.49
008-4A2	51.16	2.07	0.17	0.02	12.76	10.72	0.37	22.39	0.3	99.96
008-5A7	52.31	0.94	0.07	0.03	12.1	10.99	0.32	22.87	0.26	99.89

UTM	assemblage	collected by
820 849	2	M
822 008	4 or 5,6,7,8,14	M
823 888	4 or 5,6,7,8,14	M
824 009	4 or 5,6,7,8,14	M
824 018	8,9	A
825 011	11 or 8,9	M
827 013	2	M
827 015	5,6,7,8,14	M
828 886	11	M
829 006	5,6,7,8,14	M
830 006	4 or 5,6,7,8,14	M
831 006	4 or 5,6,7,8,14	M
831 010	5,6,7,8,14	A
832 009	5,6,7,8,14	M
833 823	4 or 5,6,7,8,14	B
833 850	4 or 5,6,7,8,14	B
833 009	4 or 5,6,7,8,14	M
833 021	5,6,7,8,14	M
833 023	11 or 8,9	B
834 047	5,6,7,8,14	M
835 023	9,10	E
836 959	8,9	M
839 956	4 or 5,6,7,8,14	B
839 000	11 or 8,9	M
840 952	2	M
840 954	8,9	E
840 056	5,6,7,8,14	A
841 004	11 or 8,9	M
841 051	5,6,7,8,14	M
841 055	5,6,7,8,14	M
842 003	5,6,7,8,14	M
842 028	5,6,7,8,14	M
842 055	5,6,7,8,14	A
844 922	2	E
844 922	2	M
845 864	4 or 5,6,7,8,14	M
847 939	5,6,7,8,14	M
847 049	2	M
849 859	5,6,7,8,14	M
849 922	5,6,7,8,14	A
849 047	4	A
847 055	5,6,7,8,14	A
844 030	2	M

UTM	assemblage	collected by
850 880	4	B
851 924	5,6,7,8,14	M
851 046	4	A
852 042	5,6,7,8,14	A
852 043	5,6,7,8,14	A
853 026	11 or 8,9	M
854 843	5,6,7,8,14	A
854 853	5,6,7,8,14	A
854 938	2	E
854 041	4	A
854 043	4	A
855 937	5,6,7,8,14	A
855 937	4 or 5,6,7,8,14	M
855 040	2	M
857 928	8,9	B
859 021	5,6,7,8,14	M
861 931	2	E
861 066	2	E
864 862	5,6,7,8,14	A
866 017	4 or 5,6,7,8,14	M
866 026	5,6,7,8,14	A
867 858	2	E
868 013	5,6,7,8,14	A
869 012	4	A
869 015	4 or 5,6,7,8,14	M
870 842	5,6,7,8,14	B
870 844	2	B
871 841	4	A
871 841	4 or 5,6,7,8,14	M
871 842	4 or 5,6,7,8,14	A
871 878	2	E
871 879	2	M
872 843	4 or 5,6,7,8,14	A
872 016	5,6,7,8,14	B
872 025	5,6,7,8,14	A
873 894	2	E
873 844	8,9	E
873 018	5,6,7,8,14	A
874 847	5,6,7,8,14	B
874 018	2	M
875 818	11 or 8,9	B
875 846	5,6,7,8,14	M
875 849	5,6,7,8,14	E

Appendix 3: UTM locations for marble thin sections (cont.)

UTM	assemblage	collected by	UTM	assemblage	collected by
875 016	5,6,7,8,14	M	902 926b	5,6,7,8,14	B
876 848	5,6,7,8,14	M	903 852	2	E
876 016	2	B	906 910	2	B
877 848	5,6,7,8,14	A	907 979	5,6,7,8,14	E
877 015	5,6,7,8,14	A	908 975	2	M
877 015	5,6,7,8,14	M	910 992	2	B
878 818	8,9	B	912 995	2	E
879 012	5,6,7,8,14	M	915 866	2	E
880 913	2	B	915 931	5,6,7,8,14	B
880 935	5,6,7,8,14	E	916 960	11 or 8,9	B
880 012	2	E	919 865	2	M
881 910	5,6,7,8,14	M	920 035	5,6,7,8,14	B
882 849	5,6,7,8,14	E	920 037	5,6,7,8,14	B
883 889	2	M	921 039	5,6,7,8,14	B
883 890	5,6,7,8,14	E	922 003	2	M
884 992	11	E	922 004	5,6,7,8,14	A
885 996	2	E	922 024	2	B
885 025	5,6,7,8,14	E	923 006	5,6,7,8,14	B
887 856	5,6,7,8,14	B	923 024	5,6,7,8,14	B
887 893	5,6,7,8,14	A	925 020	5,6,7,8,14	B
887 901	5,6,7,8,14	M	921 037	11 or 8,9	E
887 900	5,6,7,8,14	B	927 081	4	E
888 894	4	E	928 043	5,6,7,8,14	B
888 894	5,6,7,8,14	M	931 013	11 or 8,9	B
888 896	4 or 5,6,7,8,14	B	931 042	5,6,7,8,14	M
888 901	5,6,7,8,14	B	932 933	8,9	B
891 853	5,6,7,8,14	E	932 965	2	E
891 984	5,6,7,8,14	E	932 011	5,6,7,8,14	A
892 874	2	B	932 012	5,6,7,8,14	M
893 939	5,6,7,8,14	E	933 951	5,6,7,8,14	B
895 974	2	E	934 897	8,9	M
895 033	5,6,7,8,14	E	935 968	8,9	B
896 847	5,6,7,8,14	A	937 904	5,6,7,8,14	M
896 848	5,6,7,8,14	M	938 908	too altered	M
896 849	5,6,7,8,14	B	939 915	2	E
896 892	5,6,7,8,14	A	939 935a	5,6,7,8,14	B
896 892	5,6,7,8,14	M	943 973	5,6,7,8,14	E
898 901	2	B	944 941	2	M
899 899	2	B	946 977	5,6,7,8,14	B
900 964	8,9	E	947 978	8,9	B
900 968	5,6,7,8,14	B	947 952	11 or 8,9	M
901 902	5,6,7,8,14	E	947 958	2	B
902 924	5,6,7,8,14	B	953 983	11 or 8,9	B

UTM	assemblage	collected by
954 986	5,6,7,8,14	E
961 995	2	E
963 977	5,6,7,8,14	E
963 999	11	B
963 039	5,6,7,8,14	M
964 041	5,6,7,8,14	E
969 068	8,9	E
971 010	11 or 8,9	B
942 031	11 or 8,9	B
976 049	2	E
979 998	5,6,7,8,14	E
980 081	5,6,7,8,14	E
983 089a	8,9	B
984 087	11 or 8,9	A
994 025	9,10	B
003 035	5,6,7,8,14	B
005 050	2	B
010 963	5,6,7,8,14	E
016 994	2	M
020 930	9,10	B
021 973	5,6,7,8,14	B
024 010	9,10 or 11	E
025 972	11 or 8,9	B
025 008	11 or 8,9	E
026 932	2	M
026 014	9,10	B
026 017	9,10	B
028 004	8,9	E
031 971	9,10	B
032 000	5,6,7,8,14	E
033 002	too altered	B
0334 998	2	E
0335 001	11 or 8,9	B
035 997	too altered	M
036 020	11 or 8,9	B
040 026	11 or 8,9	B
042 989	11	E
042 026	9,10	E
063 030	11 or 8,9	B

UTM locations from the 31 F/1 map sheet (1994 18T, NAD 83

6-figure UTM coordinates were converted from the full grid reference by dropping the 1st and the last 2 digits from the easting and the 1st 2 and last 2 digits from the northing

eg. 869 924 = 389600 4992400

The 6-figure UTM coordinates are considered accurate to the nearest 100m.

A = Abercrombie (1983)
B = Goodwin-Bell (this study)
E = Ewert (1977)
M = McKinistry (1986?)

assemblage information corresponds to field numbers on the T-X diagrams produced in this study

2 = cc, dol, ph, qtz
4 = cc, dol, tc, trem
5,6,7,8,14 = cc, dol, ph, trem
8,9 = cc, dol, trem, diop
9,10 = cc, dol, ph, fo
11 = cc, dol, ph, diop

~ fluid is assumed to be present in all cases

Appendix 4 Trivariant assemblages corresponding to fields 1-12 on figure 4.11

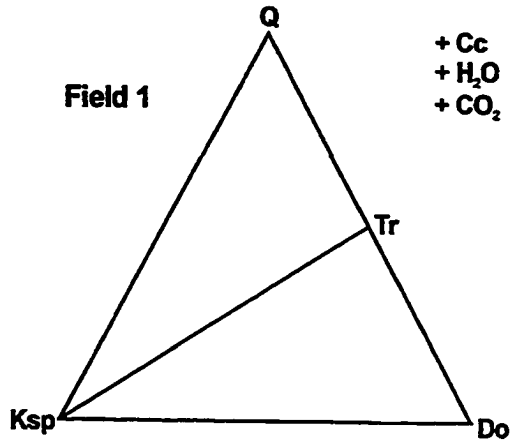

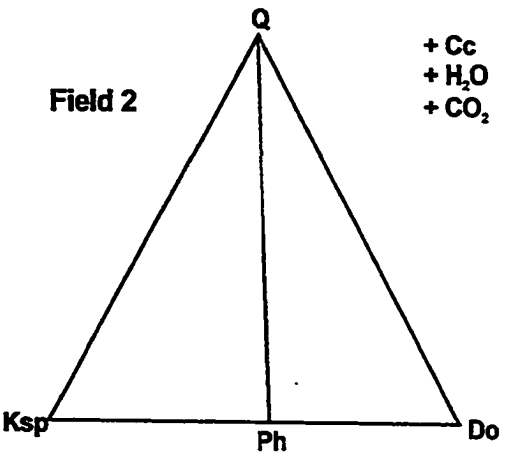

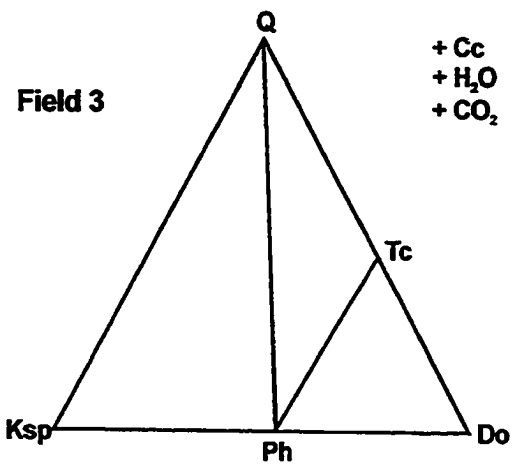

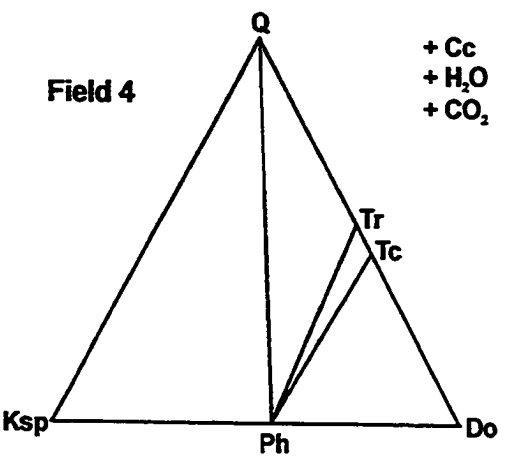

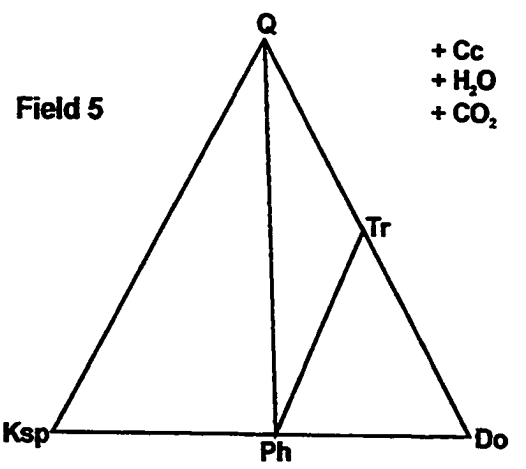

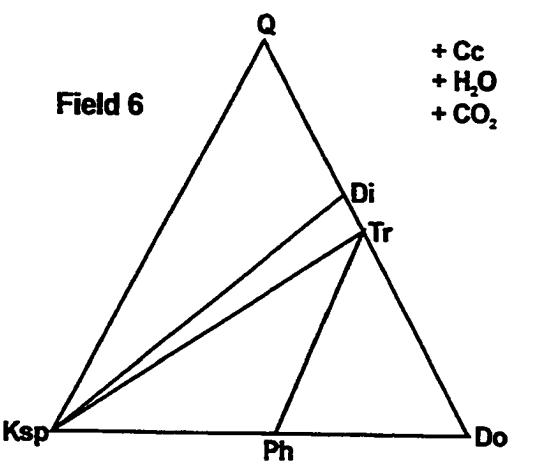

Appendix 4 (cont.) Trivariant assemblages corresponding to fields 1-12 on figure 4.11